The effects of ERCC1 deficiency on mouse hepatocytes *in vivo*

Michael Chipchase

Ph.D.

University of Edinburgh

2001

Contents

Acknowledgements

This thesis would not have been possible without the help and encouragement of my supervisor Professor David Melton, to whom I am indebted. He has always been far more positive about my results than I have been at times. I was supported by a Medical Research Council studentship and my research was funded by the Cancer Research Campaign. I was very fortunate to be able to count on the assistance of Dr. Sally Wheatley, Professor Bill Earnshaw and Dr Alan Clarke, who enabled a lot of this work through their cooperation.

Everyone in my lab has been very helpful and supportive. Dr. Fatima Nunez set up most of the experimental systems in this thesis and laid all the background down, without her this project wouldn't have existed. Ann-Marie Ketchen gave great assistance with all cell culture matters and could always answer my stupid questions. Dr. Jim Selfridge supported almost all of my mouse work and showed me which end of a mouse was which. He also gave me instruction in the fine and graceful art of Northern blots, a difficult task for someone as lacking in grace as myself. Carolanne McEwan helped me settle in when I first arrived and without her my cloning would have been nonexistent and I would never have been able to genotype my mice. Sarah and Debbie were very helpful with ideas for immunohistochemistry. I would also like to thank Dr. Derek Paisley, Dr. Kan-tai Hsia, Dr. Andrew Winter, Dr. Niki Redhead, Carolines Swann and Harrison/Homes, Dr. Mary O'Neill and Yvonne Simpson.

Much thanks must go to my friends and family for putting up with my moaning and finally, my girlfriend Allison Robb, who I won't eulogise about for fear of the curse of Fatima and Pepe.

List of Abbreviations

6-4PP – 6-4 Photoproducts

AP – Apurinic/Apyrimidinic

BER – Base Excision Repair

CDK – Cyclin Dependent Kinase

CDKI – Cyclin Dependent Kinase Inhibitor

CHR – Classical Homologous Recombination

CPD – Cyclobutane Pyrimidine Dimers

CS – Cockayne's Syndrome

CSR – Class Switch Recombination

DDB – DNA Damage Binding Activity

Def. – Deficient

dsDNA – Double Stranded DNA

DSG – Daughter Strand Gap

GGR – Global Genome Repair

ICL – DNA interstrand crosslink

IR- Ionising Radiation

MMC – Mitomycin C

MMR – Mismatch Repair

NER – Nucleotide Excision Repair

ssDNA – Single Stranded DNA

TCR – Transcription Coupled Repair

TTD – Trichiothiodystrophy

TLS – Trans Lesion Synthesis

UV- Ultra Violet

WT – Wild Type

XP – Xeroderma Pigmentosum

THE UNIVERSITY OF EDINBURGH
ABSTRACT OF THESIS (Regulation 3.5.13)

Name of Candidate: Michael David Chipchase
Address: CRC labs., MMC, Western General Hospital, University of Edinburgh
Degree: PhD Date: 10/07/01
Title of Thesis: The effects of ERCC1 deficiency on mouse hepatocytes *in vivo*

ERCC1-XPF is a structure specific endonuclease that acts in nucleotide excision repair (NER), and is also involved in repair of DNA interstrand crosslinks and removal of non-homologous 3' tails during recombination. The ERCC1 null mouse is runted and dies of liver failure before weaning, at about 3 weeks old. By three weeks after birth, some ERCC1 null hepatocytes have developed polyploidy. The liver phenotype of the ERCC1 null mouse is not observed in other NER deficiency models, which indicates that the loss of non-NER roles of ERCC1 are responsible for the liver phenotype. Development of liver polyploidy in the ERCC1 null hepatocytes has been tracked from before birth to death using FACS analysis and nuclear area distribution measurements. This has been compared to hepatocyte polyploidy development in wild type mice. The ERCC1 null mice undergo an accelerated development of polyploidy compared to age matched wild type mice. The cell cycle status of ERCC1 null hepatocytes has been investigated using a fluorescence immunostaining assay for centromeres. This reveals that the enlarged ERCC1 null hepatocytes are primarily in G2/M. Enlarged old wild type hepatocytes are also primarily in G2/M. However, normal ERCC1 null, old wild type and young wild type hepatocytes are primarily in G1/G0. The premature polyploidy liver phenotype of the ERCC1 null mouse is very similar to that seen in a transgenic mouse that overexpresses p21 in liver. Immunohistochemistry shows that p21 protein levels are increased in ERCC1 null liver. The increase in p21 protein levels tends to be confined to the enlarged, polyploid nuclei. However, no increase in p21 levels was seen in old wild type livers when measured by immunohistochemistry and Northern blot analysis. A p53-ERCC1 double null mouse was made to test if the ERCC1 phenotype was dependent on p53. ERCC1-p53 null hepatocytes have the same accelerated polyploidy and increased p21 levels as ERCC1 null hepatocytes. FACS analysis and centromeric staining assays have been used to confirm that ERCC1-p53 double null hepatocytes have the same phenotype as ERCC1 null hepatocytes. In order to compensate for the loss of ERCC1, proteins in other DNA repair pathways may be upregulated, if they have overlapping substrate specificities. The levels of MSH2, a protein involved in recombination and mismatch repair, and REF1, a protein involved in both base excision repair and redox regulation of various proteins, are upregulated in the nuclei of ERCC1 null hepatocytes. The role of ERCC1 in recombinational repair rather than NER, may be the key to understanding the phenotype of the ERCC1 null mouse. To investigate this role *in vitro*, the role of ERCC1 in the formation of UV-induced chromosome aberrations was studied. ERCC1 and XPF deficient cells have more breaks and less exchanges than wild type cells, but cells deficient in other NER proteins have the same as wild type. This indicates that ERCC1 is involved in a recombination pathway that affects aberration formation.

Word Count ((not including figure legends): 48, 477

List of Figures

List of Tables

Chapter 1 - Introduction

In order to succeed and proliferate, organisms must ensure that the information encoded in their genome remains intact. The information in the genome is constantly subject to degradation and attack by various agents and mechanisms, both external and internally generated. As a result, all organisms must have mechanisms for repairing their DNA. This thesis is concerned with ERCC1, a mammalian protein that acts as part of the nucleotide excision repair pathway (NER) and in some forms of recombinational repair.

General Types and Consequences of DNA Damage

The causes of DNA damage and its forms are various and many. Both chemical agents, such as free radicals and alkylating agents, and electromagnetic radiation, from ultraviolet light (UV) to ionising radiation (IR), can all damage DNA. These agents can alter the structure of nucleotides by modifying, fragmenting or crosslinking them and can cause single stranded (SSB) and double stranded breaks (DSB) in DNA.

Reactive oxygen species, such as superoxide anion radicals, hydroxyl radicals and nitric oxide, arise naturally during cell metabolism and through exposure to physical and chemical mutagens such as IR, UV or H_2O_2. These species can cause strand breaks, abasic sites and oxidised bases and sugars (Cadet et al., 1997; Demple and Harrison, 1994; Epe, 1996). Alkylating agents, such as mitomycin C, can modify nucleotides and if bifunctional, as is mitomycin C (MMC), can crosslink the two DNA strands (Friedberg, DNA repair and Mutagenesis). UV radiation causes cyclobutane-pyrimidine dimers (CPD) and (6-4) pyrimidine pyrimidone photoproducts (6-4PP), of these CPDs form 65-80% of the total (Friedberg, DNA Repair and Mutagenesis). There is even some evidence that UV will cause DNA interstrand crosslinking (Nejedly et al., 2001; Pospisilova, 1997). IR will cause SSBs and DSBs, which may result from the production of oxidative radicals.

DNA damage can result in disruption of normal cellular processes through blockage of transcription bubbles and DNA replication forks. Mutations can also be caused if the incorrect base is inserted opposite the damage during DNA replication. A distinction must be made between DNA damage and mutation. DNA damage does not automatically lead to mutation. There are some forms of DNA damage that cause one nucleotide to base pair like another thus leading to mutation, however in general DNA damage only leads to mutation through faulty action by the DNA processing machinery. Sometimes DNA repair systems can actually cause worse damage than was originally present. For instance, most chromosomal translocations, which can lead to cancer, are probably caused by defective recombinational DNA repair.

There are various mechanisms to repair DNA damage. They have differing, but overlapping, substrate specificities and enlist differing, but overlapping sets of proteins. The cellular response to DNA damage includes mechanisms, called checkpoints, to stall the cell cycle, to allow time for repair. Lesions that escape repair can be processed to allow their toleration. DNA repair mechanisms also act on mismatched bases and abnormal structures formed during DNA replication. DNA repair mechanisms show similarity between differing organisms but tend to be more complex in higher organisms (Eisen and Hanawalt, 1999). In general, in this thesis, mammalian systems are referred to, except where stated, sometimes gene names are prefixed with initials to denote species, ie. spcdc25 for *Schizosaccharomyces pombe* cdc25, sc for *Saccharomyces cerevisiae*.

DNA Repair

In theory, there are various ways to correct abnormal nucleotides - either the nucleotide can be repaired *in situ* and returned to its original structure or it can be removed and replaced with the correct nucleotide. If a damaged or incorrect nucleotide is replaced then a template will be needed to ensure that the correct nucleotide is used to replace it. This template can be either the undamaged complementary strand or homologous DNA. Some types of DNA damage, such as some DSBs and interstrand crosslinks, can only be repaired correctly using homologous DNA. ERCC1 is involved in multiple systems using both types of template.

Direct Reversal

Direct reversal is the simplest way to repair DNA damage. This can use photolyases, enzymes that rely on light-dependent photoreactivation (Sancar, 2000). Photolyases specific for CPDs have been found in many classes of prokaryotes and eukaryotes, but none have been found in placental mammals (Li et al., 1993). Photolyases for 6-4PP have been found in Drosophila, Xenopus and plants and two homologous genes have been found in mammals, but these seem to be involved in circadian clock regulation rather than photoreactivation (Griffin et al., 1999). Certain enzymes directly reverse alkylation damage; alkyltransferases transfer alkyl groups to an internal cysteine residue and inactivate themselves in the process (Teo et al., 1984).

Complementary Strand Repair

Systems which use the complementary strand as a template act by removing either just the damaged or incorrect base/nucleotide or by removing the damaged or incorrect base/nucleotide as part of an oligonucleotide.

Base Excision Repair

Base excision repair (BER) acts on non-bulky base adducts, e.g. methylation damage, and oxidised, reduced or fragmented bases caused by IR or oxidative damage. BER also repairs apurinic/apyridinic (AP) sites, often formed

spontaneously by oxidative damage (Nakamura and Swenberg, 1999). The initiation and recognition enzymes, DNA glycosylases, are specific for particular types of damage.

The damaged base is released in a hydrolysis reaction, from the sugar backbone of the DNA (Dianov and Lindahl, 1994; Frosina et al., 1996; Lindahl, 1995; Memisoglu and Samson, 2000). Simple DNA glycosylases, such as N-methyl purine DNA glycosylase, then require the DNA to be nicked to the 5' of the resulting AP deoxyribose by an AP endonuclease activity, provided by REF1 (Demple and Harrison, 1994; Sancar and Sancar, 1988; Wallace, 1988). The deoxyribose sugar is removed by DNA polymerase (DNA pol) β, which then fills in the gap. DNA ligase III and XRCC1 ligate the short patch. Complex DNA glycosylase-lyases, such as OGG1, OGG2 and MTH glycosylase, act differently, with intrinsic AP endonuclease activity, but REF1 is still required to provide a nick that can be acted upon by DNA polymerase β.

Long patch repair is a variant of BER and involves synthesis of 2 to 10 nucleotides (Klungland and Lindahl, 1997). DNA pol β or δ probably act with PCNA to displace the strand from the helix. The resulting flap is then removed by the endonuclease FEN1 to allow ligation by DNA ligase I. FEN1 is involved in the processing of newly synthesised Okazaki fragments prior to ligation, the flap DNA structure processed by FEN1 is often found at damaged or mismatched sites or in the process of DNA repair and recombination.

Mismatch Repair

Mismatch repair (MMR) corrects misincorporated bases after DNA synthesis, the majority of which probably result from mispairing with oxidatively damaged bases rather than mispairing with normal bases (Earley and Crouse, 1998). MMR also acts on mismatched bases in recombination intermediates.

Repair of Mismatches

In order to perform MMR, either coupled with, or after DNA replication, it is important to be able to target repair to daughter strands, otherwise correct bases may be removed rather than mismatched bases resulting in fixation of mutations. Bacteria rely on methylation to distinguish between parent and daughter strands. In eukaryotes strand discrimination probably occurs by a mechanism other than DNA methylation (Drummond and Bellacosa, 2001). In human cell extracts, strand specific MMR occurs when an ss nick is introduced on either side of a mismatch, how such nicks might be introduced in leading strands during DNA replication is unclear (Modrich, 1997). On lagging strands there are frequent nicks at the ends of Okazaki fragments.

In MMR, a heterodimer forms between MSH2 and either MSH3 or MSH6 to effect mismatch recognition (Kolodner and Marsischky, 1999; Marsischky et al., 1996). MSH2-MSH6 recognises base-base mismatches and insertion/deletion loops, whereas MSH2-MSH3 recognises only insertion/deletion loops (Das Gupta and Kolodner, 2000; Kolodner and Marsischky, 1999; Marsischky et al., 1996).

DNA mismatches induce conversion of the MSH2 heterodimer into a freely diffusible sliding clamp (Gradia et al., 1999). In yeast, a heterodimer of scMLH1 and either scPMS1, scMLH2 or scMLH3 coordinates between the mismatch recognition clamp and other proteins, the complexes probably have distinct roles in repair of mutational intermediates (Kolodner and Marsischky, 1999). Mammalian homologs of scPMS1, scMLH1 and scMLH3 have been identified (Kolodner and Marsischky, 1999). PCNA has a direct interaction with the MSH2-MSH3 and MSH2-MSH6 complexes, this may facilitate the linking of MMR to DNA replication (Clarke et al., 2000; Kolodner and Marsischky, 1999).

When error prone translesion DNA synthesis produces mismatches at UV lesions, mismatch repair probably acts on the daughter strand to prevent these mismatch mutations being fixed by NER or further replication (Mu et al., 1997). Interestingly, MMR proficient mammalian cells are more susceptible to the killing effects of

alkylating agents than MMR deficient cells. MMR probably engages in a futile cycle, attempting to repair the mismatched base opposite the damage, this may lead to strand breaks (Karran and Hampson, 1996).

Mismatch Repair and Recombination

The MMR proteins exhibit anti-recombination activity which greatly reduces genetic recombination between non-identical sequences and thereby limits genomic rearrangements involving repetitive elements (Alani et al., 1994; Ciotta et al., 1998; Datta et al., 1996; Harfe and Jinks-Robertson, 2000). Sequence divergence has been found to inhibit recombination in yeast and mammalian cells (Belmaaza et al., 1994; Lukacsovich and Waldman, 1999). In spite of the general consensus that sequence divergence inhibits mitotic recombination, there is disagreement as to whether the MMR machinery is important for this inhibition (Alani et al., 1994; Chen and Jinks-Robertson, 1999; Datta et al., 1996; De Wind et al., 1995; Selva et al., 1995). Heteroduplex recombination intermediates from diverged sequences often contain mismatches, the processing of which could require MMR. MSH2 and MSH6 possess some antirecombination activity that is not dependent on the general MMR system (Nicholson et al., 2000). Mismatch binding by MSH2-MSH6 alone may be sufficient to impede recombination. It has been suggested that the yeast MMR machinery either impedes the extension of heteroduplexes by causing the immediate resolution of recombination intermediates or triggers a reversal of the strand assimilation process (Alani et al., 1994). The extent of heteroduplex formed during recombination is longer in MMR deficient cells than in MMR proficient cells (Chen and Jinks-Robertson, 1998; Chen and Jinks-Robertson, 1999).

Nucleotide Excision Repair

Nucleotide excision repair is the most promiscuous system for repairing DNA. There are strong homologies between yeast and mammalian systems. Research has concentrated on the role of NER in the repair of damage from UV light, however, NER will also remove most damaged bases, mismatched bases (with no specificity for the mismatched bases, it will take either) and one to three nucleotide long loops, although with varying efficiencies (Batty and Wood, 2000; Fleck et al., 1999). NER is the sole repair mechanism for bulky adducts, like acetylaminofluorene-guanine,

cisplatin-guanine, psoralen-thymine adducts, and for thymine dimers and 6-4 photoproducts. NER was discovered through study of various UV sensitive cell lines and analysis of three human diseases that involve increased cancer risk and UV sensitivity. These diseases, Xeroderma Pigmentosum (XP), Cockayne's Syndrome (CS) and Trichothiodystrophy (TTD) are rare, autosomal, recessive disorders.

Xeroderma Pigmentosum

There are seven XP complementation groups, characterised by hypersensitivity to sunlight, a 1000-fold increase in skin cancers and a 20-fold increase in internal cancers (Friedberg, DNA repair and Mutagenesis; Robbins, 1988). XP patients do not have functional NER and cannot repair UV DNA damage or free radical DNA damage (Evans, 1993; Reardon, 1997; Robbins, 1988; Satoh et al., 1993). XP patients sometimes suffer from neurological abnormalities and neurodegeneration, similar to aging (Robbins, 1988; Robbins, 1989; Robbins et al., 1991). The neurodegeneration is probably caused by DNA damage, but as UV cannot reach the brain, it is proposed that DNA is damaged by reactive cellular metabolites, including the oxygen free radicals abundant in brain (Reardon et al., 1997; Robbins et al., 1989). About 20% of XP patients are classified as XPV, they have classic XP symptoms but normal NER. XPV cells are moderately sensitive to UV but excise photoproducts at a normal rate, however they suffer high rates of mutagenesis (Maher et al., 1976; Myhr et al., 1979). XPV patients are defective in Translesion synthesis (TLS), most patients have mutations in the gene that codes for DNA polymerase η (Cordonnier and Fuchs, 1999; Masutani et al., 1999; Masutani et al., 1999).

Cockayne's Syndrome

CS is characterised by growth failure, mental and neurological abnormalities, cataracts, dental caries, photosensitivity and related dermatoses. There are three CS complementation groups, genes for two of which have been cloned. CS A and CS B groups have classical CS symptoms without increased skin cancer and have near normal UV sensitivity (Henning et al., 1995; Troelstra et al., 1992). A separate patient group displays XP symptoms as well as CS. These patients have mutations in

Human	*S cerevisiae*	*S pombe*	Mouse
ERCC1	RAD10	SWI10	ERCC1
XPF	RAD1	RAD16, RAD10, RAD20, SWI9	ERCC4
XPG	RAD2	RAD13	ERCC5
XPD	RAD3	RAD15, RAD5, RHP3	ERCC2
XPA	RAD14	RHP14	XPA
XPC	RAD4	RHP4a, RHP4b	XPC
CSA	RAD28	SNF2	ERCC8
CSB	RAD26		ERCC6
HHR23a, HHR23b	RAD23	RAD26	
XPE/(DDB1& 2) (p48,p125)			DDB1-DDB2
XPB	RAD25		ERCC3

Table 1.1 Cloned human NER genes and their names in *S. cerevisiae*, *S. pombe* and mouse

the CSA, CSB, XPB, XPD or XPG genes. The lack of cancer incidence in simple CS patients may be due to the selective elimination of damaged cells by apoptosis, the transcription blockage resulting from a CS Transcription Coupled Repair (TCR) defect is a strong apoptotic signal (Balajee et al., 2000; Ljungman and Zhang, 1996).

Trichothiodystrophy

TTD patients have ichthyosis, brittle hair, photosensitivity, skeletal abnormalities, mental retardation and sometimes increased skin cancer rates (Bergmann and Egly, 2001). A group of patients have both XP and TTD symptoms and have mutations in the XPB and XPD genes. The TTD A group is probably mutant in another TFIIH subunit. TFIIH is an essential factor involved in transcription by RNA pol II.

Cross Complementation

In parallel with work on human genetic diseases, NER genes were also characterised in UV sensitive cultured rodent cell systems in which this sensitivity could be cross-complemented by 11 human genes. These cross complementing genes were given the nomenclature ERCC1 through to ERCC11, and most of them were subsequently found to correspond to genes already discovered in XP, CS and TTD. All the NER genes were mutated in either XP, CS or TTD patients, except ERCC1. This led to speculation that an ERCC1 mutation would be lethal or was associated with a different phenotype.

In this thesis I will refer to the NER genes by human nomenclature, alternative names are listed in Table 1.1. The NER genes have all been cloned, many following the cross-complementation strategy.

In Vitro Reconstitution

The NER system has been reconstituted *in vitro* (Aboussekhra et al., 1995). NER can either be reconstituted to give the dual incision steps alone or the entire repair process. The *in vitro* reconstitution was performed with XPA, TFIIH, XPG, ERCC1-XPF, XPC and RPA. These proteins were needed for the basic damage recognition and cleavage steps. The addition of RFC, PCNA, DNA polymerase ε (or δ) and DNA ligase I was needed for complete repair including the replication reaction. The complete *in vitro* NER reaction uses 25 polypeptides overall and requires IF7 and a type 2A protein phosphatase to optimise the reaction. The presence of active repair can be assayed by either measuring incision/excision or repair synthesis.

XPC is a protein of 125 kDa that copurifies with the 58 kDa HHR23B (Masutani et al., 1994). XPC binds TFIIH and has a preference for binding to damaged DNA (Sugawasa et al., 1998; Evans et al. 1997; Masutani et al., 1994; Drapkin et al., 1994; Shivji et al., 1994). XPC-HHR23B may be the primary damage sensor in Global Genome Repair (GGR) (Sugawasa et al., 1998;). XPC and TFIIH are probably involved with open complex formation and/or stabilisation (Drapkin et al., 1994; Evans et al., 1997). XPC is not required for TCR (Hanawalt, 1994; van Hoffen et al., 1995).

XPA, a 31 kDa protein with a zinc finger, acts with RPA and this complex is essential for NER (Evans et al., 1997; He et al., 1995; Li et al., 1995). XPA has a preference for binding to damaged DNA and will bind ERCC1-XPF and TFIIH (Asahina et al., 1994; Li et al., 1994; Saijo et al., 1996). The affinity of XPA binding correlates with the extent of helical distortion. It is unclear whether XPA or XPC bind first during NER, Sugawasa reported that XPC probably acts before XPA, however order of addition experiments do not support the idea that XPC acts first (Sugasawa et al., 1998; Wakasugi and Sancar, 1999). The DNA damage recognition and protein interaction properties of XPA seem to indicate that it acts as a nucleation factor with XPC.

RPA binds specifically to ssDNA and stabilises it, preventing the formation of secondary structures (Wold, 1997). RPA is a trimer of p70, p34 and p11, is essential for DNA replication, repair synthesis and the dual incision of NER, and is involved in recombination (He et al., 1995; Raderschall et al., 1999). RPA shows some preferential binding to damaged DNA and is phosphorylated at the G1/S boundary and upon DNA damage (Clugston et al., 1992; Li et al., 1995). RPA interacts with XPA, XPG, ERCC1-XPF and XPC (Bessho et al., 1997; He et al., 1995; de Laat et al., 1998; Li et al., 1995; Saijo et al., 1996). RPA is involved in orientating ERCC1-XPF and XPG in the excinuclease (de Laat et al., 1998).

PCNA is a polymerase clamp that increases the processivity of DNA pol δ and ε, and is loaded onto the template primer by RFC, an ATPase, that also loads DNA polymerases (Tsurimoto, 1999). PCNA is essential for DNA replication in mammals. PCNA seems to function as a central factor in DNA synthesis, it interacts with DNA pol δ, DNA ligase I, p21 and FEN1 (Tsurimoto, 1999). PCNA mutants in *S. cerevisiae* and *S. pombe* have increased sensitivity to DNA damage (Ayyagari et al., 1995). PCNA accumulates in actively repairing nuclei after UV irradiation and is required for *in vitro* NER, BER and MMR (Matsumoto et al., 1994; Nichols and Sancar, 1992; Umar et al., 1996).

XPB and XPD are DNA dependent ATPases and helicases that can disassociate short DNA fragments annealed to ssDNA. XPB (3'-5' helicase) and XPD (5'-3' helicase) are found in the protein complex TFIIH, which is a 9 subunit multimer involved in transcription by RNA polymerase II (Frit et al., 1999). TFIIH helicase activity is absolutely required for unwinding of DNA at lesions. TFIIH is also required where pre-unwound constructs are provided for NER, implying an additional, at least structural role. XPA and XPC-HHR23B can recruit TFIIH to damaged DNA. The ATP hydrolysis activity of TFIIH is enhanced by the presence of damaged DNA, XPA and XPC-HHR23B (Winkler et al, 2001). Perhaps XPC-HHR23B and XPA activate TFIIH by tethering it to damaged DNA or by activating TFIIH by some conformational change. Interestingly, TFIIH inhibits the action of ERCC1-XPF and XPG on artificial NER substrates and this inhibition is reversible by the addition of

ATP (Winkler et al., 2001). TFIIH probably forms a complex on the DNA and sterically inhibits ERCC1-XPF and XPG. Perhaps TFIIH inhibits incision prior to full opening of the helix in NER.

XPG has ssDNA specific endonuclease activity and is a dsDNA specific exonuclease. XPG will cleave ssDNA at a ds-ss DNA junction with a 5' ssDNA tail and requires 5 to 10 unpaired nucleotides for efficient cutting (Evans et al., 1997). XPG cleaves to the 3' side of the damage in NER (Evans et al., 1997; Matsunaga et al., 1995; O'Donavan et al., 1994). XPG performs a structural role by loosely binding TFIIH and RPA. XPG is a member of the FEN1 family of structure specific endonucleases which all act on similar but different substrates (Harrington and Lieber, 1994; O'Donavan et al., 1994). FEN1 family members have preferences for specific substrates. FEN1 will cut flaps but doesn't cleave bubbles or substrates with closed loops (Harringtone and Lieber, 1994). XPG will cleave stem loop and bubble substrates as well as flaps and splayed arms, but cannot substitute for FEN1 in BER (Evans et al., 1997; Klungland and Lindahl, 1997). XPG has a conserved PCNA interaction domain (Gary et al., 1997). The PCNA interaction domain is essential for XPG activity, perhaps PCNA helps to link the incisional and replication steps of NER. Patients with severe truncation mutations of XPG show a combined CS/XPG phenotype whereas XPG patients with missense mutations show only the XP phenotype (Nouspikel et al., 1997). This implicates XPG in TCR. *In vitro*, XPG protein even if inactivated by mutation has a stimulatory effect on transcription coupled repair of thymine glycol by NTH, the human DNA glycosylase involved in BER (Bessho, 1999; Cooper et al., 1997; Klungland et al., 1999). XPG is also involved in removal of thymine glycol and 8-oxoguanine adducts in untranscribed DNA.

ERCC1-XPF is an endonuclease complex, specific for ssDNA, that cuts 5' of the damage in NER (van Duin et al., 1986). *In vivo*, ERCC1 (33 kDa) is found in a tight complex with XPF (120 kDa) (de Laat et al., 1998; Sijbers et al., 1996). The binding between the two is so strong that cell free extracts from XPF def. cells and ERCC1 def. cells will not cross complement, indicating that there is no exchange between

protein bound in the dimer and free protein (Biggerstaff et al., 1993). C-terminal amino acids from 224 to 297 of ERCC1 are involved in binding XPF and conversely C-terminal amino acids 814 to 905 in XPF directly interact with the XPF region in ERCC1 (de Laat et, 1998; McCutchen-Maloney et al., 1999). One of the known XPF patients was shown to have a mutation in the putative ERCC1 binding region and displayed reduced levels of the ERCC1- XPF complex, supporting this model (de Laat et al., 1998). XPF mutant cells have a mild DNA repair deficiency and reduced levels of XPF and ERCC1 (Matsumura et al., 1998). The reduction in ERCC1 levels indicates how strong the interaction is between ERCC1 and XPF and the extent to which complex formation is required for protein stability. In fact, both free ERCC1 and XPF are very quickly degraded (Sijbers et al., 1996). Protein sequence comparison revealed similarity between the conserved C-terminal region of ERCC1 and the C-terminal region of XPF, including the regions necessary for the ERCC1-XPF interaction, implying that ERCC1 and XPF are related via an ancient duplication (Gaillard and Wood, 2001).

It is still unsure which of the proteins, ERCC1 or XPF actually contribute the nuclease activity, although it seems likely that it is XPF, which has an intrinsic endonuclease activity (McCutchen-Maloney et al., 1999). XPF has a region related to a helicase family, this region has many conserved acidic residues and may be a nuclease domain (Aravind et al., 1999; Sgouros et al., 1999). XPF is not a helicase but ERCC1-XPF shares the characteristics of helicases to bind with a specific polarity at junctions between ss and dsDNA.

In vitro, ERCC1-XPF will cleave one strand of dsDNA at the 5' side of a junction with ssDNA in the form of splayed arm, flap or bubble (Bessho et al., 1997; de Laat et al., 1998). The ssDNA arms protruding in the 3' direction were efficently removed from splayed arm and flap substrates. The cleavage varies from 2 to 8 nucleotides away from the junction. ERCC1-XPF will cleave synthetic structures *in vitro* to remove 3' ssDNA overhangs, and will cut 5' ssDNA overhang structures, but these incisions only lengthen the overhang rather than removing it (de Laat et al., 1998). This action suggests that in NER, ERCC1-XPF cuts the damaged strand at

the 5' end of the bubble of deannealed DNA that contains the damaged nucleotide. ERCC1-XPF will cleave at stem loop DNA junctions without the assistance of other proteins, which shows its specific intrinsic endonuclease activity.

All excision repair mutants are sensitive to DNA interstrand cross linking agents, e.g.MMC, but ERCC1 and XPF are hypersensitive. This has led to the belief that the ERCC1-XPF complex is involved with recombinational processes that could be involved in the repair of crosslinks.

ERCC1 has 35% homology over 110 amino acids at its C terminus with an *S. cerevisiae* protein called RAD10 and 56% homology over 25 amino acids at the centre of the 35% homologous region (van Duin et al., 1986). ERCC1 also has 60 extra C-terminal amino acids which are not in RAD10 and are 38% homologous to the C-terminal of UVRC, an *E coli* DNA repair protein (van Duin et al., 1988). The homologous regions form a helix-loop-helix DNA binding region in RAD10, this maybe just a common DNA binding motif or perhaps a common region for an endonuclease mechanism as well. RAD10 def. extracts have the same early incision defect as ERCC1 def. extract. RAD10 also binds very stably to a protein called RAD1 just as ERCC1 binds to XPF, although the XPF binding region of ERCC1 lies outside the region of homology with RAD10. Rad1-Rad10 has the same structural preferences as an endonuclease as ERCC1-XPF, and although RAD1 possesses the endonuclease activity it is not efficient without RAD10 (Bardwell et al., 1994; Davies et al., 1995; Habraken et al., 1994). ERCC1 is not inducible on UV irradiation of cells and this corresponds with work in yeast that shows that RAD 10, like RAD1 and RAD3 but not RAD2, is not inducible (van Duin et al., 1987). This implies that ERCC1 and RAD10 are largely equivalent in structure and function. RAD10-RAD1 is involved in the removal of non-homologous tails from invading single strands during recombination, suggesting that ERCC1-XPF may play a similar role.

ERCC1 will complement the SWI10 mutant of *S. pombe* (Rodel et al., 1997). This SWI10 mutant has a pleiotropic effect: it reduces the frequency of mating type

switching and causes increased UV radiation sensitivity (Schmidt et al., 1989). Full length ERCC1 will only complement the transposition defect, a C-terminal truncated version is needed to restore the DNA repair capacity as well. In fact, only the truncated version of ERCC1 can interact with spRAD16 (the *S. pombe* homologue of XPF) (Rodel et al., 1997).

ERCC1 and XPF homologues are known in plants (Gallego et al., 2000; Liu et al., 2000; Xu et al., 1998). The lily ERCC1 homologue will significantly correct the mitomycin C sensitivity in ERCC1 def. mammalian cells and expression is high in male generative cells in pollen but not elsewhere.

ERCC1-XPF may possibly be involved in the immunoglobulin heavy chain class switch recombination pathway (CSR), which mediates isotype switching during B cell development (Tian and Alt, 2000). CSR controls switching from IgM to other immunoglobulin types e.g. IgG. The variable region is upstream of a line of different Ig constant region sections. CSR occurs between switch regions before each Ig heavy chain constant region gene and is known to be dependent on transcription. *In vitro* transcription of switch regions in a physiological orientation seems to induce formation of stable R loops. An R loop is formed when a short RNA strand hybridises with the template strand and the non template strand exists as a single stranded loop, this is similar to the NER substrate after helicase action. ERCC1-XPF and XPG can cleave these loops either to create a DSB or SSBs that can be converted to DSBs by replication. This suggests that the NER nucleases may initiate CSR in a transcription dependent manner.

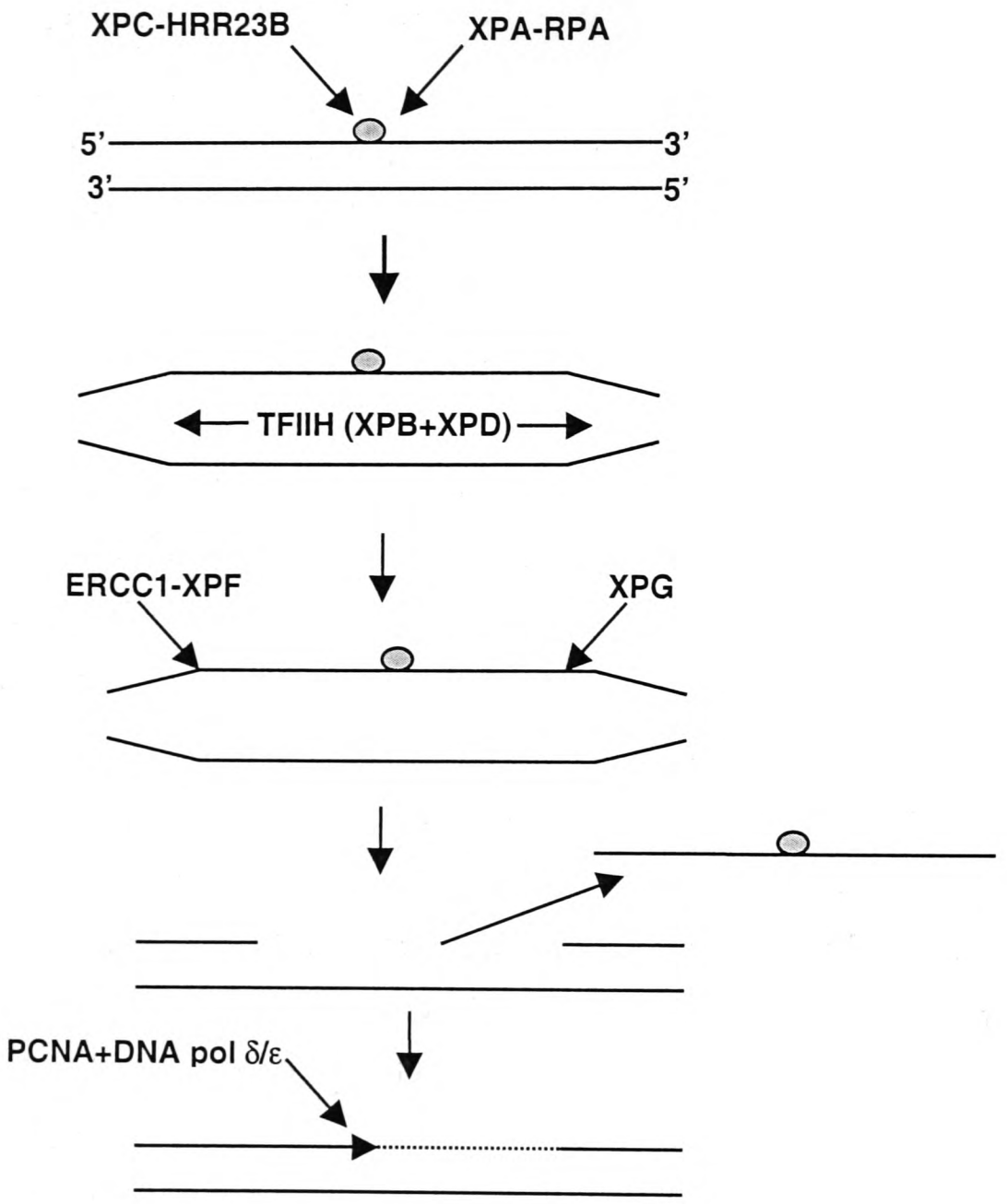

Figure 1.1 Nucleotide Excision Repair. XPC-HRR23B and XPA-RPA are involved in lesion recognition. TFIIH melts the helix around the lesion and ERCC1-XPF and XPG make the 5' and 3' incisions respectively. The oligomer containing the lesion is then removed and new DNA synthesised.

XPE and CS proteins are not required for *in vitro* NER but are required *in vivo*. XPE cells lack the UV-DDB (damage-specific DNA binding activity) which is a hetero dimer composed of the p125 and p48 proteins (Tang et al., 2000). The damage inducible p48 gene is required for the efficient GGR of CPD (Hwang et al., 1999). Here lies one important difference between rodent cells and humans. Cultured wildtype (wt) rodent cells are deficient in the GGR of CPD and lack expression of the p48 protein (Tang et al., 2000). Perhaps because of their short life spans rodents are not as concerned with the buildup of damage that does not affect transcription. Curiously, expression of human p48 protein in rodent cells results in effective GGR of CPD (Tang et al., 2000). p53 expression is required for the efficient GGR of CPDs, but is not required for TCR of CPDs and p53 regulation of NER is exerted by p48 (Hwang et al., 1999). UV-DDB recognises, with high specificity, DNA damage caused by a variety of agents (Payne and Chu, 1994). UV-DDB appears to have little or no role in naked DNA reconstitutions (Abbousekhra et al., 1995). However as XPE cells do suffer from decreased NER presumably it has some role in vivo, perhaps when the damage is presented in a chromatin context. UV-DDB may facilitate recognition of poorly recognised lesions such as CPD. Cultured CS cells are defective in TCR of CPD and thymine glycols (Cooper et al., 1997; Venema et al., 1990). CSA and CSB cells are UV sensitive and incapable of recovering RNA synthesis after inhibition by UV. They do not exhibit strand specificity for CPD repair but do repair DNA as evidenced by UV-induced DNA repair synthesis, they seem to be defective in TCR alone. It is unsure whether the TCR defective phenotype of CS cells is caused by a defect in repair or by a defect in the reinitation or perhaps initiation of transcription, as TCR is so closely coupled to transcription that a defect in transcription might stall repair entirely (Brosh et al, 1999; van Oosterwijk et al., 1996; van Oosterwijk et al., 1998).

Further investigation of *in vitro* reconstitution reactions has revealed the order of reaction and the various roles of the proteins (Evans et al., 1997; Sugasawa et al., 2001) (Figure 1.1). First either XPA-RPA or XPC binds the damage site, XPA then recruits TFIIH to give the preincision complex (this step is dependent on ATP hydrolysis). XPC or XPA-RPA help to stabilise this complex and XPG is recruited

by TFIIH to perform the incision 3' of the damage. ERCC1-XPF is recruited by XPA to incise 5' of the damage site (Saijo et al., 1996). This dual incision reaction is absolutely dependent on ATP hydrolysis and gives fragments of 24 to 32 nucleotides long but mainly of 27 to 29 nucleotides long. The fact that this size strongly correlates to the length of the optimal ssDNA binding region of RPA (30nt) suggests that RPA plays a role in positioning incisions (Kim et al., 1992). The excinuclease, as the dual excision activities are known collectively, cuts at one of the 3rd to the 5th phosphodiester bonds 3' to the damage and at one of the 21st to the 25th phosphodiester bonds 5' to the damage. Repair synthesis is PCNA dependent, and therefore must use DNA pols δ and/or ε. Antibodies raised against DNA polymerase δ inhibit repair synthesis and in reconstitution experiments DNA pol ε performed repair synthesis, indicating that both DNA polymerase delta and ε are used (Evans et al., 1997).

Although NER is the main system for the repair of UV damage there is no evidence to suggest that the levels of the NER proteins are elevated following UV irradiation (van Duin et al., 1987). However the levels of NER activity seem to be inducible after a priming dose of UV and cell extracts from UV treated cells better support NER *in vitro* (Francis and Rainbow, 1999). Host cell reactivation of reporter constructs is reduced in unstressed cells, however it is stimulated in cells subject to UV or heat shock, this indicates that blockage of transcription on the reporter is alone not enough to induce TCR, in fact p53 is required for the stimulation (McKay et al., 1997).

Damage Recognition

The exact damage recognition mechanism in NER is currently unknown (Kusumoto et al., 2001; Wood, 1999; Batty and Wood, 2000). The more a lesion distorts the DNA helix the more efficiently it is recognised and the repair rate is greater (Wood, 1999). 6-4PPs distort DNA more than CPDs and are removed from the bulk genome 5-10 times faster (Mitchell and Nairn, 1989). For effective recognition a lesion must cause distortion of DNA structure and modification of DNA chemistry (Hess et al.,

1997). CPDs are a weak NER substrate but non-complementary bases opposite the lesion increase repair efficiency (Mu et al., 1997). A 1,3 GTG cisplatin intrastrand crosslink is more distorting than a 1,2 GG crosslink and is repaired more efficiently (Bellon et al., 1991). A non-complementary base opposite the 1,2GG crosslink improves repair efficiency (Moggs et al., 1997). Distortion alone does not produce a good NER response as DNA mismatches and small loops are repaired poorly (Hess et al., 1997; Hess et al., 1997; Moggs et al., 1997; Mu et al., 1997).

The NER complex probably assembles on the damage. An ERCC1-GFP fusion protein, that will correct the NER deficiency in ERCC1 deficient cells, moves freely through the nucleus at a rate consistent with the size of ERCC1-XPF, similar results were reported in the same paper for XPA and TFIIH (Houtsmuller et al., 1999). UV treatment of cells caused a temporary immobilisation. This indicates that ERCC1-XPF, XPA and TFIIH are not part of an NER holocomplex and do not take part in processive scanning. Other evidence suggests that there may be a sub-holocomplex, based around TFIIH (Svejstrup et al., 1995). In yeast the NER repair complex seems to be assembled sequentially (Guzder et al., 1996).

Global Genome Repair and Transcription Coupled Repair

There are two pathways within NER, Global Genome Repair and Transcription Coupled Repair (Friedberg, 1996; Tornaletti and Hanawalt, 1999). Although the mechanism of GGR is relatively well understood from the *in vitro* reconstitution, that of TCR is not, and there is no *in vitro* reconstitution of TCR. However, TCR and GGR almost certainly follow a common mechanism following recognition of the lesion. As the names imply, GGR works indiscriminately over the whole genome at a relatively low rate while TCR is specifically coupled with transcription to repair lesions that would otherwise block the progress of RNA polymerases. TCR repairs the untranscribed strand at a higher rate than GGR and the transcribed strand at an even higher rate (Mellon et al., 1987). TCR seems to function to repair lesions that are poorly recognised by GGR, for example, CPD lesions are poorly repaired by GGR and tend to be repaired by TCR (Mullenders et al., 1993; van Hoffen et al., 1995).

Some oxidative damage that is thought to be primarily repaired by BER rather than NER has been shown to be subject to TCR (Le Page et al., 2000). Perhaps the TCR reaction can involve more than just NER. MMR proteins have been found to participate in TCR (Leadon and Avrutskaya, 1997). TCR of UV induced lesions requires MMR proteins in human cells, but not in yeast, and removal of thymine glycols by TCR requires MMR proteins in both (Leadon and Avrutskaya, 1997; Leadon and Avrutskaya, 1998). NER proficient cell free extracts remove 8 oxoG and thymine glycol lesions, as 26nt long oligomers and the rate of removal is similar to that for CPDs (Reardon et al., 1997). However, TCR of thymine glycol depends on XPG but not on XPA or XPF and does not require the nuclease function of XPG. Certain XPG mutations that completely abolish CPD excision repair do not affect the rate of thymine glycol repair and null XPG mutations abolish repair of CPDs and TCR of glycols (Cooper et al., 1997).

How does TCR recognise lesions? Is it by simple polymerase stalling? In this case sequence dependent stall sites may trigger the futile repair of undamaged DNA in TCR. When a polymerase stalls at a lesion, it blocks the access of repair enzymes to the lesion, so there must be some mechanism for the polymerase to either backup or disengage from the DNA.

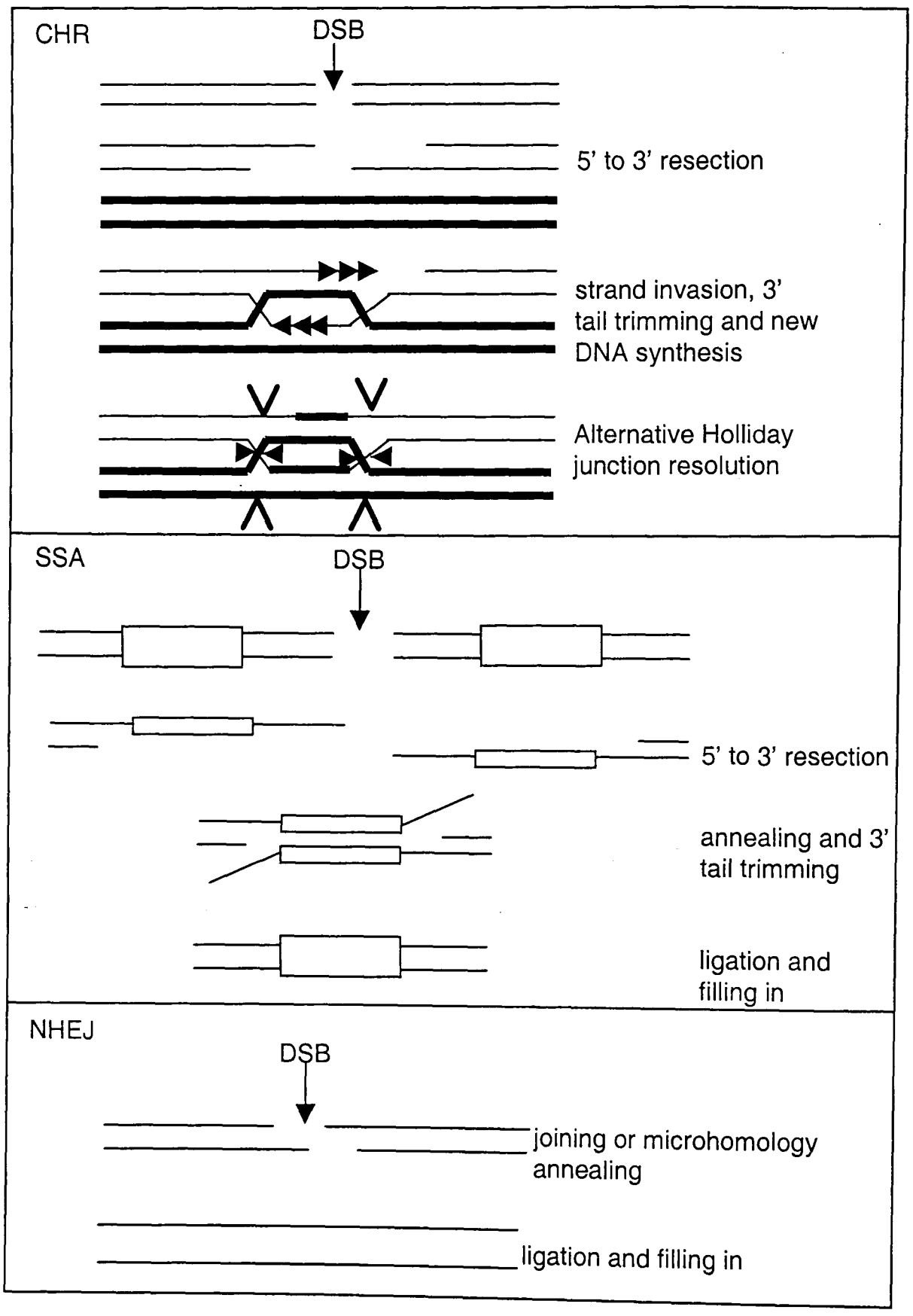

Figure 1.2 Mechanisms for Double Strand Break Repair. Classical Homologous Recombination (CHR), Single Strand Annealing (SSA) and Non-Homologous End Joining (NHEJ). During CHR (Paques and Haber, 1999), DSB formation is followed by 5' to 3' resection, strand invasion, Holliday junction formation and alternative resolution. During SSA, resection is followed by annealing of homologous regions and 3' tail trimming. During NHEJ, ends are not resected to a great extent and joining uses only short stretches of microhomology.

Double Strand Break Repair

Double strand breaks are a potentially lethal form of DNA damage as, if unrepaired, a single DSB can kill a cell. If undetected, a DSB at mitosis will lead to loss of the part of the divided chromosome without a centromere.

DSBs can be formed in a variety of ways: free radicals, IR, mechanistic stress, by endonuclease action and by the actions of replication and subsequent processing on certain types of DNA damage. They are also formed physiologically by the cell in such events as V(D)J recombination and meiotic recombination or in yeast during mating type switching.

In bacterial systems it is known that replication arrest often leads to DSB formation, a primary function of the DSB repair system in bacteria may be to rescue blocked replication forks (Kuzminov, 1995). There is much indirect evidence in yeast that replication arrest also leads to DSBs. It is well known that DSBs stimulate recombination, in fact DSBs are the sole instigators of recombination in meiotic cells and a major factor in mitotic cells (Godwin et al., 1994). Various results imply that inhibition of DNA replication induces recombination, with an assumed intermediate of DSBs (Arnaudeau et al., 2000; Bierne and Michel, 1994; Galli and Schiestl, 1996; Galli and Schiestl, 1998; Michel, 2000). There is also some direct evidence that inhibition of DNA replication leads to DSBs. The methylating agent methylmethane sulphonate generates single stranded DNA lesions *in vivo* that block DNA replication resulting indirectly in the formation of DSBs and stimulation of recombination (Chlebowicz et al., 1979; Schwartz, 1989). DNA sequences associated with unusual structures or with inhibition of DNA replication have been identified as sites of DSBs *in vivo* (Gordenin and Resnick, 1998).

The cell has evolved various mechanisms to repair DSBs, these can be divided into two sorts (Karran, 2000) (Figure 1.2). Classical homologous recombination (CHR) relies on a homologous chromosome, ideally the identical sister chromatid after DNA replication, and often results in error-free repair. Non-homologous end joining

(NHEJ) and single strand annealing (SSA) however involve the processing of DSBs so that they can be rejoined without the use of an intact homologous region, this often results in information loss.

Repair of DSBs in *S. cerevisiae* is highly accurate and is predominantly dependent on homologous recombination. In contrast, DSB repair in mammals during most of the cell cycle is accomplished primarily by NHEJ (Critchlow and Jackson, 1998; Jeggo, 1998). Cultured mammalian cells mutant in NHEJ genes (KU70, KU80, LIG4 or XRCC4) are moderately sensitive to IR whereas their yeast equivalents are resistant. Although *S. cerevisiae* and mammals use classical homologous recombination and NHEJ to different extents the mechanisms are similar between species (Takata et al., 1998). The repair of DSBs by homologous recombination is down regulated during the G_0, G1 and early S phases of the cell cycle implying that NHEJ and SSA are the predominant mechanism in this period (Takata et al., 1998). In G1 mammalian cells interchromosomal homologous recombination is exceedingly rare even after a DSB is introduced (Benjamin and Little, 1992; Godwin et al., 1994). In the rest of the cell cycle homologous recombinational repair of a break could occur by using the sister chromatid as the intact template.

In NHEJ and SSA the two broken ends are modified to make them compatible for rejoining and information between the two DNA ends is lost. Why rely on these imperfect repair processes? Mammalian genomes, unlike yeast, have a large amount of repetitive DNA. This makes homology search for repair of DSBs by homologous recombination difficult, except during late S, G2 and M, when a sister chromatid is physically positioned optimally. Otherwise homology partners for repetitive regions might be chosen inappropriately from any of the chromosomes. A homologous crossover event arising during DSB repair could result in a chromosome translocation. A mutation in a tumour supressor gene might gene-convert the good allele on the homologous chromosome if homologous recombination were in heavy use throughout the cell cycle (Liang et al., 1998). By restricting homologous recombination primarily to late S, G2 and M, a DSB arising in one chromatid can rely on the identical sister chromatid for repair without the risk of receiving a

different copy. Large regions of repetitive DNA may also provide an increased tolerance for small errors generated during repair by NHEJ.

Non-Homologous End Joining

During NHEJ the two broken DNA ends are directly joined with no overlap, or with minimal overlap and the use of short fortuitous homologies near the two ends (Jeggo, 1998; Lewis and Resnick, 2000; Lieber, 1999; Muller et al., 1999). Thus the term nonhomologous refers to the absence of extended segments of homologies between the two recombined DNA molecules. When DSBs occur in DNA, the biochemical configuration of the broken ends can be very diverse and putting the two ends back together cannot usually be achieved by a simple ligation step, processing is required. The specific proteins that are essential for NHEJ *in vivo* remain to be established, but accurate efficient endjoining in an *in vitro* assay using human cell extracts requires KU70 and KU80, DNA dependent protein kinase and is dependent on the presence of DNA ligase IV and XRCC4 (Baumann and West, 1998). DNA PK, KU70 and KU80 are involved in the recognition and binding of DSB ends. There is a propensity for the joining of the two broken DNA ends to occur at microhomology between the nucleotides proximal to the break , however microhomology is not essential for joining (Roth and Wilson, 1986). NHEJ commonly causes small deletions that extend in both directions from the break site. Such deletions typically end in a region of microhomology. When the two DNA ends do undergo alignment at points of microhomology, then there is often either excess DNA beyond the point of alignment that must be removed by nucleases or there are gaps that must be filled using polymerases. Some of these excess single stranded regions require 5' nucleases, possibly FEN1 and EXO1, and others require 3' nucleases, possibly MRE11 (Lieber, 1999; Wu et al., 1999).

Classical Homologous Recombination

Extensions of the classical homologous recombination DSB repair model have been made from bacteria to yeast to mammals (Haber, 2000; Haber, 2000; Thacker, 1999; Thompson and Schild, 1999). A DSB is first processed by the digestion of a substantial portion of the DNA strands containing the 5' ends of the break. This results in 3' ssDNA tails that can be as long as 1 kb or more. These tails are utilised

for the nucleation of a number of recombination factors that give a nucleoprotein complex that has the ability to conduct a DNA homology search. This could use either a sister chromatid or a homologous chromosome. Invasion of the homolog by the 3' tails in homologous DNA pairing and strand exchange yields a joint. The 3'ends of invading DNA act as primers for the initiation of new DNA synthesis. This process leads to the formation of two Holliday junctions, four-stranded branched structures whose alternative resolution allows formation of crossover products and completion of DSB repair. The exact mechanism of DSB end processing during classical homologous recombination is unknown but much evidence implicates the RAD50-MRE11-(NBS1/XRS2) complex (Dolganov et al., 1996; Karran, 2000).

RAD51, RAD52, RAD54, RAD55, RAD57, RDH54 and RPA are all involved in the utilisation of recombinogenic ssDNA substrates for the formation of heteroduplex DNA (Paques and Haber, 1999; Sung et al., 2000). Rad51 is at the core of CHR, it is homologous to the *E. coli* general recombinase RecA (Paques and Haber, 1999). RAD51 exhibits a homologous DNA pairing, joint formation and strand exchange activity that yields joints between two DNA molecules. In the presence of ATP, RAD51 assembles into a nucleoprotein filament on both ssDNA and dsDNA that is almost identical to the equivalent RECA filament. RAD51 is essential in mammals (Tsuzuki et al., 1996). 5 RAD51 homologues have been identified in human cells, RAD51B, RAD51C, RAD51D, XRCC2 and XRCC3 (Jones et al., 1995; Shinohara and Ogawa, 1999; Tambini et al., 1997; Tebbs et al., 1995; Thacker, 1999). These homologues may form complexes with one another and function to enhance RAD51-ssDNA filament assembly, they may all be required simultaneously for efficient recombination or may play specific recombination roles in different circumstances. *In vivo*, ssDNA filament assembly is stimulated by heterotrimeric ssDNA binding factor RPA, but an excess of RPA inhibits filament assembly. This inhibition is probably due to competition with RAD51 for binding sites on the ssDNA. RAD52 and RAD55-RAD57 help overcome this competition and mediate a productive relationship between RAD51 and RPA. RPA probably removes secondary structure in the ssDNA. RAD52 binds DNA as a ring shaped multimer, with higher affinity

for ssDNA than dsDNA. RAD52 binds specifically to DNA ends. RAD52 forms a stable stoichiometric and coimmunoprecipitable complex with RAD51, and interacts with RPA in solution and when RPA is bound to DNA. Genetic evidence indicates that RAD52 also functions in at least two other recombination pathways, Single Strand Annealing and Break Induced Recombination. Null mutations in RAD52 essentially eliminate all recombination in yeast, probably due to cumulative defects in different pathways.

RAD54 belongs to the SWI2/SNF2 protein family, involved in transcription, NER and post-replicative repair (Paques and Haber, 1999). RAD54 has a DNA dependent ATPase activity and interacts with RAD51. *In vitro*, RAD54 strongly stimulates the homologous pairing rate. The first DNA intermediate predicted in the DNA DSB repair recombination model is a D-loop structure formed between the initiating ssDNA tail and the DNA homolog. RAD51 is incapable of mediating formation of this loop *in vitro* without RAD54. RAD54 null chicken cells and mice are viable although X ray sensitive.

Alignment of the two recombining molecules is established through a series of transient joints called paranemic joints. It has been argued that this involves a DNA triplex structure held together by non-Watson-Crick bonding, or perhaps by DNA strand switching. The paranemic joints are believed to be an important intermediate that serves to capture the duplex and bring the two recombining DNA molecules into homologous registry (Paques and Haber, 1999). A more stable plectonomic joint is formed when a free DNA end is present in either the ssDNA or the dsDNA to allow for intertwining of the ssDNA strand with the complementary strand in the duplex partner. In branch migration the length of the plectonomic joint is extended. In the case of the RAD51 filament, branch migration proceeds 3'to 5' with respect to the initiating single strand, however results have suggested that migration can also proceed in the other direction. Once a stable joint is formed branch migration extends the length of the joint, resulting in the formation of a substantial amount of heteroduplex DNA. The resolvases that process Holliday junctions and other DNA intermediates in nuclear chromosomal recombination have not been identified.

There are also several putative pathways separate from CHR, these are break induced replication (BIR) and synthesis dependent strand annealing (SDSA) (not to be confused with Single Strand Annealing) (Flores-Rozas and Kolodner, 2000; Paques and Haber, 1999). BIR was discovered from very long gene conversion tracts that extended over 400kb. It is a RAD52-dependent, RAD51-independent replication driven recombination process. An initial, unstable, short DNA joint strand invasion event in a small region of perfect homology is extended by DNA replication, thus bypassing the formation of mismatched heteroduplex DNA caused by more extensive strand assimilation, that is seen in CHR. The final result of BIR is conservative DNA synthesis, where the recipient chromosome has both strands newly synthesised. SDSA accounts for the many mitotic gene conversions that are infrequently associated with crossing over. The newly synthesised DNA strands are displaced from the template and returned to the broken molecule, allowing the two newly synthesised strands to anneal to each other.

While meiotic recombination mainly involves chromosomal homologs, it is thought that most recombination events during mitotic growth occur in the late S and G2 phases and involve the sister chromatids (Paques and Haber, 1999). However in yeast there is capacity to carry out allelic (interchromosomal) recombination during mitotic growth and allelic recombinations seems to have a somewhat different genetic requirement than sister chromatid based recombination. Mutations in genes such as RAD50, MRE11 and NBS1/XRS2 that are believed to mediate sister chromatid based recombination could lead to higher levels of recombination between homologs. It has been suggested that when sister chromatid based recombination is inactivated the recombinogenic DNA substrates are channelled more often into interchromosomal recombination pathways. When the recombining DNA encompass different alleles of the same gene, then DNA mismatches will form giving heteroduplex DNA. Correction of the DNA mismatches results in the conversion on one of the recombining alleles. Gene conversion is defined as a nonreciprocal transfer of genetic information from one molecule to its homologue.

RAD1-RAD10 and MSH2-MSH3 are necessary for removal of non-homologous 3' tails during CHR repair of DSBs, but are not necessary where there are no non-homologous tails (Alani et al., 1997; Bardwell et al., 1994; Evans et al., 2000; Fishman-Lobell and Haber, 1992; Habraken et al., 1994; Ivanov and Haber, 1995; Marsischky et al., 1999; Nicholson et al., 2000; Saffran et al., 1994; Sugawara et al., 1997). When the resected tails invade a homologous donor sequence, RAD1-RAD10 (but not other NER genes), and MSH2 and MSH3, are required to cleave away non-homologous sequences at the 3' end of the tails before they can act as primers for DNA synthesis. SRS2 and RAD59 are also required for efficient removal of non-homologous ends in gene conversion (Paques and Haber, 1997; Sugawara et al., 2000).

A mutation has been found in *D. Melanogaster* in the MEI9 gene, an XPF homologue, that affects meiotic and mitotic recombination (Sekelsky et al., 1995; Sekelsky et al., 2000). This mutation leads to increased chromosomal instability, increased post meiotic segregation and lowered meiotic recombination, all of which could be explained by the misprocessing of heteroduplex intermediates in homologous recombination. dmERCC1 has been identified and interacts physically with mei9 (Sekelsky et al., 2000).

Single Strand Annealing

Single strand annealing can occur when a DSB forms between flanking homologous regions (Haber and Leung, 1996; Lin et al., 1985; Paques and Haber, 1999). A 5' to 3' exonuclease resects the ends of the DSB until the two homologous regions are exposed, these can then anneal to each other. (It is also possible that one resected end could invade the other before it is resected, in "one-ended" recombination.) This produces an intermediate with two non-homologous 3' ended tails, which must be removed before DNA synthesis and ligation can take place to seal the break. SSA is dependent on RAD52 and RAD59 (Paques and Haber, 1999; Sugawara et al., 2000). RAD52 anneals complementary DNA strands *in vitro* and its activity in SSA is stimulated by RPA (Sugiyama et al., 1998). Rad59 binds ssDNA and anneals complementary DNA strands, however its activity does not appear to depend on RPA

(Petukhova et al., 1999). RPA probably acts to modulate SSA, similar to its role in CHR. RAD1-RAD10 will cut the 3' tails at the junction between the non-annealed and annealed DNA to remove the non-homologous DNA (Ivanov and Haber, 1995; Sugawara et al., 1997). MSH2-MSH3, but not other mismatch proteins are also required for the removal of the non-homologous tails (Ivanov and Haber, 1995; Sugawara et al., 1997). MSH2 and MSH3 probably stabilise the annealed DNA structure and target RAD1-RAD10 to ssDNA overhangs (Ivanov and Haber, 1995; Paques and Haber, 1999).

In CHR the requirement for MSH2-MSH3 is present despite the long homologous sequence. During CHR the invading strand can form only an unstable side-by-side paranemic joint with its homologous sequence before the DNA end is cut off, while during SSA two single strands of DNA can form stable plectonomic molecules when the homologous segments are long enough. As CHR intermediates are less stable than SSA intermediates, this implies a role for MSH2-MSH3 in stabilisation of the intermediate structures (Evans et al., 2000). Separation of function mutations for MSH2 will destroy its MMR function but do not affect the ability to participate in the removal of non-homologous tails (Studamire et al., 1999). MSH2 and MSH2-MSH6 will bind *in vitro* to Holliday junctions (Alani et al., 1997; Marsischky et al., 1999). The meiotic specific MSH4 and MSH5 have a role in promoting meiotic crosssovers, perhaps they also stabilise intermediate structures (Paques and Haber, 1999).

In SSA, it is possible that either MSH2-MSH3 recognises the mismatch, as it recognises small loops in mismatch repair, or that it stabilises the annealed region. This would allow RAD1-RAD10 to bind and cut at the junction between homologous and non-homologous sequence. The need for MSH2-MSH3 becomes less as the length of the homologous region increases, and it is not necessary when the region is longer than 1kb, implying that the requirement may be due to stabilisation (Sugawara et al., 1997). In effect, RAD1-RAD10 is acting on the same substrate as in NER, the junction between non-annealed and annealed DNA is analogous to the melted bubble formed around the lesion in NER.

For both HRR and SSA, RAD1-RAD10 and MSH2-MSH3 are only required for the removal of nonhomologous 3' tails when the ends are 30 nt long or longer, for shorter tails alternative pathways exist (Paques and Haber, 1997; Prado and Aquilera, 1995). One alternative can remove 3'ends up to 20bp and depends at least partly on the proofreading ability of DNA polymerase δ (Paques and Haber, 1997). Another pathway can remove a non-homologous end on one side of the DSB but only after the other end has initiated strand invasion.

SSA inevitably results in a deletion as one of the two homologous regions and the sequence between the regions is lost. In yeast, SSA is nearly 100% efficient when the homologous flanking regions are at least 400bp, but 5% of the cells can survive a DSB when repeats are only 60bp (Sugawara and Haber, 1992). Repair is efficient even if the repeats are separated by as much as 15 kb. SSA may explain deletions of DNA between dispersed repeated sequences such as Alu in human DNA. These deletions may be partially suppressed by the divergence of dispersed sequences, in yeast a 3% divergence between 205bp repeats reduces SSA by a factor of 5 (Sugawara et al., 1997). The rate of production of deletions depends on the distance between two repeats, suggesting an exonuclease must traverse the whole region (Fishman-Lobell and Haber, 1992). SSA is about 3 times more frequent than gene conversion suggesting that SSA is a major pathway (Fishman-Lobell and Haber, 1992). Gene conversion accompanied by crossing over could produce a deletion between direct repeats, this would give a circular reciprocal product that would be retained only if it contained an origin of replication. Both genetic and physical experiments have failed to detect this reciprocal product except in very low levels, suggesting that SSA is the predominant route by which direct repeat deletions are produced (Fishman-Lobell and Haber, 1992; Ray et al., 1988).

scMSH2 has been shown to interact physically with a number of NER proteins: RAD1, RAD10, RAD14 and RAD25 (Bertrand et al., 1998). In *S. pombe* the NER proteins RHP14, SWI10, RAD16 can repair mismatched bases in recombination intermediates (Fleck et al., 1999). MEI9, the *D. melanogaster* homologue of XPF, is

involved in the repair of mismatches in meiotic recombination intermediates (Sekelsky et al., 1995).

RAD1-RAD10 is required for mitotic but not meiotic recombination events (Schiestl and Prakash, 1990). RAD1-RAD10 is required for spontaneous and HO-endonuclease-induced recombination between directly repeated sequences, but other NER genes are not (Ivanov and Haber, 1995; Schiestl and Prakash, 1988). Mutations in RAD1 and RAD10 decrease the efficiency of homologous integration of linear DNA fragments and circular plasmids (Schiestl and Prakash, 1990; Schiestl and Prakash, 1988; Klein, 1988). RAD1 is required for mitotic recombination stimulated by RNA polymerase I or II dependent transcription (Zehfus et al., 1990).

Mammalian 3' Tail Removal

Various studies have investigated the role of ERCC1-XPF in recombination in mammalian cells. Although, unlike in yeast, ERCC1 deficiency does not alter the frequency of either extra chromosomal or chromosomal homologous recombination, it is involved in specialised recombination types (Adair et al., 2000; Melton et al., 1998; Sargent et al., 1997; Sargent et al., 2000). ERCC1 def. cells also have a 100 times higher mutation frequency and higher genome instability than wild type cells (Melton et al., 1998). Like RAD1-RAD10, ERCC1 is probably involved in the removal of 3' non-homologous tails in recombination in mammalian cells (Adair et al., 2000).

A targeted DSB flanked by nonhomologous DNA was used to induce recombination at a tandem APRT construct (Sargent et al., 2000). This results in a greater rate of formation of APRT deletions in ERCC1 wt than in ERCC1 null cells. Presumably deletion products were formed by SSA, which would require ERCC1-XPF to remove non-homologous 3' tails. Without DSB stimulation, there was a higher frequency of rearrangement formation in the ERCC1 def. cells, than in wt. This is the same result as in a study using a tandem APRT construct but with an insert predicted to lead to the formation of large heteroduplex loops during recombination (Sargent et al., 1997). The increased rearrangements seen in ERCC1 null cells in both studies indicate that these rearrangements are not formed by faulty processing of

heteroduplex loops but more probably by the failure of ERCC1 to process 3' non-homologous tails. For effective gap repair or integration it is presumed that non-homologous tails will need to be removed. No rearrangements were formed with only one copy of APRT.

When the APRT locus was targeted in CHO cells, with selection for positive APRT recombinants, vectors were used with either long or short terminal non-homologies on either side of a DSB within the APRT gene (Adair et al., 2000). The expectation derived from yeast was that long non-homologies at least would have a lower successful recombination rate than wt, however only a very small difference in rates was seen between ERCC1 def. and wt for both lengths of non-homology. In ERCC1 null cells with long terminal non-homologies there was an increased rate of aberrant insertion/deletion recombinants, this has been interpreted as being caused by recombination starting and then being unable to complete due to unprocessed non-homologous tails, which are then a substrate for unconventional recombination.

ERCC1-XPF is probably not involved in meiotic recombination. Although the levels of both XPF and ERCC1 transcript and protein are elevated in adult mouse testis this increase occurs after the peak of meiotic recombination (Selfridge et al., submitted and Shannon et al., 1999).

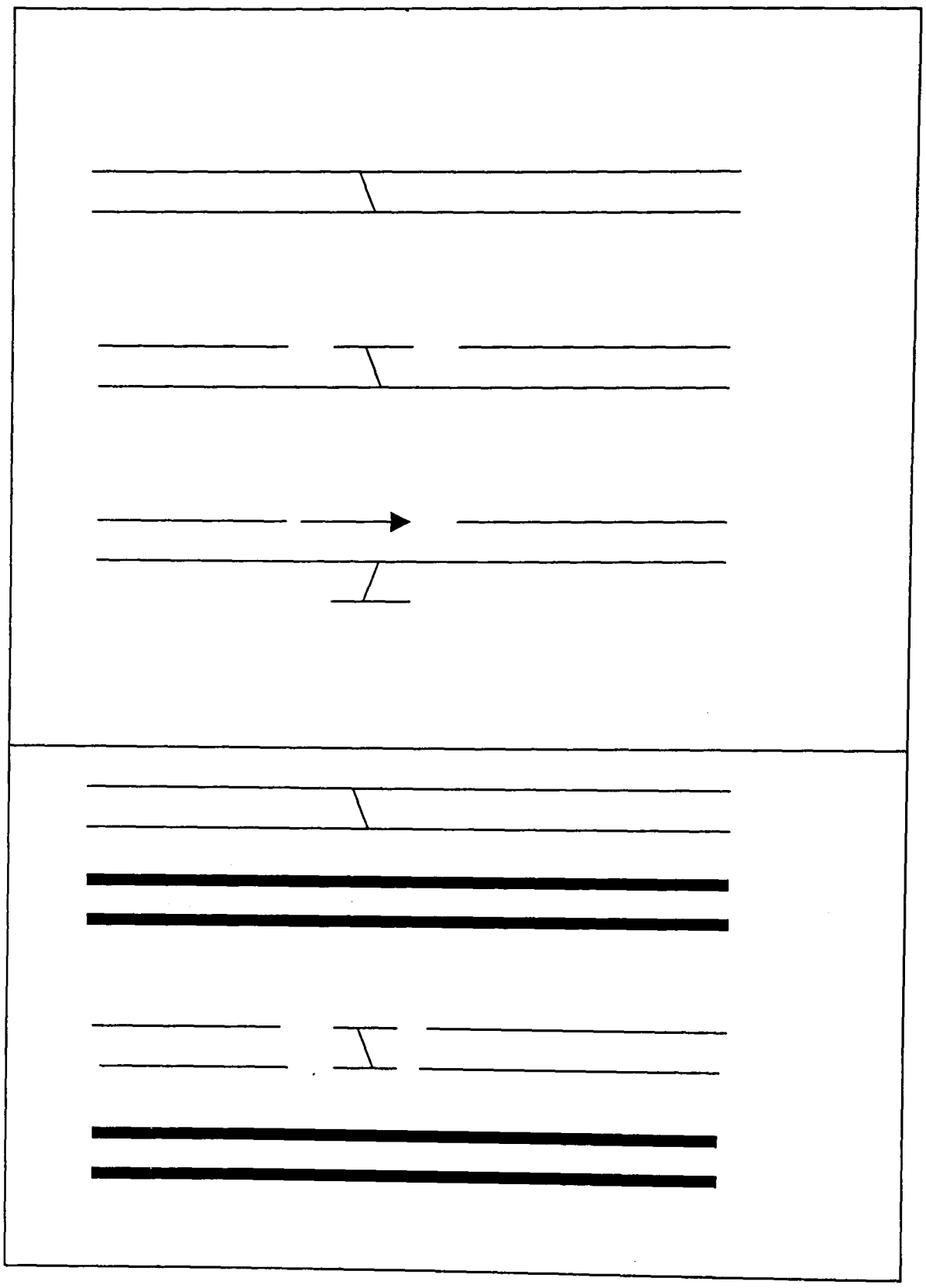

Figure 1.3 Models for the repair of DNA interstrand crosslinks. In the top model crosslinks are unlinked on one strand and a form of error prone translesion synthesis fills the gap to allow normal repair by NER. In the bottom model, the crosslink is unlinked by ERCC1-XPF, possibly forming a DSB and this serves as a substrate for recombination, involving XRCC2, XRCC3 and homologous undamaged DNA. These models are non-exclusive, the bottom mechanism probably only occurs during DNA synthesis, whereas the top mechanism may occur at any time.

Repair of Interstrand DNA Crosslinks

DNA interstrand crosslinks (ICL) require some form of recombination to effect error free repair, however the mechanism of repair is largely unknown. ICL can be caused by a variety of bifunctional agents, such as nitrous acid, nitrogen mustards, psoralen (a monofunctional agent which can be induced to form crosslinks with UV), cisplatin, mitomycin C and environmental furocoumarins. Most of these agents cause mainly non-crosslink damage such as adducts, and most of the crosslinks formed will be intrastrand. However the cell killing effects are through the highly toxic ICL. Just like DSBs, one unrepaired ICL is thought to be enough to kill a cell.

Two possible mechanisms of repair have been proposed. An error free recombinational mechanism begins with dual incision on one strand followed by strand transfer from the intact duplex with ligation and dual incision of the 2nd strand followed by the release of the crosslink and repair synthesis. The error-prone translesion synthesis mechanism involves dual incision on one strand followed by a DNA polymerase passing the lesion and creating a 3 stranded intermediate that is then repaired normally (Barre et al., 1999; Greenberg et al., 2001) (Figure 1.3).

In *E. coli*, the NER system makes a cut on either side of a crosslink on one DNA strand and initiates crosslink repair, then RecA mediated recombination replaces the removed portion and then the crosslink and oligomer can be removed by a final round of NER (Dye and Ahmad, 1995; Van Houten et al., 1986). In *S. cerevisiae*, ICL repair requires genes involved in NER and recombination, as well as additional genes (eg PSO2 and PSO3) not required for the repair of most other types of DNA damage. ICL repair in yeast, unlike that in *E. coli,* appears to involve a DSB intermediate (Dardalhon and Averbeck, 1995). A DSB is produced in an NER dependent manner and the repair then depends on the recombination proteins RAD51 and RAD52.

In mammalian systems, there is very little understanding of ICL repair. The repair of interstrand crosslinks requires ERCC1-XPF but probably not other NER genes, since

mammalian cells with mutations in other NER genes are only two to three fold sensitive to ICL (Hoy et al., 1985). Unlike other NER mutants, which are merely moderately sensitive, ERCC1 and XPF def. cells are hypersensitive to DNA ICL agents. However the exact role of ERCC1-XPF in the repair of these lesions is unknown. Either ERCC1-XPF alone or perhaps the NER system as a whole may be involved in the cleavage of ICLs (Bessho et al., 1997). ERCC1-XPF may also be involved in the downstream processing of ICLs. ERCC1 and XPF mutant cells are defective in a cell free co-incubation assay with one ICL containing and one undamaged plasmid, that stimulates DNA synthesis in both plasmids, however XPA, XPC and XPG mutants are proficient in this assay (Li et al., 1999).

The exact mechanism of ICL repair probably varies depending on the cell cycle status (Bridges and von Wright, 1981). In order to repair crosslinks without error, recombination with a sister chromatid must be used, and this is only possible in G2. ICL treatment tends to provoke a strong G2 arrest. Crosslinks are probably processed during replication, probably leading to some form of DSB. There may be a minor repair mechanism for ICLs that is not dependent on ERCC1, survival curves using ERCC1 null fibroblasts indicated an ICL resistant population, possibly active only at a certain cell cycle stage, and mouse ERCC1 mutants are more sensitive than hamster mutants to MMC indicating that there may be a subsiduary pathway operating in one but not the other (Melton et al., 1998; Weeda et al., 1997). In yeast incisions for ICL were comparable throughout the entire cell cycle (Meniel et al., 1997).

It seems unlikely that ICL repair in mammalian cells involves a typical DSB intermediate. NHEJ mutants have normal sensitivity to MMC and only weak sensitivity to other ICL agents, indicating that NHEJ is not involved in ICL repair (Caldecott and Jeggo, 1991).

Binding assays using MMC treated DNA and nuclear extracts detected two complexes in rodent cells and three in human cells that bound to ICL (Warren et al.,

1998). These complexes were missing or diminished in ERCC1 and XPA deficient cells, but were present in XPF, XPD and XPE deficient cells.

In vitro, reconstituted mammalian NER will make 2 incisions 5' to the crosslink and will remove a 22 to 28 nucleotide long undamaged strand (Bessho et al., 1997). This seems to be associated with a futile process of removal and resynthesis *in vitro*, however *in vivo*, the ssDNA region may serve as an entry point for a recombinational repair process (Mu et al., 2000). It is predictable that the NER system will recognise ICL, however to remove an oligomer that does not include the damage is unusual.

ERCC1-XPF will cut adjacent to ICL in a reaction distinct from NER and may possess the capability to initiate ICL repair (De Silva et al., 2000; Kuraoka et al., 2000). ERCC1-XPF alone will not cleave psoralen monoadducts and crosslinks in a duplex oligonucleotide. However, if a Y shaped construct is used with a crosslink at the junction between ssDNA and dsDNA, then ERCC1 will cut on the 3' ssDNA side of the crosslink and will also cut the same strand on the 5' side of the crosslink (Kuraoka et al., 2000). This has the effect of releasing one arm of the crosslink. Either recombination or some form of error prone DNA synthesis could then bypass the other arm of the crosslink. Or if ERCC1-XPF also acts on the other arm of the crosslink then a DSB would be formed which could then be repaired. As ERCC1-XPF will only cleave if one side of the crosslink is ssDNA, it seems likely that cleavage occurs as part of NER, however this may also occur at stalled replication or transcription bubbles.

Measurement of crosslink unhooking rates using comet assays show that ERCC1 and XPF mutants are extremely slow when compared to wt and other NER mutants (De Silva et al., 2000). The formation of DSBs has been studied using PFGE, this showed that DSBs are induced after ICL agent treatment but not with monoadducts. However, measurements of DSB formation using PFGE showed that all NER mutants induced DSBs at the same rate as wt, including ERCC1 and XPF. This suggests that ERCC1 may not after all be involved in the initial processing of ICLs to a DSB, or possibly that there are two routes to ICL repair, one not involving ERCC1-

XPF in early stages that involves DSB formation and another involving ERCC1 that does not involve DSB formation.

An alternative to the action of ERCC1-XPF or NER would be if a glycosylase activity could unhook the ICL (Bridges and von Wright, 1981).

Events downstream of the initial cleavage of ICL are also little understood. XRCC2 and XRCC3, RAD51 homologs, were cloned from hamster mutants that have high spontaneous chromosome instability and 60 fold greater than wt sensitivity to mitomycin C as well as a greater sensitivity to gamma rays, they are almost certainly involved in ICL repair (Cui et al., 1999; Liu et al., 1998). XRCC2 and XRCC3 mutants do not show defects in the repair of IR induced DSBs, although these are mostly repaired by NHEJ, but do show a defect in the recombinational repair of DSBs induced by I-SceI endonuclease. Although XRCC2 and XRCC3 mutants are hypersensitive to interstrand crosslinks, comet assays show that they unhook crosslinks at the same rates as their parents, this indicates that they are involved in events downstream of unhooking (De Silva et al., 2000). XRCC2 and XRCC3 mutants cannot repair the DSBs induced after ICL treatment. XRCC2 and XRCC3 mutants have also been found to be defective in a coincubation assay using damaged and undamaged plasmids, however RAD51 itself was not necessary.

It has been proposed that when replication forks meet a crosslink a DSB is formed by an unknown process (De Silva et al., 2000). XRCC2 and XRCC3 dependent recombination start to repair the DSB, but are stalled by the crosslink. ERCC1-XPF then unhooks the crosslink and recombination is completed. This would explain why ERCC1 mutants create DSBs. Obviously this model can explain repair during replication, but not during other times, although perhaps ICLs are only repaired at replication.

Mechanisms for Tolerance of DNA Damage

As well as mechanisms to repair damage, the cell also possesses mechanisms to tolerate damage. Unrepaired DNA damage can lead to blockage of replication forks, because normal replicative proofreading DNA pols cannot insert the correct base opposite the damage. Sometimes the DNA replication machinery can restart downstream of the damage. Lesions in the lagging strand result in blocked retrograde DNA synthesis, however the replication fork proceeds past the damage. This results in small daughter strand gaps (DSGs) in the lagging strand (Schwartz, 1989). Lesions in the leading strand block leading strand synthesis although lagging strand synthesis is not blocked (Cordiero-Stone et al., 1997; Cordiero-Stone et al., 1999; Svoboda and Vos, 1995; Veaute et al., 2000). Leading strand synthesis is probably reinitiated further down stream. It is possible that lesions in both the leading and lagging strands may either be tolerated without DSG formation or that DSGs may be repaired soon after formation. Persistent DSGs may lead to the creation of DSBs.

Post replication repair is the name for the process that enables replication forks to tolerate DNA damage at replication. Three mechanisms have been proposed: translesion synthesis, recombination and template switching (Barre et al., 1999; Baynton et al., 1998; Nelson et al., 1996; Xiao et al., 1998). In template switching the DNA pol temporarily switchs to the daughter strand of the undamaged complementary strand to detour around the damage. Template switching has not been demonstrated in yeast, simian or rodent cells. A recombinational mechanism relies on a sister chromosome to fill in the gap. Recombinational repair may occur, and in fact sister chromatid exchanges may be a consequence of recombinational bypass, but there is little evidence for this method. The predominant mechanism for post replication repair in eukaryotes is thought to be TLS (Lehmann. 2000; Kunz et al., 2000). In TLS a special set of polymerases are used which can insert bases opposite the damage. TLS may either be coupled to replication or be post-replicative. The tolerance of lesions in the leading strand may involve TLS following uncoupling of leading and lagging strand DNA synthesis. DNA pol η

performs non-mutagenic TLS past CPD and a limited number of other lesions but not 6-4PP (Masutani et al., 1999a; Masutani et al., 1999b). DNA pol ξ, a low processivity DNA pol, performs mutagenic lesion bypass past a variety of lesions (Gibbs et al., 1998; Lin et al., 1999).

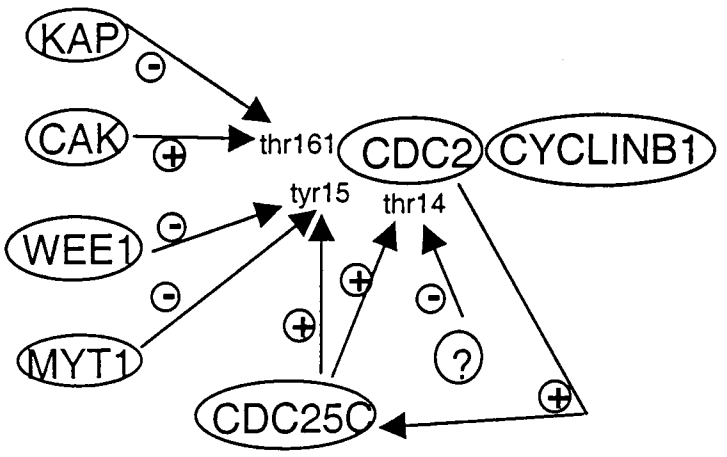

Figure 1.4 Cell Cycle Regulation. CAK activates CDC2 by phosphorylation on THR161 and KAP inactivates by phosphatase action. WEE1 and MYT1 inhibit CDC2 by phosphorylating TYR15. An unknown kinase inhibits CDC2 by phosphorylating THR14. CDC25C dephosphorylates TYR15 and THR14. CDC2 upregulates CDC25C.

The Cell Cycle

Progression through the cell cycle is mediated by a conserved family of protein kinases known as cyclin dependent kinases (cdks) (Forsburg and Nurse, 1991; Morgan, 1995; Nigg, 1995; Nurse, 1994; Pines, 1995; Sherr, 1994). Cdks are composed of a catalytic subunit and a requisite positive regulatory subunit termed a cyclin. The cdk activities that govern cell cycle progression require coordination and regulation. In most case positive regulation is mediated at the level of cyclin accumulation. However many aspects of cell cycle control require negative regulation of cdks. Negative regulation of cdk activity is achieved either by phosphorylation of the catalytic subunit or via the binding of cdk inhibitory proteins. In yeasts, CDC2 through its association with distinct cyclins activates entry into both S phase and mitosis, however in higher eukaryotes, although CDC2 is thought to be an essential cell cycle regulator, there are several distinct CDK catalytic subunits and cyclins. The D-type cyclins are associated with CDK4 and CDK6 and these complexes are required for early stages in G1 (Sherr, 1994). The cyclinE-CDK2 and cyclinA-CDK2 complexes control progression through the G1-S transition and S phase respectively (Heichmann and Roberts, 1994; Sherr, 1994). CDC2 is essential for G2-M. Cyclin A function is required for progression through S phase and into mitosis (Sherr; 1994).

At the G2-M transition in yeast and higher eukaryotes, mitosis is initiated by a cdk-cyclin complex consisting of the CDC2 protein kinase (CDK1) and a B-type cyclin (probably B1, although cyclin A may also play some role) (Clarke and Gimenez-Abian, 2000; Dunphy and Kumagai, 1991; King et al., 1994) (Figure 1.4). Activation of the CDK is controlled both by the accumulation of cyclinB and by three phosphorylation sites on the CDC2 subunit. Cdk-activating kinase (CAK) phosphorylates CDC2 on the thr161 residue essential for CDC2 catalytic activity. The phosphatase KAP will act on thr161. Prior to the onset of mitosis CDC2-cyclinB is held inactive by phosphorylations at tyr15 and thr14 of CDC2. The inhibitory kinases WEE1 and MYT1 phosphorylate CDC2 specifically on tyr15 and a distinct membrane associated kinase is thought to phosphorylate thr14. At the

onset of mitosis, the CDC25 phophastase activates the cdk by dephosphorylating CDC2 on tyr15 and thr14. *In vitro*, CDC2-cyclinB will activate CDC25C (mammalian homologue of yeast CDC25) suggesting the existence of a positive feedback loop. The control of all the cdks is probably similar to that of CDC2-cyclinB.

Cell Cycle Checkpoints

Introduction

One definition of a checkpoint is "a mechanism that establishes a dependence relationship between two cellular processes that are biochemically unrelated" (Clarke and Gimenez-Abian, 2000). One can show that yeast cells slow replication after DNA damage in S phase, due to a checkpoint and not just due to lesions impeding replication forks because mutations in checkpoint genes restore normal replication rate (Enoch et al., 1992). There are checkpoints that respond to DNA damage at the G1-S transition, during S phase and at the G2-M transition. Checkpoints usually inhibit the cyclin dependent kinases by controlling cyclin availability, binding of CDK inhibitors or CDK phosphorylation. Checkpoints can also independently inhibit other processes. The pathways that regulate the checkpoint responses of the cell to DNA damage are complex and little understood but presumably they contain sensors, transducers and effectors (Lowndes and Murgia, 2000; Murray, 1994; Zhou and Elledge, 2000).

Sensors

The identity of the sensor proteins is not known although there are several possible candidates and possibilities. These include the poly(ADP-ribose) polymerase (PARP), DNA-dependent protein kinase (DNA-PK), BRCA1, DNA polymerase ε and PCNA homologues (Enoch et al., 1992; Lowndes and Murgia, 2000; Murray, 1994; Zhou and Elledge, 2000). Evidence suggests that DNA damage checkpoint proteins detect single stranded DNA (Garvik et al., 1995; Lydall and Weinert, 1995). However many different DNA lesions can activate the DNA damage checkpoint.

Perhaps the process of repair is detected as most repair systems cause the formation of ssDNA during the process of repair. The easiest way to measure when to activate checkpoints and when to release from them may be to measure when DNA repair starts and is completed.

Transducers

The signal transducers in the DNA damage response are better understood. ATM and ATR, related and conserved protein kinases are central components (Shiloh, 2001). They are structural and functional homologues of yeast MEC1, a PI kinase. MEC1 activates RAD53 and PDS1, which probably control two independent downstream pathways, they both induce DNA repair genes after DNA damage.

AT patients have defects in ATM and are defective in such responses to IR as G1 arrest, reduction in DNA synthesis, G2 arrest and p53 induction (Beamish et al., 1996). ATM is required for p53 induction in response to IR damage but not to other types of damages such as UV, this response is speculated to act through ATR (Kastan et al., 1992). Neither ATM or ATR are thought to be involved with p53 induction independent of DNA damage. ATM controls the initial phosphorylation of proteins such as p53, MDM2, BRCA1, CHK2 and NBS1 in response to DNA damage. However, whereas AT fibroblasts are very sensitive to IR, they show little sensitivity to UV, alkylating agents or inhibitors of DNA replication. There are no known ATR mutations in human diseases, but expression of a dominant negative ATR form sensitises mammalian cells to DNA damage and reduces the G2/M checkpoint response from IR. ATM and ATR seem to have some overlapping roles in the phosphorylations they perform, but they are not redundant. DNA damage responses downstream of ATM and ATR seem to be controlled by CHK1 and CHK2 kinases, two serine/thereonine kinases.

CHK1 is required for the DNA damage checkpoint in yeast but not the replication checkpoint (Rhind and Russell; 1998). CHK1 is phosphorylated in response to DNA damage, this phosphorylation correlates with the ability of CHK1 to arrest cells in

G2. In the absence of CHK2, CHK1 can impose a checkpoint delay, although CHK1 does not appear to play an important role normally. CHK1 seems to be required for the G2 DNA damage checkpoint in mammals, CHK1 null cells die of p53 independent apoptosis and cannot arrest in G2 after IR.

CHK2 in yeast (CDS1) is required for responses to DNA damage and replication block and homologues are highly conserved (Liu et al., 2000; Rhind and Russell, 1998). CHK2 def. cells fail to upregulate p53 or trigger apoptosis after IR but not UV, however they will arrest in G2. CHK2 phosphorylates p53 *in vitro* and *in vivo* CHK2 helps to stabilise p53 after DNA damage.

Effectors

p53

p53 has an important role in activating either a cell cycle arrest or apoptosis response to DNA damage or cellular stress (Haapajarvi et al., 1999; Lowe et al., 1993; Selter and Montenarh, 1994; Smith et al., 1995). Activated p53 is also associated with senescence and differentiation. Treatment of cells with DNA damaging agents leads to increases in p53 levels and evidence suggests that DSBs are the specific lesions required for p53 induction (Kastan, 1996; Maltzman and Czyzyk, 1984; Nelson and Kastan, 1994).

Although not required for normal growth and development, p53 is crucial in the prevention of tumour development (Donehower et al., 1992; Purdie et al., 1994). Many signals that might be encountered during tumour development can activate p53, including carcinogen-induced DNA damage, telomere erosion, aberrant proliferative signals, hypoxia and loss of adhesion or survival signals. Defects in the p53 pathway are found in most human cancers and p53 null mice show a tumour prone phenotype (Donehower, 1996). p53 is essential for the G1 DNA damage checkpoint and the cell cycle arrest or apoptosis response to it (Brugaralos et al., 1995; Clarke et al., 1993; Deng et al., 1995; Lowe et al., 1993; Siu et al., 1999).

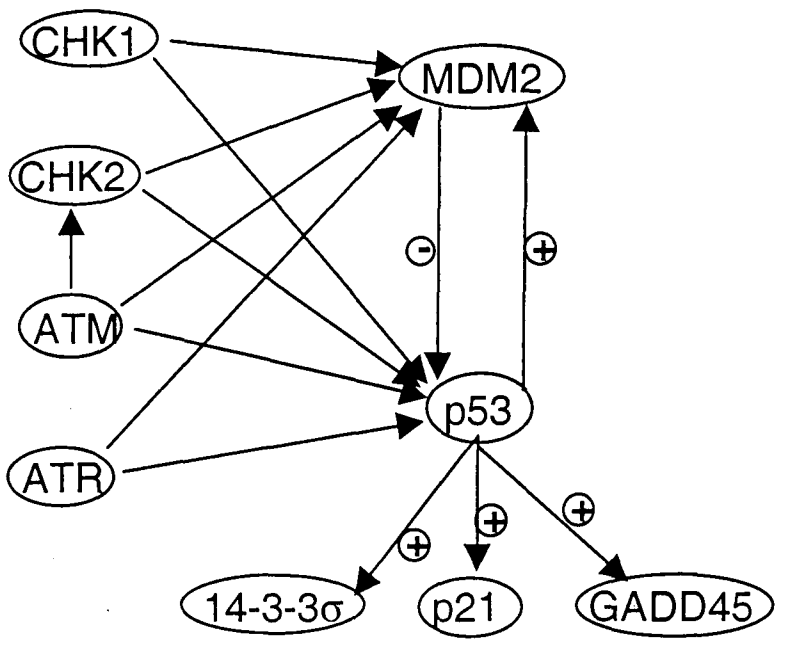

Figure 1.5 Regulation of p53 and associated proteins and genes. MDM2 targets p53 for ubiquitination and proteolysis and is induced by p53. p53 induces 14-3-3σ, p21 and GADD45. ATM phosphorylates CHK2 and ATR, ATM, CHK1 and CHK2 phosphorylate p53 and MDM2.

p53 is a sequence specific transcription factor that binds to DNA as a tetramer and activates or represses transcription from a large number of genes (el-Deiry, 1998) (Figure 1.5). The cell cycle arrest and DNA repair genes induced by p53 appear to be regulated independently of genes that mediate the apoptotic response. p53 will also act as a transcriptional repressor, through interaction with histone deacetylases. It will drive relocalisation of death receptors like FAS from the golgi to the cell surface and a direct role for p53 has been found in the mitochondria.

Regulation of p53 expression by transcription factors such as NF-κB and HOXA5, and mechanisms that control p53 translation help control the overall activity of p53 (Woods and Vousden, 2001) (Figure 1.5). However the principal mechanisms that govern p53 activity appear to be exerted at the level of regulation of p53 protein stability, control of the subcellular localisation of the p53 protein, posttranslational modifications and conformational changes that allow activation of the DNA binding activity of p53 (Kastan, 1996). The main regulator of p53 stability appears to be MDM2, which is a transcriptional target of p53 (Wu et al., 1993). MDM2 is a negative regulator of p53 and so a feedback loop exists to control p53 levels. MDM2 targets p53 for ubiquitination and subsequent proteolysis (Kastan, 1996). Phosphorylation within or close to the N-terminal MDM2 binding domain in p53 interferes with its ability to bind MDM2.

Several stress response kinases such as ATM, ATR, CHK1 and CHK2 have been shown to phosphorylate the MDM2 binding region of p53 (Ljungman, 2000). These kinase pathways appear to be critical in the activation of p53 in response to DNA damage such as UV or IR (Ljungman, 2000). Both ATM and ATR phosphorylate p53 in response to DNA damage, which enhances p53 activity. ATM activates CHK2, a kinase that phosphorylates p53 directly within the MDM2 binding domain, reducing binding to MDM2 and stabilising p53. ATM activation also induces dephosphorylation of the C-terminus of p53 and ATM can directly phosphorylate MDM2. Many other kinases have been shown to be capable of phosphorylating the N-terminus of human or mouse p53 *in vitro* including DNA-PK, JNK, p38, CK1, CAK and CHK1 (Ljungman, 2000; Shieh et al., 2000). Interaction of p53 with

REF1, by redox dependent and independent means, leads to the activation of p53 (Jayaraman et al., 1997).

Target genes of p53 include 14-3-3 σ, gadd45, mdm2, mck, bax, IGF-BP3, BTG2, p21 and cyclinG (el-Deiry, 1998).

p53 can contribute directly to DNA repair (Albrectsen et al., 1999; Lloyd and Hanawalt, 2000). p53 null mouse embryonic fibroblasts exhibit 35% to 70% of the normal unscheduled DNA synthesis indicating that p53 or p53 dependent genes are involved in NER (Smith et al., 2000). p53 is involved in the regulation of GADD45 and p48-XPE. GADD45 encodes a protein which binds PCNA and serves as a stimulator of DNA repair and inhibitor of replicative DNA synthesis (Kastan et al., 1992). p53 binds directly to XPB, XPD, RPA, CSSB and TFIIH. Li-Fraumeni cells, which are deficient in p53, have defective recovery of mRNA synthesis after UV, implying involvement of p53 or p53 dependent proteins (McKay et al., 1999).

p21

p21 is involved in cell cycle arrest and in terminal differentiation (Halevy et al., 1995; Huppi et al., 1994). It is a cyclin dependent kinase inhibitor (CDKI) and in most situations is induced by p53, in fact it is one of the principle mediators of p53 induced G1 arrest (Brugarolas et al., 1995; el-Deiry et al., 1993; el-Deiry et al., 1994; Harper et al., 1993; Harper et al., 1995; Poon et al., 1996; Waldman et al., 1995). As well as being a CDKI, p21 is also thought to be essential in low levels for the assembly of the CDK complex (at least cdk4-cyclinD), inhibition of the CDK probably occurs through increases in p21 stoichiometry (Zhang et al., 1994).

Two families of mammalian CDKIs have been described:the INK4 inhibitors and the Cip/Kip inhibitors (Awad et al., 1997; Sherr and Roberts, 1995). INK4 inhibitors are specific for cdk4 and cdk6, there are 4 known family members: p15, p16, p18 and p19. Cip/Kip inhibitors target a broader spectrum of cdks including cdk2, cdk4, cdk6 and possibly cdk1. The family consists of 3 members p21, p27 and p57. All contain a conserved N terminal cdk inhibitory domain. The cdki-cdk-cyclin complex almost certainly deforms and interferes with the cdk active site.

There is much evidence that after DNA damage p53 will upregulate p21 levels and cause G1 arrest (Brugaralos et al., 1995; Macleod et al., 1995; Reinke and Lozano, 1997; Siu et al., 1999; Waldman et al., 1995). The RAS/RAF pathway is also involved in induction of p21 in a p53 dependent manner (Ravi et al., 1999; Zhu et al., 1998). p21 is only induced after relatively low UV doses in fibroblasts, whereas BAX, a gene involved in apoptosis, is induced after high doses (Li and Ho, 1998; Reinke and Lozano, 1997).

There are also circumstances in which p21 can be induced independent of p53 (Macleod et al., 1995; Michieli et al., 1994). p21 can be induced by UV light in a p53 independent manner in cells derived from p53 null mice and in Li Fraumeni fibroblasts (Haapajarvi et al., 1999; Loignon et al., 1997; Sheikh et al., 1997). p21 expression is elevated independent of p53 in mouse hepatocytes and human hepatcarcinoma cells after cell stress (Kim et al., 2000; Serfas et al., 1997). The ERK/MAP kinase, RAF, TGFβ1 and myoblast differentiation pathways can induce p53 independent increases in p21 levels (Elbendary et al., 1994; Gartel et al., 2000, Halevy et al., 1995; Parker et al., 1995).

p21 interacts with PCNA and *in vivo* and *in vitro* studies show it prevents PCNA dependent DNA replication but will allow PCNA dependent gap filling DNA synthesis for NER (Li et al., 1994; Podust et al., 1995; Shivji et al., 1994). However, there have been observations that p21 inhibits NER and MMR (Cooper et al., 1999; Pan et al., 1995). p21 also inhibits RFC ATPase stimulation by PCNA, this is required for the loading and unloading of PCNA DNA clamps (Oku et al., 1998). p21 null mouse embryonic fibroblasts display reduced unscheduled DNA synthesis (associated with DNA repair), and p21 may facilitate NER (Sheikh et al., 1997; Smith et al., 2000).

A complex of PCNA, p21, CDK and cyclin has been reported in fibroblasts (Xiong et al., 1992). The N-terminal region of p21 binds to the CDK and the C-terminal region binds to PCNA, so p21 acts as a bridge (Chen et al., 1995). Perhaps this

enables direct coordination of cell cycle progression and DNA replication and may help control the progression from G1 to S phase. GADD45, a p53 induced gene, also binds to PCNA and binding is competitive with that of p21 (Chen et al., 1995). GADD45 expression is related to the amount of DNA damage, perhaps GADD45 is also involved in cell growth arrest by PCNA inhibition. GADD45 associates with core histones, p21 and PCNA, and is thought to be involved with the remodelling of chromatin in DNA repair (Carrier et al., 1995).

Cells in terminal differentiation or senescence pathways often have increased levels of p21. This might be expected because differentiated and senescent cells tend to withdraw from the cell cycle. p21 levels are elevated in differentiation programmes in myoblasts (independent of p53), keratinocytes and other cell types (Halevy et al., 1995; Parker et al., 1995). p21 levels also increase in senescent cells (Stein and Dulic, 1995). Cells deficient in p21 can bypass senescence (Brown et al., 1997).

Cells deficient in p21 or p53 cannot arrest in G1 following DNA damage, but will transiently arrest in G2, although they cannot maintain a G2 arrest and show uncoupling of S phase and mitosis (Brown et al., 1997; Brugarolas et al., 1995; Bunz et al., 1998; Deng et al., 1995; Waldman et al., 1996). p21 deficient cells can develop polyploidy and also undergo apoptosis. Cells over expressing p21 also develop polyploidy (Bates et al., 1998).

Cell Cycle Arrest

S Phase Arrest

p21 does not seem to be involved in S phase arrest after DNA damage (Kelly and Brown, 2000; Wyllie et al., 1996). Following UV damage, DNA repair is not inhibited by the presence of a large amount of p21 protein in the nucleus, in contrast cells undergoing DNA replication contain very low amounts of p21. Except at very high doses the cause of the reduction in S phase DNA synthesis following strand breaking agents is primarily inhibition of replicon initiation rather than chain elongation (Walters and Hildebrand, 1975). In contrast the inhibition demonstrated by p21 on replication *in vitro* affects elongation rather than initiation (Waga et al.,

1994). p21 expression in cells failed to provoke any obvious defect in S phase progression, which suggests that p21 mediated inhibition of DNA synthesis does not significantly block initiated DNA synthesis *in vivo* (Bates et al., 1998).

G1 arrest

The predominant DNA damage checkpoint in humans is the p53 and p21 dependent G1 arrest pathway, which allows time for DNA repair before transit into S phase (Bates et al., 1998; Di Leonardo, 1994). Transient transfection of p21 in fibroblasts leads to an accumulation of G1 cells (Harper et al., 1995; Niculescu et al., 1998). p21 is presumed to prevent the onset of S phase by inhibiting RB phosphorylation and thus preventing E2F activation (Dimri et al., 1996). E2F is a transcription factor involved in the activation of transcription of growth regulated genes. Overexpression of RB can arrest cells in G1 and RB is important for the G1 checkpoint. In the absence of a functional RB, G1 arrest fails and cells arrest in G2 and develop polyploidy (Niculescu et al., 1998). p21 can also regulate E2F activity in an RB independent pathway (Dimri et al., 1996).

G2/M arrest

Although the G1 DNA damage checkpoint is generally considered more commonly stimulated, the G2-M DNA damage checkpoint is also highly important (Clarke and Gimenez-Abian, 2000; O'Connell et al., 2000). This system provides a checkpoint of last resort to avoid replicated damage on one chromatid being divided from its sister, and thus being unrepairable by error free recombination. The G2-M checkpoint also allows time for the repair of damage produced during S and G2 phases. The ultimate target of the G2-M checkpoint is the tyrosine phosphorylation of cyclinA/B-CDC2 (Blasina et al., 1997; Poon et al., 1996; Rhind and Russell, 2001).

p53 and p21 play a role in regulating the G2/M transition (Chan et al., 2000; Waldman et al., 1996). Human lymphoblastoid cells arrested in G2 after DNA damage accumulate high levels of CDK bound p21 and cells with ectopic p21 expression arrested in G2 (Bates et al., 1998; Beamish et al., 1996). p21 seems to

have a role in the G2-M transition through its effect on CDK2 and CDK1/CDC2-cyclinB (Bunz et al., 1998; Guadagno and Newport, 1996). p21 blocks the initial activation step of CDC2-cyclinB that is required for G2/M progression of the cell cycle (Guadagno and Newport, 1996). In G2 arrested cells p21 was found in complexes with cyclinA but not cyclinB1, this is consistent with the binding affinities of p21 for CDK-cyclins and indicates that p21 does not block G2-M progression by a direct inhibition of CDC2-cyclinB1 (Bates et al., 1998; Dulic, 1994; Harper et al., 1993). However, CDC2-cyclinB had inhibitory phosphorylation, perhaps p21 causes this by inhibition of cyclinA-CDK1 complexes (Bates et al., 1998; Poon et al., 1996). In Xenopus egg extracts, inhibition of CDK2 leads to the inhibitory phosphorylation of CDC2 and concomitant G2 arrest (Guadagno and Newport, 1996). In normal human fibroblasts, p21 is sufficient for the inhibition of cyclinA/E-CDK2 and partly responsible for the inhibition of cyclinD-CDK4 after DNA damage, but is not responsible for the inhibition of cyclinA/B-CDC2 (Levedakou et al., 1995; Poon et al., 1996).

Part of the mechanism to arrest in G2-M after DNA damage is via the protein kinase CHK1, which is activated by phosphorylation and phosphorylates CDC25C (Chan et al., 2000; Rhind and Russell, 1997; Peng et al., 1997). Phosphorylation of CDC25C allows the protein 14-3-3σ to bind to cdc25C and inactivate its phosphatase activity (Hermeking et al., 1997; Peng et al., 1997; Rhind and Russell, 1997). The activity of CDC25C has been shown to be reduced after DNA damage. 14-3-3σ is thought to sequester CDC25 in the cytoplasm, away from CDC2 (Chan et al., 1999; Lopez-Girona et al., 1999). CDC25 regulation alone will arrest cells. MIK1 activation is required for maintenance of extended checkpoint arrest and it accumulates after prolonged activation of the checkpoint (Rhind and Russell, 2001). WEE1 levels are not altered after DNA damage and WEE1 is not required for the G2 checkpoint (Rhind and Russell, 2001).

p53 is required to maintain the G2 DNA damage checkpoint arrest in humans (Bunz et al., 1998). This may be because p53 activates transcription of p21 and 14-3-3σ. Cells deficient in p21 or 14-3-3σ are unable to maintain G2 arrest after DNA

damage. Cyclin B1 is subject to control of subcellular localisation by the nuclear export protein CRM-1 and is spatially transported during mitosis. p21 is a strong regulator of CDC2-cyclinB1, as mentioned earlier, whilst the binding of small amounts of p21 seems to be essential for CDK assembly or function, large amounts inhibit CDKs.

In cells with a prolonged G2 delay, cyclin B1 levels are reduced in a dose dependent fashion when compared to the normal levels in G2 phase (Muschel et al., 1991).

The ERCC1 Null Mouse

To study the role of ERCC1 *in vivo*, an ERCC1 null mouse was made using the embryonic stem cell method (McWhir et al., 1993). The expectation was that these mice would prove to be inviable as no human ERCC1 mutants are known. If the mice proved to be viable they might display an interesting and complex phenotype, resulting from the multiple roles of ERCC1.

Phenotype of the ERCC1 Null Mouse

The ERCC1 heterozygote phenotype is not discernible from wt. Matings between heterozygotes produced ERCC1 null mice, but in numbers smaller than expected from Mendelian segregation of non-sex linked nuclear genes. However there was no evidence of compromised viability in ERCC1 null embryos. The ERCC1 null mice displayed an extreme phenotype with severe runting and death before weaning of liver failure (McWhir et al., 1993). Increased alanine aminotransferase activity indicative of liver cell injury and significant increases in alkaline phosphatase and bilirubin indicating reduced liver excretory functions were detected. Superficial histological analysis showed a number of grossly enlarged hepatocytes. Detailed histopathology revealed polyploidy in perinatal liver progressing to severe aneuploidy by 3 weeks at which stage the mice died. Wt runts showed no pathology in liver on a superficial examination. Initial analysis of the ERCC1 null animals revealed marginly elevated p53 levels in the liver, brain and kidney. As wt mice age the number of binucleate hepatocytes increases and nuclear ploidy increases, but aneuploidy is not usually seen. In ERCC1 null hepatocytes polyploidy develops early, but is not preceded by binucleation (McWhir et al., 1993). The ERCC1 null mouse shows increased levels of disruption of mitochondrial membranes and increased levels of lipid accumulation when compared to wt (KT Hsia; personal communication).

In order to further investigate the phenotype in tissues other than liver, a mouse line was constructed with a liver specific ERCC1 transgene (Selfridge et al., submitted). This slightly runted mouse lives for up to 10 weeks before dying and it has a normal

liver. This confirms that ERCC1 null mice die of liver failure, due to the loss of ERCC1. It is interesting that the liver is the worst affected organ as although levels of ERCC1 mRNA are very low overall in mice, they are lowest in liver (McWhir et al., 1993). The ERCC1 null mice with a liver transgene develop kidney damage by 10 weeks, nuclei from proximal tubule cells are pleomorphic and many are enlarged and polyploid, this is a common response of kidney to stress (Selfridge et al., submitted).

Three other ERCC1 null lines were also created using slightly different alterations and deletions in the ERCC1 gene, one in this laboratory by Kantai Hsia and two others (Weeda et al., 1997). The Kantai Hsia mouse is a deletion rather than the original insertion mutation, although both lines produce no detectable ERCC1 protein. A complete ERCC1 null mouse and a mouse with a 7 amino acid C-terminal truncation of ERCC1 were made in the laboratory of J. Hoeijmakers. The complete null had a maximum age of 38 days and the truncation mutant had a maximum age of 78 days. However the truncation mutant on a different background had a maximum lifespan of 6 months. The skin of these animals was noted as being thin and lacking in subcutaneous fat. In spleen at 3 weeks an increased and early onset of ferritin deposition was found. Kidney nuclear abnormalities were found and dilated tubules with leaked proteinaceous material, which is indicative of renal disfunction. FACS showed increasing octaploidy in the liver, and increased nuclear size by nuclear area measurements. It was observed that the ERCC1 null hepatocytes have eosinophilic nuclear inclusions, which have been frequently observed in cells of aging animals. There was no clear increase in apoptotic nuclei seen in the liver. Subsequent analysis of the original ERCC1 null line has since revealed the features found in the other three lines. The longer life span of the two Hoejimakers ERCC1 lines is probably due to differences in genetic background.

Other NER Knockouts

The phenotype of the ERCC1 null mouse became more interesting when compared to mouse lines that were defective in other NER genes (de Boer and Hoeijmakers, 1999). These indicated further that ERCC1 had an extra function beyond NER.

XPA null mice appear normal until 13 months. However they are highly susceptible to UVB induced skin and eye tumours and to skin tumours induced by DMBA (de Vries et al., 1995). They also suffer from increased spontaneous hepatocellular carcinoma rates. This strongly mimics the human phenotype. Fibroblasts derived from XPA null mice are also UV sensitive.

CSB knockout mice are sensitive to UVB, developing erythema at low doses (van der Horst et al., 1997). They are also slightly smaller and they have possible neurological changes. Unlike CS patients they also display an increased cancer incidence. They have a TCR defect and an inability to resume RNA synthesis after UV treatment, although global genome repair is unaffected. Perhaps in humans GGR is more efficient than in mice resulting in the lack of increased cancer incidence in humans. This illustrates how although there is great conservation of the mechanisms and general regulation of NER between species, there may be differences in the degree of regulation depending on the requirements of the animal.

XPD knockout mice die before birth (de Boer et al., 1998). Mice with an XPD point mutation, that mimics a TTD patient, suffer brittle hair, developmental abnormalities, reduced lifespan, UV sensitivity, skin abnormalities and mild cancer predisposition (de Boer et al., 1999).

XPC knockout mouse lines have extreme UV sensitivity and are extremely susceptible to UV induced skin cancer, but show no obvious clinical defect or organ pathology (Sands et al., 1995).

XPG patients are rare with a wide variety of symptoms. XPG null mice have recently been made (Harada et al., 1999). These mice show growth retardation and

death before weaning (similar to the CS phenotype), probably because of failure of digestion in the abnormal intestines. These mice display no liver abnormalities beyond small cells probably resulting from starvation. The early death is probably due to the loss of the structural role of XPG in repair of oxidative damage.

The liver phenotype is unique to ERCC1 null mice amongst the other NER deficient mice that have been produced. This implies that the liver phenotype is due to the absence of ERCC1 in its roles outside NER, rather than the loss of NER. ERCC1 is probably required for the processing of 3' non-homologous tails in recombination and is involved in the repair of DNA interstrand crosslinks, of these two roles it seems probable that the loss of ICL repair is causing the phenotype in the mice. There are several candidates for endogenous ICL agents in the liver including malondialdehyde, the major byproduct of arachidonic acid metabolism and lipid peroxidation (Chaudhary et al., 1994). Adducts caused by malondialdehyde have been found in liver DNA (Smith and Pereira-Smith, 1996).

p21

Wildtype mice that had a transgene for the overexpression of p21 in the liver have been made (Wu et al., 1996). The p21 overexpression causes a phenotype remarkably similar to that displayed by the ERCC1 null line. That is: hepatocyte proliferation is severely inhibited and there is a reduction in the overall number of adult hepatocytes giving aberrant tissue organisation, runted liver and body growth and increased mortality. The mice have a population of grossly enlarged hepatocytes similar to those seen in old liver. The similarity of the p21 transgenic and ERCC1 null mice phenotypes was so great that it was decided to examine the ERCC1 null animals for increased p21 levels in the liver and other tissues and cell lines. Northern blot analysis revealed that levels of p21 mRNA were increased in ERCC1 null liver compared to wild type (Nunez et al., 2000).

p53

Due to the role of p53 in p21 control and the increase in p53 levels in ERCC1 null liver, it was decided to investigate whether the removal of p53 would affect the phenotype of the null animals. A p53 null line and the ERCC1 null line were cross bred and the few resulting p53-ERCC1 double nulls were examined. Only three of these animals were generated because they had to be bred from p53 and ERCC1 heterozygotes. Mendel predicts that 1 in every 16 of the offspring should be double null, but the frequency at three weeks was far lower than this. A similar deficiency was not observed at day 19 of gestation, indicating very high perinatal mortality (Nunez et al., 2000). This is similar to the high perinatal mortality reported in the ERCC1 null animals (McWhir et al., 1993). Measurement of the p21 mRNA levels in the double null animals showed an increase similar to the ERCC1 null animals, and the double nulls also had high levels of polyploidy in the liver.

A Model for the ERCC1 Null Mouse

A possible model for what occurs in ERCC1 null mouse hepatocytes has been proposed (Melton et al., 1998). The deficiency in ERCC1 leads to a defect in repair so more damage accumulates. The accumulating damage will be damage that is normally repaired by NER and damage that is repaired by non-NER pathways that are dependent on ERCC1. However the crucial damage is probably that which is repaired by non-NER ERCC1-dependent pathways. According to the model, due to the failure of some ERCC1-dependent repair or tolerance recombination mechanism cells accumulate double stranded breaks during replication. These double stranded breaks then cause cell cycle arrest in G2, mediated by p21 through a p53 independent pathway, although p53 levels also increase. This leads to liver polyploidy. This model results in several questions. Why is polyploidy seen in liver and not other organs? What recombination role is ERCC1 playing? What is the mechanism for the cell cycle arrest? I have investigated several of these questions in this thesis and they and the model will be discussed.

I have further investigated the role of p21 and p53 in the cell cycle arrest of ERCC1 null hepatocytes. I have studied the polyploidy development in ERCC1 null liver and have compared it to aging wt liver. I have also examined the role of ERCC1-XPF in the formation of UV-induced chromosome aberrations and in arrest of DNA replication, in order to examine the molecular causes of the ERCC1 null phenotype.

Chapter 2 - Materials and Methods

Suppliers of Laboratory Reagents

Restriction Endonucleases and other Nucleic Acid Modifying Enzymes

Boehringer Mannheim Plc

Gibco BRL Life Technologies

New England Biolabs Inc

Pharmacia LKB Biotechnology

Standard Laboratory Reagents

BDH Chemicals Ltd

Fisons Chemicals

Gibco BRL Life Technologies

ICN Flow Ltd

Sigma Chemical Co

New England Biolabs Inc

Reagents for Cell Culture

Gibco BRL Life Technologies

ICN Flow Ltd

Sigma Chemical Co

Radioactive Reagents

[α-^{32}P]dCTP 3000 Ci/mmol, Amersham RediVue

[methyl-^{3}H] thymidine 25 Ci/mmol, Amersham Life Science

Antibiotics

Penicillin G, Sigma Chemical Co

Streptomycin, Sigma Chemical Co

Primer Synthesis

Perkin-Elmer Ltd

Oswel DNA service

Cell Culture Studies

Cell Lines

CHO9: Immortalised wt Chinese Hamster ovary cell line, which is a subclone of the CHO-KK cell line (Burki et al., 1980). Cells were kindly donated by Richard Wood, ICRF, Clare Hall.

CHO 43-3B: Immortalised ERCC1-deficient Chinese hamster ovary cell line, derived from the parental CHO9 cell line (Wood and Burki,1982). Cells were kindly donated by Richard Wood, ICRF, Clare Hall. 43-3B has a mutation V98E at the 98th residue of ERCC1, this protein is unable to bind to XPA *in vitro* and is highly unstable *in vivo*, although it will bind XPF (Hayashi et al., 1998).

CHO AA8: Immortalised wt Chinese hamster ovary cell line (Thompson et al., 1980). Kindly donated by S. Squires and R. Johnson, Zoology Department, Cambridge University.

CHO UV5: Immortalised XPD (ERCC2)-deficient Chinese hamster ovary cell line, derived from the parental CHO AA8 cell line (Thompson et al., 1981). Kindly donated by S. Squires and R. Johnson, Zoology Department, Cambridge University.

CHO UV41: Immortalised XPF (ERCC4)-deficient Chinese hamster ovary cell line, derived from the parental CHO AA8 cell line. Kindly donated by R.Wood, Imperial Cancer Research Fund, Clare Hall Laboratories.

CHO UV135: Immortalised XPG (ERCC5)-deficient Chinese hamster ovary cell line, derived from the parental CHO AA8 cell line. Kindly donated by J.Hartley, Department of Oncology, Royal Free and University College Medical School, London and M.Stefanini, Istituto di Genetica ed Evoluzionistica, Pavia, Italy.

CHO UV23: Immortalised XPB (ERCC3)-deficient Chinese hamster ovary cell line, derived from the parental CHO AA8 cell line. Kindly donated by J.Hartley, Department of Oncology, Royal Free and University College Medical School, London and M.Stefanini, Istituto di Genetica ed Evoluzionistica, Pavia, Italy.

Growth of Immortalised Mammalian Cell Cultures

Cells were maintained in supplemented GMEM (10% (v/v) Foetal Calf Serum (FCS), 1× non-essential amino acids, 25 U/ml penicillin, 1mM sodium pyruvate, 25 μg/ml streptomycin) at 37°C in a 5% CO_2 atmosphere in a humidified tissue culture incubator (Forma Scientific). To passage cells, medium was aspirated, the bottom of the flask rinsed with 1-2 mls of trypsin (0.25% (w/v) trypsin (ICN Flow, Cat No. 043-5090), 1 mM EDTA in 1×PBS), then a further 1-2 mls of trypsin was added and the flask was incubated at 37°C until cells were detached. Then 5 volumes of medium were added, and cells were subjected to 5 min centrifugation at 1,300 rpm. Supernatant was discarded and the cells resuspended in an appropriate volume of medium, and an aliquot was transferred into a flask. For long term storage, cells were kept in liquid nitrogen. Cultures were trypsinised, centrifuged, the supernatant was removed, and cells were resuspended in 1ml of ice cold freezing medium (supplemented GMEM with 10 %(v/v) DMSO and 20 % (v/v) FCS). 1 ml aliquots were left at -20°C for 2 hours, then transferred to -70°C overnight before removal into liquid nitrogen. Aliquots were thawed rapidly at 37°C and diluted in 9 ml of medium, before being pelleted by centrifugation at 1,300 rpm for 5 min. The supernatant was discarded, the cells resuspended in an appropriate volume of medium, and transferred into a flask.

Chromosome aberration studies

Cells were plated the day before the experiment to allow them time to recover. They were then UV irradiated at 254 nm, using a handheld UV lamp to the required UV fluence and samples were taken 15, 27 and 35 hrs later for CHO9 and 433B cells and 20, 27 and 35 hrs later for AA8, UV5, UV41, UV135 and UV23 cells. Four hours

before taking the samples a 1:200 dilution of colcemid (10 μg/ml) was added. At the time point, shaded cells were scraped off around the periphery of the dish and removed. Cells were then trypsinised, resuspended in 5.6 g/l KCl (0.075 M) and placed in a 37°C water bath for 15 min. Cells were resuspended in Carnoy Fixative (methanol:acetic acid (3:1)) and left for 20 min, this was repeated and cells were dropped onto slides from a height, left to dry and stained with crystal violet before washing, drying and mounting with DePex. Slides were examined on an Olympus BX60 with a ccd camera and images were analysed using analySIS (Norfolk Analytical). At least 200 pictures were taken of random metaphases, selected good quality metaphases were then scored for aberrations. Well spread metaphases were selected that had between 17 and 28 chromosomes, where all the chromosomes could be distinguished and counted and the two chromatids could be resolved. Scoring was derived from Savage, 1976.

Survival Curves

Cells were plated at a calculated density with two plates for each dose. The next day plates were UV irradiated and left for 4 or 5 days in order to allow cells to grow. When the zero UV control plate became confluent, plates were fixed with Carnoy Fixative and washed in water, after drying overnight, plates were stained with crystal violet and washed with water. After overnight drying dye was extracted with 70% ethanol. Using a stained and extracted blank plate as a zero the OD was measured at 575 nm using a Perkin-Elmer, Lambda 15, UV/VIS Spectrophotometer. Taking the zero UV as 100%, survival was calculated using the OD measurements. These were then plotted on a log10 scale against dose. Duplicates were used for each dose.

Replication Arrest Studies

Cells were plated out at calculated densities and were allowed to settle overnight at 37°C. The following day they were arrested in the G1-phase of the cell cycle with overnight incubation in isoleucine-deprived medium (Galavazi et al., 1966). The cells were released from the G1 block, 6 hours before irradiation, by putting them

back into normal growth medium. After 6 hours, the cultures, which were well into S phase, were treated (F Nunez; personal communication). They were either mock irradiated or irradiated with a handheld UV lamp with the required UV fluence, or mock treated or treated with the appropriate dose of MMC for 1 hour. The cells were then processed immediately or incubated in normal medium and processed at different times after UV. Cells were rinsed in serum deprived medium and pulsed 15 min in [^{3}H]thymidine-containing (1 µCi/ml) serum deprived medium at 37 °C. After 15 min, the cells were rinsed in sterile PBS (8 mM K_2HPO_4, 1.5 mM KH_2PO_4, 150 mM NaCl), lysed in a 1% SDS solution and TCA precipitated with 0.5 volumes of 20% (v/v) TCA pre-chilled at 4°C. Samples were kept at 4°C until needed. Samples were vacuum-filtered by passing them through 2.4 cm GF/C microfibre filters (Whatman). Each filter was put into a plastic scintillation vial and 2 mls of scintillation liquid was added to it. [^{3}H]incorporation was measured as DPM counts using a scintillation counter (scintillation fluid (2.5 l Toluene, 15 g PPO (2,5-Diphenyloxazole), 0.4 g POPOP (1,4-bis[5-Phenyl-2-oxazolyl]benzene;2,2'-p-Phenylene-bis[phenyloxazole]).

Gene of interest	Name	Sequence(5`-3`)	Description	PCR conditions
Original (truncation) ERCC1 KO	033M	CCCGTGTTGAAG TTTGCG	ERCC1 exon 4 (McWhir et al. 1993b)	94°C 1 min 68°C 1 min 72°C 1 min for 35 cycles
	035M	CGAAGGGCGAAG TTCTTCCC	ERCC1 exon 5 (McWhir et al. 1993a)	
	M4956	GGTTCGAAATGC CGACCAAGCG	ERCC1 neo cassette (D. Melton, personal communication)	
p53 KO	C1045	CAAAGAGCGTTG GGCATGTG	p53 intron 7 (A. Clarke, personal communication)	94°C 1 min 62°C 1 min 72°C 1 min for 35 cycles
	C1046	CAAAGAGCGTTG GGCATGTG	p53 exon 6 (A.Clarke, personal communication)	
	C1047	CATCGCCTTCTAT CGCCTTC	p53 neo cassette (A.Clarke, personal communication)	
Kantai (complete) ERCC1 KO	033M	CCCGTGTTGAAG TTTGTGCG	ERCC1 exon 4 (McWhir et al. 1993b)	94°C 1 min 68°C 1 min 72°C 1 min for 35 cycles
	035M	CGAAGGGCGAAG TTCTTCCC	ERCC1 exon 5 (McWhir et al. 1993a)	
	262W	AGCCTACCCTCT GGTAGATTGTCG	HPRT (D. Melton, personal communication)	94°C 1 min 67°C 1 min 72°C 1.5 min for 35 cycles
	B1235	CCTCAGGACCAC CCACCAGGAGGA AG	ERCC1 exon 2 (D. Melton, personal communication)	

Table 2.1 PCR primers and conditions for mouse genotyping

Mouse Studies

Mouse Breeding

The ERCC1 null animals and littermates were on an outbred background segregating for 129/O1a and BALB-c (McWhir et al., 1993). ERCC1 null animals were produced by cross-breeding of two ERCC1 heterozygous animals. No difference has been observed between female and male animals with respect to liver phenotype and so no discrimination was made between the sexes when selecting animals for experiments. The p53/ERCC1 null animals were on an outbred background, derived from the ERCC1 129/O1a and BALB-c background and an extremely outbred background from the p53 stock. The ERCC1/p53 null animals were produced from a crossbred ERCC1 het/p53 heterozygous stock.

PCR genotyping of mice

In order to determine the genotype of an individual, PCR reactions were performed on genomic DNA samples extracted from tail. 0.5 cm of tail was incubated overnight in 2 ml of Tail buffer (10 mM Tris pH8, 0.4 M NaCl, 1 mM EDTA pH8, 1% SDS) with 280 μg/ml proteinase K at 37°C. Visible debris was removed by centrifugation and 1 μl of supernatant was used as substrate for a genotyping PCR reaction. Cycle conditions employed for different primer pairs are outlined in Table 2.1. 20 μl of each reaction was subjected to agarose gel electrophoresis, and products visualised by ultra-violet illumination.

Electrophoresis of DNA in agarose gels

DNA was separated in 0.7-2% (w/v) electrophoresis grade agarose with 0.5 μg/ml ethidium bromide in 1×TBE buffer (0.9 M Tris-HCl, 0.9 M boric acid, 20 mM EDTA, pH 8.0). Prior to loading, DNA samples were mixed with1/5 volume of 5× sample buffer (20% (w/v) glycerol, 100 mM EDTA, 0.1% bromophenol blue) and heated at 65°C for 5 min. Electrophoresis was carried out horizontally across a

potential difference of 1-10 V/cm. Bacteriophage lambda DNA cut with HindIII and ΦX174 DNA cut with HaeIII were used as size markers. DNA was visualised with short wave UV illumination, except for DNA in preparative gels which was visualised with long wave UV from a handheld lamp.

FACS Analysis

About 8 mm^3 of tissue was cut into small pieces and suspended in 100 µl of citrate buffer (sucrose (85.5 mg/ml), trisodium citrate (11.76 mg/ml), DMSO 0.05% (v/v), pH 7.6). This was incubated for 10 min at room temperature with 0.45ml solution A (trypsin (0.03 mg/ml) in stock solution (trisodium citrate (1 mg/ml), Tris (0.06 mg/ml), spermine tetrahydrochloride (0.5 mg/ml), NP40 (1 µl/ml)) was added to separate the tissue into individual cells and to lyse plasma but not nuclear membranes. Then 0.325 ml solution B (Trypsin inhibitor (0.5 mg/ml) and ribonuclease A (0.1 mg/ml) in stock solution) was added and the preparation was incubated for a further 10 min at room temperature to inhibit trypsin and digest RNA. Finally 0.25 ml propidium iodide (0.42 mg/ml) and spermine tetrahydrochloride (1 mg/ml) in stock solution was added and incubated for 10 min on ice to stain DNA before filtration through gauze. Samples were analysed on a Coulter EPICSXL or a Becton-Dickinson FACScan machine. The percentage of cells in each distinct peak was calculated.

The Coulter EPICS-XL FACS machine was set up as follows. The Becton-Dickinson FACScan machine was set up in a very similar way.

The preparative method used prepares individual nuclei. To eliminate background from RNA, an RNAse was used during the preparation as described. For each sample preparation the same amount of tissue was used (8 mm^3) in order that the flow and number of nuclei would be the same for each sample. This ensures that the dye/DNA ratio does not vary greatly, which means greater reliability in terms of peak positions from experiment to experiment. Low flow rates were used to ensure consistency.

Before each use of the machine, fluorescent Flowcheck beads (Beckman Coulter) were used. These confirm that the machine is functioning as expected and that all fluorescence collectors are working. A 3 week old wild type control sample was used to set the G0 peak to the same red fluorescence value, each time the machine was used, by altering the appropriate settings. The 3 week old wild type liver sample, as a relatively quiescent tissue, has a pattern with a high G1/G0 peak and a small G2 peak and so is effective for calibrating the machine. The Flowcheck beads also allow further confirmation that the machine is attributing the same fluorescence value to a certain fluoresence each time.

The instrument used can focus the laser beam used for detection down to an ellipse with a cross-section of less than 10 μm^2, this means that the difference between two nuclei stuck together and one larger nuclei can be revealed by pulse shape analysis, i.e. by comparing the shape/size of the absorbance to the intensity. Two G1 nuclei stuck together will have a greater cross section than one G2 nuclei, although the same DNA content. Most cytometers enable two parameters the pulse height and width to be measured, the pulse area can be calculated from this. A G2 cell will have the same DNA content and hence peak area as a doublet G1, but will have a greater peak width because the two cells take longer to traverse the laser, the total DNA content is the same but the two cells have a high fluorescence in the beam for longer. A dot plot of DNA peak against DNA area, FL3 peak against FL3 as used in this system shows that singleton nuclei fall in a constant straight line slope, whereas doublet nuclei fall off this slope, from this plot only singleton nuclei were selected. Smaller debris were also gated off using this plot, the debris falls at the smaller end and by comparison of previous plots and controls was be selected for removal.

Logarithmic scales were used on some of the plots to illustrate peaks that were not visible on some of the linear scale plots. The logarithmic plots compress the peaks on a plot, as they display a greater range of fluorescence, this means that smaller peaks are more visible. Due to the way that logarithmic plots are calculated using a digital to analogue converter and then displayed it is not always easy to compare the

positions of peaks. Unlike with linear plots, where it is easy to say that the nuclei in one peak have twice the amount of DNA as those in another peak due to their positions on the X axis, with logarithmic plots it is not easy to be sure of this. In order to establish that peaks were allocated properly control samples of young wild type liver were used.

Preparation of RNA from cells and mouse tissues

The following method is adapted from Chomczynksi and Sacchi, 1987. Fresh cells or tissue were placed in a sterile polycarbonate centrifuge tube containing up to 7 ml of RNAzol solution (Biogenesis Ltd., Bournemouth, UK) and homogenised. Subsequently, 0.1 volumes of chloroform was added, the tube was shaken vigorously for 30 sec and stored on ice for 5 min and then centrifuged for 15 min at 10,000 rpm in an HB4 rotor precooled to 4°C in a Sorvall RC5 Centrifuge. The aqueous phase was transferred to a fresh tube and RNA precipitated by the addition of 1 volume of isopropanol. The sample was stored at 4°C for at least 15 min before a 15 min centrifugation as above. The RNA pellet was washed in 75% ethanol, centrifuged for 8 min at 5,000 rpm and resuspended in sterile H_20. RNA was stored at -70°C.

RNA Concentration

RNA was diluted in distilled water and the OD of absorbance at wavelengths 260 nm and 280 nm was measured by a spectrophotometer (Perkin-Elmer, Lambda 15, UV/VIS Spectrophotometer). An $OD_{260\ nm}$ value of 1.0 represents a concentration of 40 mg/ml. A ratio of $OD_{260\ nm}$/ $OD_{280\ nm}$ over 2.0 represents a pure preparation of nucleic acid.

Electrophoresis of RNA in agarose gels

RNA samples were electrophoresed through 1.4% (w/v) agarose gels made with 1×MOPS (a dilution of 10×MOPS (200 mM MOPS, 50 mM sodium acetate, 10 mM EDTA, pH 7.0)), 0.66 M formaldehyde and 0.5 μg/ml ethidium bromide. Samples

were prepared by the addition of 30 µg of total RNA (in 20 µl d.H_20) to an equal volume of FSB (100 µl 10×MOPS, 200 µl formamide, 120 µl de-ionised 37% (w/v) formaldehyde) and one quarter volume of standard sample buffer (20% glycerol, 100mM EDTA, 0.1% bromophenol blue) was also added and the sample heated for 5 minutes at 65 °C then cooled on ice prior to electrophoresis for 3-4 hours at 100V.

Following electrophoresis, gels were washed three times for 20 mins in 10×SSC (a dilution of 20 SSC buffer (3 M NaCl, 0.3 M tri-sodium citrate, pH 7.0)) at room temperature to remove formaldehyde and ethidium bromide. The RNA was transferred to Genescreen Plus nylon membrane (Du Pont; Stevenage; UK) by capillary action using 10×SSC as the transfer buffer. Transfer was for 12 to 24 hours. On completion of transfer the membrane was washed in 2×SSC for 10 mins then baked at 80°C for 2 hours.

DNA labelled to high activities was obtained using the randomly primed DNA labeling method (Feinberg and Vogelstein, 1983). DNA probes were denatured, annealed to random hexamer primers and extended by the Klenow fragment of E. coli DNA polymerase I in the presence of [α-^{32}P]dCTP. Probes were labelled as follows:100 ng of double stranded DNA was made up to 32 µl with H_2O then denatured by boiling for 5 min and allowed to cool at 37 °C for 10 min. 10 µl of OLB (0.025 M $MgCl_2$, 5 mM β-mercaptoethanol, 0.1 mM each of dGTP, dTTP and dATP, 0.25 M Tris HCl, 1 M HEPES buffer and 0.3 ml of random hexanucleotides (OD260nm=90) per ml of final OLB), 2 ml of 10 mg/ml BSA, 5 µl (50 µCi) of α[^{32}P]dCTP (3000 Ci/mmol) and 10 units of Klenow enzyme were then added. The reaction was incubated overnight at room temperature. Probes were purified with TE buffer (10 mM Tris-HCl, 0.1 mM EDTA, pH 8.0) through a Nick Column, Sephadex G-50, DNA grade (Pharmacia Biotech).

Pre-hybridisations were performed in a temperature controlled rotisserie in 30 ml of prehybridisation buffer (6×SSC, 1% SDS, 10%(w/v) dextran sulphate, 100mg/ml of denatured herring sperm DNA). Blots were prehybridised for a minimum of 2 hours at 65°C. DNA probes (10 ng) were heat denatured with 300 µl of 10 mg/ml herring

sperm DNA and added to the prehybridisation solution. For p21 Northerns, a cloned PCR product of the mouse p21 cDNA was used. After overnight hybridisation the solution was discarded and blots were rinsed for 2×5 min in 2×SSC at room temperature, followed by 2×30 min in 2×SSC, 1%(w/v) SDS at 65° C then 2×30 min in 0.1×SSC at room temperature. Membranes were autoradiographed at –80°C, typically overnight, using Cronex X-ray film (DuPont) in a cassette with intensifying screens (Cronex Lightning plus, DuPont). Signals were also visualised using a Molecular Dynamics PhosphorImager and analysed with ImageJ software.

Radiolabelled probes were stripped from Northern Blots by washing for 4× 5 mins in boiling 0.01×SSC, 0.01% (w/v) SDS. Blots were autoradiographed to confirm that stripping was complete. The membrane was reprobed after prehybridisation as above.

Reprobing was with a 1.2kb cloned fragment of glyceraldehyde-3-phosphate dehydrogenase cDNA (Fort et al., 1985).

Cloning of p21 probe

Total mouse embryonic cDNA was used for a PCR reaction with two primers designed to anneal within the p21 coding region to generate a product of approximately 490 base pairs. The sequence of one primer was 5' ACCATGTCCAATCCTGGTGATGTCCG. The sequence of the other primer was 5' GGGCACTTCAGGGTTTTCTCTTGCAG. Primers were derived from the complete mouse p21 cDNA sequence (GenBank Acc. No. U09507).

A product of the expected size was purified from a 1% agarose gel. DNA was electrophoresed using low melting point agarose in 1×TBE and 0.5 mg/ml ethidium bromide. The desired fragment was visualised by long wave UV illumination and excised and recovered from the agarose by phenol extraction. The gel slice volume was estimated, then 0.5 volumes of TE, 1 µl glycogen (Boehringer Mannheim) and 5 µl 20% SDS was added to the gel slice and heated to 70°C until the agarose melted. Liquified agarose was extracted 3 times with 1 volume of Tris buffered phenol (pH 8.0) and once with 1 volume of choloform. The aqueous phase was retained and

DNA precipitated by the addition of 0.1 volume 3 M sodium acetate and 1 volume of isopropanol. DNA was pelleted by a 10 min centrifugation at 13 krpm and the DNA pellet was resuspended in distilled H_20.

pBluescript was used as a cloning vector (Thummel, 1988). The vector was cleaved with EcoRV to produce a blunt end. Typically for restriction enzyme digests 2-5U of restriction endonuclease were used per µg of DNA. Manufacturers buffers and recommended conditions were used. Reactions were terminated with the addition of DNA sample buffer and 10 min heating at 65°C. The PCR product was treated with a T4 polynucleotide kinase to add a 5' phosphate to each end.

Between 100 and 200 ng of insert DNA was incubated with linearised vector DNA at an insert to vector molar ratio of 5:1. Ligation was in a 10-20 µl volume with 50 mM Tris-Cl pH 7.6, 10 mM MgCl2, 1 mM DTT, 1 mM ATP and 5% (w/v) PEG8000. This was incubated overnight at 15°C with one unit of T4 DNA ligase.

The p21 vector was then used to transform *E coli*. The method used was a modification of Nishimura et al. (1990). A 500 µl aliquot of an overnight culture of the DH5α *E coli* strain (*supE*44Δ*lacU*169 (*Φ*80*lac*2Δ*M*15) *hsdR*17*recA*1*endA*1*gyrA*96*thi*-1*relA*1) (Gibco BRL) was used to inoculate 50 ml L broth (1% (w/v) Bactotryptone, 0.5% (w/v) Bactoyeast extract and 0.5% NaCl) supplemented with $MgSO_4$ (10mM) and glucose (0.2% (w/v)). This culture was incubated at 37°C until the culture reached mid-logarithmic phase whereupon it was chilled on ice for 10 min and pelleted by centrifugation at 1500g for 10 min at 4°C. Cells were resuspended in Transformation Buffer (50mM $CaCl_2$, 10 mM Tris, pH7.5) and left on ice for 30 min. Cells were then pelleted and resuspended in Transformation Buffer. Cells were transformed by the addition of approx 100 pg of plasmid DNA to 100 µl of competent cells followed by mixing and a 15 min incubation on ice. Cells were heat shocked for 3 min at 37°C then placed on ice for 1 min. Then 0.4 ml of 37°C L broth was added and the cells incubated for 1 hr in the absence of antibiotic selection. A number of aliquots were then plated to dryness on L broth agar 90mm petri dishes, with appropriate antibiotic selection (ampicillin to

100 μg/ml) and 30 μl of 2% (w/v) X-Gal (in dimethylformamide) and 20 μl of 100 mM IPTG to aid the identification of recombinants. Plates were incubated at 37°C for at least 20 hr before scoring or picking of colonies. Typical transformation efficiencies were between 10^5 and 10^8 transformants per μg of DNA. Recombinant colonies appeared white and non-recombinant colonies were blue using IPTG/X-Gal.

p21 vector was purified as follows. A single bacterial colony was used to inoculate 50 ml of TB containing an appropriate antibiotic and grown overnight at 37°C with vigorous aeration. The cells were pelleted by centrifugation for 15 min and 4°C in an HB4 rotor in a Sorvall RC5 centrifuge at 10,000 rpm. The bacterial pellet was resuspended in 10 ml of solution P1 (50 mM Tris-HCl pH 8.0, 10 mM EDTA, 100 mg/ml RNase A), then 10 ml of solution P2 was added (20 mM NaOH, 1% (w/v) SDS). The sample was stored at room temperature for 5 min. Then 10 ml of P3 (2.55 M potassium acetate, pH 4.8) was added and the cell preparation was left on ice for 10-15 min. Then chromosomal DNA, SDS and protein was sedimented by centrifugation at 13, 000 rpm in an HB4 rotor for 30 min at room temperature. A Qiagen500 column was equilibrated with 10 ml buffer QBT (750 mM NaCl, 50 mM MOPS, 15% ethanol, 0.15% (w/v) TritonX100, pH 7.0). The supernatant was applied through a Whatman filter. After washing twice with 30ml buffer QC (1 M NaCl, 50 mM MOPS, 15% ethanol, pH 7.0), the DNA was eluted with 15 ml buffer QF (1.25 M NaCl, 50 mM MOPS , 15% ethanol, pH 8.2). DNA was precipitated with 0.6 volumes of isopropanol and centrifuged at room temperature. Pelleted DNA was washed with 70% ethanol, air dried and redissolved in water and stored at –20°C. Diagnostic restriction enzyme digests were used to confirm that the correct cDNA fragment was present in the plasmid.

It was then cleaved with EcoRI and HindIII, and gel purified as above.

Centromeric staining of hepatocytes

Livers were gently pressed onto a glass coverslip after dissection. This method allows single hepatocytes to detach from liver in a non-disruptive manner so that their nuclei remain intact. Liver cells prepared in this was were allowed to air dry for 5 minutes and they were then fixed in 4% (v/v) formaldehyde in PBS (10×PBS (100 mM NaPO4 pH7.4, 1.5 M NaCl, 10 mM EGTA)). After washing in PBS the cells were permeabilised in KB buffer (10×KB (100 mM Tris.HCl pH 7.7, 1.5 M NaCl, 1% BSA)) with 0.1% Triton (v/v), washed twice in PBS and incubated for 30 min in the primary antibody diluted optimally (NR antibody (a gift of Professor W. Earnshaw, ICMB (Earnshaw and Rothfield, 1985)), 1:1000 in PBS/1% BSA/0.1% Sodium Azide). The coverslips were washed again twice in PBS/1% BSA/0.1% Sodium Azide and subsequently incubated in a 1:1000 dilution of the biotinylated secondary antibody (anti-human IgG) in the same solution for 30 min at room temperature. After this they were washed again and incubated for a further 30 min in Streptavidin/Texas Red-complex, 1:1000 dilution in PBS/1% BSA/0.1% Sodium Azide at room temperature. Finally the cells were washed and stained with DAPI (0.5 μg/ml in PBS) for 5 min, mounted on slides with Vectashield mounting medium and sealed with nail varnish.

Red dots within the nucleus of the hepatocytes corresponding to the centromeres in the chromosomes were scored using a fluoresence microscope (Axioplan 2, Zeiss) usinga 100×/NA 1.4 oil immersion objective lens. The images presented in this thesis were acquired by F. Nunez, Dr Sally Wheatley and Professor Bill Earnshaw using deconvolution, a technique to compress many focal planes into one image and to remove out of focus light. Pictures were processed using Adobe Photoshop.

Batch	Catalogue number	Antigen	Antibody Dilution	Fixative	Time in DAB (min)	Notes
C-19	Sc-397	P21/ Waf1	5:1000	Formalin	8	
N-20	Sc-494	MSH2	1:50	Formalin	8	
C-20	Sc-334	Ref1	1:4000	Formalin	10	No citrate recovery
CM5	NCL-p53-CM5p	P53	1:50	Formalin	3	
FL-261	Sc-7907	PCNA	1:5000	Formalin	2	
FL-261	Sc-7907	PCNA	1:1000	Methacarn	2	
C-Fos(4)	Sc-52	C-FOS	1:50	Formalin	3	
C-19	Sc-954	Cdc2	1:50	Formalin	4	

Table 2.2 Antibodies and conditions for immunohistochemistry. All antibodies were polyclonal rabbit anti-mouse.

Hepatocyte Nuclear Area Measurement

Liver samples were collected, fixed overnight (4% formaldehyde in PBS), and embedded in paraffin. Sections (3 μm) were cut and these were stained with haemotoxylin and eosin. The AxioHOME system (Zeiss) was used to measure the area of hepatocytes. The software used, BASIC Morphometry, allows the drawing around the periphery of each nucleus in a field and the area of each hepatocyte measured is calculated automatically in μm2. Typically, a 100×/NA oil immersion objective lens was used for the measurements and all of the nuclei in a given field would be measured. Results were analysed using Microsoft Excel and Sigma Plot software. For some experiments an Olympus BX60 with a ccd camera was used with analySIS (Norfolk Analytical) to measure hepatocyte areas. The two systems were compared and gave equivalent results.

In all studies, except those comparing the truncation and complete knockouts, results from both knockouts were pooled and treated as one.

Immunohistochemistry

General protocol – variations in Table 2.2. Liver samples were collected, fixed overnight (formalin (4% formaldehyde in PBS) or methacarn (methanol:chloroform:acetic acid, 3:2:1)), and embedded in paraffin. Sections (3μm) were cut and mounted on poly-L-lysine coated slides. Sections were dewaxed in xylene and rehydrated in an ethanol-water series. Endogenous peroxidase activity was blocked in H_2O_2:Methanol:Water (1:50:50). After washing in water, antigen retrieval used about 250 ml of a pH6 citrate buffer with 3×5 min in a plastic tub in a 700 W microwave. Sections were allowed to cool for 20 min and washed in a TBST buffer (pH 7.6, 0.145M NaCl, 12.5mM TrisHCl, 0.5% Tween20). Sections were then blocked for 5 min in Donkey serum (1:5 in PBS) (Diagnostics Scotland, Law Hospital, Carluke, Scotland) before incubation in primary antibody in TBS (TBST

without Tween20) overnight at 4°C. Sections were washed for 4×10 min in TBST before incubation for 1 hr in 1:50 biotinylated donkey anti-rabbit in TBS (Diagnostics Scotland). After washing for 2×10 mins in TBST, sections were incubated for 1 hr in StreptABComplex/HRP solution prepared according to the manufacturers instructions (Dako Ltd). After washing in TBST colour was developed in DAB solution prepared according to the manufacturers instructions (Dako Ltd). Sections were counterstained in 50% acidified haematoxylin (16 ml of glacial acetic acid per 350 ml undiluted stain) (Sigma Diagnostics) and Scott's Tap Water (1%(w/v) K_2CO_3, 10% (w/v)$MgSO_4$). They were then dehydrated using an ethanol-water series and cleared in xylene, before mounting in DePex.

All primary antibodies were acquired from Santa Cruz Biotechnology (www.scbt.com). Except for p53 which was acquired from Novocastra Laboratories Ltd (www.novocastra.co.uk).

PCNA immunohistochemistry was carried out using both formalin and methacarn fixed samples. Whilst formalin fixation acts on the entire population of PCNA, methacarn fixation may possibly only fix the active PCNA bound to DNA (Bravo et al., 1987; Burford-Mason et al., 1994).

All histology images presented here were acquired on an Olympus BX60 with a ccd camera and images were analysed using analySIS (Norfolk Analytical). Except where noted all image were taken with a 20× objective. The camera compensates automatically for lighter images so that immunohistochemistry images with light staining appear relatively darker than they appear down the microscope.

Chapter 3 – Cell cycle studies in ERCC1 null liver

Chapter Summary and Background

ERCC1 null mice have high levels of hepatocyte polyploidy and their appearance is similar to aged wt animals (McWhir et al., 1993; Weeda et al., 1997). The levels of polyploidy increase in wt mice as they age. This indicates that the ERCC1 null mice maybe suffering from accelerated ageing. I have confirmed that the development of polyploidy in the ERCC1 null mouse is accelerated compared to the development of polyploidy in the ageing wt mouse. The enlarged hepatocytes in both ERCC1 null and ageing wt mice are arrested in G2/M. The increased polyploidy is not a side effect of the runting observed in the ERCC1 null animals and the development of polyploidy is the same in the original insertion null animal and in a deletion knockout.

ERCC1 null hepatocytes have accelerated development of polyploidy and enlarged nuclei are detectable from birth

Nuclear Area Measurements

In order to document the development of polyploidy in ERCC1 null hepatocytes and to compare it to ageing wt samples, measurements were made of nuclear area to calculate area distributions. The area of hepatocyte nuclei is proportional to their volume and the volume is proportional to the DNA content (Bohm and Noltemeyer, 1981; Brasch, 1980; Epstein and Gatens, 1967; Kudryavtsev et al., 1993; Medvedev, 1986). Measurements of nuclear area can therefore be used to study changes in the DNA content of nuclei. This gives a semi-quantitative method of comparing the level of polyploidy.

The liver is composed of hepatocytes (parenchymal cells) and non-hepatocytes (non-parenchymal cells, such as lymphocytes and structural cells). The hepatocytes perform the metabolic functions of the liver and are roughly hexagonal in shape when viewed in any cross section. It is possible to easily differentiate between

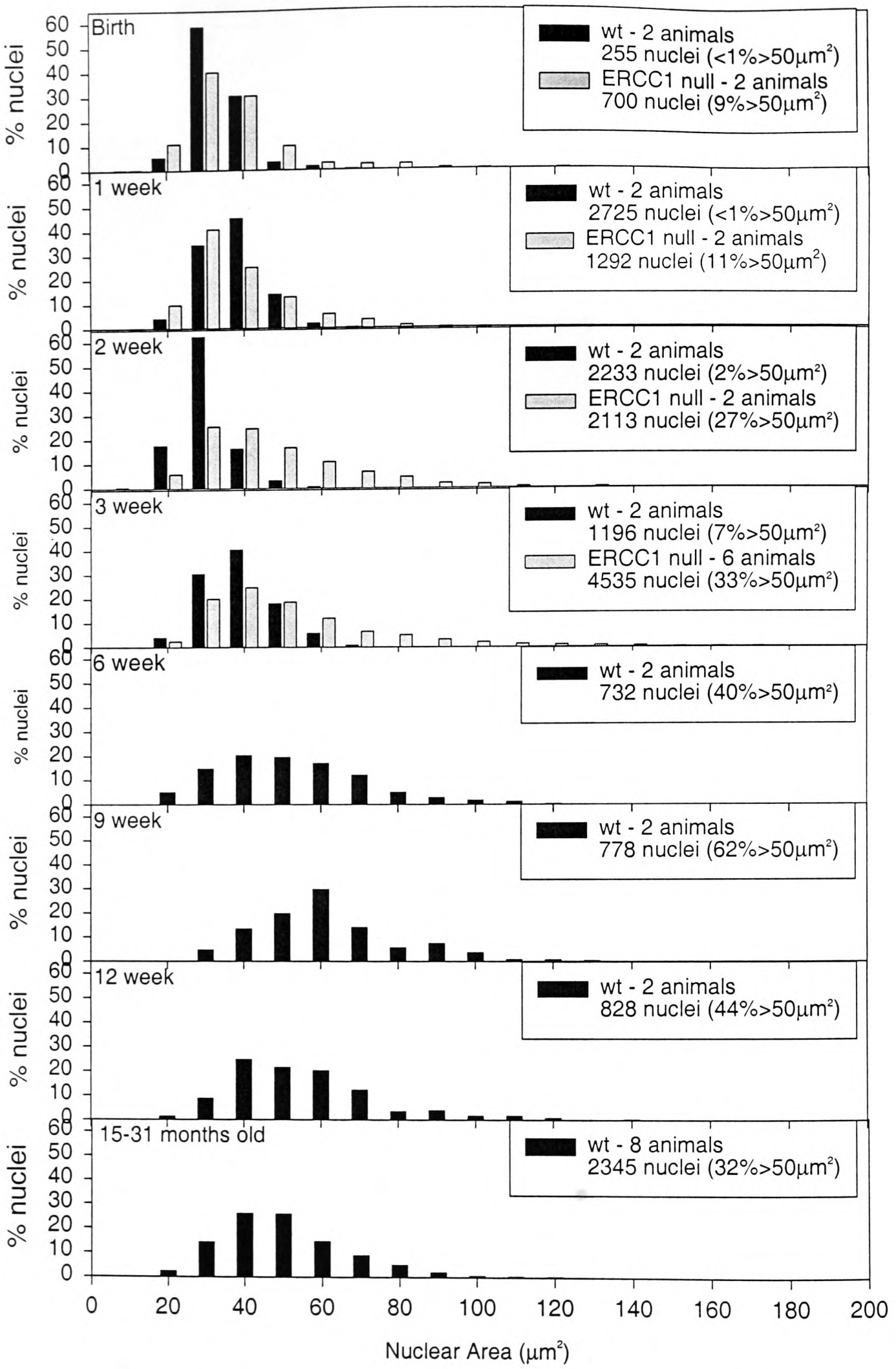

Figure 3.1 Hepatocyte Nuclear Area Distributions for ERCC1 null and wt animals from birth to death. The number of animals examined, total number of nuclei and percentage of the nuclei over 50 μm^2 is indicated. Each bar covers a range from 9.99 below the stated value to the value, e.g. 20 μm2 is 10.01 to 20 μm2.

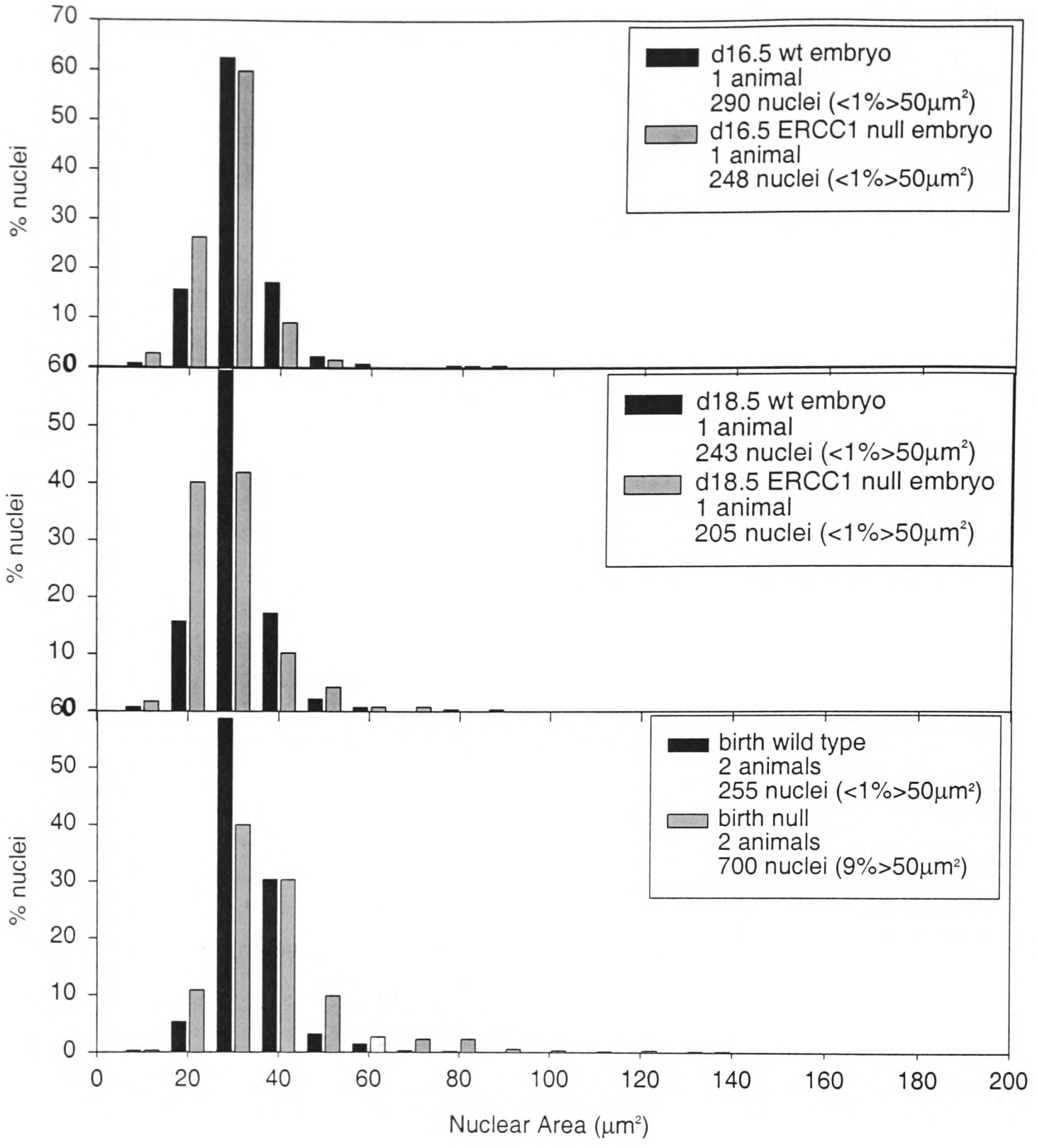

Figure 3.2 Distribution of the nuclear area of hepatocyte nuclei for ERCC1 null and wt animals for d16.5, d18.5 embryonic and birth. Number of animals studied, number of nuclei measured and percentage of those nuclei over 50 μm^2.Each bar covers a range from 9.99 below the stated value to the value, e.g. 20 μm2 is 10.01 to 20 μm2.

hepatocytes and non-hepatocytes because non-hepatocytes have condensed nuclei which take up stain strongly, whereas hepatocytes have much larger weakly staining nuclei, with a non homogenous staining pattern. The cytoplasm of hepatocytes often appears to have many small gaps in the tissue. This is because of the presence of lipid storage droplets in the liver, which can be often extracted by histology preparation protocols. The number and size of droplets/gaps depends on the nutritional status of the animal. Nuclear area measurements were only made of hepatocytes as there is no indication that non-hepatocytes display the polyploidy phenotype. Measurements were not made in the areas around the portal veins, as these areas have a high proportion of non-hepatocytes, or of the areas immediately adjacent to the edge of sections, as hepatocytes in those areas do not display the polyploidy phenotype so distinctly.

At birth, it is already possible to distinguish a difference between ERCC1 null and wt area distributions (Figure 3.1). There is clearly a higher proportion of large nuclei in the ERCC1 null samples than the wt sample. Less than 1% of wt nuclei at birth are over 50 μm^2, compared to 9% of ERCC1 null nuclei. 50 μm^2 has been chosen as a good cutoff mark for so called "normal" nuclei as the great majority of the nuclei in the 3 week old wild type samples are smaller than this. The relative proportion of large nuclei develops in the ERCC1 null samples over the three weeks after birth, until at 3 weeks old, 33% of ERCC1 null nuclei are over 50 μm^2, whereas only 7% of wt nuclei are over 50 μm^2. However, at 6 weeks old, 40% of wt nuclei appear to be over 50 μm^2 and at later ages the percentage of nuclei over 50 μm^2 stays between 32% and 62%. The nuclear area distributions indicate that by 6 weeks the level of polyploidy in wt hepatocytes is equivalent to that seen in 3 week old ERCC1 null hepatocytes. Before birth, less than 1% of nuclei are larger than 50 μm^2 in both ERCC1 null and wt samples and there appears to be no difference between the genotypes (Figure 3.2). These results work confirm and extend the results of McWhir and Weeda, who showed that enlarged nuclei were present in ERCC1 null hepatocytes (Weeda et al., 1997; McWhir et al., 1993).

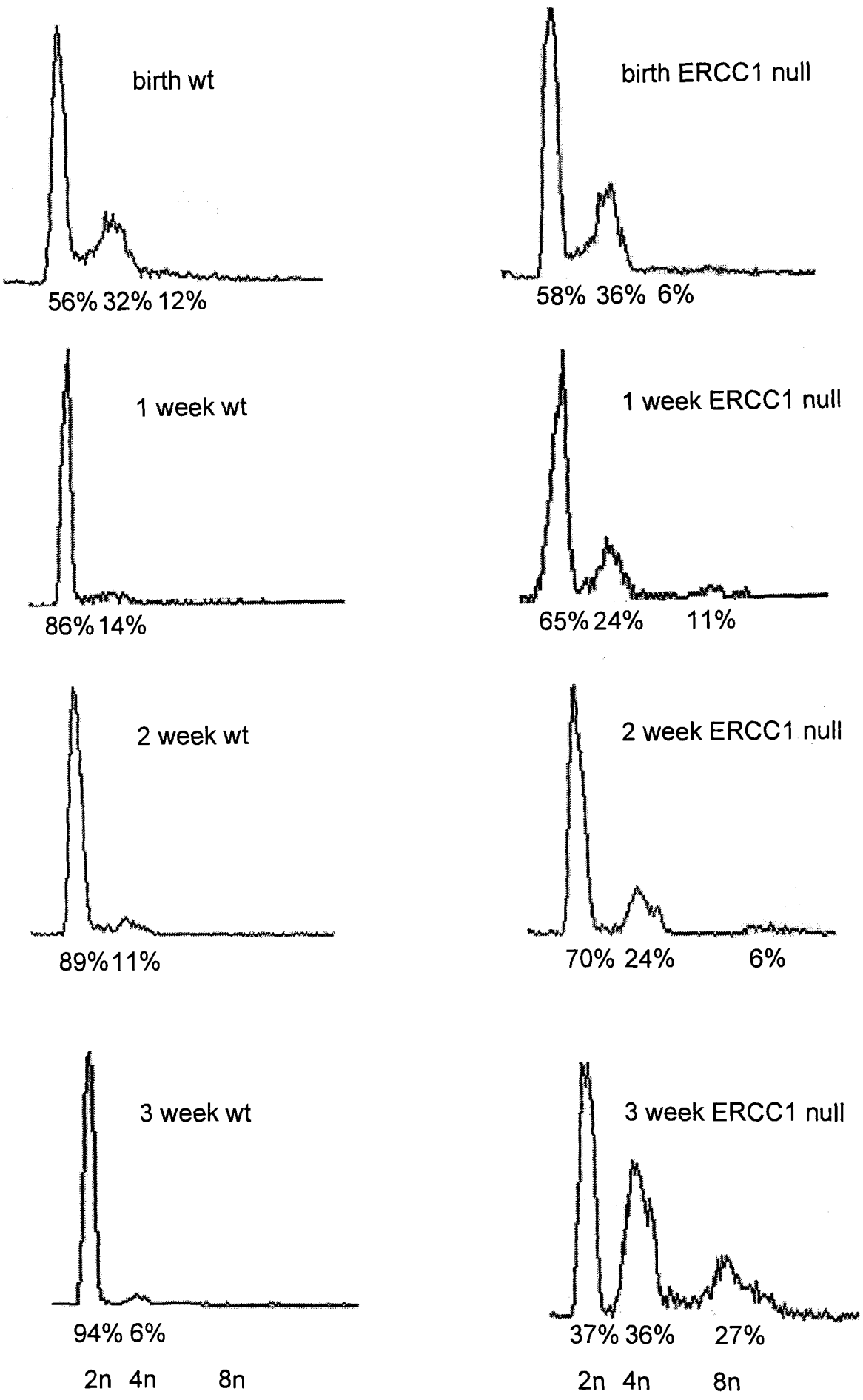

Figure 3.3 FACS profiles of ERCC1 null and wt liver from birth to 3 weeks old. The position of nuclei with 2n, 4n and 8n DNA content is indicated, as is the percentage of cells in each peak. These are typical examples of profiles taken from at least 4 animals for each age and genotype.

Although a proportion of the nuclei drastically increase in size, the vast majority stay about the same size. This means that the difference between the ERCC1 null, aged wild type and young wild type size distributions is not as obvious as when examining a picture of a section. A comparison of the percentage of nuclei that are greater than 50 μm^2 shows explicitly how the proportion of enlarged nuclei increase with age in both genotypes.

It might be expected that the distributions would show a smooth increase in the number of enlarged cells with age, however only a trend is obvious, and there is quite a large variation about the trend. This variation reflects the fact that the exact development of polyploidy varies between individual animals. The distributions shown are averages taken from a number of animals but the variation is still obvious. There is also a large variation in the proportion of enlarged nuclei between the different areas of the same liver, the large numbers of nuclei measured should correct for this, but it may still contribute to the variation in distributions.

FACS Profiles

FACS profiles have also been used to compare the development of polyploidy during ageing in wt and ERCC1 null liver. The FACS profiles measure the incorporation of propidium iodide into individual nuclei. This gives a direct way to precisely compare DNA content. The method used prepares individual nuclei. The FACS profiles tell a slightly different story to the nuclear area distributions. For all profiles, except the log profiles, at least 4 animals were tested and the samples shown are typical of those tested. Variation between animals was high especially in animals with high levels of polyploidy, but a trend could always be clearly distinguished from animals of one age to those of the next shown.

At birth, in both wt and ERCC1 null liver over 30% of nuclei have 4n DNA content and around 10% have over 4n DNA content (Figure 3.3). In 1 week old ERCC1 null liver, 24% of nuclei have 4n DNA content and 11% have 8n DNA content. In 1 week old wt liver however, only 14% of nuclei have 4n DNA content and none have greater than 4n. The proportions of nuclei with different DNA contents stays the

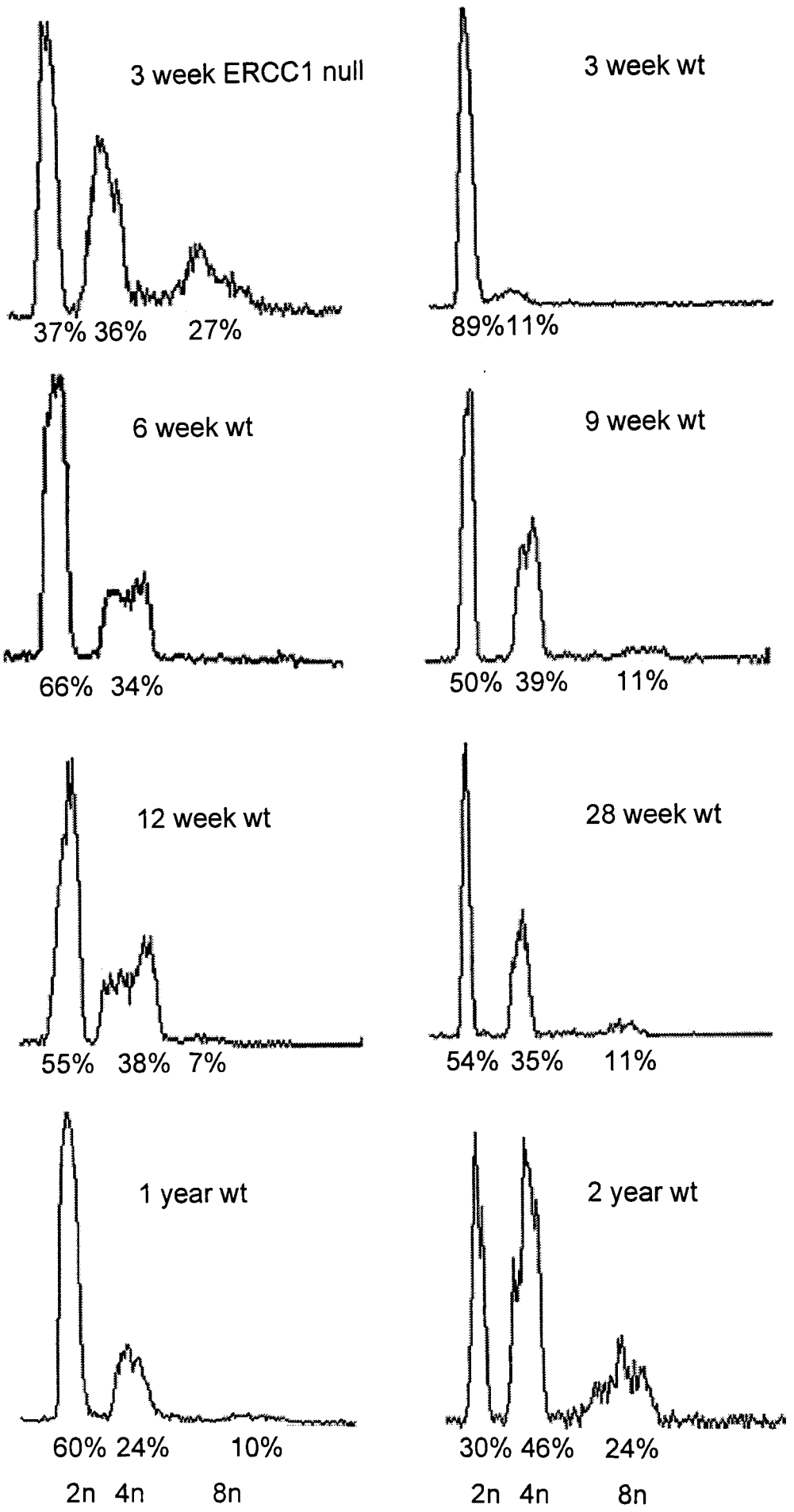

Figure 3.4 FACS profiles of ERCC1 null and wt liver from 3 weeks to 2 years. The position of nuclei with 2n, 4n and 8n DNA content is indicated, as is the percentage of cells in each peak. These are typical examples of profiles taken from at least 4 animals for each age and genotype.

same at about 2 weeks old, but at 3 weeks old 36% of ERCC1 null nuclei are 4n and 27% are 8n, whereas about 94% of wt nuclei are 2n and only 6% are 4n. Figure 3.3 shows how over the 3 weeks from birth the ploidy level of ERCC1 null liver increases, with an increased proportion of 4n nuclei and the appearance of an 8n peak. This contrasts strongly with the wt samples which stay roughly the same throughout the 3 weeks. Although the trend can clearly be seen from 1 week old to 3 weeks, there appears to be an anomaly at birth. These profiles show an increased number of 4n nuclei. It is clear from the nuclear area distributions and examination of sections that there are no enlarged hepatocytes in the wt samples at birth. The FACS profiles measure all the cells in the liver, which around birth has a large number of rapidly dividing cells involved in haematogenesis. A high proportion of these cells will be in G2 leading to a high 4n DNA content peak. This means that the birth FACS profiles provide a picture of the ploidy status in the liver as a whole, but are not informative about hepatocyte ploidy. The increased 4n peak at birth is due to haematogenic cells. The birth samples may have a small peak at greater than 4n due to the presence of polyploid megakaryocytes.

After 3 weeks when the ERCC1 null animals die, the ploidy level continues to develop in wt liver (Figure 3.4). In 6 week liver 34% of nuclei are 4n and by 1 year old 24% of nuclei are 4n and 10% are 8n. At 2 years old 46% of nuclei are 4n and 24% are 8n. The wt liver seems to attain the same level of polyploidy as the 3 week ERCC1 null liver at between 1 and 2 years old.

There seems to be some discrepancy between the nuclear area distributions and the FACS profiles. The nuclear area distributions indicate that by 6 weeks old, the wt samples have a similar area distribution to that seen in 3 week ERCC1 null samples. However, the FACS profiles indicate that level of polyploidy only becomes comparable to a 3 week ERCC1 null in 2 year old wt samples. I can give no comprehensive explanation for this discrepancy, but I believe the FACS profiles probably give a more accurate view of the polyploidy development as FACS profiles measure the DNA content in a nucleus directly. Nuclear area distributions measure DNA content indirectly by measuring the area of nuclei in a section and assuming

that the area of a nucleus is proportional to volume which is proportional to DNA content. Nuclear area measurements also do not measure the area of a nucleus at its widest point but at a thin slice taken at random through the nucleus. This means that the profiles are more flattened than they would be if only the true mid-cross-sectional area was measured. If the liver were composed of nuclei of one particular size only, the distribution would be stretch between the true mid-cross-sectional area of the nuclei and the smallest areas measured and all sizes would have the same value. When sections were analysed, below a certain size it was not possible to differentiate nuclei and this puts a lower limit on the areas measured.

The larger 8n cells only form a small proportion of the total even in the 3 week old ERCC1 null and 2 year old wt FACS profiles, which should give a true representation of the proportions of cells of different ploidy levels. The larger cells form a small proportion of the total and so they will not appear to a significant degree in the nuclear area distributions. The tendency of the nuclear area distributions to be flattened will also disguise the presence of increased numbers of very large cells. Perhaps the fact that the FACS profiles take a non-specific piece of liver, which includes the edge of the tissue, whereas the nuclear area distributions only take measurements from the centre of the tissue contributes. If the development of aging related polyploidy started in the middle of the tissue and then proceeded to the outside, then the nuclear area distributions measurements would detect this polyploidy earlier and the FACS profiles would detect it later. However, the FACS profiles nevertheless give a better description of the polyploidy development.

It would be interesting to use statistical testing to compare the nuclear area distributions. However, the most often recommended test to compare non-parametric distributions is the Kolmogorov-Smirnov test, which has not proved useful in this case. This test gives a significant difference to pairs of samples, even when by eye no difference can be seen.

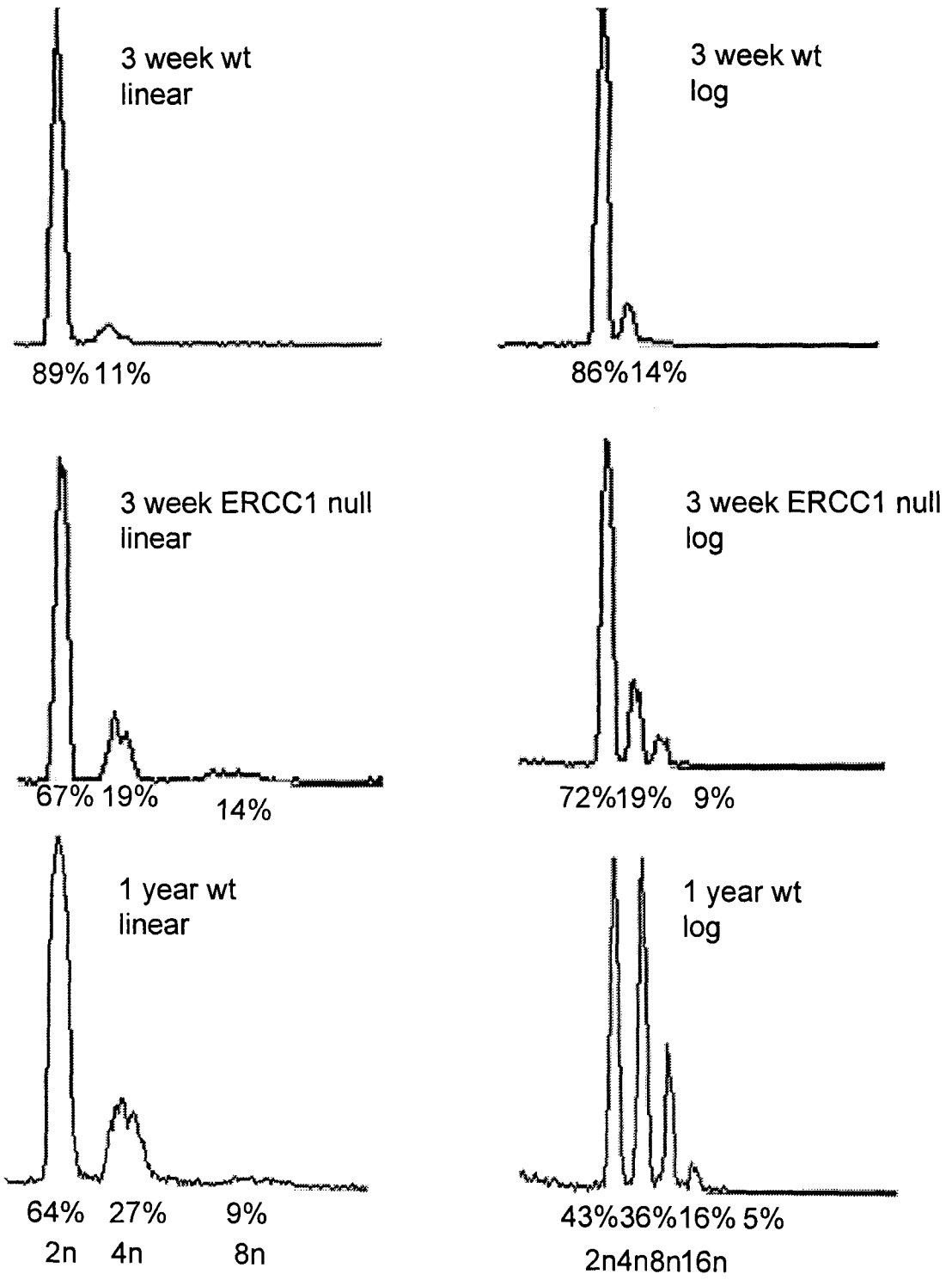

Figure 3.5 Linear and Log FACS profiles of ERCC1 null and wt liver at 3 weeks and 1 year old. The position of nuclei with 2n, 4n and 8n DNA content is indicated, as is the percentage of cells in each peak. The same sample was used for both log and linear profiles. Due to time constraints only one animal was examined for each type under log conditions, however the linear profiles are typical for animals of the ages and genotypes shown.

The settings used to acquire most of the FACS profiles show only three peaks for the 3 week ERCC1 null and old wt samples, however some other samples were measured using both logarithmic settings and the normal linear settings. Figure 3.5 shows how the logarithmic setting compresses the peaks and shows the presence of a 16n peak clearly visible in the 1 year old wt sample, this peak is however not clearly visible in the ERCC1 null sample. Unfortunately, this particular ERCC1 null sample does not display a particularly high level of polyploidy. There are differences between the percentages of cells in a particular peak between the log and linear profiles. This reflects both the fact that they are taken from slightly different parts of the tissue and differences in measuring peak areas between the log and linear profiles.

Both FACS profiles and nuclear area distribution measurements have been made as the two methods highlight different aspects of polyploidy development. The nuclear area distributions have the advantage that they are specific to hepatocytes and show how the distributions change over time. The FACS profiles allow one to see how the specific ploidy levels in the liver change, however they are not specific to hepatocytes.

The nuclear area distributions and FACS profiles show that the rate of development of polyploidy in the ERCC1 null mice is much faster than that seen in wild type mice. In fact, by birth there are already signs of polyploid nuclei in the ERCC1 null hepatocytes. However, the levels of polyploidy in the ERCC1 null mice do not exceed those in the aged wild type mice, in fact 16n nuclei have been seen in wt but not in ERCC1 null liver (although the sample tested was atypical). As the aged wild type mice are not dying of liver failure, but have a greater or equal polyploidy level than the ERCC1 null liver, it appears that the accelerated polyploidy, whilst a symptom of the phenotype, is not the cause of death.

ERCC1 null hepatocytes and enlarged hepatocytes in aged wild type animals are arrested in G2/M

Correction of FACS profiles

The FACS profiles and nuclear area distributions show clearly that the development of liver polyploidy is accelerated in the ERCC1 null liver, however, they give no information on hepatocyte cell cycle status. Further study of the FACS profiles reveals some information about the cell cycle status of the hepatocytes. Examination of FACS profiles of the ERCC1 null livers indicates that there is an increased 4n peak and the appearance of an 8n DNA content peak (Figure 3.4). However there still appears to be a significant proportion of nuclei in G1/2n. This is probably deceptive, as discussed earlier, because the FACS analyses include all of the cells from the liver; the hepatocytes that display the phenotype and various types of non-hepatocytes, including vascular tissue and white blood cells. The presence of these non-hepatocytes will increase the relative height of the G1 peak, as like most mature cells in the body they will be quiescent and have 2n DNA content.

In order to gain a more accurate reflection of the cell cycle status of the hepatocytes the relative proportions of non-hepatocytes and hepatocytes were calculated by examining liver sections. The calculations were made based on measurements from the central part of the tissue, avoiding any large blood vessels, and so these proportions probably underestimate the contribution of non-hepatocytes to FACS profiles. Non-hepatocytes are more common around the periphery of the liver and around blood vessels. The vast majority of non-hepatocytes in liver will tend to be in G1/G0, for these calculations it has been assumed that 100% are in G1/G0. About 35% of the cells in ERCC1 null livers were non-hepatocytes, compared to about 22% in wt livers. The difference in these figures is because the hepatocytes in ERCC1 null liver tend to be larger, so there are less hepatocytes in a given area, whereas the number of non-hepatocytes stays the same. The proportions of hepatocytes and non-

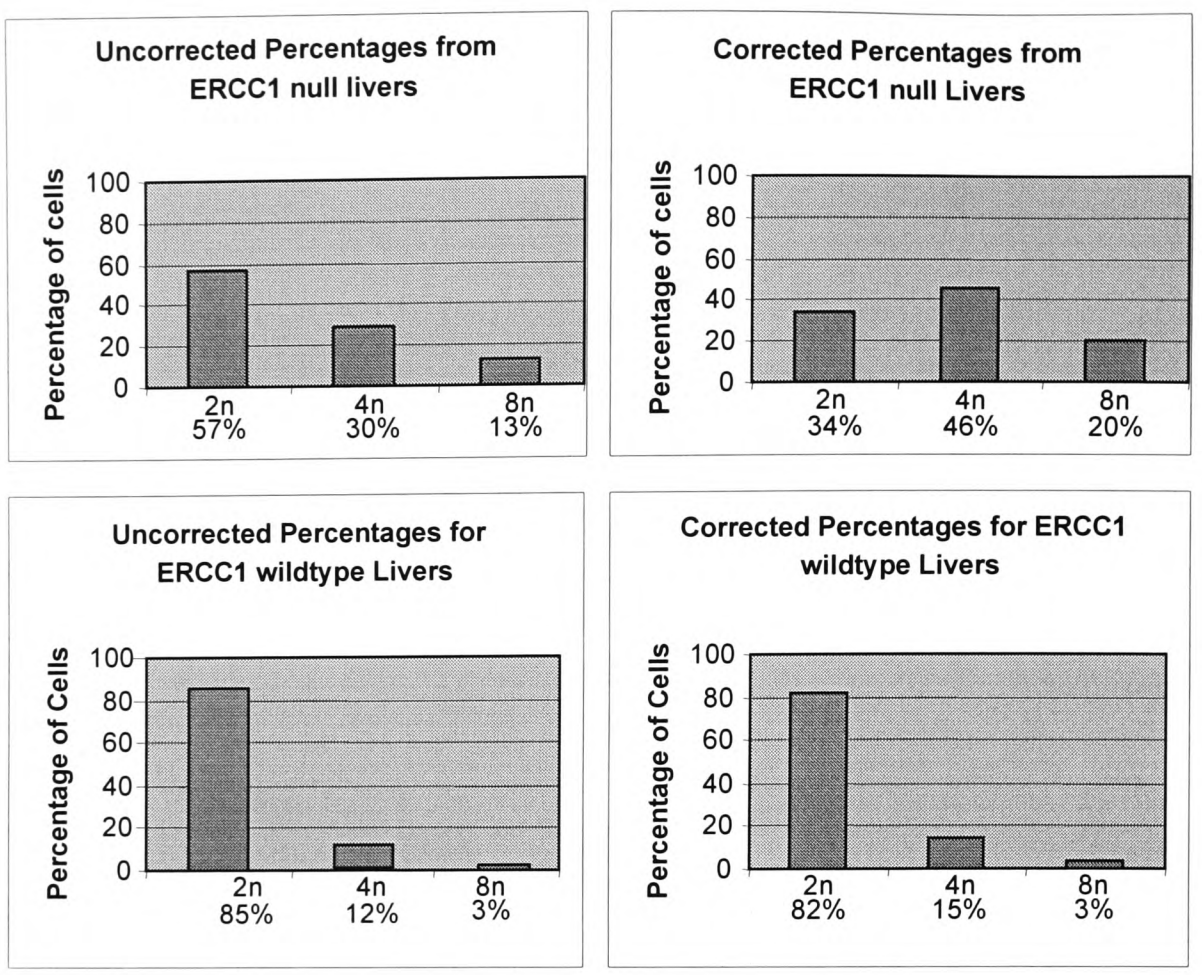

Figure 3.6 Corrected and uncorrected FACS profiles for 3 week old ERCC1 null and wt liver. Each genotype is the average of 2 animals. Corrected FACS profiles were calculated by subtracting the percentage of non-hepatocytes from the G1/G0 fraction. Fractions were then recalculated to total 100%.

Genotype	Small Nuclei - % in G2/M	SD	Enlarged Nuclei - % in G2/M	SD	Number of animals
3 week old wt	32	6	0	N/A	6
3 week old ERCC1 null	36	9	62	7	5
3 week old wt runt	36	4	0	N/A	2
Aged wt (~2 years old)	29	9	84	7	4

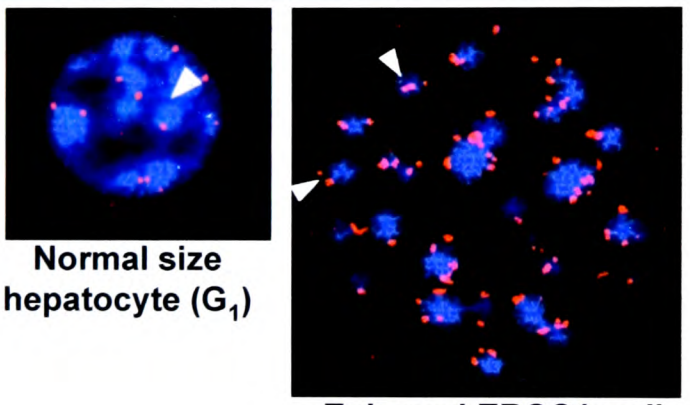

Normal size hepatocyte (G_1)

Enlarged ERCC1-null hepatocyte (G_2)

Figure 3.7 Percentage of small and enlarged nuclei in G2/M from centromeric immunostaining assay. Binding of the NR antibody to centromeres was visualised with a Texas Red-conjugated tertiary antibody. Each centromeric structure is represented by a red spot. The DNA is stained with DAPI and presents a blue colour. In normal size nuclei (mostly G1) the majority of structures appear as single spots, in enlarged nuclei (mostly G2) they appear as double spots. Nuclei were scored as G1 or G2 by eye and at least 50 nuclei were counted per sample. SD is the standard deviation.

hepatocytes were combined with the relative numbers of 2n, 4n and 8n nuclei derived from the FACS profiles to produce a profile that did not include the G1 contribution from non-hepatocytes. Figure 3.6 shows the corrected FACS profile for the ERCC1 null samples, this shows an increased relative proportion of 4n and 8n nuclei in the corrected sample. After correction for non-hepatocytes 34% of 3 week ERCC1 null nuclei have 2n DNA content, 46% have 4n and 20% have 8n DNA content. For 3 week wt nuclei 82% have 2n DNA content, 15% have 4n and 3% have 8n DNA content. This shows that only a small number of ERCC1 null hepatocytes are diploid and in G1. The majority of ERCC1 null hepatocytes are either diploid and in G2 or tetraploid and in G1. In order to distinguish between these two alternatives, and to study the cell cycle status in more detail, a more complex assay was required.

Centromeric Staining Assay

To further investigate the cell cycle status of the hepatocytes, a trial of a fluorescense immunostaining assay was carried out by F. Nunez. This used a primary antibody (NR) which recognises the cenpA, cenpB and cenpC antigens of the centrosome (Earnshaw and Rothfield, 1985). Cells in G1/G0 and S have single centromeres which can be seen as single dots whereas those in G2 have double centromeres which can be resolved as individual paired dots (Brenner et al., 1981). This trial showed that around 70% of 3 week wt hepatocytes were at G1 and 30% at G2/M, whereas in 3 week ERCC1 null samples 75% of the hepatocytes were in G2/M. This seemed to indicate that the ERCC1 null hepatocytes are arrested in G2/M.

I have extended this assay to study whether the enlarged or normal nuclei or both are arrested in G2/M (Figure 3.7). There is no significant difference between the normal sized nuclei in the ERCC1 null and 3 week old wild type samples (by Student's *t* test), and ~30% are in G2/M. However, the enlarged nuclei in the ERCC1 null sample have a statistically significant increase in the number of nuclei in G2/M when compared to normal sized wt samples ($p=0.01$) and 62% of nuclei are in G2/M. The aged wild type nuclei have the same spread of cell cycle status as the ERCC1 null nuclei ($p=0.01$), 29% of the small nuclei are in G2/M, whereas 84% of the enlarged

nuclei are in G2/M . These results show two populations of hepatocytes in the ERCC1 null and aged wild type liver; smaller hepatocytes that are spread through the cell cycle in the normal proportions and enlarged hepatocytes that are largely arrested in G2. Thus the increased 4n peak in FACS profiles of 3 week ERCC1 null liver is probably due to a mixture of diploid G2 and tetraploid G1 nuclei.

The interpretation of these results depends crucially on the division of nuclei into enlarged and normal classes. It is not possible to draw a clear division between enlarged nuclei and normal nuclei. The great majority of nuclei are a very similar size and are easy to differentiate from the grossly enlarged nuclei, but the split is somewhat subjective. When analysing preparations only cells that were clearly normal size were taken as normal, and only cells that were clearly enlarged were taken as enlarged. This inevitably leaves a small number of nuclei unassigned between the two classes. As normal sized nuclei in G2 would be expected to be larger than their brethren in G1, there may be a propensity to select against normal G2 cells. This would tend to reduce the percentage of cells scored in G2 in the normal population. However, as the corrected FACS profiles reveal, there are a large number of cells with 4n DNA content compared to 2n in the ERCC1 null sample, this means that as long as the vast majority of nuclei were taken as normal, it is unlikely that the result was skewed badly for the normal nuclei.

Even if the cell cycle status of the classes of nuclei is skewed slightly, it is still possible to say that the overall proportion of nuclei in G2 is greater in the ERCC1 null than in the wildtype. Measurement of the cell cycle status in the trial experiments still show an increased G2 percentage in the ERCC1 null samples, when no attempt was made to separate the normal and enlarged nuclei. Non-hepatocytes were easy to distinguish from hepatocytes because of the relatively condensed nuclei and were not scored.

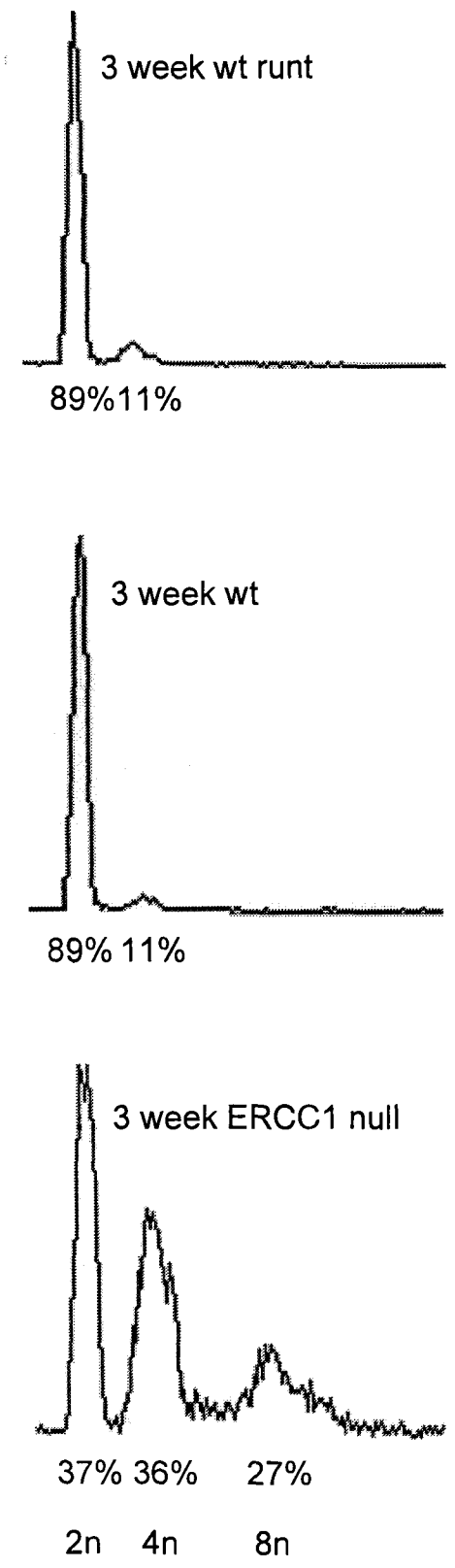

Figure 3.8 Wt runt liver has the same FACS profile as normal wt liver, not the same as ERCC1 null liver. All samples are ~3 weeks old. The position of nuclei with 2n, 4n and 8n DNA content is indicated, as is the percentage of cells in each peak. These are typical examples of profiles taken from at least 4 animals for each age and genotype.

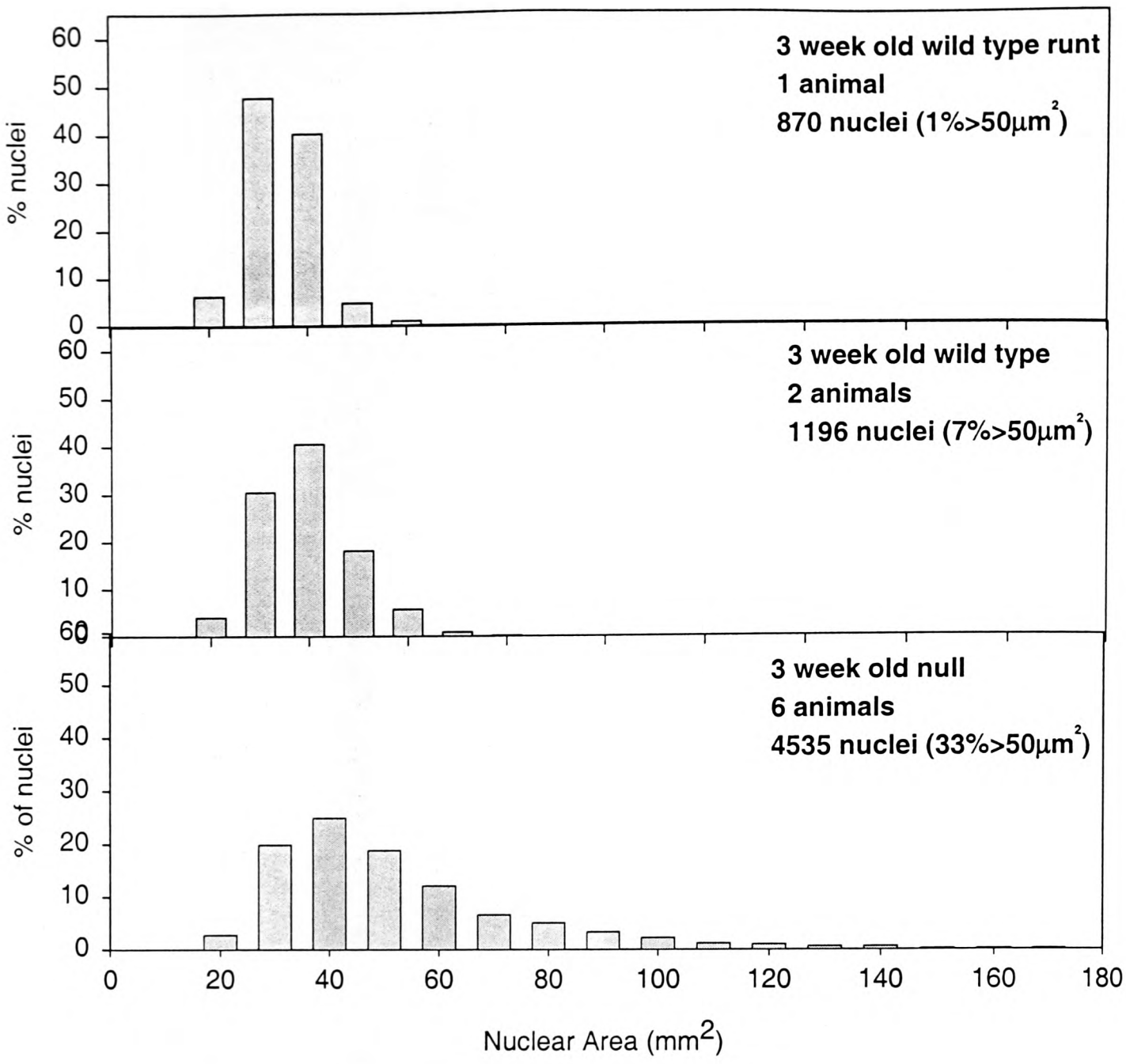

Figure 3.9 Hepatocyte Nuclear Area Distributions for ERCC1 null, wt and wt runt. The number of animals examined, total number of nuclei and percentage of the nuclei over 50 μm^2 is indicated.

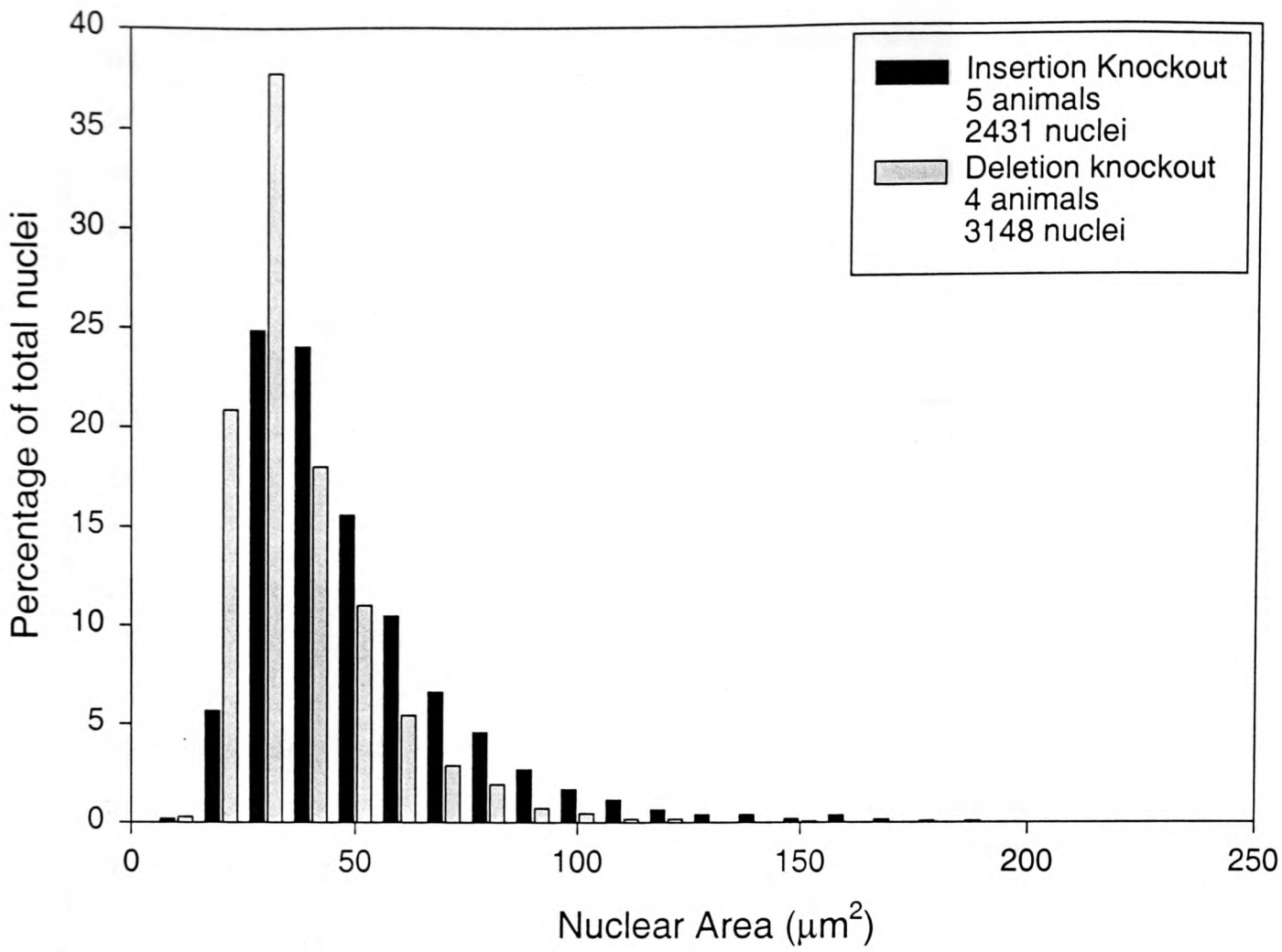

Figure 3.10 Hepatocyte Nuclear Area Distributions comparing 3 week old insertion and deletion ERCC1 null. The number of animals examined and total number of nuclei is indicated.

The ERCC1 null phenotype is not a feature of runted animals

As the ERCC1 null mice are runted, it was possible that the high level of polyploidy and G2/M arrest seen in the hepatocytes was an aspect of the runting, rather than a direct result of the ERCC1 deficiency. To test this a study was made of several wt runts of a similar genetic background to the ERCC1 null animals. A comparison of the wt runts with the ERCC1 null runts and normal wt animals, shows that the FACS profiles, nuclear size distributions and centromeric staining assay results are the same for wild type runts as for normal wt animals (Figure 3.7, 3.8, 3.9). Wt runts have a tight nuclear area distribution, a low level of 4n nuclei and a low level of G2/M nuclei, the same as normal wt animals. This result indicates that the gross cell cycle and polyploidy phenotype seen in the ERCC1 nulls is not a side effect of runting but is due to other reasons.

The original ERCC1 insertion null phenotype is not significantly different from a deletion knockout

The original ERCC1 null line was an insertion knockout (McWhir et al., 1993). A deletion ERCC1 null line has also been constructed in order to see if this displayed an altered phenotype (KT Hsia; personal communication). Nuclear area distributions have been used to compare the phenotypes of the two different knockouts. Figure 3.10 shows that there appears to be no difference in distribution between insertion and deletion ERCC1 null liver. This indicates that the original insertion ERCC1 null animal is effectively the same as the deletion knockout. In the rest of this thesis, results from the two lines have been combined and treated as one. However, results for all experiments showed no difference between the two lines.

Discussion

Just as ERCC1 null hepatocytes display an increase in polyploidy with age, so do wt hepatocytes (Epstein and Gatens, 1967). At 2 weeks old about half of all the hepatocytes are binuclear and by 4 weeks old about 80%. This level of binucleation stays the same until at least 1 year old. Nuclei are predominantly 2n and 4n at 4 weeks old, but 8n nuclei appear and numbers increase rapidly, whilst the levels of 2n nuclei decrease. From 6 weeks old 16n nuclei are found, although the levels never increase above 8% (Bohm and Noltemeyer, 1981). Whilst in ERCC1 null hepatocytes there is a high level of polyploidy by 3 weeks when the animals die, in wt animals it takes more time to reach a similar state of ploidy. The wt mice do not die when they reach the same level of polyploidy as the ERCC1 null mice, which indicates that the increased polyploidy is not directly causing death in the ERCC1 nulls. In fact, a development of polyploidy is seen in many organs as they age, including blood, muscle, cornea, thyroid, pancreas, endometrium, placenta, urinary bladder and neural tissues (Brodsky and Uryvaeva, 1977; Harris, 1971; Kudryavtsev et al., 1993). In wt mouse liver development the number of binucleate cells also increases with age, interestingly, ERCC1 null livers have a lower rate of binucleation than wt liver (Nunez et al., 2000). In 3 week old ERCC1 null liver 3% of hepatocytes were binucleate (n=13), compared to 8% of hepatocytes in wt liver (n=7), this was a significant difference (p=0.05) (Nunez et al., 2000). It would seem likely that there is a connection between polyploidy and binucleation. Binucleate cells, in a similar way to polyploidy nuclei, have arrested before the completion of mitosis. It could be suggested that binucleate cells have escaped the particular arrest in G2/M of polyploidy nuclei and have progressed further, only to meet a block before the completion of cytokinesis. Perhaps this represents a further way to increase/maintain liver metabolic function without cell division and the concurrent cancer risk.

The polyploidy in old wt hepatocytes is associated with increased accumulation of the lipid peroxidation product lipofuscin and increased cytoplasmic complexity (Hall et al., 1989; Sigal et al., 1995). Interestingly, increased levels of disruption of mitochondrial membranes and increased levels of lipid accumulation are seen in the

ERCC1 null mouse when compared to wild type (KT Hsia; personal communication).

The accelerated polyploidy in the ERCC1 null hepatocytes could be caused directly by increased levels of DNA damage, or by non-specific damage to the liver due to the effects of DNA repair deficiency. The ploidy of hepatocytes tends to increase with any sort of liver damage, for instance alcohol. Polyploidy is associated with hypertrophic responses in tissues and with cell aging, as observed in cultured fibroblasts undergoing senescence (Biesterfeld et al., 1994; Katz, 1994). It is thought that the development of polyploidy may be to increase the effectiveness of the liver under stress. Hepatocytes may accumulate damage more quickly than other cells because of their role in metabolising toxins.

Liver polyploidy develops as mice age and the development of polyploidy tends to be greater in mice than in other mammals, such as humans. Polyploidisation is restricted to the periods of active growth and development in human liver and does not attain as great a level as in mouse and there is no rapid increase in binucleation and polyploid cells in post natal growth (Kudryavtsev et al., 1993). Polyploidy in rat liver only develops until 12-14 months old and does not continue like in mouse, the ploidy level generally only reach tetraploidy. In mice, polyploidy development continues until death and accumulation of up to 32N nuclei is seen. Mouse liver mass declines near death, but polyploidy still continues to develop (Medvedev, 1986).

Polyploidy maybe a mechanism to allow the liver to preserve its full metabolic function under toxic load, without cell division of damaged cells, which could lead to cancer (Medvedev, 1986). Liver function is important for metabolism of proteins, carbohydrates and fat. Hepatocytes that are damaged by toxins cannot be replaced by new hepatocytes because the mitosis of cells with damaged DNA would increase cancer risk. Polyploid hepatocytes have redundant extra copies of vital genes and this is thought to increase toxin and carcinogen resistance. In fact, hepatocytes do not readily undergo apoptosis after DNA damage (Bellamy et al., 1997). The

increased size of polyploid cells allows the liver to adapt to ageing related cellular loss and still preserve function. Cell size is generally proportional to DNA content and so polyploid cells can have more functional capability than diploid cells (Gregory et al., 2001). Polyploidy may be a defence mechanism against intrinsic DNA damage in order to preserve at least one good copy of essential genes as liver ages.

Polyploidy occurs by endoreduplication, in which there are three possibilities which could occur in liver, either continuous rounds of DNA replication, with distinct gap phases, occur in the absence of mitosis, S phase reoccurs without a gap or there are multiple initiations within a given S phase (Grafi, 1998). Hepatocytes have unusual proliferative abilities for somatic cells, although normally relatively quiescent, after partial hepatectomy the liver mass is restored rapidly by the development of polyploidy with most hepatocytes undergoing two or three rounds of DNA synthesis (Brodsky and Uryvaeva, 1977; Gerlyng et al., 1993). Hepatocytes from adult animals can divide repeatedly after transplantation into reduced liver, suggesting extensive replication potential in hepatocytes, however it is unknown whether all transplanted hepatocytes participate in this replication, or merely a subset (Laconi et al., 1998; Mignon et al., 1998; Overturf et al., 1997; Sigal et al., 1999). Liver regenerative capacity is decreased in older animals with greater proportions of polyploid hepatocytes (Brodsky and Uryvaeva, 1977). After mild insults to liver, hepatocytes can regenerate, however where the regenerative capacity of hepatocytes is compromised it is proposed that oval cells that may be derived from the biliary cells can serve as progenitors (Alison, 1998; Dabeva et al., 1995).

The enlarged hepatocyte nuclei in both ERCC1 null and ageing wt samples are arrested in G2-M. As the nuclei are undergoing endoreduplication to become polyploid, they must be cycling but missing out M phase. As they probably suffer from accumulated DNA damage, they probably arrest naturally in G2 before the mechanism activates that allows them to skip mitosis.

Chapter 4 – Changes in protein expression in ERCC1 null liver

Chapter Summary and Background

The accelerated development of liver polyploidy in ERCC1 null mice is very similar to that of transgenic mice that overexpress p21 in the liver, and in fact the ERCC1 null mice have increased p21 mRNA levels in the liver (Nunez et al., 2000). Thus it seems likely that the p21 increase in the ERCC1 null livers is the cause of the accelerated polyploidy. If the increase in p21 levels is causing the accelerated polyploidy then the increase should be found mainly in those nuclei which are polyploid. In order to test this, and to confirm that the levels of p21 protein are increased in ERCC1 null liver, immunohistochemistry has been used. This shows that there are increased levels of p21 protein in the ERCC1 null hepatocytes and that this increase is mostly in the enlarged nuclei. A small increase in p21 levels was seen in old wt liver samples. p53 levels have been shown to be slightly increased in ERCC1 null hepatocytes, but the ERCC1 null phenotype is p53-independent. REF1 and MSH2, DNA repair proteins, are also upregulated in ERCC1 null hepatocytes.

Increased p21 levels in ERCC1 null hepatocytes

In order to confirm that the staining seen was specifically for p21, a UV irradiated skin sample was used as a positive control. This was from a time course of skin samples after UV irradiation where the p21 immunochemistry staining conformed to that seen in a published time course (Lu et al., 1999). Preliminary Western analysis of ERCC1 null and wild type tissue using the p21 antibody suggests that the antibody mainly detects a protein corresponding to the expected molecular weight for p21 (D. Melton; personal communication). The variability in increases in staining levels in ERCC1 null liver corresponds well to that seen in Northern analysis of p21 levels in ERCC1 null liver. High levels of increases are also seen in both immunohistochemistry and Northern analysis. This all suggests that the antibody being used detects p21 and that the vast majority of signal seen is derived from increases in p21 levels rather than other proteins. It would be an extreme coincidence if another protein (not p21) that was specifically detected by the antibody was also expressed in greatly increased levels in ERCC1 null liver. The

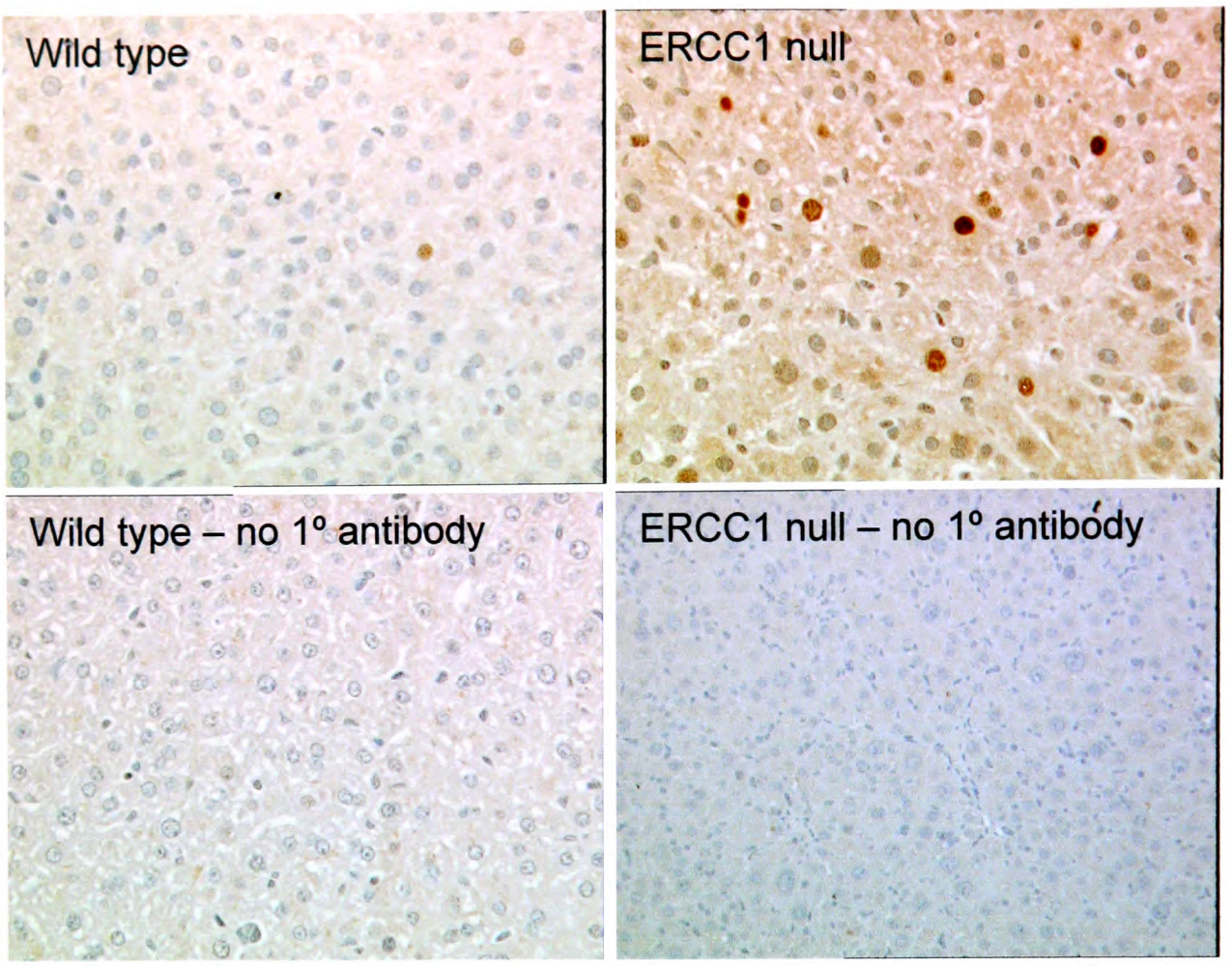

Mean % staining		
ERCC1 null	STDEV	n=
27	25	8
wt	STDEV	n=
4	4	5

% staining for individual samples	
ERCC1 null	Wildtype
73.1	8.5
57.9	6.5
24.8	1.3
24	1.1
21.4	0.4
14.8	
2.3	
1.5	

Figure 4.1 p21 immunohistochemistry on 3 week old ERCC1 null and wild type liver. Typical staining patterns are shown for ERCC1 null, wild type and control samples without primary antibody. The percentage of nuclei that stain positive for p21 is also shown, both as an average and for individual samples from different animals.

highly nuclear specific nature of the immunohistochemistry staining indicates that the antibody is specifically detecting one protein.

Preliminary immunohistochemistry studies showed that p21 expression in individual hepatocyte nuclei tends to be either on (at a high level) or off (at a low level) and that it is relatively easy to segregate nuclei by eye into those which stain positive for p21 and those which do not. Scoring in this way showed that whilst ~4% of the hepatocyte nuclei in 3 week wt sections were stained, ~27% of hepatocyte nuclei in the 3 week ERCC1 nulls stained positive for p21 (Figure 4.1). This confirms that p21 protein levels are increased in the ERCC1 null liver and that the increase is specifically associated with hepatocytes rather than just with other cell types. On a visual inspection, the larger nuclei in the ERCC1 null samples appear to be stained more often than the small nuclei.

Figure 4.1 shows a large variation in the amount of staining between samples of the same genotype. Some of the heterogeneity in staining may possibly be artifactual. Due to technical constraints it was only possible to stain 5 samples at once, including a positive control. Although the percentage of stained nuclei in the positive control was calculated to confirm that the level of staining was the same, there were small differences between staining sets. The level of staining would vary by perhaps 10%, i.e. if a sample normally had 30% of nuclei staining this would vary between about 27% and 33%. This may contribute somewhat to the heterogeneity, however as will be discussed later the heterogeneity in staining may be connected to heterogeneity in nuclear area distribution

In general, the background cytoplasmic staining in the ERCC1 null samples was stronger than in the wt samples, this is slightly unexpected as p21 is mainly a nuclear protein. If this is merely background then it could be making the ERCC1 null samples appear more strongly stained than they really are, however this cytoplasmic staining is probably due to the nature of the ERCC1 null sections in having more p21 present rather than true background. An increase in nuclear p21 levels means higher

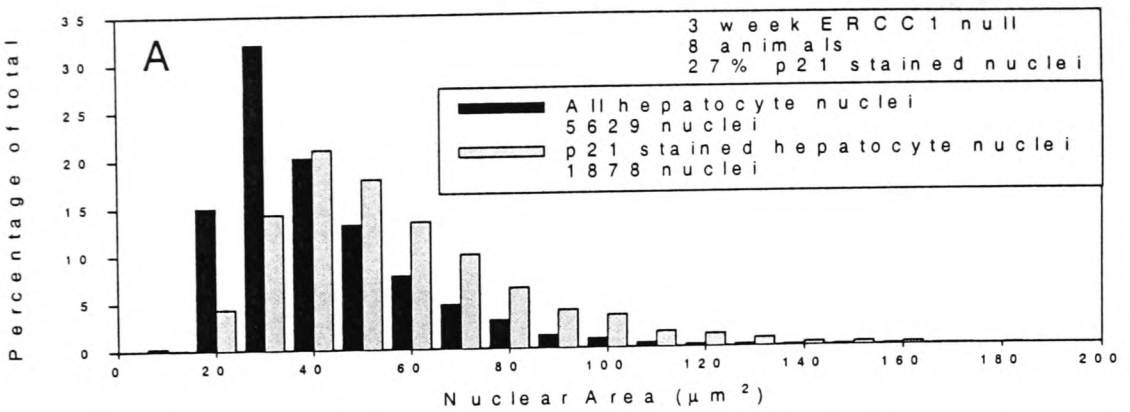

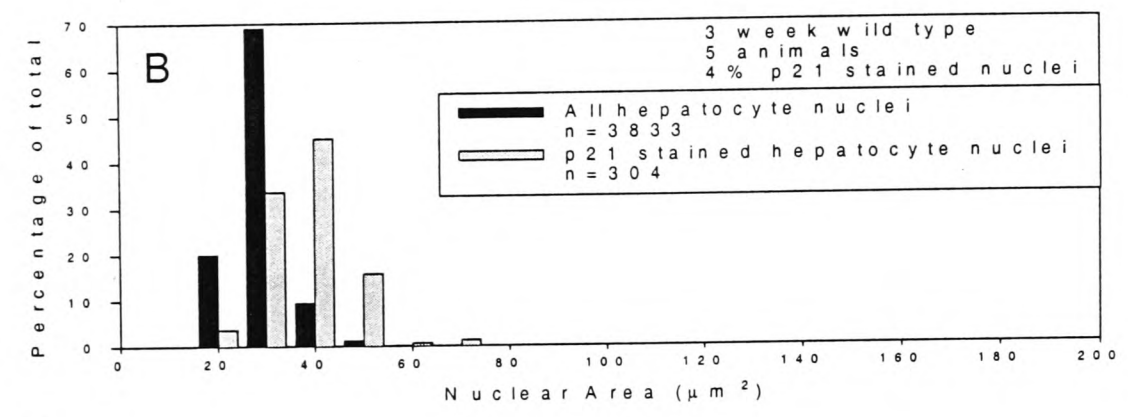

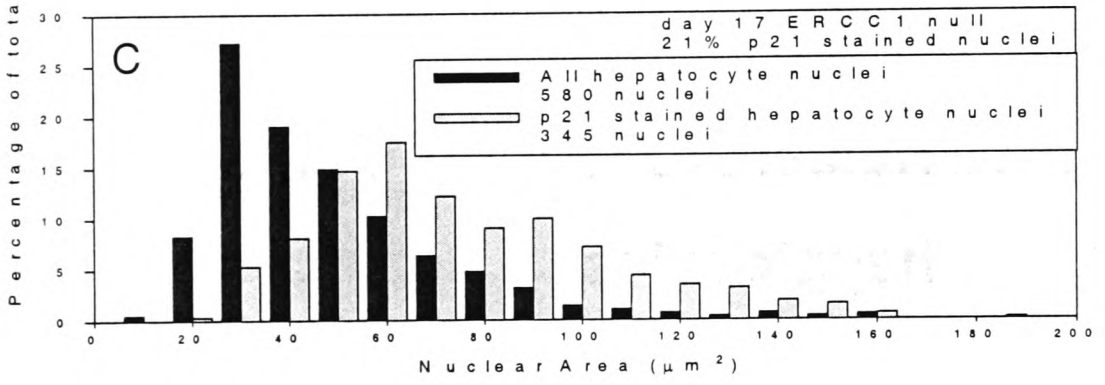

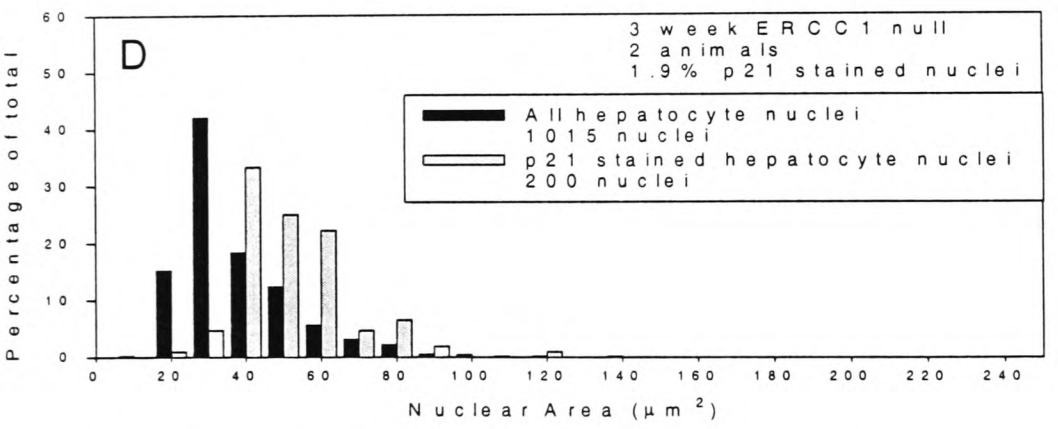

Figure 4.2 Nuclear size distribution graphs for p21 stained liver. p21 stained nuclei tend to be larger than the total population average. Distributions are shown for a summary of all 8 ERCC1 null animals tested (A), a summary of 5 wt animals (B), a d17 ERCC1 null animal with a high level of p21 staining (C) and a summary of 2 ERCC1 null animals with a low level of p21 staining (D).

levels of translation, perhaps increased levels of newly translated p21 are being detected before transport into the nucleus.

p21 stained nuclei are restricted to the enlarged ERCC1 null hepatocytes

In order to test whether the p21 staining is directly associated with the polyploid nuclei, measurements were made of nuclear area in the ERCC1 null and wt samples that had been stained for the presence of p21. The area distribution of the stained nuclei was calculated and also the area distribution of all the nuclei in a sample; both stained and unstained.

Figure 4.2 shows a graphical comparison of the nuclear area distributions for the ERCC1 null nuclei; for all nuclei and for stained nuclei. Most of the stained nuclei are over 40 μm^2 whereas most of the total nuclei are under 40 μm^2. This demonstrates that the stained nuclei tend to fall within the larger part of the population. The example shown in panel C illustrates this particularly well, but it is also apparent in the summary graph in panel A. The increased p21 levels are associated with the increased polyploidy in the ERCC1 null hepatocytes.

In light of the apparent tendency of the p21 stained nuclei in the ERCC1 null liver to be restricted to the enlarged nuclei, nuclear area distributions have also been measured for the p21 stained and total populations in the 3 week wt samples. Using a graphical analysis it appears that the p21 stained nuclei in the wt samples also tend to fall in the larger part of the nuclear area distribution (panel B). This is despite the fact that the wt samples do not have a high percentage of enlarged nuclei.

There is a large degree of heterogeneity in the percentage of p21 staining in different ERCC1 null samples (Figure 4.1). Heterogeneity in p21 mRNA levels in ERCC1 null liver has been observed before (Nunez et al., 2000). The two ERCC1 null samples in Figure 4.2 (panel D) with a low level of p21 staining appear to have less exaggerated accelerated polyploidy development. Only 12 % of the total nuclei in

the samples in panel D are over 50μm^2, whereas 19.2% of the total nuclei from all 8 samples tested are over 50μm^2. This confirms that the presence of increased p21 levels does correlate with polyploid nuclei.

The percentage of ERCC1 null nuclei in the enlarged (over 50 μm^2) class and normal (below 50 μm^2) class that stain positive for p21 has been calculated. This shows that 53% of the enlarged nuclei stain positive for p21, compared with 23% of the normal sized nuclei. The percentage of p21 stained nuclei in wt samples is so low that the comparative figures for wt samples are insignificant. This correlation between enlarged nuclei and increased p21 levels seems high but there are a significant proportion of enlarged ERCC1 null nuclei without increased p21 levels and there are also a significant proportion of small wt nuclei with increased p21 levels. This makes it difficult to say whether p21 is causing the increase in ploidy. p21 maybe causing the increase in ploidy for at least some of the enlarged nuclei. Perhaps the activation of other factors, as well as p21, is necessary to increase the ploidy. This would explain why some of the normal sized nuclei stained positive for p21. Perhaps there are also other pathways that activate the increase in ploidy. This would explain why some of the enlarged nuclei do not stain positive for p21. Alternatively, it may be the case that p21 levels are only increased at certain stages in polyploidy development. After stimulation of liver polyploidy by partial hepatectomy, p21 levels are increased in G1 phase and following S phase, but not during S phase (Albrecht et al., 1997). Perhaps the normal nuclei with increased p21 levels are close to entering an endoreduplication cycle and the enlarged nuclei without increased p21 levels have past the stage where p21 is involved.

The wt samples also seem to have more p21 staining in the larger cells, although they have few enlarged cells (Figure 4.2 (panel B)). This is unexpected. I believe this is a real result and not due to some bias. It could be imagined that in the nuclear area measurements the stained nuclei are measured as slightly bigger than they actually are, because the stain could diffuse beyond the boundaries of the nucleus and make it appear larger. This is probably untrue as both unstained and stained nuclei seem to

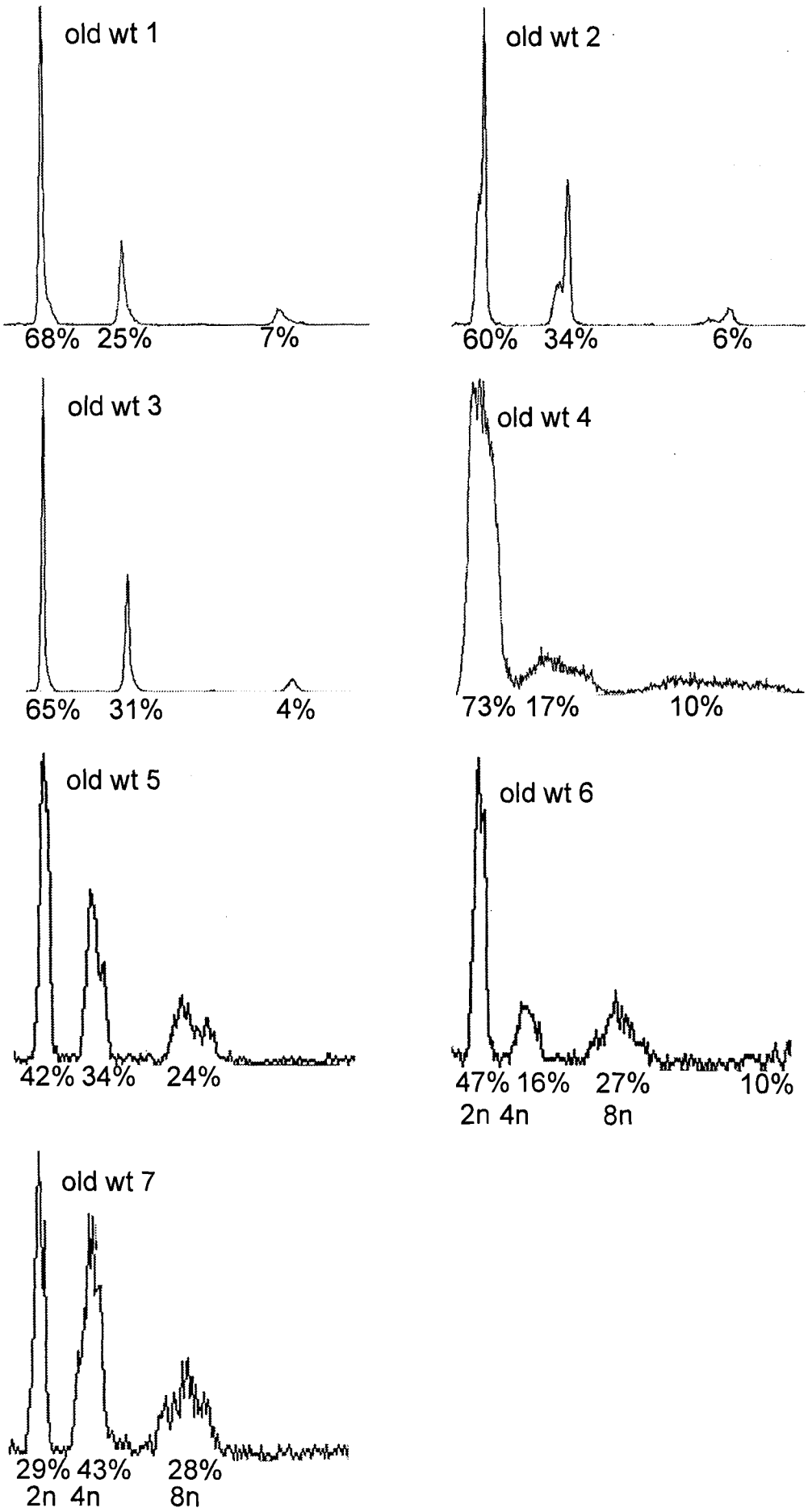

Figure 4.3 FACS profiles of old wt liver. Ages between 18 and 27 months old. Samples 1-3 were measured on a Coulter XPICS XL machine. Samples 4-7 were measured on a Beckman Dickinson FACScan machine

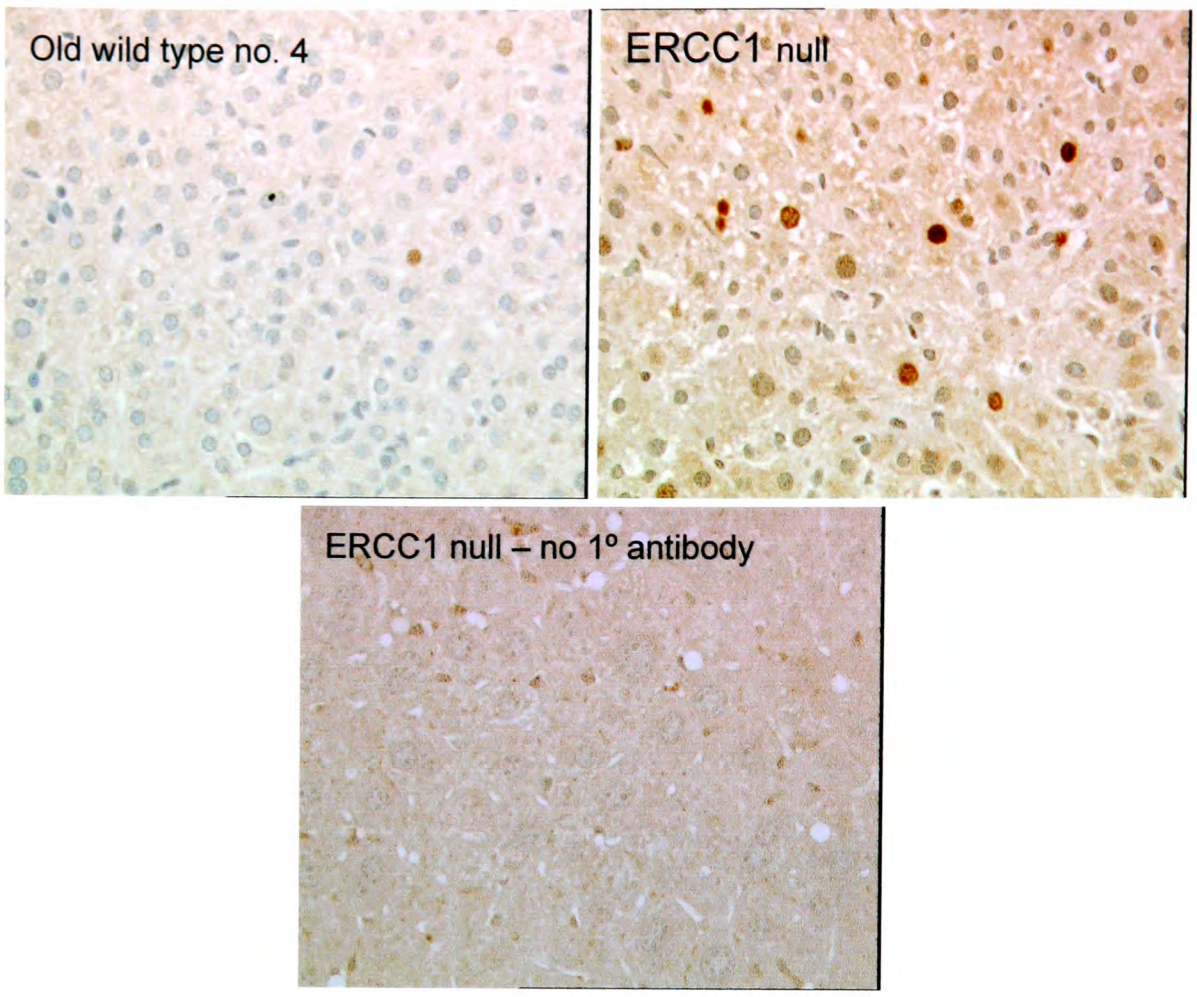

Figure 4.4 p21 immunostaining patterns for old wild type and ERCC1 null liver. The old wt section was 1 of 4 from a total of 7 that had low levels of background and did not appear to display increased levels of p21

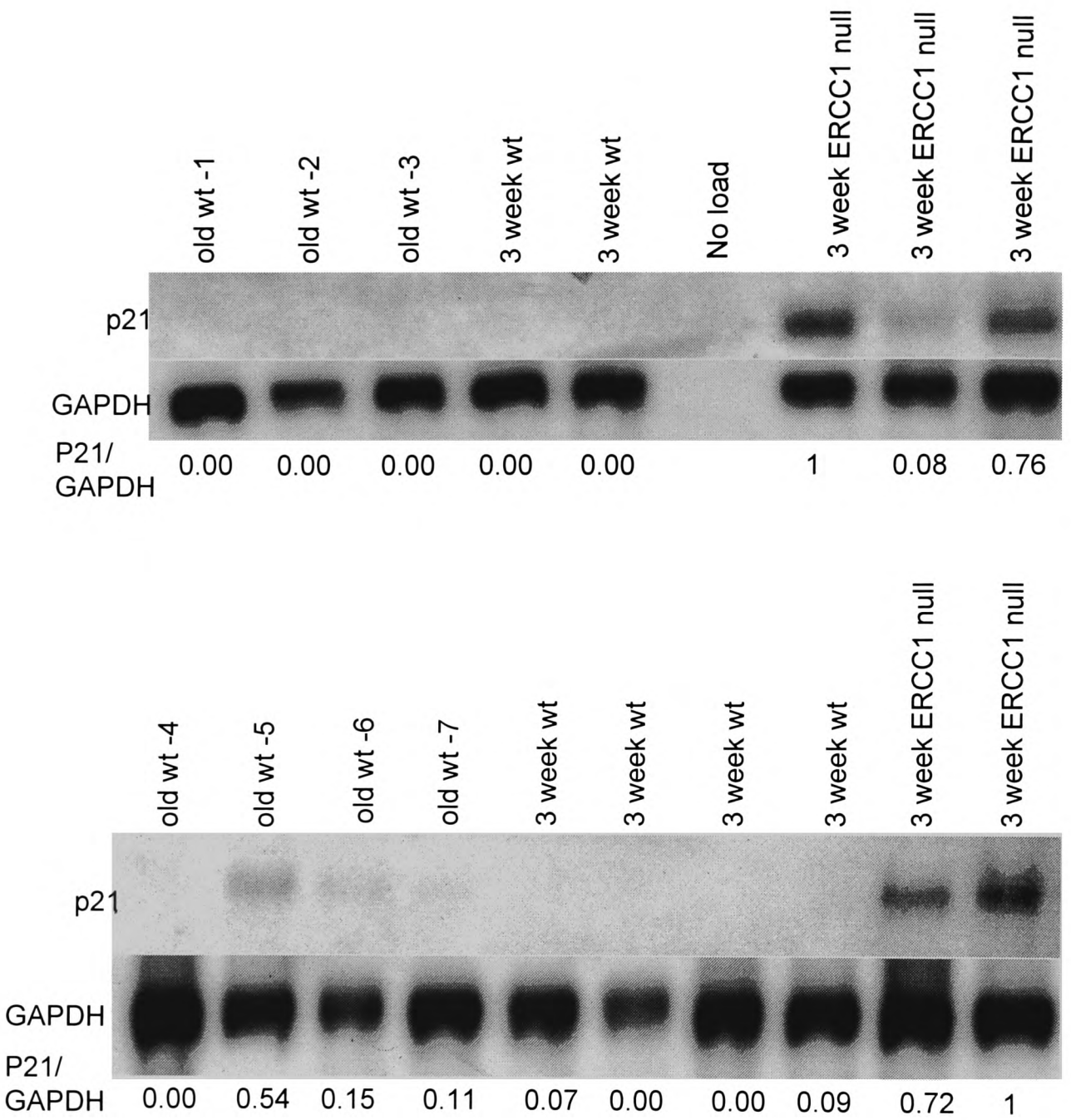

Figure 4.5 p21 northern autoradiography of total mRNA extracted from old wild type, 3 week old wild type and 3 week old ERCC1 null liver. Blots were reprobed with GAPDH for a loading control and the ratio of p21/GAPDH signal was calculated using a phosphorimage analysis system. Ratios were normalised to 1 using a 3 week ERCC1 null sample used in both blots

have distinct boundaries and the boundaries appear the same in both the stained and unstained nuclei (Figure 4.1).

It is not possible to say if the p21 is really causing the liver polyploidy, it is possible that it is merely a side effect of some other process that causes the polyploidy. However, the increased p21 levels are certainly associated with the polyploidy.

There is no increase in p21 levels in aged wildtype liver

The ERCC1 null livers display an accelerated polyploidy compared to wild type animals and appear to be the same as aged wild type by measurements of nuclear area, centromeric status and FACS. However, it is important to know whether the polyploidy in aged wild type animals is also correlated with an increase in p21 levels. To investigate this, immunohistochemistry has been used to investigate the p21 levels in 7 old wt animals aged between 18 and 27 months old. All of which had high levels of polyploidy (Figure 4.3). FACS profiles were measured on two different machines because of a move of laboratory. Although 4 out of the 7 samples (old wt 1-4) appeared to have no increase in p21 levels, 3 of the samples (old wt 5-7) seemed to have increased staining (Figure 4.4). These 3 samples were all processed at the same time, although with one other sample that does not show increased p21. The 3 samples may have slightly higher polyploidy levels than the other samples. Unfortunately, the background was very high for the 3 samples which appeared to show increased levels of staining and it did not prove possible to obtain sections that did not show high levels of background. This indicated that the apparent increase in staining could be artifactual.

In order to test, whether there really is a p21 increase in some of the old wt samples, Northern blot analysis was used to study the levels of p21 mRNA (Figure 4.5). The old wt samples were between 18 and 27 months old. Out of four ERCC1 null samples tested, three had a p21/GAPDH ratio between 0.72 and 1, one other had a ratio of 0.08. Old wt samples 1-4 had a ratio of 0 and old wt 5, 6 and 7 had ratios of 0.54, 0.15 and 0.11 respectively. Four 3 week wt samples had ratios of 0 and two

had ratios of 0.07 and 0.09. The Northern Blots, which were done in parallel, show that 4 out of 7 old wt samples have no detectable increase in p21 mRNA levels. However, the three old wt samples, which showed apparent increases in p21 staining do show a small increase in p21 levels. Some old wt liver samples appear to have increased p21 levels whereas some do not.

Discussion

The increase in p21 levels and the polyploidy could be caused by accumulated DNA damage, although I have not shown a direct link. ERCC1 null liver will accumulate damage faster and hence have increased levels of p21 earlier and so this may trigger increased ploidy. In young wt liver there is no accumulated DNA damage and so no polyploidy. In old wt liver damage accumulates in some nuclei but not in others and so there is variablity in p21 expression.

The stochastic nature of DNA damage may explain why some nuclei develop polyploidy and others do not. Presumably some nuclei suffer more DNA damage than others and thus polyploidy development is stimulated. This could perhaps be explained if ICL were causing the crucial damage in ERCC1 null liver. These are rare enough that the stochastic nature of their formation could become apparent in the ploidy development. ICL, even at a very low frequency, can also arrest the cell cycle in G2.

There may be two explanations for the small increase of p21 levels in some old wt liver samples, but not others. Possibly there are two different mechanisms that cause liver polyploidy, one dependent on p21 and one not. ERCC1 null liver polyploidy would be mostly caused by the p21 dependent pathway whereas polyploidy in old wt samples could be caused mainly by the p21 independent pathway and possibly sometimes by the p21 dependent pathway. p21 is not necessary for G2 arrest and polyploidy development, as has been demonstrated in p21 null cells (Bates et al., 1998; Niculescu et al., 1998; Waldman et al., 1996). Alternatively, the lack of p21 increases may be connected to the fact that p21 is probably not increased during S

phase and that the polyploidy in wt hepatocytes develops very slowly compared to ERCC1 null samples. Perhaps S phase in the old hepatocytes lasts a long time relative to ERCC1 null hepatocytes and so p21 levels are not increased in most nuclei or possibly endoreduplication is not always active and the nuclei are mostly dormant with p21 only activated when endoreduplication occurs. Polyploidy development may be coordinated across the tissue, perhaps in old wt liver some cells induce p21 due to increased DNA damage and these cells then communicate with and promote polyploidy development in other cells that do not have increased DNA damage.

The old wt liver samples seem to have small increases in p21 levels, apart from one sample, which has an increase comparable to some ERCC1 null samples. Is the size of the relatively small increase in p21 levels in some old wt liver samples important? This may be due to variation between animals and the small number of old wt animals tested. However, the low p21 increase may be connected to the idea of a p21 independent and dependent polyploidy development pathway. Hepatocytes are normally quiescent except in aging and after damage. p21 is required for the formation of various cdk complexes in the cell cycle, however in high levels it inhibits them, perhaps the small increases in old wt liver are necessary for one form of polyploidy development, but the higher levels seen in ERCC1 null samples are necessary for the other.

As discussed earlier the polyploidy may be described as being part of a protective terminal differentiation pathway. p21 is important in the differentiation of several cell types (Elbendary et al., 1994; Jiang et al., 1994; Parker et al., 1995). p21 is upregulated in various human liver diseases, such as alcoholic cirrhosis and chronic active hepatitis (Albrecht et al., 1997).

The level of p21 in rodent liver has been investigated before using immunohistochemistry. This work showed that in normal rat liver, only rare hepatocytes stain positive for p21, whereas by 5 days after partial hepatectomy, which induces polyploidy, there was a considerable increase in the number of p21

stained nuclei (Sigal et al., 1999). Although an increase in the level of p21 staining was demonstrated, this did not approach the levels seen in the ERCC1 null hepatocytes. This demonstrates the similarity between the induced polyploidy in livers after partial hepactectomy and that seen in normal liver. Mice with a p21 liver transgene for overexpression of p21 have accelerated liver polyploidy development (Wu et al., 1996). In these mice, p21 complexes with cyclin D1 and cdk4 leading to inhibition of hepatocyte entry into S phase during postnatal growth and partial hepactectomy. p21 overexpression after partial hepactectomy is in agreement with roles for p21 in G2/M arrest, polyploidisation and terminal differentiation, similar to other systems.

p21 null mice are viable, with no increased cancer incidence however p21 null fibroblasts cannot arrest in G1 after DNA damage (Brugarolaset al., 1995, Deng et al., 1995). Human fibroblasts and tumour cells deficient for p21 also cannot arrest in G1, these cells show p21 is involved in p53 mediated G2 arrest and coupling of DNA synthesis and mitosis (Brown et al., 1997; Waldman et al., 1995). In the absence of p21 endoreduplication often occurs. This would seem a contradiction as increased levels of p21 lead to endoreduplication and so does a deficiency in p21. However, this my be due to the role of p21 in both inhibiting CDKs and promoting their formation. With high levels of p21 CDKs are inhibited but without p21 their formation is reduced. Both situations lead to reduced CDK activity.

Several other proteins belong to the same CIP/INK family as p21 and they have similar roles. Perhaps some of these proteins may play a role in the polyploidy in ERCC1 null liver. p16 could not be detected in rat liver and no evidence has been found for activation after partial hepatectomy (Awad et al., 2000; Sigal et al., 1999). p27 and p18 levels are constant throughout development, p19 expression is low in adults, p15 levels are high in adults but low in embryos and p57 levels were high in embryos and low in adults (Awad et al., 2000). This indicates that p15 and p57 play a role in liver development, perhaps p15 is involved in the maintenance of hepatocytes in a quiescent state. p27 has been shown to be induced after partial

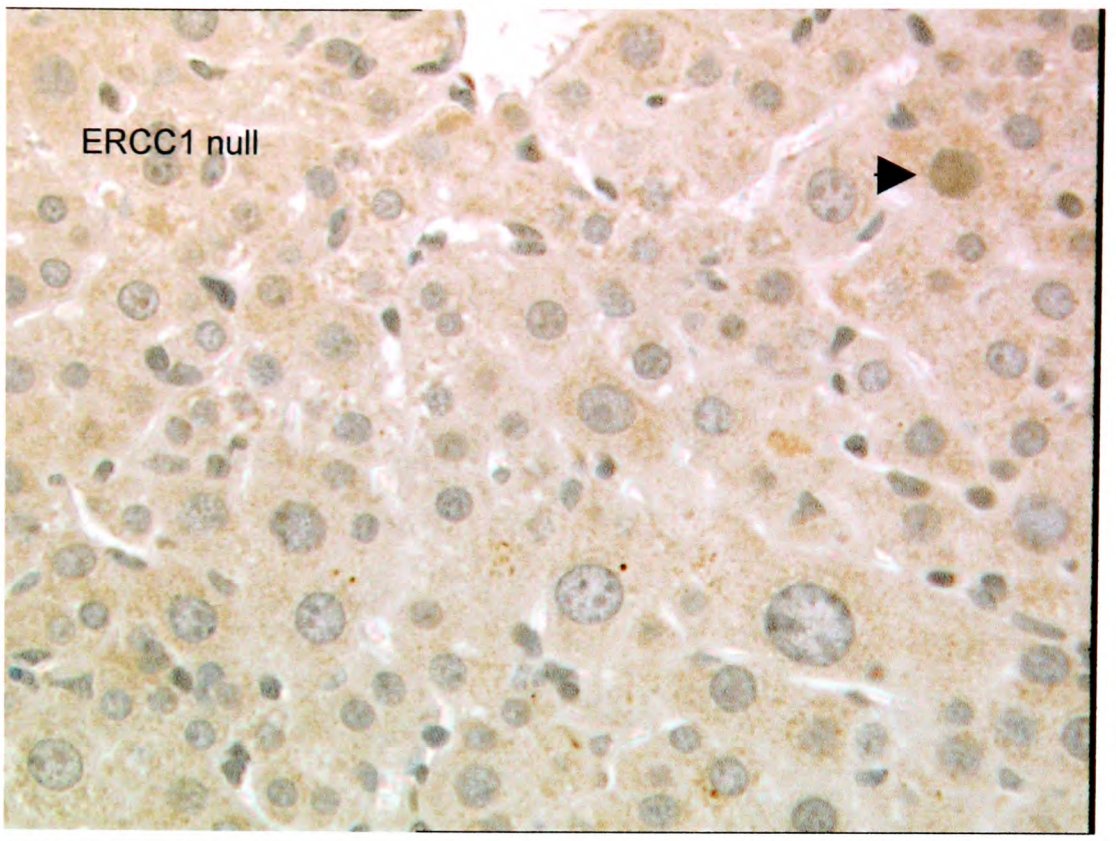

Figure 4.6 p53 immunostaining patterns for ERCC1 null and wt liver sections. The arrow indicates the stained nucleus.

hepatectomy (Albrecht et al., 1998). It may be interesting to study the levels of the other CIP/INK family members in ERCC1 null liver.

Although there is an increase in p53 expression in ERCC1 null livers the phenotype is p53 independent

It has previously been shown that p53 levels are increased in ERCC1 null hepatocytes (McWhir et al., 1993). These experiments showed large increases in p53 staining in ERCC1 null hepatocytes, however I have been unable to repeat this. Although some increase in p53 staining is visible this is at the level of occasional nuclei in a section rather than the staining of about 10% of nuclei seen previously (Figure 4.6). Possibly my detection is not sufficiently sensitive, but positive controls from UV irradiated skin showed the expected level of staining, so this seems unlikely (F Nunez; personal communication).

Increases in p21 levels may cause the polyploidy in ERCC1 null hepatocytes. The major mechanism for p21 induction is through p53. Although p53 levels may not be greatly increased in the ERCC1 null hepatocytes, it was of interest to see whether p53 was causing the p21 increase and hence the polyploidy.

In order to test this, an ERCC1-p53 double null mouse was bred from heterozygotes for the ERCC1 null allele and heterozygotes for a p53 null allele (Purdie et al., 1994). The assumption was that as the ERCC1-p53 double null could not produce p53 in response to the enhanced DNA damage, so there would be no increase in p21 levels and thus the accelerated polyploidy might be corrected. However, the ERCC1-p53 null mouse still suffers from the accelerated polyploidy, as shown by nuclear area measurements, and in fact, may die on average a few days earlier than the typical ERCC1 null mice (Nunez et al., 2000). The simple p53 null mouse does not have a liver phenotype. p53 null mice generally die from lymphomas before 6 months old but appear relatively normal before then and certainly no gross liver

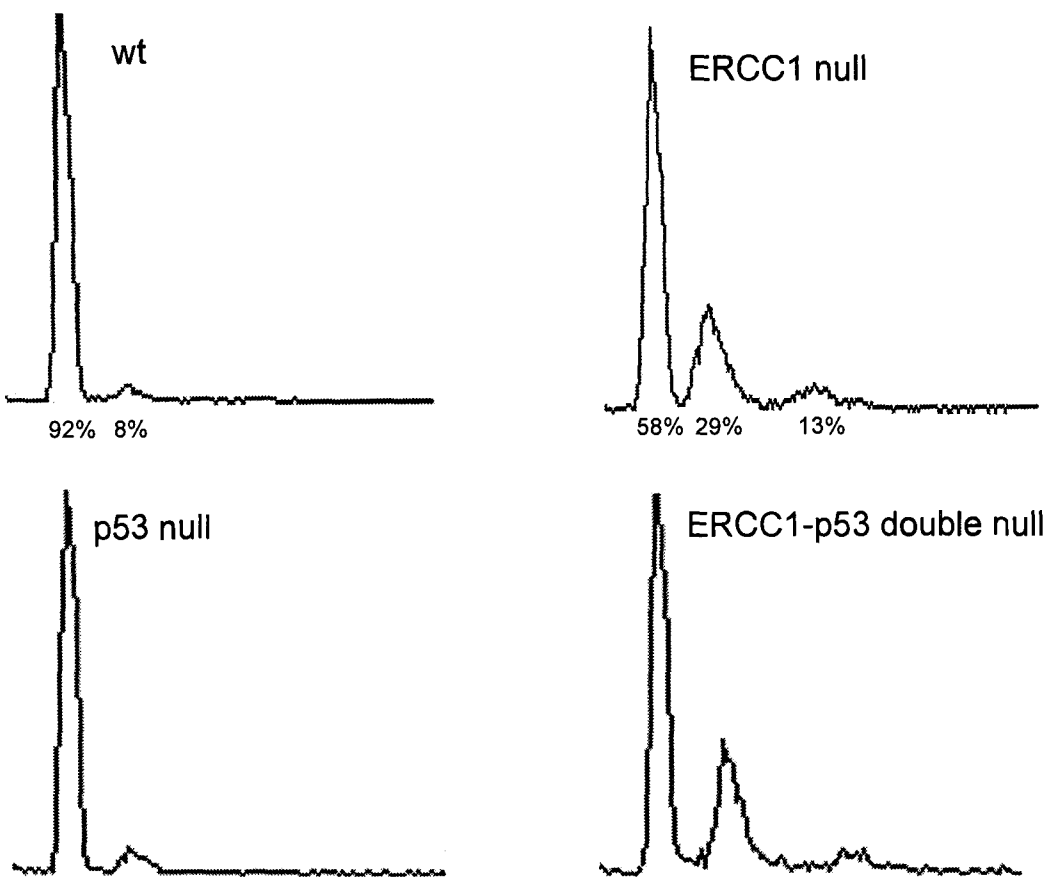

Figure 4.7 FACS profiles of 3 week old wt, ERCC1 null, p53 null and ERCC1-p53 double null liver.

Genotype	Small Nuclei - % in G2/M	S D	Enlarged Nuclei - % in G2/M	S D	Number of animals
3 week old wildtype	32	6	0	n/a	6
3 week old ERCC1 null	36	9	62	7	5
3 week old ERCC1-p53 double null	19	n/a	50	n/a	1
3 week old p53 null	29	n/a	0	n/a	1

Table 4.1 Percentage of small and enlarged nuclei in G2/M. Calculated from results of centromeric immunostaining assay. SD is Standard Deviation.

abnormalities are reported (Donehower et al., 1992; Purdie et al., 1994). ERCC1-p53 null liver also has increased p21 mRNA levels (Nunez et al., 2000). In order to confirm that the liver phenotype of the ERCC1-p53 double null was the same as that of the ERCC1 null, the cell cycle status of the hepatocytes was studied using FACS analysis and the centromeric staining assay. The FACS profile of ERCC1-p53 double liver is very similar to an ERCC1 null sample and the p53 null sample is very similar to a wt sample (Figure 4.7). The cell cycle distribution of ERCC1-p53 double null hepatocytes, measured using the centromeric staining assay, is very similar to that from ERCC1 null hepatocytes and the p53 null is very similar to wt (Table 4.1). This data confirms that ERCC1-p53 null liver has the same accelerated polyploidy phenotype as the ERCC1 null liver. This confirms that the increase in p21 levels in ERCC1 null hepatocytes is not caused by p53. Other models have also shown that p21 activation can be p53 independent (Michieli et al., 1994).

REF1 is upregulated in ERCC1 null hepatocytes

REF1/APE1/HAP1/APEX (apurinic/apyrimidinic endonuclease/redox effector factor) is an apurinic/apyrimidinic (AP) endonuclease involved in BER, a redox regulator of DNA binding proteins and bioreductive drugs and it binds in a complex to the negative response element of the parathyroid hormone gene (Evans et al., 2000). AP sites arise naturally and are the consequence of spontaneous hydrolysis of the bond between base and deoxyribose sugar, of some forms of oxidative damage and of exogenous agents. They are also formed by the action of DNA glycosylases in BER. REF1 hydrolyses the phosphodiester bonds at AP sites to remove the damaged nucleotide from the backbone. REF1 is the major if not exclusive endonuclease for this purpose in mammalian cells (Friedberg, DNA repair and mutagenesis; Barzilay, 1996). REF1 can also rescue inactivation by cysteine oxidation of various transcription factors (Xanthoudakis et al., 1992; Xanthoudakis and Curran, 1992). A REF1 knockout is lethal and the REF1 protein is required for the redox-independent activation of p53 *in vitro* (Jayaraman et al., 1997; Xanthoudakis et al., 1996). REF1 is translocated to the nucleus and is upregulated in B lymphocytes after exposure to H_2O_2 (Tell et al., 2000). The DNA binding activity

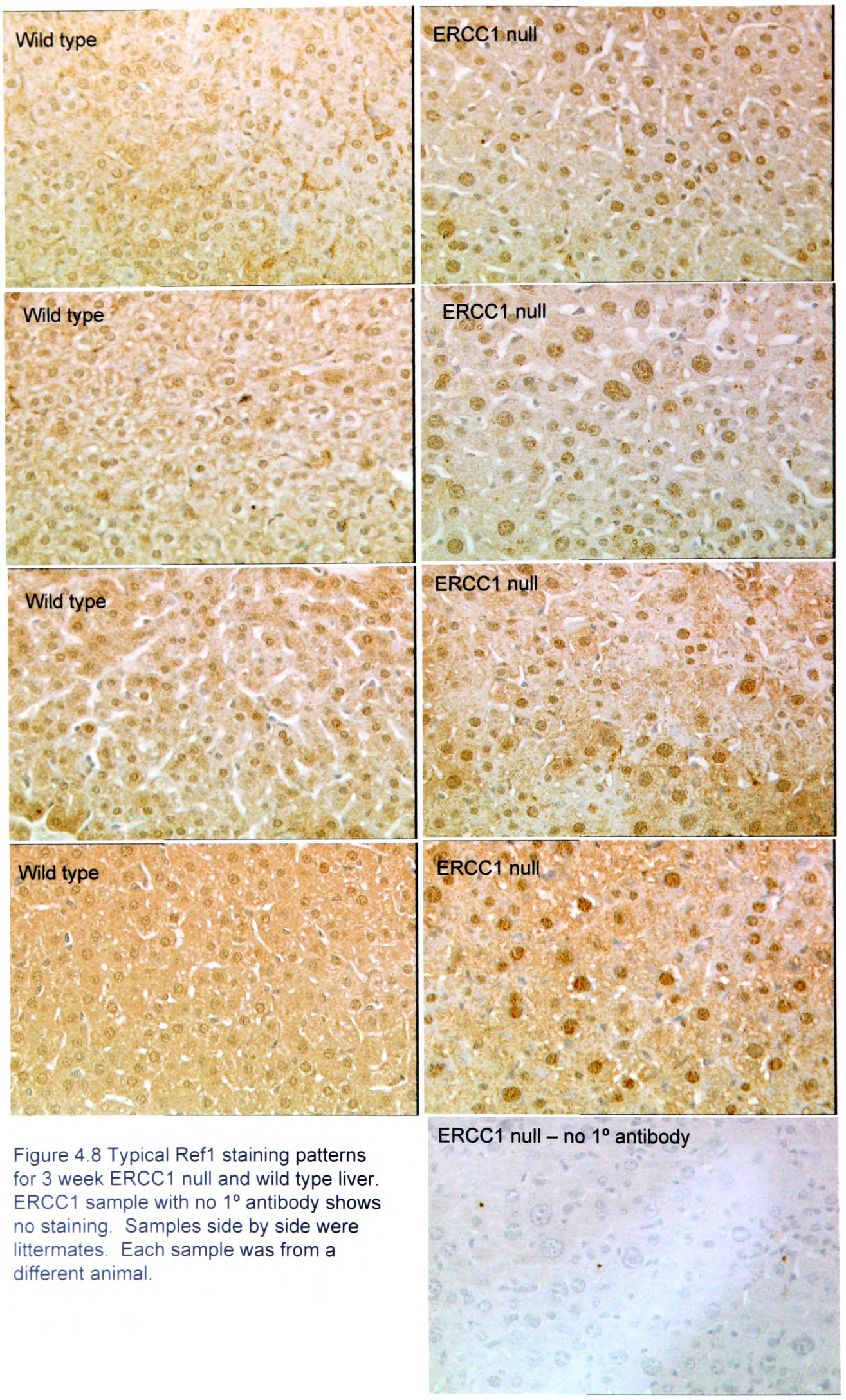

Figure 4.8 Typical Ref1 staining patterns for 3 week ERCC1 null and wild type liver. ERCC1 sample with no 1° antibody shows no staining. Samples side by side were littermates. Each sample was from a different animal.

of recombinant NF-Y heterotrimeric transcription factor is stimulated by REF1 or DTT (Nakshatri et al., 1996). REF1 also mediates AP-1 activation after heat shock (Diamond et al., 1999) There is some indication that REF1 may have roles outside the nucleus, immunohistochemistry shows that in some populations of cell staining is mainly cytoplasmic however this may be just inactive REF1 in unstressed cells (Kakolyris et al., 1998).

I have used immunohistochemistry to examine whether REF1 levels are up regulated in ERCC1 null hepatocytes. REF1 might be upregulated to compensate for the DNA repair functions of ERCC1. All the hepatocyte nuclei display some level of REF1 staining, mostly in the nucleus, however it appears that the staining is significantly stronger in ERCC1 null liver (Figure 4.8). There appears to be no difference in the amount of staining between the enlarged and normal size nuclei. Western blot analysis has also shown that REF1 levels are increased in ERCC1 null liver (Kan-Tai Hsia; personal communication).

REF1 appears to have two roles, regulation of the redox state of some transcription factors and as an AP endonuclease. Why it is upregulated in ERCC1 null hepatocytes? It is highly likely that BER is upregulated in ERCC1 null liver. There is some overlap between BER and NER in repair of alkylation damage and recent evidence suggests that NER is also involved in the repair of oxidative damage. In fact, HPLC shows that levels of 8-oxoguanine, a major product of oxidative damage, are increased in ERCC1 null liver compared to wildtype (D Melton; personal communication; Grollman and Moriya, 1993). This is similar to an aspect of the phenotype of the mouse OGG1 knockout. OGG1 is the DNA glycosylase that repairs 8-oxoG. No histological abnormalities were detected in the livers of OGG1 null mice, but increased levels of 8-oxoG were detected. Extracts from OGG1 null mice tissues cannot excise 8-oxoG but there there is significant slow removal *in vivo* from proliferating cells, this may be by MMR or NER (Klungland et al., 1999). However, some studies have found no influence of NER on 8-oxoG repair, this may be because BER is the main repair process and NER only becomes important under heavy load (Dianov et al., 1998).

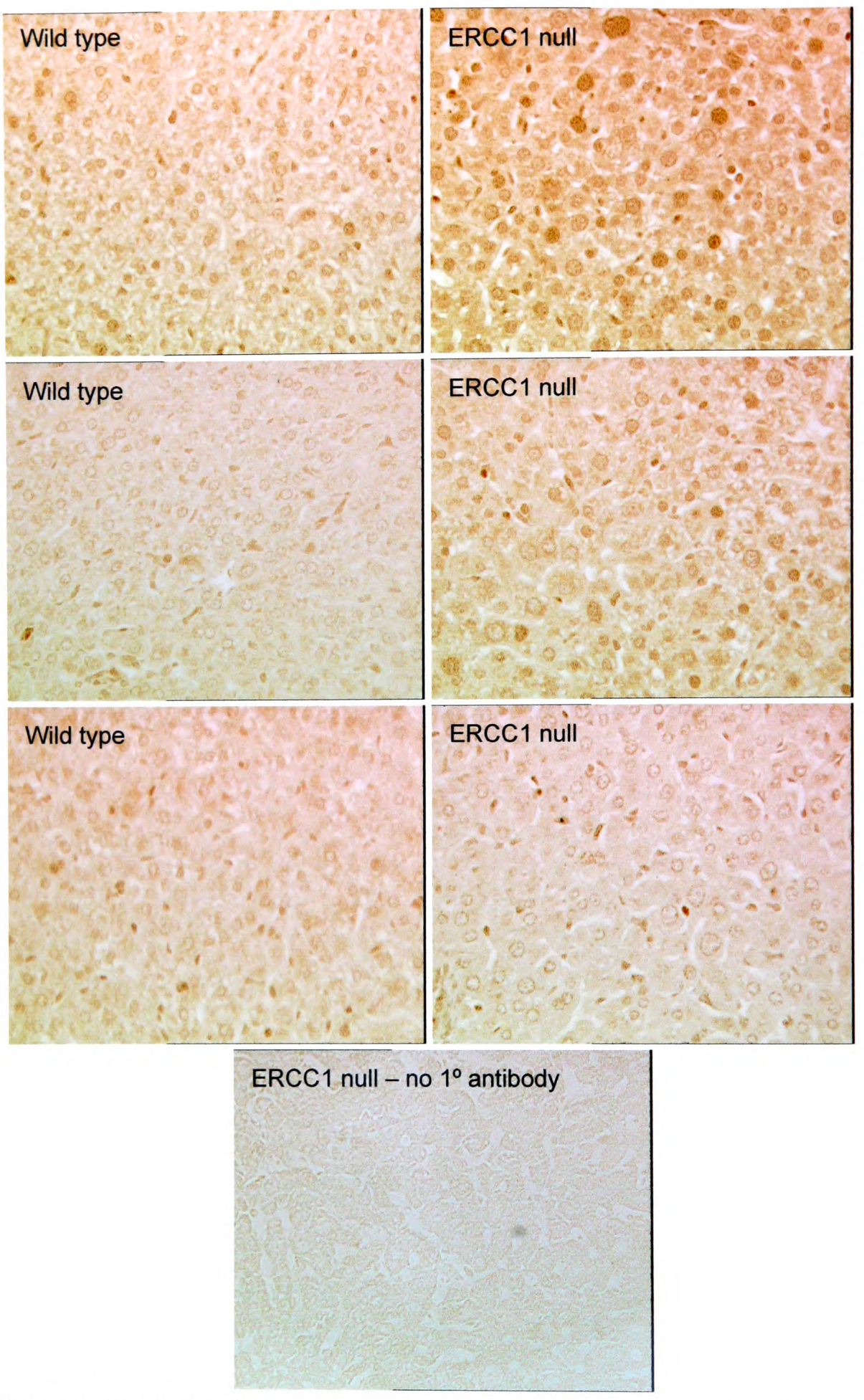

Figure 4.9 Typical MSH2 staining patterns for 3 week ERCC1 null and wild type liver. ERCC1 null sample with no 1° antibody shows no staining. Samples side by side were littermates. Each sample was from a different animal.

It is not known whether the increased levels of oxidative DNA damage in ERCC1 null mice are caused by decreased repair due to the loss of NER or by increased amounts of oxidative radicals caused by the breakdown in cellular systems. ERCC1 null liver has increased amounts of disruption to mitochondrial membranes compared to wt and this could allow more oxidative radicals to attack DNA. The increased mitochondrial disruption is probably caused by reduced production of mitochondrial proteins from the nucleus. However, there is no increase in levels of HO-1 (haemoxygenase), a marker for oxidative stress, in ERCC1 null liver (Melton; personal communication). This indicates that there is no overall increase in oxidative stress in ERCC1 null liver and that REF1 levels are probably increased due its role in BER.

In order to confirm whether the BER pathway as a whole is upregulated, further study of different markers is necessary, perhaps such proteins as the DNA glycosylases.

MSH2 is upregulated in ERCC1 null hepatocytes

As discussed earlier, MSH2 is involved in MMR and recombination. I have investigated the levels of MSH2 in ERCC1 null hepaptocytes. MSH2 staining tends, like that of REF1, to be homogenous, however more MSH2 staining is evident in ERCC1 null hepatocytes than in wild type (Figure 4.9). There appears to be no difference in staining between enlarged and normal sized nuclei. Western blot analysis has also shown that there are greater levels of MSH2 protein in ERCC1 null liver than wt liver (KT Hsia; personal communication).

Why are the levels of an MMR protein increased in ERCC1 null liver? Obviously ERCC1 and MSH2 are connected in their recombination associated roles and it is possible that MSH2 levels are increased to compensate for the loss of ERCC1 in this aspect, but the link is more probably between MSH2 and the loss of NER. MMR seems to have roles in the processing of both UV lesions and oxidative damage.

Whilst NER will repair some small looped mismatches, MMR will repair some UV damage where the recognition system mistakenly recognises a mismatch. MMR is also involved in regulatory responses to DNA damage. MSH2 levels are upregulated in response to UV light and this upregulation is dependent on p53 and c-jun and their interaction (Scherer et al., 2000).

The MMR system is thought to be involved in the recognition of DNA lesions such as those caused by UV and then the transmission of a signal to the apoptotic machinery (De Weese et al., 1998; Hickman and Samson, 1999). Cancer cell lines from XPA null mice show reduced levels of MMR proteins such as MSH2 and reduced MMR activity and it is proposed that the absence of MMR proteins may mean that no signal is passed to the apoptotic machinery on UV damage and thus the cells survive longer (Ichikawa et al., 2000). Double XPA and MSH2 mutant cells derived from the human XP12RO cell line are not more UV sensitive than the simple XPA mutant (O'Driscoll et al., 1999). MSH2 and ERCC1 double mutant cells derived from ERCC1 mutants CHO9 43-3B show highly elevated levels of UV induced mutation rates compared to wild type and simple ERCC1 mutants, however the UV sensitivity is not greatly increased (Nara et al., 2001). However in the absence of MMR alone, UV-induced mutation rates are not much influenced (Tobi et al., 1999). This implies that in the absence of NER, MMR is required for the reduced mutation rates but its absence does not affect survival. MSH2-ERCC1 double null mice die before birth with high levels of necrosis in the liver whereas MSH2 null mice are healthy until 2 months old when they start to suffer from a high frequency of lymphoid tumours and ERCC1 null mice die at 3 weeks old of liver failure (D Melton, personal communication; Reitmair et al., 1995; Weeda et al., 1997).

However, MSH2, as part of MMR, also has another connection to NER. MMR seems to be involved in the processing of oxidative damage. The majority of replication associated mismatches are probably caused by mispairing with oxidatively damaged bases rather than mispairing with normal bases (Earley and Crouse, 1998). The ERCC1 null liver has increased amounts of oxidative damage

and although the ERCC1 null hepatocytes are quiescent in terms of cell division, they are going through cycles of DNA synthesis as the ploidy levels increase and this will induce the formation of mismatches and mutations. Consistent with the involvement of MMR in this process, synergistic mutator effects were observed when OGG1 and MSH6 were simultaneously eliminated from yeast cells and purified MSH2-MSH6 strongly binds to oligonucleotides containing mismatches of 8oxoG with either A or C (Ni et al., 1999). Presumably the increased oxidative damage in the ERCC1 null hepatocytes is causing increased mismatches and general damage and MSH2 is overexpressed to deal with this. This sharing of substrates will contribute to the overexpression of MSH2.

c-FOS

c-FOS and c-JUN are members of a multigene family implicated in a number of stress induced signal transduction cascades. They associate in homo or hetero dimers to form the transcription factor AP1. AP1 may regulate expression of downstream target genes in cellular responses to oxidative stress. Regulation of AP1 probably depends on the redox state of the cell. Both c-FOS and c-JUN have a conserved cysteine located in the DNA binding domain. These will only allow DNA binding in the sulphydryl state, so these cysteines act as a switch depending on the redox state of the cell. REF1 regulates the redox state of these cysteines. Both c-FOS and c-JUN are induced following heat shock (shown to cause increased oxidative stress levels), the AP1 DNA binding activity also increases, however this increase is prevented by the immunodepletion of REF1 from extracts. Levels of c-FOS might be increased if ERCC1 null liver has increased levels of oxidative DNA damage. Western blot analysis may show that c-FOS is upregulated in ERCC1 null liver (KT Hsia; personal communication). However, I have been unable to confirm this by immunohistochemistry. I have shown staining of c-FOS in both ERCC1 null and wt but no difference in intensity could be detected.

PCNA

PCNA (Proliferating Cell Nuclear Antigen) is involved in DNA synthesis where it acts as a processivity factor. Although PCNA upregulation in ERCC1 null liver has been observed by Western, I have been unable to confirm an increase in PCNA levels by immunohistochemistry. I have shown strong nuclear staining of PCNA in both formalin and methacarn fixed samples, but no difference in intensity of staining is seen between ERCC1 null and wt samples.

CDC2

CDC2 is an essential cell cycle regulator in all eukaryotes. In mammalian cells CDC2, in a complex with cyclin B, is essential for the G2-M phase transition. In yeast, CDC2 complexes with different cyclins to control entry to S-phase and mitosis. After IR, changes in CDC2 activity in human diploid cells have been found and this is associated with altered phosphorylation activity. CDC2 mRNA and protein levels are also found to be down regulated by ionising radiation in a p53-dependent, p21-dependent manner. As CDC2 is important in regulation of the G2-M transition in mammalian cells and ERCC1 null hepatocytes are arrested in G2 it was decided to investigate levels of CDC2 protein in the ERCC1 null hepatocytes using immunohistochemistry. However, although nuclear CDC2 was detected in hepatocytes, no change was observed between ERCC1 null and wt hepatocytes.

Future Work

14-3-3σ is a protein that is involved, similarly to p21, in the response downstream of p53 activation (Hermeking et al., 1997). 14-3-3σ is also induced by various forms of DNA damage. The exogenous expression of 14-3-3σ results in a G2 arrest similar to that seen in irradiated cells, however it is followed by polyploidy. 14-3-3σ sequesters cyclinB-cdc2 complexes in the cytoplasm during a DNA damage induced G2 arrest, this is a complementary role to p21 which inactivates cdc2-cyclinB in the

nucleus. Cells lacking both p21 and 14-3-3σ are significantly more sensitive to DNA damage or exogenous p53 than cells deficient in either p21 or 14-3-3σ, this implies that p21 and 14-3-3σ have complementary roles in the G2/M checkpoints. Cells lacking 14-3-3σ can arrest in G1 but cannot maintain a stable G2 arrest after adriamycin treatment. The above work shows the close connection between p21 and 14-3-3σ in the mechanics of G2 arrest, it is highly likely that 14-3-3σ is upregulated in the ERCC1 null hepatocytes. It would be interesting to test this. However, at present only mouse derived antibodies are commercially available for 14-3-3σ, introducing technical challenges.

Discussion

Although immunohistochemistry does allow the pinpointing of increases in protein levels to individual cells there are some disadvantages to the technique. One of these is the "edge effect", when sections are stained more staining is apparent at the edges of the section than in the centre. Presumably this is due to antibody and reagents diffusing into the section more easily at the edge, although it is difficult to see how this could work given the fact that the sections are essentially two dimensional anyway. In general this is no great disadvantage because it does not extend more than a few cell widths from the edge of the section, however in my experiments it must be considered. The comparison of the wild type and ERCC1 null samples relies on them both staining to the same degree. The wild type livers because they are much bigger obviously result in bigger sections and so it is always easily possible to find an area well away from the edge of the section, however the ERCC1 null sections are much smaller because the livers they are taken from are much smaller. This means that it is much harder to find areas well away from the edge of the section. Could this mean that some of the areas taken have been close enough to the edge to have the staining increased artifactually? It is possible, but I have been careful to always select areas well enough away from the edges not to have the staining increased by the edge effect.

Another disadvantage to immunohistochemistry is that staining is often heterogeneous in nature. To combat this sections have only been measured when the staining is reasonably homogeneous.

Whilst immunohistochemistry is ideally suited to quantifying large increases in protein levels in particular nuclei as is seen in p21 staining, and in fact in this case is probably more useful than Western analysis, it is not very useful where there is an increase in the amount of protein across all of the nuclei, which is only detectable in the case of a large increase.

The question I am really trying to ask in the latter part of this chapter is what pathways in the hepatocyte change when ERCC1 is not functional? I have tried to address this by examining the levels of various proteins, hoping to use them as some sort of indicator for the relative activities of various pathways. However, it is very difficult to do this for DNA repair. The sheer interconnectivity of all of the pathways means that often, as with MSH2 and REF1, the most interesting proteins are those which are involved in more than one pathway. Despite the difficulties of trying to use individual protein levels as markers, I believe it is probably one of the best ways. Other possible methods might be to perhaps use protein extracts to measure the levels of *in vitro* repair using an artificial substrate. Or to examine the levels of DNA damage directly by HPLC, however this bears the disadvantage of not knowing are the increased or decreased levels of damage compared to wt because of changes in damage caused or changes in the level of the repair process, and because repair substrates overlap between pathways, which pathway is repairing the damage? All of these methods suffer from disadvantages and perhaps only by using them all can we gain a clear picture of what is really going on in the ERCC1 null liver.

Chapter 5 – The role of ERCC1 in the formation of UV-induced chromosome aberrations

Chapter Summary and Background

Cells that progress through S phase and into mitosis with unrepaired UV lesions can form chromosome aberrations that are visible in condensed metaphase chromosomes. ERCC1 and XPF null cells have a higher ratio of breaks to exchanges than wt and other NER null cells.

Introduction

DNA damaging agents promote the formation of chromosome aberrations, which can be seen by examination of stained metaphase chromosomes, i.e. after chromosome condensation and before separation (Evans, 1962).

Chromosome aberrations take the form of a variety of different structures. There are various ways to assign these to different classes and there is some debate over which class certain aberrations fall into. Structures can be first classified by whether they are chromosome or chromatid-type aberrations depending on whether they involve both chromatids of a chromosome, in which case they are called chromosome type aberrations, or involve just one chromatid, where they are known as chromatid type aberrations.

S independent agents, like IR and a few chemical agents (eg. bleomycin and neocarzinostatin), can cause aberrations when cells are treated at any stage of the cell cycle. They induce chromosome type aberrations when cells are treated in G1 phase and chromatid-type in cells treated in S or G2. S dependent agents like UV, can cause aberrations only when cells are treated and allowed to proceed through S phase. They cause chromatid type aberrations after G1 or early S phase treatment.

Both chromosome-type and chromatid-type aberrations can be further subdivided into breaks (which result in an acentric fragment) and exchanges (the rearrangement of chromatids or chromosomes). A break can be defined as: the apparent complete severance of a chromatid (Savage, 1990). Exchanges can be either complete, where

all of the ends are joined, or incomplete where 2 or more ends remain unjoined. An exchange can be defined as: any aberration resulting from the interaction of two or more lesions, and includes interchanges (different chromosomes) and intrachanges (same chromosomes) (Savage, 1990).

Chromosome aberrations visible with crystal violet staining are only part of the spectrum of chromosome rearrangements. For instance, events like inversions are only seen where they occur across a centromere and so affect the length of chromosome arms. The chromosome aberrations studied here are primary aberrations, formed in the first S phase after DNA damage. Some primary aberrations will result in structures which cannot be separated by the cell, resulting in terminal arrest. However, aberrations which progress successfully through to the next stage of the cell cycle are often changed into secondary aberrations, which are stable enough to be transmitted through the generations.

Formation of Chromosome Aberrations

There are two theories to explain the formation of chromosome aberrations, the breakage-reunion theory and the exchange theory. The breakage reunion theory states that all exchanges are formed from a primary break in the chromosome and that whether intrachanges, interchanges or no exchanges are seen depends on how breaks rejoin, i.e. 4 ends from two breaks can rejoin to form no aberration (original partner ends), an exchange where the ends are rejoined with the wrong end, or a break can form where no rejoining occurs. The exchange theory proposes that exchanges are formed from a primary lesion which is not a break, these lesions interact to form exchanges and all breaks are the result of incomplete exchanges. These two models are still current. Recent data comes out in support of the breakage reunion theory; using model predictions, breakage reunion fits best with observed patterns (Sachs et al., 2000). However, indirect evidence suggests that DSBs are the ultimate lesion involved in aberration formation (Natarajan and Zwanenburg, 1980). The formation of exchanges relies on lesions on both interacting chromosomes, as

shown by nuclear fusion experiments with non-irradiated and irradiated HeLa cells (Cornforth, 1989).

It is possible that both the breakage-reunion and exchange theories are correct to some degree depending on the original lesion. As these two models are largely based on data from IR studies, they may not be entirely applicable to UV induced chromosome aberrations. UV lesions tend to not cause strand breaks, at least directly, thus one would think that they cause lesions according to the exchange theory (Savage, 1976). However, there is evidence that the breakage-reunion theory applies. After treatment with wortmannin, an inhibitor of DNA-PK, in G2, the number of breakage type aberrations was enhanced whereas the yield of chromatid type exchanges was almost completely suppressed (Ishii and Ikushima, 1999). DNA-PK is crucial for the NHEJ pathway of DSB repair. This indicates that NHEJ is crucial in the formation of exchanges. They suggest that in the presence of wortmannin, NHEJ or another DNA-PK dependent pathway, cannot function and exchange formation is inhibited leaving more breaks to go through to metaphase. Other inhibitors of DNA synthesis and repair used in G2 will also potentiate S-dependent agent induced chromosome aberrations (Palitti et al., 1983). Perhaps there are multiple routes to form chromosome aberrations, this might explain how NHEJ genes and NER genes could be both involved in aberration formation. Possibly the exchange theory reflects the repair of DSGs, whereas the breakage-reunion theory reflects the repair of DSBs that form from some DSGs.

Recent evidence suggests that CPD lesions in active genes are important in triggering the formation of aberrations (De Santis et al., 2000). CSB null CHO cells suffer a high frequency of aberrations even at low doses of UV. This is despite the fact that wt hamster cells display little or no repair of CPDs outside active genes. Wt hamster cells would be expected to have large numbers of CPD lesions during S phase but these do not trigger high levels of aberrations. However, in wt cells CPDs are repaired well in active genes. In CSB cells this repair does not happen and high levels of chromosome aberrations are seen.

Chromosome Aberrations in NER Deficient Cells

The frequency of S phase dependent chromosome exchanges induced by UV light is dramatically reduced in ERCC1 null cells when compared to the frequency of breaks (Melton et al., 1998). In wt hamster cells there were 6.15 exchanges/breaks and in ERCC1 def. hamster cells there were 0.36 exchanges/breaks. This implies that ERCC1 has some role in the formation of chromosome exchanges. Is this due to the lack of NER function in ERCC1 null cells or due to the loss of the role of ERCC1 in recombinational pathways? In order to test this the ratio of exchanges to breaks has been studied in ERCC1, XPF, XPD, XPB and XPG def. cell lines. If, as expected, the reduction in the rate of exchanges is due to the loss of a recombinational function of ERCC1-XPF, then the rate of exchanges should be reduced in ERCC1 and XPF def. cells, but the same as wt in XPD, XPB and XPG def. cells.

In order to induce aberrations, unsynchronised cultures were UV irradiated and allowed to grow for a sufficient time so that cells that were in G1 when irradiated might progress through S phase to metaphase. Then chromosome spreads were prepared. In all experiments spreads were prepared at three different time points after UV. This is necessary, both in order to ensure a large number of cells are caught at metaphase, and because use of just one fixation point may select for cells that were at one particular part of G1 during irradiation and this could prejudice the results.

Obviously the higher the number of UV lesions in a cell, the higher the number of chromosome aberrations that might be expected to form. It was decided to irradiate cultures with equitoxic doses rather than equal doses because otherwise the number of aberrations seen in the highly UV sensitive mutants would be extremely high and the number seen in wt and less UV sensitive mutants would be very low. This would make it very difficult to make a real comparison between the different cell lines. In order to make a true comparison between the different cell lines the effective damage must be the same for all of them. Using equitoxic doses should ensure that a wt and mutant line have the same effective amount of damage. Although the damage immediately after irradiation will be higher in the wt than the mutant, the wt will

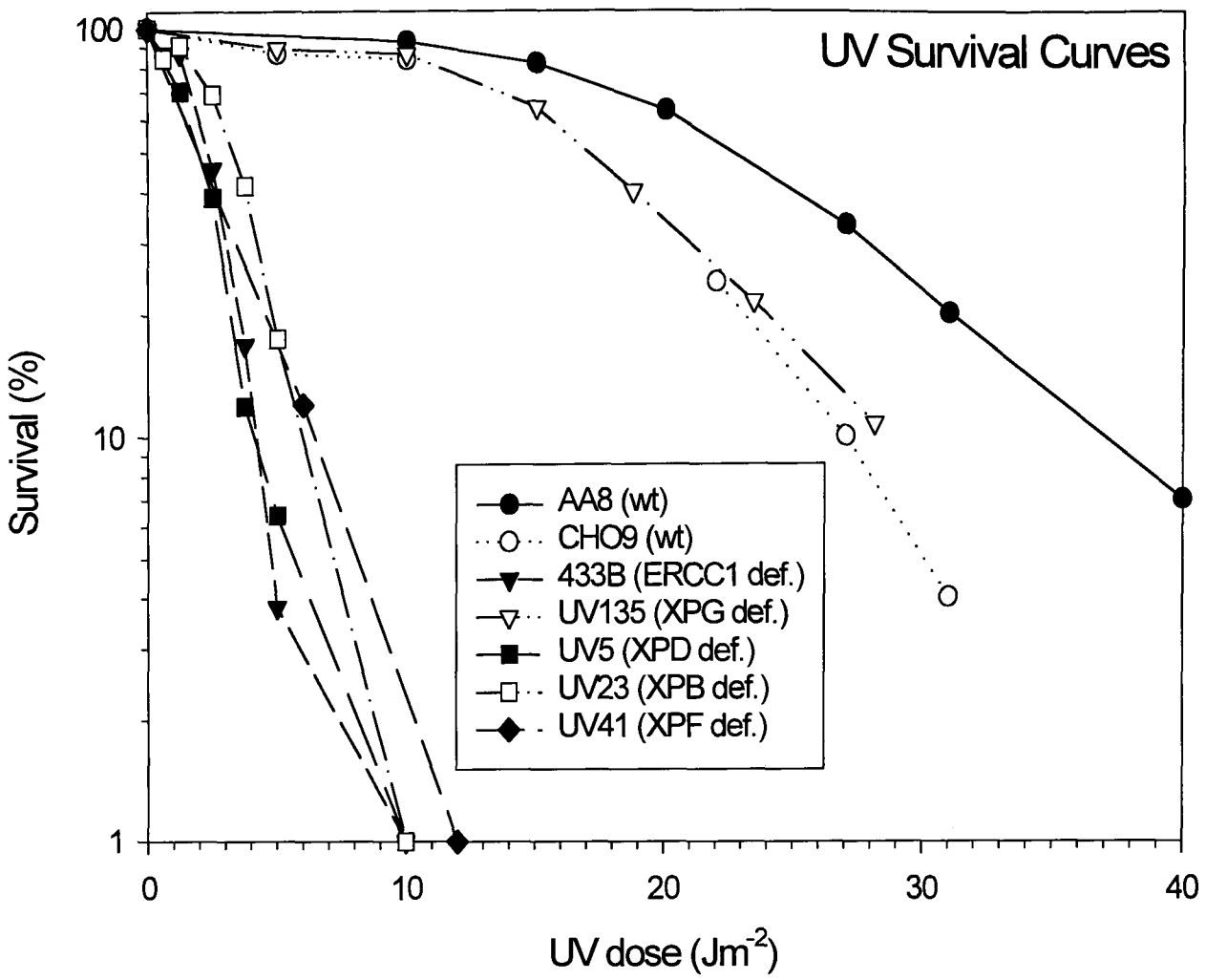

Figure 5.1 UV survival curves for NER def. and wt cell lines. Cultures were plated at calculated densities, allowed to rest overnight and then UV irradiated at a selection of doses. After about 4 days growth the zero UV plate reached confluence. Cells were then dyed with Crystal Violet, the dye was extracted and OD575 nm values were compared to the zero UV sample to calculate % survival. Survival curves were the average of 2 experiments.

Cell line	Genotype	Breaks/cell	Exchanges/cell	Aberrations/cell	Dose (Jm-^{2})	Approx Survival at Dose
CHO9	wt	0.26	0.41	0.67	12	70%
433B	ERCC1def.	0.35	0.15	0.5	3	30%
AA8	wt	0.23	0.28	0.51	26	33%
UV41	XPF def.	0.6	0.35	0.95	5	15%
UV5	XPD def.	0.39	0.45	0.84	5.9	5%
UV23	XPB def.	0.12	0.2	0.31	3.4	50%
UV135	XPG def.	0.25	0.41	0.66	23.4	21%

Table 5.1 Rates of chromosome aberrations and doses for wt and NER def. cell lines. Aberration rates were calculated for at least 100 metaphases.

repair the damage at a much greater rate than the mutant, so that by the time the aberrations are formed the amount of damage should be equal in each cell line.

Initially, UV survival curves were used to calculate the dose at which about 30% of the cells were still able to grow (Figure 5.1). All of the NER mutants except XPG were very sensitive to UV. Trial experiments were then used to find a dose at which about two thirds of cells had aberrations, although as aberration formation is random, some cells had many events where others had none. The source was roughly calibrated by comparing published survival curves with those obtained in our laboratory. The doses given should be relatively consistent through the experiments but comparisons with published work are difficult. There will be some error in dose across these experiments as the UV emission of the bulb varies over time. Fortunately the real basis for equitoxicity in these experiments is that the number of aberrations per cell is about the same across all cell lines, if this is so, as can be seen in Table 5.1, then the doses may be assumed to be equitoxic. In order to study cell lines where the ratio of exchanges to breaks changes, it is probably best to compare the total aberrations per cell rather than just exchanges or breaks.

As can be seen in Table 5.1, there is only a rough correspondence, between the percentage survival and the number of aberrations per cell at the UV dose, for each cell line. It might be expected that the lower the survival, the greater the number of aberrations, however, for instance UV5 has a particularly low survival but no more aberrations than UV41 which has a greater survival at the given dose. An explanation for this might be that the survival curves are not particularly accurate especially for the highly UV sensitive cell lines. Where the curve is steep, a small difference in dose can make a large difference in the calculated survival, and so errors in the curves are amplified. The survival curves were only used to calculate a rough starting dose for trial experiments on each cell line so these errors are not of concern. There may be a further discrepancy due to the fact that survival curves are calculated from the fraction of cells still growing about 5 days after UV treatment, whereas the chromosome aberrations are studied only 24 hours after UV. The errors

breaks

simple and complex interchanges

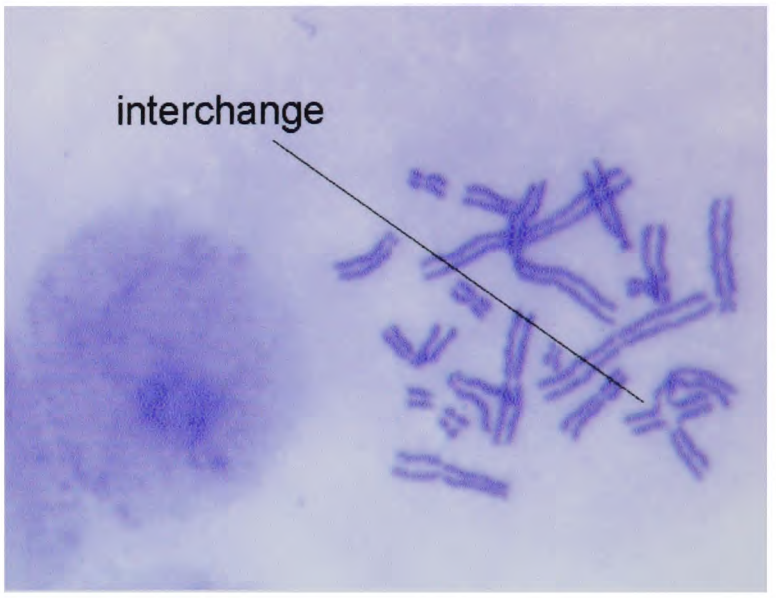

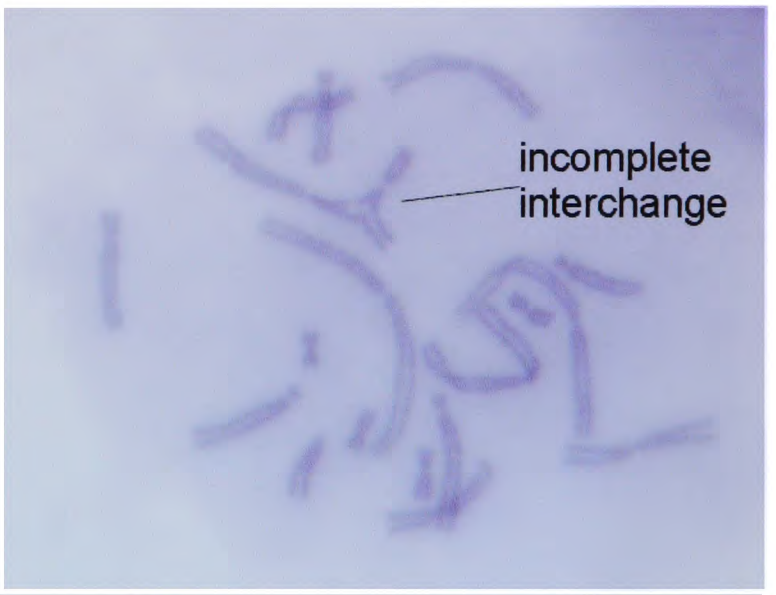

intrachange

Figure 5.2 Pictures and Diagrams of typical UV-induced chromosome aberrations. Cells were UV irradiated, allowed to proceed to metaphase and chromosome spreads were prepared and stained with Crystal Violet. Pictures were acquired at 400times magnification using a ccd camera.

in survival curves may possibly affect the interpretation of the experiments and mean it is possible that they do not reflect the true situation. When comparing the rate of aberrations I have summed the rate of breaks and exchanges to calculate a total rate of aberrations. This may be flawed if these aberrations are produced by unconnected processes and changes in one do not affect and reflect changes in the other.

There is a theory that proposes that the rate of exchanges and breaks changes in a different fashion with increasing dose (Sachs et al, 2000). This is based on IR data that shows that the rate of breaks increases linearly with increasing dose and that the yield is unaffected by altering the dose rate or by splitting the dose into two different doses. The data also shows that the rate of exchanges increases in proportion to the square of the dose, provided the doses are given in the same relatively short period of time. This fits with the idea that breaks (one hit aberrations) are caused by one lesion and exchanges (two hit aberrations) are caused by two lesions. This implies that the ratio of breaks and exchanges would alter quite naturally with increasing dose. The theory predicts that a higher dose would give a greater increase in the number of exchanges than the increase in the number of breaks.

This data and the corresponding theory should not affect my analysis, because the UV doses given to the different mutants are equitoxic and because the UV doses are given over minutes rather than the hours that are relevant to the IR based theory and to the repair process. If the theory was affecting these experiments than as the number of exchanges increases with a higher effective rate of irradiation and the 433B line is subjected to an effective higher rate than its parental line, CHO9, so it should have more exchanges, which is the reverse of what is observed.

Scoring of Chromosome Aberrations

Aberrations have been scored using five different classes: breaks, interchanges, intrachanges, incomplete interchanges and incomplete intrachanges (Figure 5.2). Incomplete structures have been recorded separately from the complete exchanges and the "breaks" in the incomplete exchanges in a separate class from normal breaks.

There is some controversy over what exactly constitutes a break for scoring purposes. A reasonable consensus is that a break exists where a space between two stained ends can be seen in a chromatid and the two ends are misaligned. Otherwise the space between the ends is classified as a gap. This controversy exists because it is thought that some spaces, i.e. gaps, are merely where chromosome decondensation has occurred and are not really breaks in the DNA strand. Obviously using the classification above, some breaks will be classified as gaps and not scored, but as long as the classification is consistent for all these experiments it should not affect the results.

For the purposes of analysis aberrations have been divided into two classes: all the exchanges and all the breaks. Breaks from incomplete exchanges have been included with breaks, as it is not, in reality, possible to tell which breaks are derived from incomplete exchanges and which are not. Although some publications use more detailed scoring systems, many simply score into either breaks or exchanges (De Santis et al., 2001).

One of the problems of studying chromosome aberrations is that scoring by its essence is subjective and this can bias results. Even with a rigorous selection of good metaphases and a scoring criteria there is still the possibility of bias. It is sometimes recommended that two independent investigators score experiments and then collate the results, however this has not been possible here. To try and combat possible bias, some experiments have been blind scored, these gave similar results to those which were not blind scored and this is a reasonable confirmation that any systematic bias is not too extreme and should not affect these results.

For each cell line, a zero UV control was scored for about 50 metaphases. All of the non-irradiated cell lines had only one or two aberrations in the 50 metaphases examined. This figure is low enough to be discounted.

Cell Line	Genotype	No. of Exp	No. of Metaphases	Mean of Total Exchanges/ Total Breaks	SD
CHO9	wt	1	176	1.57	
433B	ERCC1 def	1	168	0.43	
AA8 (total)	wt	2	296	1.27	0.09
AA8 (normal)			92	1.33	
AA8 (blind)			204	1.20	
UV41 (total)	XPF def.	2	270	0.60	0.04
UV41(normal)			123	0.57	
UV41 (blind)			147	0.63	
UV5	XPD def.	2	346	1.19	0.07
UV23	XPB def.	1	148	1.67	
UV135	XPG def.	1	120	1.63	

Table 5.2 Ratio of total exchanges to total breaks for UV-induced chromosome aberrations using various wt and NER def. cell lines. One experiment was blind scored for AA8 and UV41 cell lines. Results for AA8 and UV41 are given as total results (blind and normal summed), blind scored and normal.

ERCC1 def. cells have a higher ratio of breaks to exchanges than wt

An ERCC1 def. cell line shows a lower ratio of exchanges to breaks than a wild type cell line (Melton et al., 1998). So for every exchange event more breaks will be seen in the ERCC1 def. cells than in wt cells. If this effect is due to the loss of NER then it would be expected that other NER deficient cell lines would display the same effect. However, if the effect is due to the loss of the roles of ERCC1-XPF outside NER then it would be expected that other NER deficient cell lines would have the same ratio as wt.

In order to test the experimental method and method of scoring, it was decided to repeat published work studying the ERCC1 null 433B cell line and its wt parent CHO9 (Melton et al., 1998). The results suggest that the ERCC1 def. cell line has a ratio of 0.43 exchanges to breaks as compared to 1.57 for the wt parent (Table 5.2). This confirms the previous work and validates my method. However, the new data only shows a 3 fold difference between wt and ERCC1 null rather than the published 10 fold difference. This is probably due to different scoring methods. However, even a 3 fold difference between wt and ERCC1 def. is enough to merit investigation of other NER genes.

Although both new and published data was obtained using the same cell lines the doses used are rather different. In the published experiments 6.5J/m^2 were used for the wt line and 1.5 J/m^2 for the ERCC1 def. line, whereas my experiments used 12 and 3 J/m^2 respectively. This is surprising and may reflect the lack of a calibrated UV source in these experiments.

XPF def. cells have a higher ratio of breaks to exchanges than wt

After confirmation of the ERCC1 result it was decided to investigate an XPF def. cell line. This cell line and the XPD, XPB and XPG def. cell lines are derived from the wt AA8 parent rather than CHO9 and so AA8 has been used as the wt control. Both parental lines are derived from CHO cells and so the results should be relatively comparable, however because there may be unknown differences between the parents, the results have initially been analysed separately.

The experiment was repeated twice for the XPF def. cells and one of the experiments was scored blind in order to test whether there was any systematic bias in the scoring used. The wt cell line was tested in the same experiments, using blind scoring. The wt cell line had a ratio of 1.27 exchanges to breaks whereas the XPD def. cell line had a ratio of only 0.60, i.e. a greater than 2 fold difference (Table 5.2). The XPD def. cell line has a lower ratio of exchanges to breaks than the wt cell line, a similar result to that observed for ERCC1 def. cells.

The studies on ERCC1 and XPF def. cells confirm the work of Melton at al. (Melton et al., 1998). That is, the ratios of exchanges to breaks are higher in wt than in ERCC1 and XPF def. cells. This implies that ERCC1-XPF has some role in the formation of either breaks or exchanges, or both. Loss of ERCC1-XPF may promote the formation of breaks and/or inhibit the formation of exchanges. Obviously if the formation of breaks and exchanges is explicitly connected then changing one would naturally effect the other.

XPD, XPB and XPG def. cells have the same ratio of breaks to exchanges as wt

To test whether ERCC1-XPF is involved in aberration formation via its role in NER or its role in recombination, cell lines def. for XPD, XPB and XPG were tested. Two

experiments were performed for the XPD def. cell line and one each for the XPB and XPG cell lines. The ratios of exchanges to breaks are 1.19, 1.67 and 1.63 for the XPD, XPB and XPG def. cell lines respectively, these are close to the 1.27 ratio seen in wt cells. This shows that simple NER defective cell lines have about the same ratio of exchanges to breaks as wt.

Analysis of Results and Conclusions

By inspection there appears to be quite a difference in the ratio of exchanges to breaks between the wt (AA8) and XPF def. (UV41) cell lines and statistical testing confirms this. Using a T-test a significant difference was found between wt (AA8) and XPF def. (UV41) ($p=0.034$, 95% confidence interval –0.245 to 1.575). The nature of these experiments makes effective simple statistical testing difficult. Although over a hundred metaphases have been studied for each experiment, only a few independent experiments have been performed due to time limitations and this means it is difficult to show strong statistical significance.

The XPD, XPB and XPG def. cell lines all show very similar ratios of exchanges and breaks when compared to wt (AA8). The data was pooled for the simple NER def. cell lines and T-testing shows no significant difference from wt ($p=0.38$, 95% confidence interval –0.631 to 0.32). However a strongly statistically significant difference was found between the simple NER def. cell lines and the XPF def. cell line ($p=0.0048$, 95% confidence interval 0.38 to 1.259).

If the results for the XPF def. (UV41) and ERCC1 def. (433B) cell lines are collated and compared to the other NER def. cell lines a strong statistical difference is seen ($p=0.02$, 95% confidence interval 0.47 to 1.285).

This work has shown that an XPF and an ERCC1 def. cell line have a lower ratio of exchanges to breaks than simple NER def. cell lines and a wt cell line. This indicates that the reduction in the exchange over break ratio is due to the roles of ERCC1-XPF outside NER. What are the possible mechanisms by which ERCC1-XPF might be

involved in the formation of chromosome aberrations? Evidence indicates that ERCC1 is involved in the removal of non-homologous tails in SSA and homologous recombination. It may also be involved in the cleavage of ICL. So how is the loss of these roles likely to affect chromosome aberration formation? UV induced chromosome aberrations probably form when unrepaired damage is present during DNA replication in S phase. Replication past damage will result in a DSG opposite the damage and to repair these, or the DSBs formed from them, without error, may involve a recombinational event. Normally and ideally DSGs will be repaired by recombination using the sister chromatid as a template, failure of this could result in a break. This recombinational repair is analogous to NER in that it uses the information from the original complementary strand before replication for repair. The roles of ERCC1-XPF seem to be in processing non-homologous ends during recombination, and there should be no need for this in recombination between entirely homologous sister chromatids. Exchanges are probably formed when a partially homologous region of a non-homologous chromosome is used incorrectly to repair a DSG. ERCC1-XPF may be required for the processing of non-homologous ends formed in these recombination intermediates. The absence of ERCC1-XPF may mean that these intermediates cannot be processed and so a break is created. This would explain why ERCC1-XPF null cells have a higher ratio of breaks to exchanges than wt. Alternatively, perhaps breaks form at replication forks and SSA can sometime be used to repair these. If 4 ends rejoin incorrectly, using SSA to form an exchange, then ERCC1-XPF would be required to process the 3'ends. In the absence of ERCC1, SSA will fail and the breaks will not be repaired.

As mentioned earlier there is a possibility that the changed ratio of exchanges and breaks varies merely with the amount of UV, and has nothing to do with genotype. However this is extremely unlikely when the doses that I have used are considered. The dose for the XPF def. cell line falls between those for the wt AA8 line and the XPB and XPD def. cell lines, if the ratio of events changed merely with dose then one would expect there to be a trend however the XPF cell line has clearly different results to those found for the wt and XPB cell line.

The formation of chromosome aberrations has been studied previously using NER def. cell lines. Although there are no studies involving multiple NER def. cell lines there are various studies with one deficient line and a wt control and it is necessary to consider my results in light of these. Published work has seen an increased number of UV induced chromosomal aberrations in UV61; a CSB deficient cell line (defective in TCR) compared to wt (De Santis et al., 2001). A summation of their data across all doses shows 27 breaks and 11 exchanges for the AA8 wt cell line and 146 breaks and 123 exchanges for the UV61. Other work provides data on chromosome aberrations in wt cells alone (Palitti et al., 1983). It shows 18 breaks and 2 exchanges studying UV induced chromosome aberrations in a CHO cell line. The induction of chromosomal aberrations has also been previously studied in the 433B cell line (Darroudi and Natarajan, 1985). The results show that 433B cells have a higher (about 4 times) incidence of spontaneous chromosome aberrations and this is mainly due to breaks. It is difficult to say whether the above results contradict or support these current results. Scoring methods and hence results differ between researchers and so it is difficult to compare separate experiments. There have been no studies published with a comparison across several cell lines and without this, it is difficult to compare my work with others.

Chapter 6 - The response of DNA replication in NER deficient cell lines to UV and DNA crosslinking agents

Chapter Summary and Background

Cell cycle arrest can occur at various points after DNA damage. In order to study this in ERCC1 and other NER def. cell lines it was decided to examine how the level of replicative DNA synthesis changes after DNA damage in S phase. These experiments were prompted by results which indicated a possible difference between the UV response of ERCC1 def. 433B cells, XPD def. UV5 cells and wt (AA8 and CHO9) cells (F. Nunez, 1999). The response of 433B and UV5 cells to treatment with UV and MMC in S phase has been examined by using the incorporation of tritiated thymidine as a measure of DNA synthesis. MMC is a bifunctional DNA alkylating agent that causes DNA adducts, DNA intrastrand crosslinks and DNA interstrand links. Although the interstrand crosslinks form a small proportion of the overall damage, they have the largest effect on the cell. One unrepaired interstrand crosslink can be enough to arrest the cell cycle.

Introduction – UV induced arrest of DNA replication

In order for a cell to progress through the cell cycle it must pass various checkpoints, these ensure that the cell is in a suitable condition to proceed. There are 4 main sets of checkpoints: those at the G1 to S phase transition, those within S phase, at the G2 to M transition and within M phase. Several of the checkpoints respond to DNA damage. If a cell has large amounts of DNA damage it will not proceed into S phase. DNA damage will also delay the completion of S phase and the transition from G2 into M phase.

Enlarged ERCC1 null hepatocytes arrest in G2, this indicates that they bypass the normal G1/S DNA damage checkpoint and that there maybe altered cell cycle regulation in ERCC1 null cells. This altered regulation maybe due to special characteristics of hepatocytes but may also be due directly to the ERCC1 deficiency.

This makes it interesting to study the response to DNA damage in the 433B (ERCC1 def.) cell line.

Previously published work using the tritiated thymidine incorporation assay has detected no unexpected features of the response of DNA replication in 433B (ERCC1 def.) and CHO9 (wt) cells to DNA damage in S phase (Wood et al., 1982). However, possible abnormalities in the response of 433B cells have been recently detected (F Nunez, 1999). Two assays were used one at a low dose (10 J/m^2) and one at a higher dose (20 J/m^2). The low dose assay relied on the enzyme DenV, which cuts the damaged strand of DNA at thymidine dimer sites. By using radioactive labelling of replicating DNA by nucleotide incorporation, it is possible to differentiate replicating DNA from the bulk DNA. Samples from irradiated cells at various time points after irradiation were digested with DenV and electrophoresed on an alkaline gel. The size of the tail that is produced from digested nuclei gives an indication of the amount of digestion. This gives a measure of the number of thymidine dimers by the number of enzyme sensitive sites. This assay showed poor removal of dimers after UV in both ERCC1 def. and wt cells. DenV will also cut at thymidine dimers opposite DSGs leading to a DSB, which can be detected using AFIGE (Asymmetric Field Inversion Gel Electrophoresis). The rationale was that DSGs would be formed where a replication fork stalls at damage and this gives a measure of replication arrest. This relies on the proportion of DSGs that form DSBs being stable whatever the dose or genotype.

The results of this assay were interpreted as indicating that there was very little arrest of DNA replication after UV as the numbers of DSBs decreased rapidly in both wt and ERCC1 def.. However this assay is not really measuring arrest of replication directly, merely an after effect of the stalling of replication. The number of DSBs formed reflects the kinetics of formation and survival of the DSGs, not directly the arrest or stalling of replication forks. This makes the experiments very hard to interpret. The more complex an experiment is, as is the DenV AFIGE assay, the more assumptions must be made to interpret the results, and the more assumptions that are made the more likely that one of them will be wrong and that the

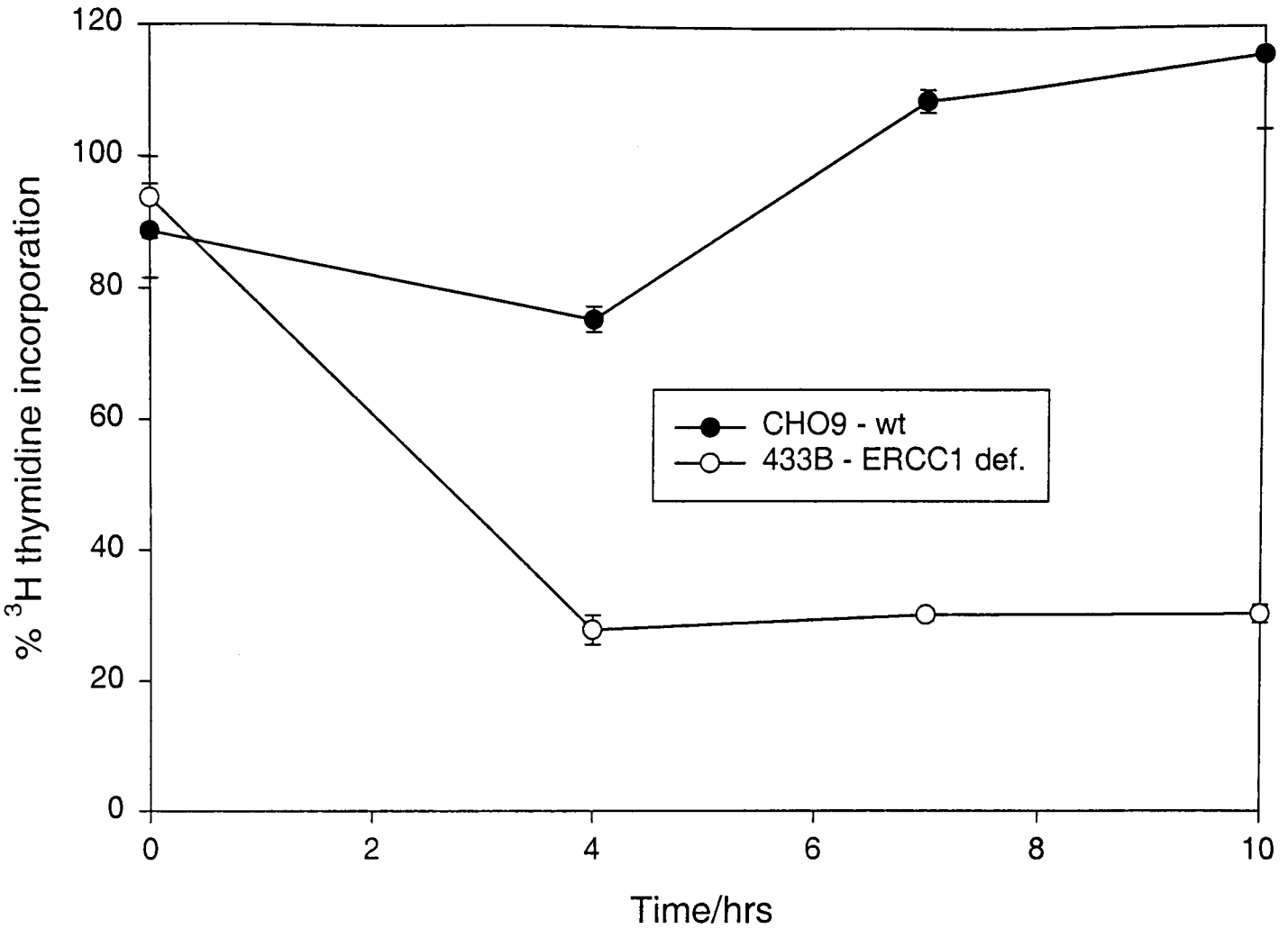

Figure 6.1 Incorporation of ^{3}Hthymidine after UV during S phase. Cells were synchronised in G0, released and allowed to proceed into S phase. They were then given a dose of 10 J/m^2 of UV. 15 minute pulses of tritiated thymidine were used to assay for DNA synthesis. Points are plotted as a percentage relative to a non-irradiated sample. Each curve is the mean of at least 3 experiments. Error bars represent standard error.

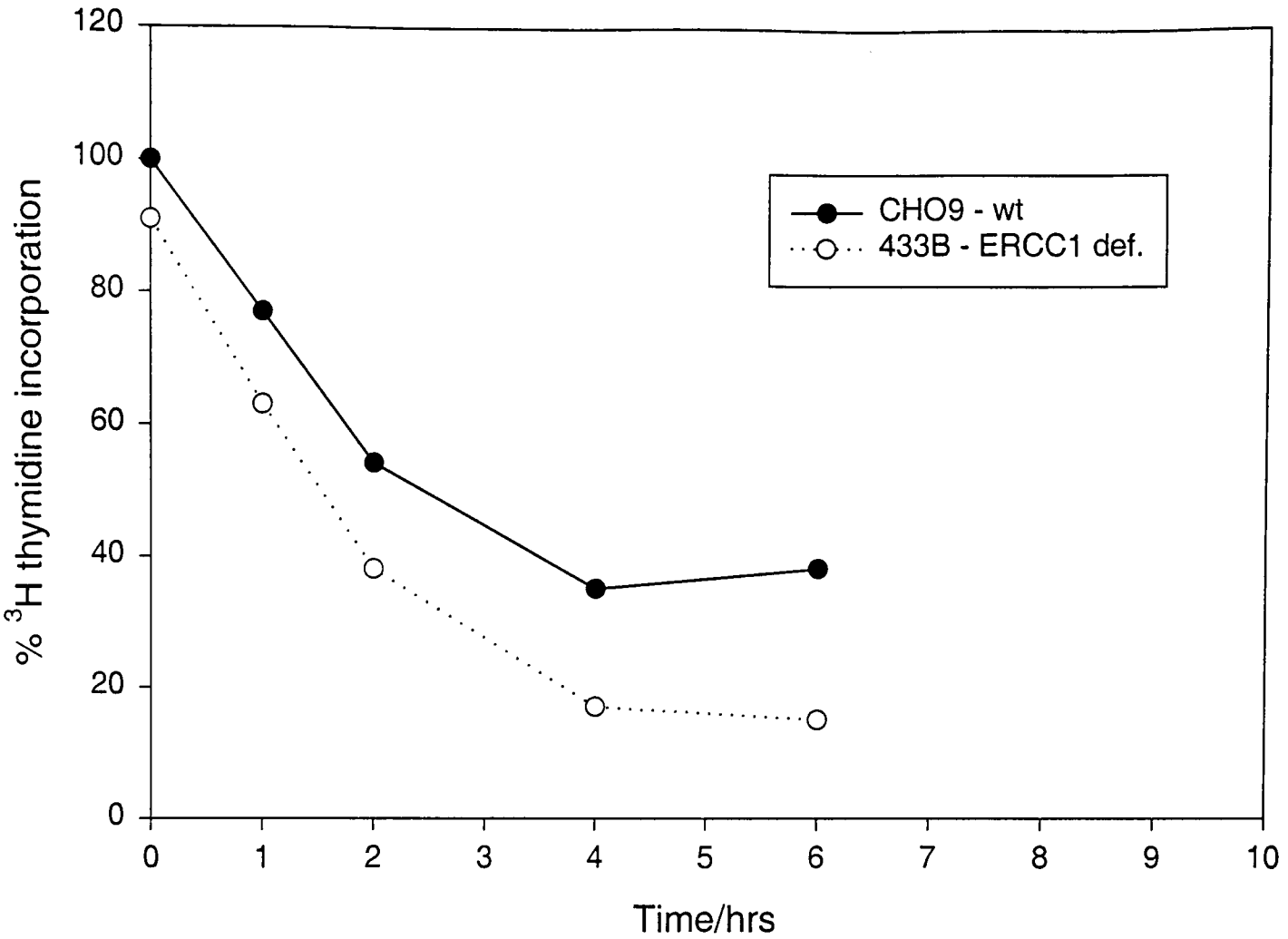

Figure 6.2 Incorporation of ^{3}H-thymidine after UV during S phase (F Nunez, 1999). Cells were synchronised in G0, released and allowed to proceed into S phase. They were then given a dose of 20 J/m^{2} of UV. 15 minute pulses of tritiated thymidine were used to assay for DNA synthesis. Points are plotted as a percentage relative to a non-irradiated sample.

interpretation of the experiments will be wrong. The AFIGE assay also indicated that the ERCC1 def. cells might possibly arrest for a shorter time than wt after DNA damage.

On the basis of the above experiments, and their original interpretation, further experiments were performed using a simpler assay and a higher dose (F Nunez, 1999). Cells were arrested in G1 using isoleucine deprivation, released from arrest and allowed to proceed in synchrony into S phase. S phase cells were UV irradiated and then the level of DNA synthesis was measured at various time points after irradiation, by using pulses of tritiated thymidine. The incorporation in the UV irradiated samples was taken as a percentage of incorporation in unirradiated cells to study the effect of the irradiation. These experiments showed a terminal arrest of replication in the ERCC1 def. cells and a nearly terminal arrest of wt cells. This appeared to contradict the results of the DenV assays, which appeared to show very little arrest of replication as measured by DSB formation. Although the thymidine assay used a higher dose than the DenV assay, it seems unlikely that little arrest occurs at 10 J/m^2 and yet both genotypes are arrested at 20 J/m^2.

ERCC1 deficient cells arrest DNA replication at low doses

In order to try and resolve the difference between the results of the two assays, I investigated the arrest of 433B (ERCC1 def.) and CHO9 (wt) cells using the thymidine incorporation assay at the low dose originally used with the DenV assay (Figure 6.1). The percentage incorporation of thymidine in 433B (ERCC1 def.) cells compared to unirradiated controls falls to around 30% by 4 hrs after irradiation and does not recover by 10 hours. The percentage incorporation of thymidine in CHO9 (wt) cells compared to unirradiated controls falls to around 75% by 4 hours and recovers to 100% by 7 hours. This can be compared to the results of F Nunez (Figure 6.2). Measurements at 0 hrs after irradiation do not show 100% incorporation because incorporation is detected over 15 minute pulses, so arrest has some time to take effect. These results show that 433B (ERCC1 def.) cells do arrest

DNA replication at low doses of 10 J/m^2 and suggests that the results from and original interpretation of the DenV assay are probably misleading.

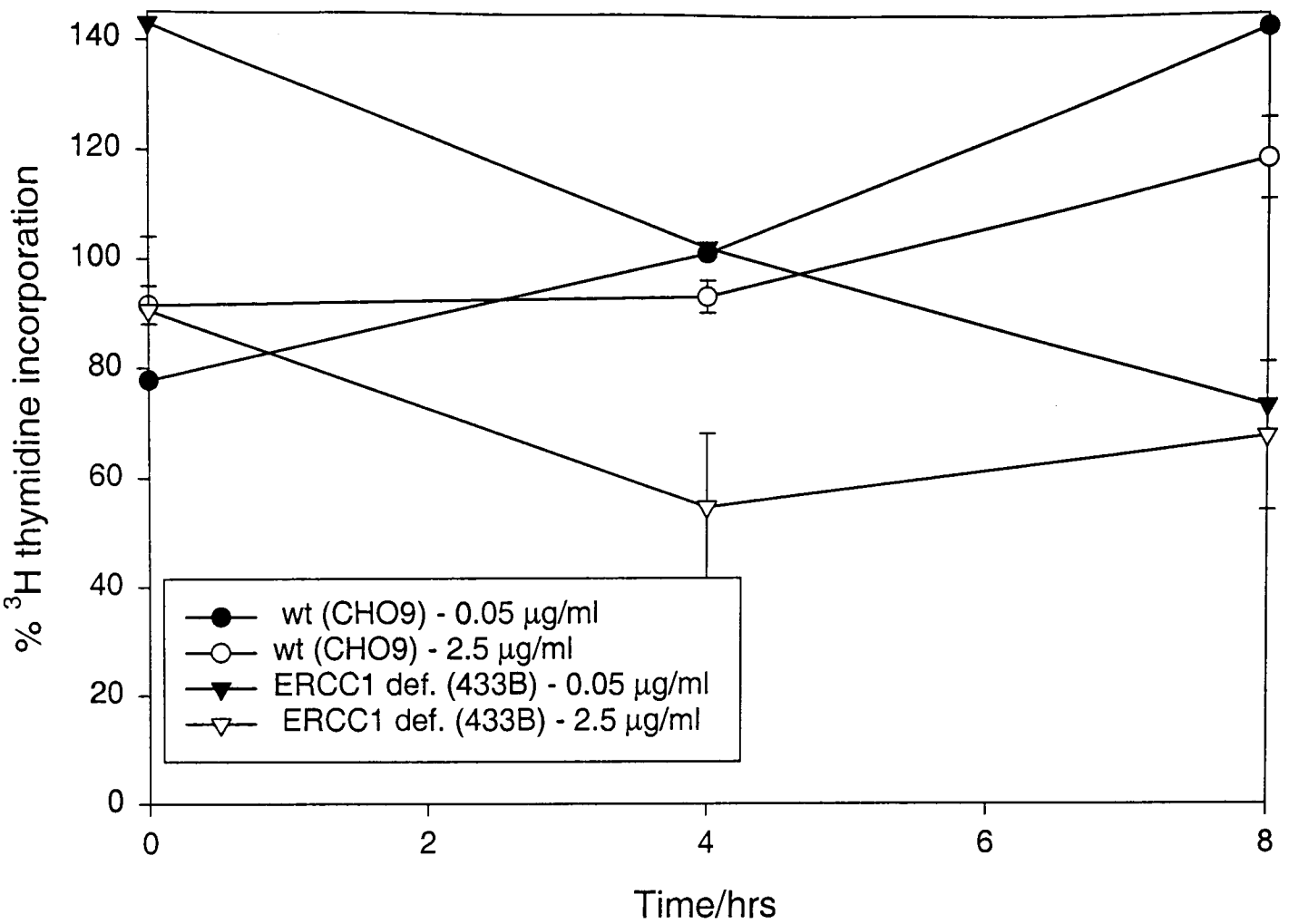

Figure 6.3 Incorporation of ^{3}Hthymidine after Mitomycin C during S phase. Cells were synchronised in G0, released and allowed to proceed into S phase. They were then given a dose of either 2.5 or 0.05 µg/ml of Mitomycin C. 15 minute pulses of tritiated thymidine were used to assay for DNA synthesis. Points are plotted as a percentage relative to a non-irradiated sample. Each curve is the mean of 2 experiments. Error bars represent standard error.

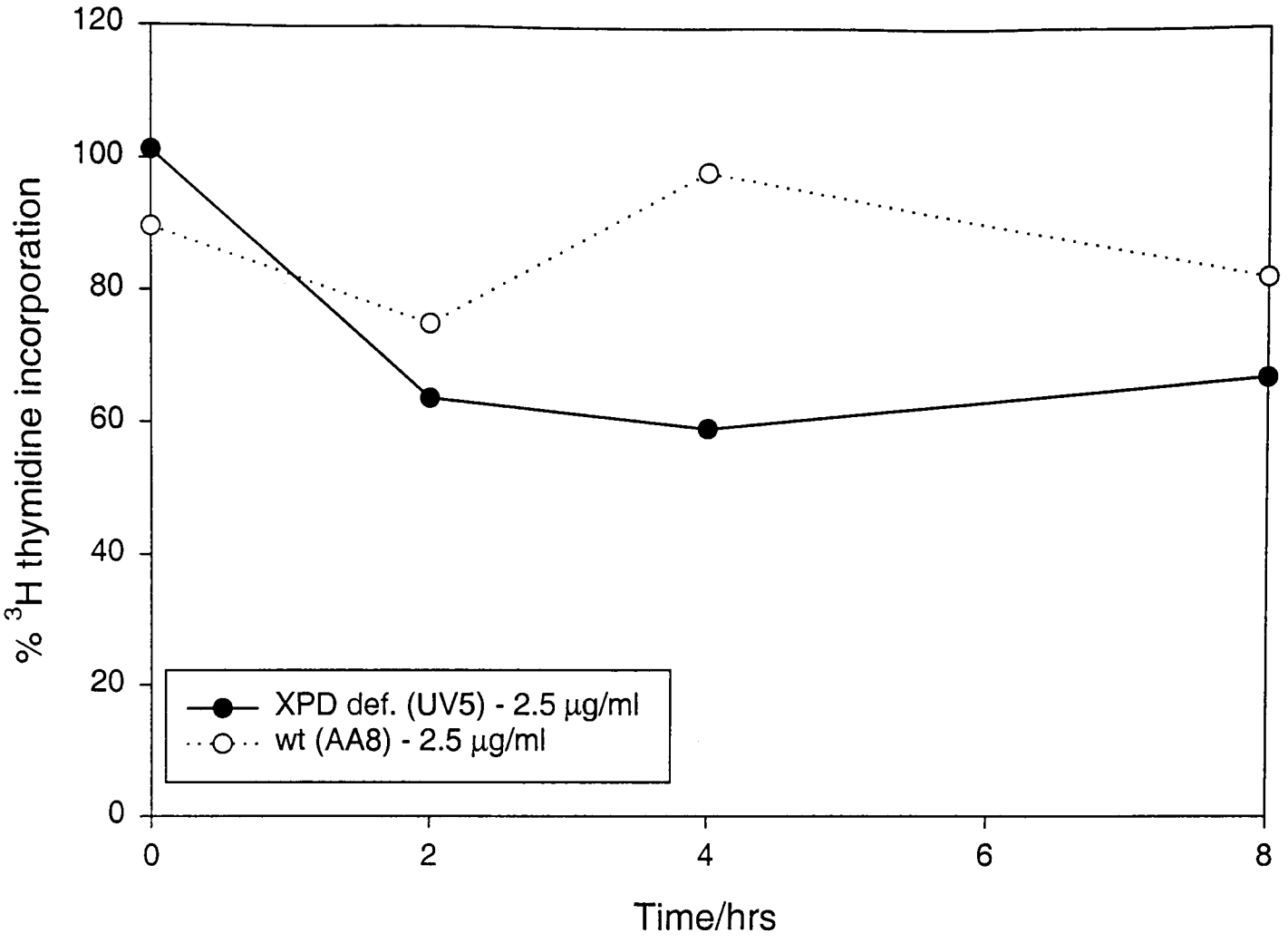

Figure 6.4 Incorporation of ^{3}H-thymidine after Mitomycin C treatment during S phase. Cells were synchronised in G0, released and allowed to proceed into S phase. They were then given a dose of 2.5 µg/ml of Mitomycin C. 15 minute pulses of tritiated thymidine were used to assay for DNA synthesis. Points are plotted as a percentage relative to an untreated sample.

Introduction – MMC induced arrest of DNA replication

ERCC1 deficient cells are hypersensitive to ICL agents and ERCC1 is involved in the repair of this type of damage. The thymidine incorporation assay has been used to study the responses of ERCC1 def. and XPD def. cells to ICL damage in order to see if arrest of DNA synthesis occurred in the same way in an ERCC1 mutant and another NER mutant. This assay also allows the investigation of the dose of crosslinking agent required for arrest in S phase. It is known that cells treated with low doses of ICL agents arrest in G2, however it was interesting to investigate the question of whether cells would arrest in S phase and what dose would be required relative to that needed for arrest in G2.

ERCC1 and XPD def. cells show replication arrest after DNA crosslinking treatment only at extremely high cell killing doses

Two doses of MMC were used for these experiments, 0.05 and 2.5 μg/ml (Figure 6.3, Figure 6.4). There is no clear reduction in thymidine incorporation after MMC treatment except in 433B (ERCC1 def.) cells and UV5 (XPD def.) cells, where incorporation reduces to about 60% by 4 and 2 hours respectively, after treatment with 2.5 μg/ml. This is unexpected if compared to the amount of MMC required to kill these cells. The D50 (dose required for 50% survival) for MMC was 0.325 μg/ml for CHO9 (wt) and 0.0075 μg/ml for 433B (ERCC1 def.) (Melton et al., 1998). The dose required to significantly arrest replication is 300 times greater than that required to kill half the cells. XPD def. (UV5) cells have a sensitivity to MMC between those of 433B and CHO9. It is unexpected that XPD and ERCC1 def. cells both arrest replication to about the same degree after the same dose of MMC, even though ERCC1 def. cells are much more sensitive to MMC than XPD def. cells.

Discussion

These results show that a far greater dose of MMC is required to arrest cells in S phase than to kill them and this dose is the same for hypersensitive ERCC1 def. cells and less sensitive XPD def. cells, ie. the response is not affected by ERCC1 deficiency. Perhaps the main process of repair occurs after S phase as there is no sensitive checkpoint in S phase to allow repair of ICL. Published data suggests that ERCC1-XPF is probably involved the repair of DNA interstrand crosslinks, but the other NER genes, including XPD, are not.

Vastly higher doses of ICL agents are required to arrest cells in S-phase than to kill cells. It only requires one unrepaired ICL to kill a cell, but it seems that many ICL are required to arrest a cell in S-phase. At the doses used ERCC1 def. cells arrest to about the same degree as other NER def. cells, this may reflect the fact that MMC forms mostly single stranded adducts, as well as the cell killing ICL adducts.

These results are interesting given that the ERCC1 null hepatocytes arrest in G2/M. Perhaps the G2 arrest is caused by a small number of crosslinks that are not enough to arrest the cell in S phase but are detected in G2/M.

Previous experiments have shown that cisplatin DNA crosslinks do not inhibit S phase and cause only a G2/M arrest in both *S. cerevisiae* and mammalian cells (Grossmann et al., 1999; Grossmann et al., 2000; Sorenson et al., 1990; Sorenson and Eastman, 1988). My results have shown that MMC can only arrest DNA replication in mammalian cells at hyper cell killing doses.

Chapter 7 - Overall Conclusions

I have shown that:

- ERCC1 null hepatocytes have accelerated development of polyploidy and that the enlarged ERCC1 null hepatocytes are arrested in G2/M, as are enlarged old wt hepatocytes.
- ERCC1 null liver has increased levels of p21 and that the p21 tends to be found in the enlarged nuclei.
- Most old wt liver samples do not have greatly increased levels of p21.
- The phenotype of the ERCC1 null mouse is p53 independent and that BER and MMR genes are overexpressed in ERCC1 null hepatocytes.
- ERCC1-XPF is involved in the formation of chromosome aberrations, but that other NER proteins are not. In ERCC1 and XPF def. cells there are less exchanges and more breaks.
- ERCC1 def. cells respond in the same way as other NER def. cells to UV treatment during S phase and that a hyper cell killing dose of interstrand crosslinks is required to arrest a cell in S phase, whereas it is known that just one crosslink will arrest a cell in G2.

These results allow a greater understanding of the causes of the ERCC1 null phenotype. Other NER def. mice display no similar liver phenotype implying that the loss of NER is not causing the ERCC1 null liver phenotype.

Considering my data and previous data, I propose a model to explain the hepatocyte phenotype of the ERCC1 null mouse. DNA damage accumulates in ERCC1 null hepatocytes due to the loss of DNA repair pathways that depend on ERCC1-XPF. This damage is likely to be DNA interstrand crosslink damage as well as other damage that is normally repaired by NER. The increased DNA damage leads to increased activity by the MMR and BER pathways. The loss of ERCC1 means that interstrand crosslinks cannot be repaired. The load of crosslinks and associated damage is not high enough to arrest DNA replication. The formation of chromosome exchanges may be an error prone way for cells to repair DNA damage, at least to tolerate the damage to allow DNA replication. Without ERCC1 this repair cannot function and the increased number of chromosome breaks, i.e. DSBs, formed is a

strong signal for polyploidy development in the liver. The increased DNA damage promotes the induction of p53 and p21 in nuclei, although p21 induction in this case does not require p53. The increase in p21 levels is a response to DNA damage and may also trigger polyploidy. Increased levels of p21 only appear at certain stages in the development of polyploidy and appear before the polyploidy is apparent, thus explaining why p21 increases are not seen in some enlarged nuclei and are seen in some small nuclei. The polyploidy development is accelerated compared to the normal polyploidy development in ageing wt liver. Small p21 increases are only seen in old wt liver because either the development of polyploidy is extremely slow, over 2 years, and p21 only appears at certain stages or because p21 is not involved in the normal development of polyploidy. The small increases are expected if p21 levels are increased due to DNA damage, because of the stochastic nature of that damage and because there will be low levels of DNA damage in old wt animals compared to ERCC1 null. The ERCC1 null polyploid nuclei arrest in G2, like old wt polyploid nuclei, as part of the normal process of polyploidy development.

This model comes with the caveat that I have not shown that there is a direct link between ERCC1 deficiency, increased levels of DNA damage, increased levels of p21 and accelerated polyploidy, but I have shown some association between these, at least in the case of the ERCC1 mouse liver that I have studied.

References

Aboussekhra, A., Biggerstaff, M., Shivji, M.K., Vilpo, J.A., Moncollin, V., Podust, V.N., Protic, M., Hubscher, U., Egly, J.M., and Wood, R.D. (1995). Mammalian DNA nucleotide excision repair reconstituted with purified protein components. Cell *80*, 859-868.

Adair, G.M., Rolig, R.L., Moore-Faver, D., Zabelshansky, M., Wilson, J.H., and Nairn, R.S. (2000). Role of ERCC1 in removal of long non-homologous tails during targeted homologous recombination. EMBO J. *19*, 5552-5561.

Alani, E., Reenan, R.A., and Kolodner, R.D. (1994). Interaction between mismatch repair and genetic recombination in Saccharomyces cerevisiae. Genetics *137*, 19-39.

Alani, E., Lee, S., Kane, M.F., Griffith, J., and Kolodner, R.D. (1997). Saccharomyces cerevisiae MSH2, a mispaired base recognition protein, also recognizes Holliday junctions in DNA. J.Mol.Biol. *265*, 289-301.

Albrecht, J.H., Meyer, A.H., and Hu, M.Y. (1997). Regulation of cyclin-dependent kinase inhibitor p21(WAF1/Cip1/Sdi1) gene expression in hepatic regeneration. Hepatology *25*, 557-563.

Albrechtsen, N., Dornreiter, I., Grosse, F., Kim, E., Wiesmuller, L., and Deppert, W. (1999). Maintenance of genomic integrity by p53: complementary roles for activated and non-activated p53. Oncogene *18* , 7706-7717.

Alison, M. (1998). Liver stem cells: a two compartment system. Curr.Opin.Cell Biol. *10*, 710-715.

Aravind, L., Walker, D.R., and Koonin, E.V. (1999). Conserved domains in DNA repair proteins and evolution of repair systems. Nucleic.Acids.Res. *27*, 1223-1242.

Arnaudeau, C., Tenorio, M.E., Jenssen, D., and Helleday, T. (2000). Inhibition of DNA synthesis is a potent mechanism by which cytostatic drugs induce homologous recombination in mammalian cells. Mutat.Res. *461*, 221-228.

Asahina, H., Kuraoka, I., Shirakawa, M., Morita, E.H., Miura, N., Miyamoto, I., Ohtsuka, E., Okada, Y., and Tanaka, K. (1994). The XPA protein is a zinc metalloprotein with an ability to recognize various kinds of DNA damage. Mutat.Res. *315*, 229-237.

Awad, M.M., Sanders, J.A., and Gruppuso, P.A. (2000). A potential role for p15(Ink4b) and p57(Kip2) in liver development. FEBS Lett. *483*, 160-164.

Ayyagari, R., Impellizzeri, K.J., Yoder, B.L., Gary, S.L., and Burgers, P.M. (1995). A mutational analysis of the yeast proliferating cell nuclear antigen indicates distinct roles in DNA replication and DNA repair. Mol.Cell Biol. *15*, 4420-4429.

Balajee, A.S., Proietti, D.S., Brosh, R.M.J., Selzer, R., and Bohr, V.A. (2000). Role of the ATPase domain of the Cockayne syndrome group B protein in UV induced apoptosis. Oncogene *19*, 477-489.

Bardwell, A.J., Bardwell, L., Tomkinson, A.E., and Friedberg, E.C. (1994). Specific cleavage of model recombination and repair intermediates by the yeast Rad1-Rad10 DNA endonuclease. Science *265*, 2082-2085.

Barre, F.X., Asseline, U., and Harel-Bellan, A. (1999). Asymmetric recognition of psoralen interstrand crosslinks by the nucleotide excision repair and the error-prone repair pathways. J.Mol.Biol. *286*, 1379-1387.

Barzilay, G., Walker, L.J., Rothwell, D.G., and Hickson, I.D. (1996). Role of the HAP1 protein in repair of oxidative DNA damage and regulation of transcription factors. Br.J.Cancer Suppl. *27:S145-50.*, S145-S150

Bates, S., Ryan, K.M., Phillips, A.C., and Vousden, K.H. (1998). Cell cycle arrest and DNA endoreduplication following p21Waf1/Cip1 expression. Oncogene *17*, 1691-1703.

Batty, D.P. and Wood, R.D. (2000). Damage recognition in nucleotide excision repair of DNA. Gene *241*, 193-204.

Baumann, P. and West, S.C. (1998). DNA end-joining catalyzed by human cell-free extracts. Proc.Natl.Acad.Sci.U.S.A. *95*, 14066-14070.

Baynton, K., Bresson-Roy, A., and Fuchs, R.P. (1998). Analysis of damage tolerance pathways in Saccharomyces cerevisiae: a requirement for Rev3 DNA polymerase in translesion synthesis. Mol.Cell Biol. *18*, 960-966.

Beamish, H., Williams, R., Chen, P., and Lavin, M.F. (1996). Defect in multiple cell cycle checkpoints in ataxia-telangiectasia postirradiation. J.Biol.Chem. *271*, 20486-20493.

Bellamy, C.O., Clarke, A.R., Wyllie, A.H., and Harrison, D.J. (1997). p53 Deficiency in liver reduces local control of survival and proliferation, but does not affect apoptosis after DNA damage. FASEB J. *11*, 591-599.

Bellon, S.F., Coleman, J.H., and Lippard, S.J. (1991). DNA unwinding produced by site-specific intrastrand cross-links of the antitumor drug cis-diamminedichloroplatinum(II). Biochemistry *30*, 8026-8035.

Belmaaza, A., Milot, E., Villemure, J.F., and Chartrand, P. (1994). Interference of DNA sequence divergence with precise recombinational DNA repair in mammalian cells. EMBO J. *13*, 5355-5360.

Benjamin, M.B. and Little, J.B. (1992). X rays induce interallelic homologous recombination at the human thymidine kinase gene. Mol.Cell Biol. *12*, 2730-2738.

Bergmann, E. and Egly, J.M. (2001). Trichothiodystrophy, a transcription syndrome. Trends.Genet. *17*, 279-286.

Bertrand, P., Tishkoff, D.X., Filosi, N., Dasgupta, R., and Kolodner, R.D. (1998). Physical interaction between components of DNA mismatch repair and nucleotide excision repair. Proc.Natl.Acad.Sci.U.S.A. *95*, 14278-14283.

Bessho, T., Sancar, A., Thompson, L.H., and Thelen, M.P. (1997). Reconstitution of human excision nuclease with recombinant XPF-ERCC1 complex. J.Biol.Chem. *272*, 3833-3837.

Bessho, T., Mu, D., and Sancar, A. (1997). Initiation of DNA interstrand cross-link repair in humans: the nucleotide excision repair system makes dual incisions 5' to the cross-linked base and removes a 22- to 28-nucleotide-long damage-free strand. Mol.Cell Biol. *17*, 6822-6830.

Bessho, T. (1999). Nucleotide excision repair 3' endonuclease XPG stimulates the activity of base excision repairenzyme thymine glycol DNA glycosylase. Nucleic.Acids.Res. *27*, 979-983.

Bierne, H. and Michel, B. (1994). When replication forks stop. Mol.Microbiol. *13*, 17-23.

Biesterfeld, S., Gerres, K., Fischer-Wein, G., and Bocking, A. (1994). Polyploidy in non-neoplastic tissues. J.Clin.Pathol. *47*, 38-42.

Biggerstaff, M., Szymkowski, D.E., and Wood, R.D. (1993). Co-correction of the ERCC1, ERCC4 and xeroderma pigmentosum group F DNA repair defects in vitro. Embo J *12*, 3685-92.

Blasina, A., Paegle, E.S., and McGowan, C.H. (1997). The role of inhibitory phosphorylation of CDC2 following DNA replication block and radiation-induced damage in human cells. Mol.Biol.Cell *8*, 1013-1023.

Bohm, N. and Noltemeyer, N. (1981). Development of binuclearity and DNA-polyploidization in the growing mouse liver. Histochemistry *72*, 55-61.

Brasch, K. (1980). Endopolyploidy in vertebrate liver: an evolutionary perspective. Cell Biol.Int.Rep *4*, 217-226.

Bravo, R., Frank, R., Blundell, P.A. and Macdonald –Bravo, H. (1987). Cyclin/PCNA is the auxiliary protein of DNA polymerase delta. Nature *326*, 515-517

Brenner, S., Pepper, D., Berns, M.W., Tan, E., and Brinkley, B.R. (1981). Kinetochore structure, duplication, and distribution in mammalian cells: analysis by human autoantibodies from scleroderma patients. J.Cell Biol. *91*, 95-102.

Bridges, B.A. and von Wright, A. (1981). Influence of mutations at the rep gene on survival of Escherichia coli following ultraviolet light irradiation or 8-methoxypsoralen photosensitization: evidence for a recA+ rep+-dependent pathway for repair of DNA crosslinks. Mutat.Res. *82*, 229-238.

Brodsky, W.Y. and Uryvaeva, I.V. (1977). Cell polyploidy: its relation to tissue growth and function. Int.Rev.Cytol. *50:275-332.*, 275-332.

Brosh, R.M.J., Balajee, A.S., Selzer, R.R., Sunesen, M., Proietti, D.S., and Bohr, V.A. (1999). The ATPase domain but not the acidic region of Cockayne syndrome group B gene product is essential for DNA repair. Mol.Biol.Cell *10*, 3583-3594.

Brown, J.P., Wei, W., and Sedivy, J.M. (1997). Bypass of senescence after disruption of p21CIP1/WAF1 gene in normal diploid human fibroblasts. Science *277*, 831-834.

Brugarolas, J., Chandrasekaran, C., Gordon, J.I., Beach, D., Jacks, T., and Hannon, G.J. (1995). Radiation-induced cell cycle arrest compromised by p21 deficiency. Nature *377*, 552-557.

Bunz, F., Dutriaux, A., Lengauer, C., Waldman, T., Zhou, S., Brown, J.P., Sedivy, J.M., Kinzler, K.W., and Vogelstein, B. (1998). Requirement for p53 and p21 to sustain G2 arrest after DNA damage. Science *282*, 1497-1501.

Burford-Mason, A.P., Mackay, A.J., Cummins, M. and Dardick, I. (1994). Detection of PCNA in paraffin embedded specimens is dependent on pre-embedding tissue handling and fixation. Arch. Pathol. Lab. Med. *118*, 1007-1013.

Burki, H.J., Lam, C.K., and Wood, R.D. (1980). UV-light-induced mutations in synchronous CHO cells. Mutat.Res. *69*, 347-356.

Cadet, J., Berger, M., Douki, T., and Ravanat, J.L. (1997). Oxidative damage to DNA: formation, measurement, and biological significance. Rev.Physiol.Biochem.Pharmacol. *131:1-87.*

Caldecott, K. and Jeggo, P. (1991). Cross-sensitivity of gamma-ray-sensitive hamster mutants to cross-linking agents. Mutat.Res. *255*, 111-121.

Carrier, F., Georgel, P.T., Pourquier, P., Blake, M., Kontny, H.U., Antinore, M.J., Gariboldi, M., Myers, T.G., Weinstein, J.N., Pommier, Y., and Fornace, A.J.J. (1999). Gadd45, a p53-

responsive stress protein, modifies DNA accessibility on damaged chromatin. Mol.Cell Biol *19*, 1673-1685.

Chan, T.A., Hwang, P.M., Hermeking, H., Kinzler, K.W., and Vogelstein, B. (2000). Cooperative effects of genes controlling the G(2)/M checkpoint. Genes Dev. *14*, 1584-1588.

Chaudhary, A.K., Nokubo, M., Reddy, G.R., Yeola, S.N., Morrow, J.D., Blair, I.A., and Marnett, L.J. (1994). Detection of endogenous malondialdehyde-deoxyguanosine adducts in human liver. Science *265*, 1580-1582.

Chen, J., Jackson, P.K., Kirschner, M.W., and Dutta, A. (1995). Separate domains of p21 involved in the inhibition of Cdk kinase and PCNA. Nature *374*, 386-388.

Chen, W. and Jinks-Robertson, S. (1998). Mismatch repair proteins regulate heteroduplex formation during mitotic recombination in yeast. Mol.Cell Biol. *18*, 6525-6537.

Chen, W. and Jinks-Robertson, S. (1999). The role of the mismatch repair machinery in regulating mitotic and meiotic recombination between diverged sequences in yeast. Genetics *151*, 1299-1313.

Chlebowicz, E. and Jachymczyk, W.J. (1979). Repair of MMS-induced DNA double-strand breaks in haploid cells of Saccharomyces cerevisiae, which requires the presence of a duplicate genome. Mol.Gen.Genet. *167*, 279-286.

Chomczynski, P. and Sacchi, N. (1987). Single-step method of RNA isolation by acid guanidinium thiocyanate-phenol-chloroform extraction. Anal.Biochem. *162*, 156-159.

Ciotta, C., Ceccotti, S., Aquilina, G., Humbert, O., Palombo, F., Jiricny, J., and Bignami, M. (1998). Increased somatic recombination in methylation tolerant human cells with defective DNA mismatch repair. J.Mol.Biol. *276*, 705-719.

Clark, A.B., Valle, F., Drotschmann, K., Gary, R.K., and Kunkel, T.A. (2000). Functional interaction of proliferating cell nuclear antigen with MSH2-MSH6 and MSH2-MSH3 complexes. J.Biol.Chem. *275*, 36498-36501.

Clarke, A.R., Purdie, C.A., Harrison, D.J., Morris, R.G., Bird, C.C., Hooper, M.L., and Wyllie, A.H. (1993). Thymocyte apoptosis induced by p53-dependent and independent pathways. Nature *362*, 849-852.

Clarke, D.J. and Gimenez-Abian, J.F. (2000). Checkpoints controlling mitosis. Bioessays *22*, 351-363.

Clugston, C.K., McLaughlin, K., Kenny, M.K., and Brown, R. (1992). Binding of human single-stranded DNA binding protein to DNA damaged by the anticancer drug cis-diamminedichloroplatinum (II). Cancer Res. *52*, 6375-6379.

Cooper, M.P., Balajee, A.S., and Bohr, V.A. (1999). The C-terminal domain of p21 inhibits nucleotide excision repair In vitro and In vivo. Mol.Biol.Cell *10*, 2119-2129.

Cooper, P.K., Nouspikel, T., Clarkson, S.G., and Leadon, S.A. (1997). Defective transcription-coupled repair of oxidative base damage in Cockayne syndrome patients from XP group G. Science *275*, 990-993.

Cordeiro-Stone, M., Zaritskaya, L.S., Price, L.K., and Kaufmann, W.K. (1997). Replication fork bypass of a pyrimidine dimer blocking leading strand DNA synthesis. J.Biol.Chem. *272*, 13945-13954.

Cordeiro-Stone, M., Makhov, A.M., Zaritskaya, L.S., and Griffith, J.D. (1999). Analysis of DNA replication forks encountering a pyrimidine dimer in the template to the leading strand. J.Mol.Biol. *289*, 1207-1218.

Cordonnier, A.M. and Fuchs, R.P. (1999). Replication of damaged DNA: molecular defect in xeroderma pigmentosum variant cells. Mutat.Res. *435*, 111-119.

Cornforth, M.N. (1989). On the nature of interactions leading to radiation-induced chromosomal exchange. Int.J.Radiat.Biol. *56*, 635-643.

Critchlow, S.E. and Jackson, S.P. (1998). DNA end-joining: from yeast to man. Trends Biochem Sci *23*, 394-8.

Cui, X., Brenneman, M., Meyne, J., Oshimura, M., Goodwin, E.H., and Chen, D.J. (1999). The XRCC2 and XRCC3 repair genes are required for chromosome stability in mammalian cells. Mutat.Res. *434*, 75-88.

Dardalhon, M. and Averbeck, D. (1995). Pulsed-field gel electrophoresis analysis of the repair of psoralen plus UVA induced DNA photoadducts in Saccharomyces cerevisiae. Mutat.Res. *336*, 49-60.

Darroudi, F. and Natarajan, A.T. (1985). Cytological characterization of repair-deficient CHO cell line 43-3B. I. Induction of chromosomal aberrations and sister-chromatid exchanges by UV and its modulation with 3-aminobenzamide. Mutat.Res. *149*, 239-247.

Das, G.R. and Kolodner, R.D. (2000). Novel dominant mutations in Saccharomyces cerevisiae MSH6. Nat.Genet. *24*, 53-56.

Datta, A., Adjiri, A., New, L., Crouse, G.F., and Jinks, R.S. (1996). Mitotic crossovers between diverged sequences are regulated by mismatch repair proteins in Saccaromyces cerevisiae. Mol.Cell Biol. *16* , 1085-1093.

Davies, A.A., Friedberg, E.C., Tomkinson, A.E., Wood, R.D., and West, S.C. (1995). Role of the Rad1 and Rad10 proteins in nucleotide excision repair and recombination. J.Biol.Chem. *270*, 24638-24641.

de Boer, J., de Wit, J., van Steeg, H., Berg, R.J., Morreau, H., Visser, P., Lehmann, A.R., Duran, M., Hoeijmakers, J.H., and Weeda, G. (1998). A mouse model for the basal transcription/DNA repair syndrome trichothiodystrophy. Mol.Cell *1*, 981-990.

de Boer, J., van Steeg, H., Berg, R.J., Garssen, J., de Wit, J., van Oostrum, C.T., Beems, R.B., van der Horst, G.T., van Kreijl, C.F., de Gruijl, F.R., Bootsma, D., Hoeijmakers, J.H., and Weeda, G. (1999). Mouse model for the DNA repair/basal transcription disorder trichothiodystrophy reveals cancer predisposition. Cancer Res. *59*, 3489-3494.

de Boer, J. and Hoeijmakers, J.H. (1999). Cancer from the outside, aging from the inside: mouse models to study the consequences of defective nucleotide excision repair. Biochimie *81*, 127-137.

de Laat, W.L., Appeldoorn, E., Sugasawa, K., Weterings, E., Jaspers, N.G., and Hoeijmakers, J.H. (1998). DNA-binding polarity of human replication protein A positions nucleases in nucleotide excision repair. Genes Dev. *12*, 2598-2609.

de Laat, W.L., Sijbers, A.M., Odijk, H., Jaspers, N.G., and Hoeijmakers, J.H. (1998). Mapping of interaction domains between human repair proteins ERCC1 and XPF. Nucleic.Acids.Res. *26*, 4146-4152.

de Laat, W.L., Appeldoorn, E., Jaspers, N.G., and Hoeijmakers, J.H. (1998). DNA structural elements required for ERCC1-XPF endonuclease activity. J.Biol.Chem. *273*, 7835-7842.

De Santis, P., Garcia, C.L., Balajee, A.S., Brea, C.G., Bassi, L., and Palitti, F. (2001). Transcription coupled repair deficiency results in increased chromosomal aberrations and apoptotic death in the UV61 cell line, the Chinese hamster homologue of Cockayne's syndrome B. Mutat.Res. *485*, 121-132.

De Silva., I, McHugh, P.J., Clingen, P.H., and Hartley, J.A. (2000). Defining the roles of nucleotide excision repair and recombination in the repair of DNA interstrand cross-links in mammalian cells. Mol.Cell Biol. *20*, 7980-7990.

de Vries, A., van Oostrom, C.T., Hofhuis, F.M., Dortant, P.M., Berg, R.J., de Gruijl, F.R., Wester, P.W., van Kreijl, C.F., Capel, P.J., and van Steeg, H. (1995). Increased susceptibility to ultraviolet-B and carcinogens of mice lacking the DNA excision repair gene XPA. Nature *377*, 169-173.

de Wind, N., Dekker, M., Berns, A., Radman, M., and te, R.H. (1995). Inactivation of the mouse Msh2 gene results in mismatch repair deficiency, methylation tolerance, hyperrecombination, and predisposition to cancer. Cell *82*, 321-330.

Deng, C., Zhang, P., Harper, J.W., Elledge, S.J., and Leder, P. (1995). Mice lacking p21CIP1/WAF1 undergo normal development, but are defective in G1 checkpoint control. Cell *82*, 675-684.

DeWeese, T.L., Shipman, J.M., Larrier, N.A., Buckley, N.M., Kidd, L.R., Groopman, J.D., Cutler, R.G., te, R.H., and Nelson, W.G. (1998). Mouse embryonic stem cells carrying one or two defective Msh2 alleles respond abnormally to oxidative stress inflicted by low-level radiation. Proc.Natl.Acad.Sci.U.S.A. *95*, 11915-11920.

Di Leonardo, A., Linke, S.P., Clarkin, K., and Wahl, G.M. (1994). DNA damage triggers a prolonged p53-dependent G1 arrest and long-term induction of Cip1 in normal human fibroblasts. Genes Dev. *8*, 2540-2551.

Diamond, D.A., Parsian, A., Hunt, C.R., Lofgren, S., Spitz, D.R., Goswami, P.C., and Gius, D. (1999). Redox factor-1 (Ref-1) mediates the activation of AP-1 in HeLa and NIH 3T3 cells in response to heat shock. J.Biol.Chem. *274*, 16959-16964.

Dianov, G. and Lindahl, T. (1994). Reconstitution of the DNA base excision-repair pathway. Curr.Biol. *4*, 1069-1076.

Dianov, G., Bischoff, C., Piotrowski, J., and Bohr, V.A. (1998). Repair pathways for processing of 8-oxoguanine in DNA by mammalian cell extracts. J.Biol.Chem. *273*, 33811-33816.

Dimri, G.P., Nakanishi, M., Desprez, P.Y., Smith, J.R., and Campisi, J. (1996). Inhibition of E2F activity by the cyclin-dependent protein kinase inhibitor p21 in cells expressing or lacking a functional retinoblastoma protein. Mol.Cell Biol. *16*, 2987-2997.

Dolganov, G.M., Maser, R.S., Novikov, A., Tosto, L., Chong, S., Bressan, D.A., and Petrini, J.H. (1996). Human Rad50 is physically associated with human Mre11: identification of a conserved multiprotein complex implicated in recombinational DNA repair. Mol.Cell Biol. *16*, 4832-4841.

Donehower, L.A., Harvey, M., Slagle, B.L., McArthur, M.J., Montgomery, C.A.J., Butel, J.S., and Bradley, A. (1992). Mice deficient for p53 are developmentally normal but susceptible to spontaneous tumours. Nature *356*, 215-221.

Donehower, L.A. (1996). The p53-deficient mouse: a model for basic and applied cancer studies. Semin.Cancer Biol. *7*, 269-278.

Drapkin, R., Reardon, J.T., Ansari, A., Huang, J.C., Zawel, L., Ahn, K., Sancar, A., and Reinberg, D. (1994). Dual role of TFIIH in DNA excision repair and in transcription by RNA polymerase II. Nature *368*, 769-772.

Drummond, J.T. and Bellacosa, A. (2001). Human DNA mismatch repair in vitro operates independently of methylation status at CpG sites. Nucleic.Acids.Res. *29*, 2234-2243.

Dulic, V., Kaufmann, W.K., Wilson, S.J., Tlsty, T.D., Lees, E., Harper, J.W., Elledge, S.J., and Reed, S.I. (1994). p53-dependent inhibition of cyclin-dependent kinase activities in human fibroblasts during radiation-induced G1 arrest. Cell *76*, 1013-1023.

Dunphy, W.G. and Kumagai, A. (1991). The cdc25 protein contains an intrinsic phosphatase activity. Cell *67*, 189-196.

Dye, K. and Ahmad, S.I. (1995). Repair of phage lambda DNA damaged by near ultraviolet light plus 8-methoxypsoralen. J.Gen.Virol. *76*, 723-726.

Earley, M.C. and Crouse, G.F. (1998). The role of mismatch repair in the prevention of base pair mutations in Saccharomyces cerevisiae. Proc.Natl.Acad.Sci.U.S.A. *95*, 15487-15491.

Earnshaw, W.C. and Rothfield, N. (1985). Identification of a family of human centromere proteins using autoimmune sera from patients with scleroderma. Chromosoma *91*, 313-321.

el-Deiry, W.S., Tokino, T., Velculescu, V.E., Levy, D.B., Parsons, R., Trent, J.M., Lin, D., Mercer, W.E., Kinzler, K.W., and Vogelstein, B. (1993). WAF1, a potential mediator of p53 tumor suppression. Cell *75*, 817-825.

el-Deiry, W.S., Harper, J.W., O'Connor, P.M., Velculescu, V.E., Canman, C.E., Jackman, J., Pietenpol, J.A., Burrell, M., Hill, D.E., and Wang, Y. (1994). WAF1/CIP1 is induced in p53-mediated G1 arrest and apoptosis. Cancer Res. *54*, 1169-1174.

el-Deiry, W.S. (1998). Regulation of p53 downstream genes. Semin.Cancer Biol. *8*, 345-357.

Elbendary, A., Berchuck, A., Davis, P., Havrilesky, L., Bast, R.C.J., Iglehart, J.D., and Marks, J.R. (1994). Transforming growth factor beta 1 can induce CIP1/WAF1 expression independent of the p53 pathway in ovarian cancer cells. Cell Growth Differ. *5*, 1301-1307.

Enoch, T., Carr, A.M., and Nurse, P. (1992). Fission yeast genes involved in coupling mitosis to completion of DNA replication. Genes Dev. *6*, 2035-2046.

Epe, B. (1996). DNA damage profiles induced by oxidizing agents. Rev.Physiol.Biochem.Pharmacol. *127:223-49.*, 223-249.

Epstein, C.J. and Gatens, E.A. (1967). Nuclear ploidy in mammalian parenchymal liver cells. Nature *214*, 1050-1051.

Evans, A.R., Limp-Foster, M., and Kelley, M.R. (2000). Going APE over ref-1. Mutat.Res. *461*, 83-108.

Evans, E., Fellows, J., Coffer, A., and Wood, R.D. (1997). Open complex formation around a lesion during nucleotide excision repair provides a structure for cleavage by human XPG protein. EMBO J. *16*, 625-638.

Evans, E., Moggs, J.G., Hwang, J.R., Egly, J.M., and Wood, R.D. (1997). Mechanism of open complex and dual incision formation by human nucleotide excision repair factors. EMBO J. *16*, 6559-6573.

Evans, E., Sugawara, N., Haber, J.E., and Alani, E. (2000). The Saccharomyces cerevisiae Msh2 mismatch repair protein localizes to recombination intermediates in vivo. Mol.Cell *5*, 789-799.

Evans, M. K. (1962) Chromosome aberrations induced by ionizing radiations. Int.Rev.Cytol. 13, 221-317.

Evans, M.K., Robbins, J.H., Ganges, M.B., Tarone, R.E., Nairn, R.S., and Bohr, V.A. (1993). Gene-specific DNA repair in xeroderma pigmentosum complementation groups A, C, D, and F. Relation to cellular survival and clinical features. J.Biol.Chem. *268*, 4839-4847.

Feinberg, A.P. and Vogelstein, B. (1983). A technique for radiolabeling DNA restriction endonuclease fragments to high specific activity. Anal.Biochem. *132*, 6-13.

Fishman-Lobell, J. and Haber, J.E. (1992). Removal of nonhomologous DNA ends in double-strand break recombination: the role of the yeast ultraviolet repair gene RAD1. Science *258*, 480-484.

Fleck, O., Lehmann, E., Schar, P., and Kohli, J. (1999). Involvement of nucleotide-excision repair in msh2 pms1-independent mismatch repair. Nat.Genet. *21*, 314-317.

Flores-Rozas, H. and Kolodner, R.D. (2000). Links between replication, recombination and genome instability in eukaryotes. Trends.Biochem.Sci. *25*, 196-200.

Fort P, Marty L, Piechaczyk M, el Sabrouty S, Dani C, Jeanteur P, Blanchard JM. (1985). Various rat adult tissues express only one major mRNA species from the glyceraldehyde-3-phosphate-dehydrogenase multigenic family. Nucleic Acids Res 13:1431-1442.

Forsburg, S.L. and Nurse, P. (1991). Cell cycle regulation in the yeasts Saccharomyces cerevisiae and Schizosaccharomyces pombe. Annu.Rev.Cell Biol. *7:227-56.*, 227-256.

Francis, M.A. and Rainbow, A.J. (1999). UV-enhanced reactivation of a UV-damaged reporter gene suggests transcription-coupled repair is UV-inducible in human cells. Carcinogenesis *20*, 19-26.

Friedbeg, E.C. (1994). DNA repair and Mutagenesis

Friedberg, E.C. (1996). Relationships between DNA repair and transcription. Annu.Rev.Biochem. *65:15-42.*, 15-42.

Frit, P., Bergmann, E., and Egly, J.M. (1999). Transcription factor IIH: a key player in the cellular response to DNA damage. Biochimie *81*, 27-38.

Frosina, G., Fortini, P., Rossi, O., Carrozzino, F., Raspaglio, G., Cox, L.S., Lane, D.P., Abbondandolo, A., and Dogliotti, E. (1996). Two pathways for base excision repair in mammalian cells. J.Biol.Chem. *271*, 9573-9578.

Gaillard, P.H. and Wood, R.D. (2001). Activity of individual ERCC1 and XPF subunits in DNA nucleotide excision repair. Nucleic.Acids.Res. *29*, 872-879.

Galavazi, G., Schenk, H. and Bootsma, D. (1966). Synchronization of mammalian cells in vitro by inhibition of the DNA synthesis. I. Optimal conditions. Exp. Cell. Research. 41, 428-437.

Gallego, F., Fleck, O., Li, A., Wyrzykowska, J., and Tinland, B. (2000). AtRAD1, a plant homologue of human and yeast nucleotide excision repair endonucleases, is involved in dark repair of UV damages and recombination. Plant J. *21*, 507-518.

Galli, A. and Schiestl, R.H. (1996). Hydroxyurea induces recombination in dividing but not in G1 or G2 cell cycle arrested yeast cells. Mutat.Res. *354*, 69-75.

Galli, A. and Schiestl, R.H. (1998). Effects of DNA double-strand and single-strand breaks on intrachromosomal recombination events in cell-cycle-arrested yeast cells. Genetics *149*, 1235-1250.

Gartel, A.L., Najmabadi, F., Goufman, E., and Tyner, A.L. (2000). A role for E2F1 in Ras activation of p21(WAF1/CIP1) transcription. Oncogene *19*, 961-964.

Garvik, B., Carson, M., and Hartwell, L. (1995). Single-stranded DNA arising at telomeres in cdc13 mutants may constitute a specific signal for the RAD9 checkpoint. Mol.Cell Biol. *15*, 6128-6138.

Gary, R., Ludwig, D.L., Cornelius, H.L., MacInnes, M.A., and Park, M.S. (1997). The DNA repair endonuclease XPG binds to proliferating cell nuclear antigen (PCNA) and shares sequence elements with the PCNA-binding regions of FEN-1 and cyclin-dependent kinase inhibitor p21. J.Biol.Chem. *272*, 24522-24529.

Gerlyng, P., Abyholm, A., Grotmol, T., Erikstein, B., Huitfeldt, H.S., Stokke, T., and Seglen, P.O. (1993). Binucleation and polyploidization patterns in developmental and regenerative rat liver growth. Cell Prolif. *26*, 557-565.

Gibbs, P.E., McGregor, W.G., Maher, V.M., Nisson, P., and Lawrence, C.W. (1998). A human homolog of the Saccharomyces cerevisiae REV3 gene, which encodes the catalytic subunit of DNA polymerase zeta. Proc.Natl.Acad.Sci.U.S.A. *95*, 6876-6880.

Godwin, A.R., Bollag, R.J., Christie, D.M., and Liskay, R.M. (1994). Spontaneous and restriction enzyme-induced chromosomal recombination in mammalian cells. Proc.Natl.Acad.Sci.U.S.A. *91*, 12554-12558.

Gordenin, D.A. and Resnick, M.A. (1998). Yeast ARMs (DNA at-risk motifs) can reveal sources of genome instability. Mutat.Res. *400*, 45-58.

Gradia, S., Subramanian, D., Wilson, T., Acharya, S., Makhov, A., Griffith, J., and Fishel, R. (1999). hMSH2-hMSH6 forms a hydrolysis-independent sliding clamp on mismatched DNA. Mol.Cell *3*, 255-261.

Greenberg, R.B., Alberti, M., Hearst, J.E., Chua, M.A., and Saffran, W.A. (2001). Recombinational and mutagenic repair of psoralen interstrand crosslinks in Saccharomyces cerevisiae. J.Biol.Chem.

Griffin, E.A.J., Staknis, D., and Weitz, C.J. (1999). Light-independent role of CRY1 and CRY2 in the mammalian circadian clock. Science *286*, 768-771.

Grollman, A.P. and Moriya, M. (1993). Mutagenesis by 8-oxoguanine: an enemy within. Trends.Genet. *9*, 246-249.

Grossmann, K.F., Brown, J.C., and Moses, R.E. (1999). Cisplatin DNA cross-links do not inhibit S-phase and cause only a G2/M arrest in Saccharomyces cerevisiae. Mutat.Res. *434*, 29-39.

Grossmann, K.F., Ward, A.M., and Moses, R.E. (2000). Saccharomyces cerevisiae lacking Snm1, Rev3 or Rad51 have a normal S-phase but arrest permanently in G2 after cisplatin treatment. Mutat.Res. *461*, 1-13.

Guadagno, T.M. and Newport, J.W. (1996). Cdk2 kinase is required for entry into mitosis as a positive regulator of Cdc2-cyclin B kinase activity. Cell *84*, 73-82.

Guzder, S.N., Sung, P., Prakash, L., and Prakash, S. (1996). Nucleotide excision repair in yeast is mediated by sequential assembly of repair factors and not by a pre-assembled repairosome. J.Biol.Chem. *271*, 8903-8910.

Haapajarvi, T., Kivinen, L., Heiskanen, A., des, B.C., Datto, M.B., Wang, X.F., and Laiho, M. (1999). UV radiation is a transcriptional inducer of p21(Cip1/Waf1) cyclin-kinase inhibitor in a p53-independent manner. Exp.Cell Res. *248*, 272-279.

Haber, J.E. and Leung, W.Y. (1996). Lack of chromosome territoriality in yeast: promiscuous rejoining of broken chromosome ends. Proc.Natl.Acad.Sci.U.S.A. *93*, 13949-13954.

Haber, J.E. (2000). Lucky breaks: analysis of recombination in Saccharomyces. Mutat.Res. *451*, 53-69.

Haber, J.E. (2000). Recombination: a frank view of exchanges and vice versa. Curr.Opin.Cell Biol. *12*, 286-292.

Habraken, Y., Sung, P., Prakash, L., and Prakash, S. (1994). Holliday junction cleavage by yeast Rad1 protein. Nature *371*, 531-534.

Halevy, O., Novitch, B.G., Spicer, D.B., Skapek, S.X., Rhee, J., Hannon, G.J., Beach, D., and Lassar, A.B. (1995). Correlation of terminal cell cycle arrest of skeletal muscle with induction of p21 by MyoD. Science *267*, 1018-1021.

Hall, N.A., Lake, B.D., Palmer, D.N., Jolly, R.D., and Patrick, A.D. (1989). Glycoconjugates in storage cytosomes from ceroid-lipofuscinosis (Batten's disease) and in lipofuscin from old-age brain. Adv.Exp.Med.Biol. *266:225-41; discussion 242.*, 225-241.

Hanawalt, P.C. (1994). Transcription-coupled repair and human disease. Science *266*, 1957-1958.

Harada, Y.N., Shiomi, N., Koike, M., Ikawa, M., Okabe, M., Hirota, S., Kitamura, Y., Kitagawa, M., Matsunaga, T., Nikaido, O., and Shiomi, T. (1999). Postnatal growth failure, short life span, and early onset of cellular senescence and subsequent immortalization in mice lacking the xeroderma pigmentosum group G gene. Mol.Cell Biol. *19*, 2366-2372.

Harfe, B.D. and Jinks-Robertson, S. (2000). Mismatch repair proteins and mitotic genome stability. Mutat.Res. *451*, 151-167.

Harper, J.W., Adami, G.R., Wei, N., Keyomarsi, K., and Elledge, S.J. (1993). The p21 Cdk-interacting protein Cip1 is a potent inhibitor of G1 cyclin-dependent kinases. Cell *75*, 805-816.

Harper, J.W., Elledge, S.J., Keyomarsi, K., Dynlacht, B., Tsai, L.H., Zhang, P., Dobrowolski, S., Bai, C., Connell-Crowley, L., and Swindell, E. (1995). Inhibition of cyclin-dependent kinases by p21. Mol.Biol.Cell *6*, 387-400.

Harrington, J.J. and Lieber, M.R. (1994). The characterization of a mammalian DNA structure-specific endonuclease. EMBO J. *13*, 1235-1246.

Harris, M. (1971). Polyploid series of mammalian cells. Exp.Cell Res. *66*, 329-336.

Hayashi, T., Takao, M., Tanaka, K., and Yasui, A. (1998). ERCC1 mutations in UV-sensitive Chinese hamster ovary (CHO) cell lines. Mutat.Res. *407*, 269-276.

He, Z., Henricksen, L.A., Wold, M.S., and Ingles, C.J. (1995). RPA involvement in the damage-recognition and incision steps of nucleotide excision repair. Nature *374*, 566-569.

Heichman, K.A. and Roberts, J.M. (1994). Rules to replicate by. Cell *79*, 557-562.

Henning, K.A., Li, L., Iyer, N., McDaniel, L.D., Reagan, M.S., Legerski, R., Schultz, R.A., Stefanini, M., Lehmann, A.R., and Mayne, L.V. (1995). The Cockayne syndrome group A gene encodes a WD repeat protein that interacts with CSB protein and a subunit of RNA polymerase II TFIIH. Cell *82*, 555-564.

Hermeking, H., Lengauer, C., Polyak, K., He, T.C., Zhang, L., Thiagalingam, S., Kinzler, K.W., and Vogelstein, B. (1997). 14-3-3 sigma is a p53-regulated inhibitor of G2/M progression. Mol.Cell *1*, 3-11.

Hess, M.T., Schwitter, U., Petretta, M., Giese, B., and Naegeli, H. (1997). Bipartite substrate discrimination by human nucleotide excision repair. Proc.Natl.Acad.Sci.U.S.A. *94*, 6664-6669.

Hess, M.T., Gunz, D., Luneva, N., Geacintov, N.E., and Naegeli, H. (1997). Base pair conformation-dependent excision of benzo[a]pyrene diol epoxide-guanine adducts by human nucleotide excision repair enzymes. Mol.Cell Biol. *17*, 7069-7076.

Hickman, M.J. and Samson, L.D. (1999). Role of DNA mismatch repair and p53 in signaling induction of apoptosis by alkylating agents. Proc.Natl.Acad.Sci.U.S.A. *96*, 10764-10769.

Houtsmuller, A.B., Rademakers, S., Nigg, A.L., Hoogstraten, D., Hoeijmakers, J.H., and Vermeulen, W. (1999). Action of DNA repair endonuclease ERCC1/XPF in living cells. Science *284*, 958-961.

Hoy, C.A., Thompson, L.H., Mooney, C.L., and Salazar, E.P. (1985). Defective DNA cross-link removal in Chinese hamster cell mutants hypersensitive to bifunctional alkylating agents. Cancer Res. *45*, 1737-1743.

Huppi, K., Siwarski, D., Dosik, J., Michieli, P., Chedid, M., Reed, S., Mock, B., Givol, D., and Mushinski, J.F. (1994). Molecular cloning, sequencing, chromosomal localization and expression of mouse p21 (Waf1). Oncogene *9*, 3017-3020.

Hwang, B.J., Ford, J.M., Hanawalt, P.C., and Chu, G. (1999). Expression of the p48 xeroderma pigmentosum gene is p53-dependent and is involved in global genomic repair. Proc.Natl.Acad.Sci.U.S.A. *96*, 424-428.

Ichikawa, M., Nakane, H., Marra, G., Corti, C., Jiricny, J., Fitch, M., Ford, J.M., Ikejima, M., Shimada, T., Yoshino, M., Takeuchi, S., Nakatsu, Y., and Tanaka, K. (2000). Decreased UV sensitivity, mismatch repair activity and abnormal cell cycle checkpoints in skin cancer cell lines derived from UVB-irradiated XPA-deficient mice. Mutat.Res. *459*, 285-298.

Ishii, Y. and Ikushima, T. (1999). Involvement of G2-dependent DNA double-strand break repair in the formation of ultraviolet light B-induced chromosomal aberrations. Mutat.Res. *427*, 99-103.

Ivanov, E.L. and Haber, J.E. (1995). RAD1 and RAD10, but not other excision repair genes, are required for double-strand break-induced recombination in Saccharomyces cerevisiae. Mol.Cell Biol. *15*, 2245-2251.

Jayaraman, L., Murthy, K.G., Zhu, C., Curran, T., Xanthoudakis, S., and Prives, C. (1997). Identification of redox/repair protein Ref-1 as a potent activator of p53. Genes Dev. *11*, 558-570.

Jeggo, P.A. (1998). Identification of genes involved in repair of DNA double-strand breaks in mammalian cells. Radiat.Res. *150*, S80-S91

Jiang, H., Lin, J., Su, Z.Z., Collart, F.R., Huberman, E., and Fisher, P.B. (1994). Induction of differentiation in human promyelocytic HL-60 leukemia cells activates p21, WAF1/CIP1, expression in the absence of p53. Oncogene *9*, 3397-3406.

Jones, N.J., Zhao, Y., Siciliano, M.J., and Thompson, L.H. (1995). Assignment of the XRCC2 human DNA repair gene to chromosome 7q36 by complementation analysis. Genomics *26*, 619-622.

Kakolyris, S., Kaklamanis, L., Giatromanolaki, A., Koukourakis, M., Hickson, I.D., Barzilay, G., Turley, H., Leek, R.D., Kanavaros, P., Georgoulias, V., Gatter, K.C., and Harris, A.L. (1998). Expression and subcellular localization of human AP endonuclease 1 (HAP1/Ref-1) protein: a basis for its role in human disease. Histopathology *33*, 561-569.

Karran, P. and Hampson, R. (1996). Genomic instability and tolerance to alkylating agents. Cancer Surv. *28:69-85.*, 69-85.

Karran, P. (2000). DNA double strand break repair in mammalian cells. Curr.Opin.Genet.Dev. *10*, 144-150.

Kastan, M.B., Onyekwere, O., Sidransky, D., Vogelstein, B., and Craig, R.W. (1991). Participation of p53 protein in the cellular response to DNA damage. Cancer Res. *51*, 6304-6311.

Kastan, M.B., Zhan, Q., el-Deiry, W.S., Carrier, F., Jacks, T., Walsh, W.V., Plunkett, B.S., Vogelstein, B., and Fornace, A.J.J. (1992). A mammalian cell cycle checkpoint pathway utilizing p53 and GADD45 is defective in ataxia-telangiectasia. Cell *71*, 587-597.

Katz, A.M. (1994). The cardiomyopathy of overload: an unnatural growth response in the hypertrophied heart. Ann.Intern.Med. *121*, 363-371.

Kelly, T.J. and Brown, G.W. (2000). Regulation of chromosome replication. Annu.Rev.Biochem. *69:829-80.*, 829-880.

Kim, C., Snyder, R.O., and Wold, M.S. (1992). Binding properties of replication protein A from human and yeast cells. Mol.Cell Biol. *12*, 3050-3059.

Kim, W.H., Kang, K.H., Kim, M.Y., and Choi, K.H. (2000). Induction of p53-independent p21 during ceramide-induced G1 arrest in human hepatocarcinoma cells. Biochem.Cell Biol. *78*, 127-135.

King, R.W., Jackson, P.K., and Kirschner, M.W. (1994). Mitosis in transition. Cell *79*, 563-571.

Klein, H.L. (1988). Different types of recombination events are controlled by the RAD1 and RAD52 genes of Saccharomyces cerevisiae. Genetics *120*, 367-377.

Klungland, A. and Lindahl, T. (1997). Second pathway for completion of human DNA base excision-repair: reconstitution with purified proteins and requirement for DNase IV (FEN1). EMBO J. *16*, 3341-3348.

Klungland, A., Rosewell, I., Hollenbach, S., Larsen, E., Daly, G., Epe, B., Seeberg, E., Lindahl, T., and Barnes, D.E. (1999). Accumulation of premutagenic DNA lesions in mice defective in removal of oxidative base damage. Proc.Natl.Acad.Sci.U.S.A. *96*, 13300-13305.

Klungland, A., Hoss, M., Gunz, D., Constantinou, A., Clarkson, S.G., Doetsch, P.W., Bolton, P.H., Wood, R.D., and Lindahl, T. (1999). Base excision repair of oxidative DNA damage activated by XPG protein. Mol.Cell *3*, 33-42.

Kolodner, R.D. and Marsischky, G.T. (1999). Eukaryotic DNA mismatch repair. Curr.Opin.Genet.Dev. *9*, 89-96.

Kudryavtsev, B.N., Kudryavtseva, M.V., Sakuta, G.A., and Stein, G.I. (1993). Human hepatocyte polyploidization kinetics in the course of life cycle. Virchows Arch.B.Cell Pathol.Incl.Mol.Pathol. *64*, 387-393.

Kunz, B.A., Straffon, A.F., and Vonarx, E.J. (2000). DNA damage-induced mutation: tolerance via translesion synthesis. Mutat.Res. *451*, 169-185.

Kuraoka, I., Kobertz, W.R., Ariza, R.R., Biggerstaff, M., Essigmann, J.M., and Wood, R.D. (2000). Repair of an interstrand DNA cross-link initiated by ERCC1-XPF repair/recombination nuclease. J.Biol.Chem. *275*, 26632-26636.

Kusumoto, R., Masutani, C., Sugasawa, K., Iwai, S., Araki, M., Uchida, A., Mizukoshi, T., and Hanaoka, F. (2001). Diversity of the damage recognition step in the global genomic nucleotide excision repair in vitro. Mutat.Res. *485*, 219-227.

Kuzminov, A. (1995). Collapse and repair of replication forks in Escherichia coli. Mol.Microbiol. *16*, 373-384.

Laconi, E., Oren, R., Mukhopadhyay, D.K., Hurston, E., Laconi, S., Pani, P., Dabeva, M.D., and Shafritz, D.A. (1998). Long-term, near-total liver replacement by transplantation of isolated hepatocytes in rats treated with retrorsine. Am.J.Pathol. *153*, 319-329.

Le Page, F., Kwoh, E.E., Avrutskaya, A., Gentil, A., Leadon, S.A., Sarasin, A., and Cooper, P.K. (2000). Transcription-coupled repair of 8-oxoguanine: requirement for XPG, TFIIH, and CSB and implications for Cockayne syndrome. Cell *101*, 159-171.

Leadon, S.A. and Avrutskaya, A.V. (1997). Differential involvement of the human mismatch repair proteins, hMLH1 and hMSH2, in transcription-coupled repair. Cancer Res. *57*, 3784-3791.

Leadon, S.A. and Avrutskaya, A.V. (1998). Requirement for DNA mismatch repair proteins in the transcription-coupled repair of thymine glycols in Saccharomyces cerevisiae. Mutat.Res. *407*, 177-187.

Lehmann, A.R. (2000). Replication of UV-damaged DNA: new insights into links between DNA polymerases, mutagenesis and human disease. Gene *253*, 1-12.

Lewis, L.K. and Resnick, M.A. (2000). Tying up loose ends: nonhomologous end-joining in Saccharomyces cerevisiae. Mutat.Res. *451*, 71-89.

Li, G. and Ho, V.C. (1998). p53-dependent DNA repair and apoptosis respond differently to high- and low-dose ultraviolet radiation. Br.J.Dermatol. *139*, 3-10.

Li, L., Elledge, S.J., Peterson, C.A., Bales, E.S., and Legerski, R.J. (1994). Specific association between the human DNA repair proteins XPA and ERCC1. Proc.Natl.Acad.Sci.U.S.A. *91*, 5012-5016.

Li, L., Lu, X., Peterson, C.A., and Legerski, R.J. (1995). An interaction between the DNA repair factor XPA and replication protein A appears essential for nucleotide excision repair. Mol.Cell Biol. *15*, 5396-5402.

Li, L., Peterson, C.A., Lu, X., Wei, P., and Legerski, R.J. (1999). Interstrand cross-links induce DNA synthesis in damaged and undamaged plasmids in mammalian cell extracts. Mol.Cell Biol. *19*, 5619-5630.

Li, Y., Jenkins, C.W., Nichols, M.A., and Xiong, Y. (1994). Cell cycle expression and p53 regulation of the cyclin-dependent kinase inhibitor p21. Oncogene *9*, 2261-2268.

Li, Y.F., Kim, S.T., and Sancar, A. (1993). Evidence for lack of DNA photoreactivating enzyme in humans. Proc.Natl.Acad.Sci.U.S.A. *90*, 4389-4393.

Liang, F., Han, M., Romanienko, P.J., and Jasin, M. (1998). Homology-directed repair is a major double-strand break repair pathway in mammalian cells. Proc.Natl.Acad.Sci.U.S.A. *95*, 5172-5177.

Lieber, M.R. (1999). The biochemistry and biological significance of nonhomologous DNA end joining: an essential repair process in multicellular eukaryotes. Genes Cells *4*, 77-85.

Lin, F.L., Sperle, K., and Sternberg, N. (1985). Recombination in mouse L cells between DNA introduced into cells and homologous chromosomal sequences. Proc.Natl.Acad.Sci.U.S.A. 82, 1391-1395.

Lin, W., Wu, X., and Wang, Z. (1999). A full-length cDNA of hREV3 is predicted to encode DNA polymerase zeta for damage-induced mutagenesis in humans. Mutat.Res. *433*, 89-98.

Lindahl, T. (1995). Recognition and processing of damaged DNA. J.Cell Sci.Suppl. *19:73-7.*, 73-77.

Liu, N., Lamerdin, J.E., Tebbs, R.S., Schild, D., Tucker, J.D., Shen, M.R., Brookman, K.W., Siciliano, M.J., Walter, C.A., Fan, W., Narayana, L.S., Zhou, Z.Q., Adamson, A.W., Sorensen, K.J., Chen, D.J., Jones, N.J., and Thompson, L.H. (1998). XRCC2 and XRCC3, new human Rad51-family members, promote chromosome stability and protect against DNA cross-links and other damages. Mol.Cell *1*, 783-793.

Liu, Q., Guntuku, S., Cui, X.S., Matsuoka, S., Cortez, D., Tamai, K., Luo, G., Carattini-Rivera, S., DeMayo, F., Bradley, A., Donehower, L.A., and Elledge, S.J. (2000). Chk1 is an essential kinase that is regulated by Atr and required for the G(2)/M DNA damage checkpoint. Genes Dev. *14*, 1448-1459.

Liu, Z., Hossain, G.S., Islas-Osuna, M.A., Mitchell, D.L., and Mount, D.W. (2000). Repair of UV damage in plants by nucleotide excision repair: Arabidopsis UVH1 DNA repair gene is a homolog of Saccharomyces cerevisiae Rad1. Plant J. *21*, 519-528.

Ljungman, M. and Zhang, F. (1996). Blockage of RNA polymerase as a possible trigger for u.v. light-induced apoptosis. Oncogene *13*, 823-831.

Ljungman, M. (2000). Dial 9-1-1 for p53: mechanisms of p53 activation by cellular stress. Neoplasia. *2*, 208-225.

Lloyd, D.R. and Hanawalt, P.C. (2000). p53-dependent global genomic repair of benzo[a]pyrene-7,8-diol-9,10-epoxide adducts in human cells. Cancer Res. *60*, 517-521.

Loignon, M., Fetni, R., Gordon, A.J., and Drobetsky, E.A. (1997). A p53-independent pathway for induction of p21waf1cip1 and concomitant G1 arrest in UV-irradiated human skin fibroblasts. Cancer Res. *57*, 3390-3394.

Lopez-Girona, A., Furnari, B., Mondesert, O., and Russell, P. (1999). Nuclear localization of Cdc25 is regulated by DNA damage and a 14-3-3 protein. Nature *397*, 172-175.

Lowe, S.W., Schmitt, E.M., Smith, S.W., Osborne, B.A., and Jacks, T. (1993). p53 is required for radiation-induced apoptosis in mouse thymocytes. Nature *362*, 847-849.

Lowndes, N.F. and Murguia, J.R. (2000). Sensing and responding to DNA damage. Curr.Opin.Genet.Dev. *10*, 17-25.

Lu, Y.P., Lou, Y.R., Yen, P., Mitchell, D., Huang, M.T. and Conney, M.H. (1999). Time Course for Early Adaptive Responses to Ultraviolet B Light in the Epidermis of SKH-1 Mice. Cancer Res. 59, 4591-4602.

Lukacsovich, T. and Waldman, A.S. (1999). Suppression of intrachromosomal gene conversion in mammalian cells by small degrees of sequence divergence. Genetics *151*, 1559-1568.

Lydall, D. and Weinert, T. (1995). Yeast checkpoint genes in DNA damage processing: implications for repair and arrest. Science *270*, 1488-1491.

Macleod, K.F., Sherry, N., Hannon, G., Beach, D., Tokino, T., Kinzler, K., Vogelstein, B., and Jacks, T. (1995). p53-dependent and independent expression of p21 during cell growth, differentiation, and DNA damage. Genes Dev. *9*, 935-944.

Maher, V.M., Ouellette, L.M., Curren, R.D., and McCormick, J.J. (1976). Frequency of ultraviolet light-induced mutations is higher in xeroderma pigmentosum variant cells than in normal human cells. Nature *261*, 593-595.

Maltzman, W. and Czyzyk, L. (1984). UV irradiation stimulates levels of p53 cellular tumor antigen in nontransformed mouse cells. Mol.Cell Biol. *4*, 1689-1694.

Marsischky, G.T., Filosi, N., Kane, M.F., and Kolodner, R. (1996). Redundancy of Saccharomyces cerevisiae MSH3 and MSH6 in MSH2-dependent mismatch repair. Genes Dev. *10*, 407-420.

Marsischky, G.T., Lee, S., Griffith, J., and Kolodner, R.D. (1999). 'Saccharomyces cerevisiae MSH2/6 complex interacts with Holliday junctions and facilitates their cleavage by phage resolution enzymes. J.Biol.Chem. *274*, 7200-7206.

Masutani, C., Sugasawa, K., Yanagisawa, J., Sonoyama, T., Ui, M., Enomoto, T., Takio, K., Tanaka, K., van der Spek, P.J., and Bootsma, D. (1994). Purification and cloning of a nucleotide excision repair complex involving the xeroderma pigmentosum group C protein and a human homologue of yeast RAD23. EMBO J. *13*, 1831-1843.

Masutani, C., Kusumoto, R., Yamada, A., Dohmae, N., Yokoi, M., Yuasa, M., Araki, M., Iwai, S., Takio, K., and Hanaoka, F. (1999a). The XPV (xeroderma pigmentosum variant) gene encodes human DNA polymerase eta. Nature *399*, 700-704.

Masutani, C., Araki, M., Yamada, A., Kusumoto, R., Nogimori, T., Maekawa, T., Iwai, S., and Hanaoka, F. (1999b). Xeroderma pigmentosum variant (XP-V) correcting protein from HeLa cells has a thymine dimer bypass DNA polymerase activity. EMBO J. *18*, 3491-3501.

Matsumoto, Y., Kim, K., and Bogenhagen, D.F. (1994). Proliferating cell nuclear antigen-dependent abasic site repair in Xenopus laevis oocytes: an alternative pathway of base excision DNA repair. Mol.Cell Biol. *14*, 6187-6197.

Matsumura, Y., Nishigori, C., Yagi, T., Imamura, S., and Takebe, H. (1998). Characterization of molecular defects in xeroderma pigmentosum group F in relation to its clinically mild symptoms. Hum.Mol.Genet. *7*, 969-974.

Matsunaga, T., Mu, D., Park, C.H., Reardon, J.T., and Sancar, A. (1995). Human DNA repair excision nuclease. Analysis of the roles of the subunits involved in dual incisions by using anti-XPG and anti-ERCC1 antibodies. J.Biol.Chem. *270*, 20862-20869.

McCutchen-Maloney, S.L., Giannecchini, C.A., Hwang, M.H., and Thelen, M.P. (1999). Domain mapping of the DNA binding, endonuclease, and ERCC1 binding properties of the human DNA repair protein XPF. Biochemistry *38*, 9417-9425.

McKay, B.C., Francis, M.A., and Rainbow, A.J. (1997). Wildtype p53 is required for heat shock and ultraviolet light enhanced repair of a UV-damaged reporter gene. Carcinogenesis *18*, 245-249.

McKay, B.C., Ljungman, M., and Rainbow, A.J. (1999). Potential roles for p53 in nucleotide excision repair. Carcinogenesis *20*, 1389-1396.

McWhir, J., Selfridge, J., Harrison, D.J., Squires, S., and Melton, D.W. (1993). Mice with DNA repair gene (ERCC-1) deficiency have elevated levels of p53, liver nuclear abnormalities and die before weaning. Nat.Genet. *5*, 217-224.

Medvedev, Z.A. (1986). Age-related polyploidization of hepatocytes: the cause and possible role. A mini-review. Exp.Gerontol. *21*, 277-282.

Mellon, I., Spivak, G., and Hanawalt, P.C. (1987). Selective removal of transcription-blocking DNA damage from the transcribed strand of the mammalian DHFR gene. Cell *51*, 241-249.

Melton, D.W., Ketchen, A.M., Nunez, F., Bonatti-Abbondandolo, S., Abbondandolo, A., Squires, S., and Johnson, R.T. (1998). Cells from ERCC1-deficient mice show increased genome instability and a reduced frequency of S-phase-dependent illegitimate chromosome exchange but a normal frequency of homologous recombination. J.Cell Sci. *111*, 395-404.

Memisoglu, A. and Samson, L. (2000). Base excision repair in yeast and mammals. Mutat.Res. *451*, 39-51.

Meniel, V., Magana-Schwencke, N., Averbeck, D., and Waters, R. (1997). Preferential incision of interstrand crosslinks induced by 8-methoxypsoralen plus UVA in yeast during the cell cycle. Mutat.Res. *384* , 23-32.

Michel, B. (2000). Replication fork arrest and DNA recombination. Trends.Biochem.Sci. *25*, 173-178.

Michieli, P., Chedid, M., Lin, D., Pierce, J.H., Mercer, W.E., and Givol, D. (1994). Induction of WAF1/CIP1 by a p53-independent pathway. Cancer Res. *54*, 3391-3395.

Mignon, A., Guidotti, J.E., Mitchell, C., Fabre, M., Wernet, A., De La Coste, A., Soubrane, O., Gilgenkrantz, H., and Kahn, A. (1998). Selective repopulation of normal mouse liver by Fas/CD95-resistant hepatocytes. Nat.Med. *4*, 1185-1188.

Mitchell, D.L. and Nairn, R.S. (1989). The biology of the (6-4) photoproduct. Photochem.Photobiol. *49*, 805-819.

Modrich, P. (1997). Strand-specific mismatch repair in mammalian cells. J.Biol.Chem. *272*, 24727-24730.

Moggs, J.G., Szymkowski, D.E., Yamada, M., Karran, P., and Wood, R.D. (1997). Differential human nucleotide excision repair of paired and mispaired cisplatin-DNA adducts. Nucleic.Acids.Res. *25*, 480-491.

Morgan, D.O. (1995). Principles of CDK regulation. Nature *374*, 131-134.

Mu, D., Tursun, M., Duckett, D.R., Drummond, J.T., Modrich, P., and Sancar, A. (1997). Recognition and repair of compound DNA lesions (base damage and mismatch) by human mismatch repair and excision repair systems. Mol.Cell Biol. *17*, 760-769.

Mu, D., Bessho, T., Nechev, L.V., Chen, D.J., Harris, T.M., Hearst, J.E., and Sancar, A. (2000). DNA interstrand cross-links induce futile repair synthesis in mammalian cell extracts. Mol.Cell Biol. *20*, 2446-2454.

Mullenders, L.H., Hazekamp-van Dokkum, A.M., Kalle, W.H., Vrieling, H., Zdzienicka, M.Z., and van Zeeland, A.A. (1993). UV-induced photolesions, their repair and mutations. Mutat.Res. *299*, 271-276.

Muller, C., Calsou, P., Frit, P., and Salles, B. (1999). Regulation of the DNA-dependent protein kinase (DNA-PK) activity in eukaryotic cells. Biochimie *81*, 117-125.

Murray, A. (1994). Cell cycle checkpoints. Curr.Opin.Cell Biol. *6*, 872-876.

Muschel, R.J., Zhang, H.B., Iliakis, G., and McKenna, W.G. (1991). Cyclin B expression in HeLa cells during the G2 block induced by ionizing radiation. Cancer Res. *51*, 5113-5117.

Myhr, B.C., Turnbull, D., and DiPaolo, J.A. (1979). Ultraviolet mutagenesis of normal and xeroderma pigmentosum variant human fibroblasts. Mutat.Res. *62*, 341-353.

Nakamura, J. and Swenberg, J.A. (1999). Endogenous apurinic/apyrimidinic sites in genomic DNA of mammalian tissues. Cancer Res. *59*, 2522-2526.

Nakshatri, H., Bhat-Nakshatri, P., and Currie, R.A. (1996). Subunit association and DNA binding activity of the heterotrimeric transcription factor NF-Y is regulated by cellular redox. J.Biol.Chem. *271*, 28784-28791.

Nara, K., Nagashima, F., and Yasui, A. (2001). Highly elevated ultraviolet-induced mutation frequency in isolated Chinese hamster cell lines defective in nucleotide excision repair and mismatch repair proteins. Cancer Res. *61*, 50-52.

Natarajan, A.T. and Zwanenburg, T.S. (1982). Mechanisms for chromosomal aberrations in mammalian cells. Mutat.Res. *95*, 1-6.

Nejedly, K., Kittner, R., Pospisilova, S., and Kypr, J. (2001). Crosslinking of the complementary strands of DNA by UV light: dependence on the oligonucleotide composition of the UV irradiated DNA. Biochim.Biophys.Acta *1517*, 365-375.

Nelson, J.R., Lawrence, C.W., and Hinkle, D.C. (1996). Thymine-thymine dimer bypass by yeast DNA polymerase zeta. Science *272*, 1646-1649.

Nelson, W.G. and Kastan, M.B. (1994). DNA strand breaks: the DNA template alterations that trigger p53-dependent DNA damage response pathways. Mol.Cell Biol. *14*, 1815-1823.

Ni, T.T., Marsischky, G.T., and Kolodner, R.D. (1999). MSH2 and MSH6 are required for removal of adenine misincorporated opposite 8-oxo-guanine in S. cerevisiae. Mol.Cell *4*, 439-444.

Nichols, A.F. and Sancar, A. (1992). Purification of PCNA as a nucleotide excision repair protein. Nucleic.Acids.Res. *20*, 2441-2446.

Nicholson, A., Hendrix, M., Jinks-Robertson, S., and Crouse, G.F. (2000). Regulation of mitotic homeologous recombination in yeast. Functions of mismatch repair and nucleotide excision repair genes. Genetics *154*, 133-146.

Niculescu, A.B., Chen, X., Smeets, M., Hengst, L., Prives, C., and Reed, S.I. (1998). Effects of p21(Cip1/Waf1) at both the G1/S and the G2/M cell cycle transitions: pRb is a critical determinant in blocking DNA replication and in preventing endoreduplication. Mol.Cell Biol. *18*, 629-643.

Nigg, E.A. (1995). Cyclin-dependent protein kinases: key regulators of the eukaryotic cell cycle. Bioessays *17*, 471-480.

Nouspikel, T., Lalle, P., Leadon, S.A., Cooper, P.K., and Clarkson, S.G. (1997). A common mutational pattern in Cockayne syndrome patients from xeroderma pigmentosum group G: implications for a second XPG function. Proc.Natl.Acad.Sci.U.S.A. *94*, 3116-3121.

Nunez, F. (1999) The Mechanism of Cell Cycle Arrest in the ERCC1-Deficient Mouse Model. Thesis – University of Edinburgh.

Nunez, F., Chipchase, M.D., Clarke, A.R., and Melton, D.W. (2000). Nucleotide excision repair gene (ERCC1) deficiency causes G(2) arrest in hepatocytes and a reduction in liver binucleation: the role of p53 and p21. FASEB J. *14*, 1073-1082.

Nurse, P. (1994). Ordering S phase and M phase in the cell cycle. Cell *79*, 547-550.

O'Connell, M.J., Walworth, N.C., and Carr, A.M. (2000). The G2-phase DNA-damage checkpoint. Trends.Cell Biol. *10*, 296-303.

O'Donovan, A., Davies, A.A., Moggs, J.G., West, S.C., and Wood, R.D. (1994). XPG endonuclease makes the 3' incision in human DNA nucleotide excision repair. Nature *371*, 432-435.

O'Driscoll, M., Martinelli, S., Ciotta, C., and Karran, P. (1999). Combined mismatch and nucleotide excision repair defects in a human cell line: mismatch repair processes methylation but not UV- or ionizing radiation-induced DNA damage. Carcinogenesis *20*, 799-804.

Oku, T., Ikeda, S., Sasaki, H., Fukuda, K., Morioka, H., Ohtsuka, E., Yoshikawa, H., and Tsurimoto, T. (1998). Functional sites of human PCNA which interact with p21 (Cip1/Waf1), DNA polymerase delta and replication factor C. Genes Cells *3*, 357-369.

Overturf, K., al-Dhalimy, M., Ou, C.N., Finegold, M., and Grompe, M. (1997). Serial transplantation reveals the stem-cell-like regenerative potential of adult mouse hepatocytes. Am.J.Pathol. *151*, 1273-1280.

Palitti, F., Tanzarella, C., Degrassi, F., De Salvia, R., Fiore, M., and Natarajan, A.T. (1983). Formation of chromatid-type aberrations in G2 stage of the cell cycle. Mutat.Res. *110*, 343-350.

Pan, Z.Q., Reardon, J.T., Li, L., Flores-Rozas, H., Legerski, R., Sancar, A., and Hurwitz, J. (1995). Inhibition of nucleotide excision repair by the cyclin-dependent kinase inhibitor p21. J.Biol.Chem. *270*, 22008-22016.

Paques, F. and Haber, J.E. (1997). Two pathways for removal of nonhomologous DNA ends during double-strand break repair in Saccharomyces cerevisiae. Mol.Cell Biol. *17*, 6765-6771.

Paques, F. and Haber, J.E. (1999). Multiple pathways of recombination induced by double-strand breaks in saccharomyces cerevisiae Microbiol Mol Biol Rev *63*, 349-404.

Parker, S.B., Eichele, G., Zhang, P., Rawls, A., Sands, A.T., Bradley, A., Olson, E.N., Harper, J.W., and Elledge, S.J. (1995). p53-independent expression of p21Cip1 in muscle and other terminally differentiating cells. Science *267*, 1024-1027.

Payne, A. and Chu, G. (1994). Xeroderma pigmentosum group E binding factor recognizes a broad spectrum of DNA damage. Mutat.Res. *310*, 89-102.

Peng, C.Y., Graves, P.R., Thoma, R.S., Wu, Z., Shaw, A.S., and Piwnica-Worms, H. (1997). Mitotic and G2 checkpoint control: regulation of 14-3-3 protein binding by phosphorylation of Cdc25C on serine-216. Science *277*, 1501-1505.

Petukhova, G., Stratton, S.A., and Sung, P. (1999). Single strand DNA binding and annealing activities in the yeast recombination factor Rad59. J.Biol.Chem. *274*, 33839-33842.

Pines, J. (1995). Cyclins and cyclin-dependent kinases: a biochemical view. Biochem.J. *308*, 697-711.

Podust, V.N., Podust, L.M., Goubin, F., Ducommun, B., and Hubscher, U. (1995). Mechanism of inhibition of proliferating cell nuclear antigen-dependent DNA synthesis by the cyclin-dependent kinase inhibitor p21. Biochemistry *34*, 8869-8875.

Poon, R.Y., Jiang, W., Toyoshima, H., and Hunter, T. (1996). Cyclin-dependent kinases are inactivated by a combination of p21 and Thr-14/Tyr-15 phosphorylation after UV-induced DNA damage. J.Biol.Chem. *271*, 13283-13291.

Pospisilova, S. and Kypr, J. (1997). UV light-induced crosslinking of the complementary strands of plasmid pUC19 DNA restriction fragments. Photochem.Photobiol. *65*, 945-948.

Prado, F. and Aguilera, A. (1995). Role of reciprocal exchange, one-ended invasion crossover and single-strand annealing on inverted and direct repeat recombination in yeast: different requirements for the RAD1, RAD10, and RAD52 genes. Genetics *139*, 109-123.

Purdie, C.A., Harrison, D.J., Peter, A., Dobbie, L., White, S., Howie, S.E., Salter, D.M., Bird, C.C., Wyllie, A.H., and Hooper, M.L. (1994). Tumour incidence, spectrum and ploidy in mice with a large deletion in the p53 gene. Oncogene *9*, 603-609.

Raderschall, E., Golub, E.I., and Haaf, T. (1999). Nuclear foci of mammalian recombination proteins are located at single-stranded DNA regions formed after DNA damage. Proc.Natl.Acad.Sci.U.S.A. *96*, 1921-1926.

Ravi, R.K., McMahon, M., Yangang, Z., Williams, J.R., Dillehay, L.E., Nelkin, B.D., and Mabry, M. (1999). Raf-1-induced cell cycle arrest in LNCaP human prostate cancer cells. J.Cell Biochem. *72*, 458-469.

Ray, A., Siddiqi, I., Kolodkin, A.L., and Stahl, F.W. (1988). Intra-chromosomal gene conversion induced by a DNA double-strand break in Saccharomyces cerevisiae. J.Mol.Biol. *201*, 247-260.

Reardon, J.T., Bessho, T., Kung, H.C., Bolton, P.H., and Sancar, A. (1997). In vitro repair of oxidative DNA damage by human nucleotide excision repair system: possible explanation for neurodegeneration in xeroderma pigmentosum patients. Proc.Natl.Acad.Sci.U.S.A. *94*, 9463-9468.

Reinke, V. and Lozano, G. (1997). Differential activation of p53 targets in cells treated with ultraviolet radiation that undergo both apoptosis and growth arrest. Radiat.Res. *148*, 115-122.

Reitmair, A.H., Schmits, R., Ewel, A., Bapat, B., Redston, M., Mitri, A., Waterhouse, P., Mittrucker, H.W., Wakeham, A., and Liu, B. (1995). MSH2 deficient mice are viable and susceptible to lymphoid tumours. Nat.Genet. *11*, 64-70.

Rhind, N., Furnari, B., and Russell, P. (1997). Cdc2 tyrosine phosphorylation is required for the DNA damage checkpoint in fission yeast. Genes Dev. *11*, 504-511.

Rhind, N. and Russell, P. (1998). Mitotic DNA damage and replication checkpoints in yeast. Curr.Opin.Cell Biol. *10*, 749-758.

Rhind, N. and Russell, P. (2001). Roles of the mitotic inhibitors Wee1 and Mik1 in the G(2) DNA damage and replication checkpoints. Mol.Cell Biol. *21*, 1499-1508.

Robbins, J.H. (1988). Xeroderma pigmentosum. Defective DNA repair causes skin cancer and neurodegeneration. JAMA *260*, 384-388.

Robbins, J.H. (1989). A childhood neurodegeneration due to defective DNA repair: a novel concept of disease based on studies xeroderma pigmentosum. J.Child Neurol. *4*, 143-146.

Robbins, J.H., Brumback, R.A., Mendiones, M., Barrett, S.F., Carl, J.R., Cho, S., Denckla, M.B., Ganges, M.B., Gerber, L.H., and Guthrie, R.A. (1991). Neurological disease in xeroderma pigmentosum. Documentation of a late onset type of the juvenile onset form. Brain *114*, 1335-1361.

Rodel, C., Jupitz, T., and Schmidt, H. (1997). Complementation of the DNA repair-deficient swi10 mutant of fission yeast by the human ERCC1 gene. Nucleic.Acids.Res. *25*, 2823-2827.

Roth, D.B. and Wilson, J.H. (1986). Nonhomologous recombination in mammalian cells: role for short sequence homologies in the joining reaction. Mol.Cell Biol. *6*, 4295-4304.

Sachs, R.K., Rogoff, A., Chen, A.M., Simpson, P.J., Savage, J.R., Hahnfeldt, P., and Hlatky, L.R. (2000). Underprediction of visibly complex chromosome aberrations by a recombinational-repair ('one-hit') model. Int.J.Radiat.Biol. *76*, 129-148.

Saffran, W.A., Greenberg, R.B., Thaler-Scheer, M.S., and Jones, M.M. (1994). Single strand and double strand DNA damage-induced reciprocal recombination in yeast. Dependence on nucleotide excision repair and RAD1 recombination. Nucleic.Acids.Res. *22*, 2823-2829.

Saijo, M., Kuraoka, I., Masutani, C., Hanaoka, F., and Tanaka, K. (1996). Sequential binding of DNA repair proteins RPA and ERCC1 to XPA in vitro. Nucleic.Acids.Res. *24*, 4719-4724.

Sancar, A. and Sancar, G.B. (1988). DNA repair enzymes. Annu.Rev.Biochem. *57:29-67.*, 29-67.

Sancar, G.B. (2000). Enzymatic photoreactivation: 50 years and counting. Mutat.Res. *451*, 25-37.

Sands, A.T., Abuin, A., Sanchez, A., Conti, C.J., and Bradley, A. (1995). High susceptibility to ultraviolet-induced carcinogenesis in mice lacking XPC. Nature *377*, 162-165.

Sargent, R.G., Brenneman, M.A., and Wilson, J.H. (1997). Repair of site-specific double-strand breaks in a mammalian chromosome by homologous and illegitimate recombination. Mol.Cell Biol. *17*, 267-277.

Sargent, R.G., Meservy, J.L., Perkins, B.D., Kilburn, A.E., Intody, Z., Adair, G.M., Nairn, R.S., and Wilson, J.H. (2000). Role of the nucleotide excision repair gene ERCC1 in formation of recombination-dependent rearrangements in mammalian cells. Nucleic.Acids.Res. *28*, 3771-3778.

Satoh, M.S., Jones, C.J., Wood, R.D., and Lindahl, T. (1993). DNA excision-repair defect of xeroderma pigmentosum prevents removal of a class of oxygen free radical-induced base lesions. Proc.Natl.Acad.Sci.U.S.A. *90*, 6335-6339.

Savage, J.R. (1976). Classification and relationships of induced chromosomal structual changes. J.Med.Genet. *13*, 103-122.

Savage, J.R. (1990) Mutation and the Environment, Part B:385-396, Wiley-Liss Inc.

Scherer, S.J., Maier, S.M., Seifert, M., Hanselmann, R.G., Zang, K.D., Muller-Hermelink, H.K., Angel, P., Welter, C., and Schartl, M. (2000). p53 and c-Jun functionally synergize in the regulation of the DNA repair gene hMSH2 in response to UV. J.Biol.Chem. *275*, 37469-37473.

Schiestl, R.H. and Prakash, S. (1990). RAD10, an excision repair gene of Saccharomyces cerevisiae, is involved in the RAD1 pathway of mitotic recombination. Mol.Cell Biol. *10*, 2485-2491.

Schmidt, H., Kapitza-Fecke, P., Stephen, E.R., and Gutz, H. (1989). Some of the swi genes of Schizosaccharomyces pombe also have a function in the repair of radiation damage. Curr.Genet. *16*, 89-94.

Schmucker, D.L. (1990). Hepatocyte fine structure during maturation and senescence. J.Electron Microsc.Tech. *14*, 106-125.

Schwartz, J.L. (1989). Monofunctional alkylating agent-induced S-phase-dependent DNA damage. Mutat.Res. *216*, 111-118.

Sekelsky, J.J., McKim, K.S., Chin, G.M., and Hawley, R.S. (1995). The Drosophila meiotic recombination gene mei-9 encodes a homologue of the yeast excision repair protein Rad1. Genetics *141*, 619-627.

Sekelsky, J.J., Hollis, K.J., Eimerl, A.I., Burtis, K.C., and Hawley, R.S. (2000). Nucleotide excision repair endonuclease genes in Drosophila melanogaster. Mutat.Res. *459*, 219-228.

Selter, H. and Montenarh, M. (1994). The emerging picture of p53. Int.J.Biochem. *26*, 145-154.

Selva, E.M., New, L., Crouse, G.F., and Lahue, R.S. (1995). Mismatch correction acts as a barrier to homeologous recombination in Saccharomyces cerevisiae. Genetics *139*, 1175-1188.

Serfas, M.S., Goufman, E., Feuerman, M.H., Gartel, A.L., and Tyner, A.L. (1997). p53-independent induction of p21WAF1/CIP1 expression in pericentral hepatocytes following carbon tetrachloride intoxication. Cell Growth Differ. *8*, 951-961.

Sgouros, J., Gaillard, P.H., and Wood, R.D. (1999). A relationship betweena DNA-repair/recombination nuclease family and archaeal helicases. Trends.Biochem.Sci. *24*, 95-97.

Shannon, M., Lamerdin, J.E., Richardson, L., McCutchen-Maloney, S.L., Hwang, M.H., Handel, M.A., Stubbs, L., and Thelen, M.P. (1999). Characterization of the mouse Xpf DNA repair gene and differential expression during spermatogenesis. Genomics *62*, 427-435.

Sheikh, M.S., Chen, Y.Q., Smith, M.L., and Fornace, A.J.J. (1997). Role of p21Waf1/Cip1/Sdi1 in cell death and DNA repair as studied using a tetracycline-inducible system in p53-deficient cells. Oncogene *14*, 1875-1882.

Sherr, C.J. (1994). G1 phase progression: cycling on cue. Cell *79*, 551-555.

Sherr, C.J. and Roberts, J.M. (1995). Inhibitors of mammalian G1 cyclin-dependent kinases. Genes Dev. *9*, 1149-1163.

Shieh, S.Y., Ahn, J., Tamai, K., Taya, Y., and Prives, C. (2000). The human homologs of checkpoint kinases Chk1 and Cds1 (Chk2) phosphorylate p53 at multiple DNA damage-inducible sites. Genes Dev. *14*, 289-300.

Shinohara, A. and Ogawa, T. (1999). Rad51/RecA protein families and the associated proteins in eukaryotes. Mutat.Res. *435*, 13-21.

Shivji, M.K., Grey, S.J., Strausfeld, U.P., Wood, R.D., and Blow, J.J. (1994). Cip1 inhibits DNA replication but not PCNA-dependent nucleotide excision-repair. Curr.Biol. *4*, 1062-1068.

Shivji, M.K., Eker, A.P., and Wood, R.D. (1994). DNA repair defect in xeroderma pigmentosum group C and complementing factor from HeLa cells. J.Biol.Chem. *269*, 22749-22757.

Sigal, S.H., Gupta, S., Gebhard, D.F.J., Holst, P., Neufeld, D., and Reid, L.M. (1995). Evidence for a terminal differentiation process in the rat liver. Differentiation. *59*, 35-42.

Sigal, S.H., Rajvanshi, P., Gorla, G.R., Sokhi, R.P., Saxena, R., Gebhard, D.R.J., Reid, L.M., and Gupta, S. (1999). Partial hepatectomy-induced polyploidy attenuates hepatocyte replication and activates cell aging events. Am.J.Physiol. *276*, G1260-G1272

Sijbers, A.M., van der Spek, P.J., Odijk, H., van den Berg, J., van Duin, M., Westerveld, A., Jaspers, N.G., Bootsma, D., and Hoeijmakers, J.H. (1996). Mutational analysis of the human nucleotide excision repair gene ERCC1. Nucleic.Acids.Res. *24*, 3370-3380.

Sijbers, A.M., de Laat, W.L., Ariza, R.R., Biggerstaff, M., Wei, Y.F., Moggs, J.G., Carter, K.C., Shell, B.K., Evans, E., de Jong, M.C., Rademakers, S., de Rooij, J., Jaspers, N.G., Hoeijmakers, J.H., and Wood, R.D. (1996). Xeroderma pigmentosum group F caused by a defect in a structure-specific DNA repair endonuclease. Cell *86*, 811-822.

Siu, W.Y., Yam, C.H., and Poon, R.Y. (1999). G1 versus G2 cell cycle arrest after adriamycin-induced damage in mouse Swiss3T3 cells. FEBS Lett. *461*, 299-305.

Smith, J.R. and Pereira-Smith, O.M. (1996). Replicative senescence: implications for in vivo aging and tumor suppression. Science *273*, 63-67.

Smith, M.L., Chen, I.T., Zhan, Q., O'Connor, P.M., and Fornace, A.J.J. (1995). Involvement of the p53 tumor suppressor in repair of u.v.-type DNA damage. Oncogene *10*, 1053-1059.

Smith, M.L., Ford, J.M., Hollander, M.C., Bortnick, R.A., Amundson, S.A., Seo, Y.R., Deng, C.X., Hanawalt, P.C., and Fornace, A.J.J. (2000). p53-mediated DNA repair responses to UV radiation: studies of mouse cells lacking p53, p21, and/or gadd45 genes. Mol.Cell Biol. *20*, 3705-3714.

Sorenson, C.M. and Eastman, A. (1988). Influence of cis-diamminedichloroplatinum(II) on DNA synthesis and cell cycle progression in excision repair proficient and deficient Chinese hamster ovary cells. Cancer Res. *48*, 6703-6707.

Sorenson, C.M., Barry, M.A., and Eastman, A. (1990). Analysis of events associated with cell cycle arrest at G2 phase and cell death induced by cisplatin. J.Natl.Cancer Inst. *82*, 749-755.

Stein, G.H. and Dulic, V. (1995). Origins of G1 arrest in senescent human fibroblasts. Bioessays *17*, 537-543.

Studamire, B., Price, G., Sugawara, N., Haber, J.E., and Alani, E. (1999). Separation-of-function mutations in Saccharomyces cerevisiae MSH2 that confer mismatch repair defects but do not affect nonhomologous-tail removal during recombination. Mol.Cell Biol. *19*, 7558-7567.

Sugasawa, K., Ng, J.M., Masutani, C., Iwai, S., van der Spek, P.J., Eker, A.P., Hanaoka, F., Bootsma, D., and Hoeijmakers, J.H. (1998). Xeroderma pigmentosum group C protein complex is the initiator of global genome nucleotide excision repair. Mol.Cell *2*, 223-232.

Sugasawa, K., Okamoto, T., Shimizu, Y., Masutani, C., Iwai, S., and Hanaoka, F. (2001). A multistep damage recognition mechanism for global genomic nucleotide excision repair. Genes Dev. *15*, 507-521.

Sugawara, N. and Haber, J.E. (1992). Characterization of double-strand break-induced recombination: homology requirements and single-stranded DNA formation. Mol.Cell Biol. *12*, 563-575.

Sugawara, N., Paques, F., Colaiacovo, M., and Haber, J.E. (1997). Role of Saccharomyces cerevisiae Msh2 and Msh3 repair proteins in double-strand break-induced recombination. Proc.Natl.Acad.Sci.U.S.A. *94* , 9214-9219.

Sugawara, N., Ira, G., and Haber, J.E. (2000). DNA length dependence of the single-strand annealing pathway and the role of Saccharomyces cerevisiae RAD59 in double-strand break repair. Mol.Cell Biol. *20* , 5300-5309.

Sugiyama, T., New, J.H., and Kowalczykowski, S.C. (1998). DNA annealing by RAD52 protein is stimulated by specific interaction with the complex of replication protein A and single-stranded DNA. Proc.Natl.Acad.Sci.U.S.A. *95*, 6049-6054.

Sung, P., Trujillo, K.M., and Van Komen, S. (2000). Recombination factors of Saccharomyces cerevisiae. Mutat.Res. *451*, 257-275.

Svejstrup, J.Q., Wang, Z., Feaver, W.J., Wu, X., Bushnell, D.A., Donahue, T.F., Friedberg, E.C., and Kornberg, R.D. (1995). Different forms of TFIIH for transcription and DNA repair: holo-TFIIH and a nucleotide excision repairosome. Cell *80*, 21-28.

Svoboda, D.L. and Vos, J.M. (1995). Differential replication of a single, UV-induced lesion in the leading or lagging strand by a human cell extract: fork uncoupling or gap formation. Proc.Natl.Acad.Sci.U.S.A. *92*, 11975-11979.

Takata, M., Sasaki, M.S., Sonoda, E., Morrison, C., Hashimoto, M., Utsumi, H., Yamaguchi-Iwai, Y., Shinohara, A., and Takeda, S. (1998). Homologous recombination and non-homologous end-joining pathways of DNA double-strand break repair have overlapping roles in the maintenance of chromosomal integrity in vertebrate cells. EMBO J. *17*, 5497-5508.

Tambini, C.E., George, A.M., Rommens, J.M., Tsui, L.C., Scherer, S.W., and Thacker, J. (1997). The XRCC2 DNA repair gene: identification of a positional candidate. Genomics *41*, 84-92.

Tang, J.Y., Hwang, B.J., Ford, J.M., Hanawalt, P.C., and Chu, G. (2000). Xeroderma pigmentosum p48 gene enhances global genomic repair and suppresses UV-induced mutagenesis. Mol.Cell *5*, 737-744.

Tebbs, R.S., Zhao, Y., Tucker, J.D., Scheerer, J.B., Siciliano, M.J., Hwang, M., Liu, N., Legerski, R.J., and Thompson, L.H. (1995). Correction of chromosomal instability and sensitivity to diverse mutagens by a cloned cDNA of the XRCC3 DNA repair gene. Proc.Natl.Acad.Sci.U.S.A. *92*, 6354-6358.

Tell, G., Zecca, A., Pellizzari, L., Spessotto, P., Colombatti, A., Kelley, M.R., Damante, G., and Pucillo, C. (2000). An 'environment to nucleus' signaling system operates in B lymphocytes: redox status modulates BSAP/Pax-5 activation through Ref-1 nuclear translocation. Nucleic.Acids.Res. *28*, 1099-1105.

Teo, I., Sedgwick, B., Demple, B., Li, B., and Lindahl, T. (1984). Induction of resistance to alkylating agents in E. coli: the ada+ gene product serves both as a regulatory protein and as an enzyme for repair of mutagenic damage. EMBO J. *3*, 2151-2157.

Thacker, J. (1999). A surfeit of RAD51-like genes? Trends.Genet. *15*, 166-168.

Thacker, J. (1999). The role of homologous recombination processes in the repair of severe forms of DNA damage in mammalian cells. Biochimie *81*, 77-85.

Thompson, L.H., Fong, S., and Brookman, K. (1980). Validation of conditions for efficient detection of HPRT and APRT mutations in suspension-cultured Chinese hamster ovary cells. Mutat.Res. *74*, 21-36.

Thompson, L.H., Busch, D.B., Brookman, K., Mooney, C.L., and Glaser, D.A. (1981). Genetic diversity of UV-sensitive DNA repair mutants of Chinese hamster ovary cells. Proc.Natl.Acad.Sci.U.S.A. *78*, 3734-3737.

Thompson, L.H. and Schild, D. (1999). The contribution of homologous recombination in preserving genome integrity in mammalian cells. Biochimie *81*, 87-105.

Tian, M. and Alt, F.W. (2000). Transcription-induced cleavage of immunoglobulin switch regions by nucleotide excision repair nucleases in vitro. J.Biol.Chem. *275*, 24163-24172.

Tobi, S.E., Levy, D.D., Seidman, and Kraemer (1999). Sequence-dependent mutations in a shuttle vector plasmid replicated in a mismatch repair deficient human cell line. Carcinogenesis *20*, 1293-1301.

Tornaletti, S. and Hanawalt, P.C. (1999). Effect of DNA lesions on transcription elongation. Biochimie *81*, 139-46.

Troelstra, C., van Gool, A., de Wit, J., Vermeulen, W., Bootsma, D., and Hoeijmakers, J.H. (1992). ERCC6, a member of a subfamily of putative helicases, is involved in Cockayne's syndrome and preferential repair of active genes. Cell *71*, 939-953.

Tsurimoto, T. (1999). PCNA binding proteins. Front.Biosci. *4:D849-58.*, D849-D858

Tsuzuki, T., Fujii, Y., Sakumi, K., Tominaga, Y., Nakao, K., Sekiguchi, M., Matsushiro, A., Yoshimura, Y., and MoritaT (1996). Targeted disruption of the Rad51 gene leads to lethality in embryonic mice. Proc.Natl.Acad.Sci.U.S.A. *93*, 6236-6240.

Umar, A., Buermeyer, A.B., Simon, J.A., Thomas, D.C., Clark, A.B., Liskay, R.M., and Kunkel, T.A. (1996). Requirement for PCNA in DNA mismatch repair at a step preceding DNA resynthesis. Cell *87*, 65-73.

van der Horst, G.T., van Steeg, H., Berg, R.J., van Gool, A.J., de Wit, J., Weeda, G., Morreau, H., Beems, R.B., van Kreijl, C.F., de Gruijl, F.R., Bootsma, D., and Hoeijmakers, J.H. (1997).

Defective transcription-coupled repair in Cockayne syndrome B mice is associated with skin cancer predisposition. Cell *89*, 425-435.

van Duin, M., de Wit, J., Odijk, H., Westerveld, A., Yasui, A., Koken, H.M., Hoeijmakers, J.H., and Bootsma, D. (1986). Molecular characterization of the human excision repair gene ERCC-1: cDNA cloning and amino acid homology with the yeast DNA repair gene RAD10. Cell *44*, 913-923.

van Duin, M., Koken, M.H., van den Tol, J., ten Dijke, P., Odijk, H., Westerveld, A., Bootsma, D., and Hoeijmakers, J.H. (1987). Genomic characterization of the human DNA excision repair gene ERCC-1. Nucleic.Acids.Res. *15*, 9195-9213.

van Duin, M., van den Tol, J., Warmerdam, P., Odijk, H., Meijer, D., Westerveld, A., Bootsma, D., and Hoeijmakers, J.H. (1988). Evolution and mutagenesis of the mammalian excision repair gene ERCC-1. Nucleic.Acids.Res. *16*, 5305-5322.

van Hoffen, A., Venema, J., Meschini, R., van Zeeland, A.A., and Mullenders, L.H. (1995). Transcription-coupled repair removes both cyclobutane pyrimidine dimers and 6-4 photoproducts with equal efficiency and in a sequential way from transcribed DNA in xeroderma pigmentosum group C fibroblasts. EMBO J. *14*, 360-367.

Van Houten, B., Gamper, H., Holbrook, S.R., Hearst, J.E., and Sancar, A. (1986). Action mechanism of ABC excision nuclease on a DNA substrate containing a psoralen crosslink at a defined position. Proc.Natl.Acad.Sci.U.S.A. *83*, 8077-8081.

van Oosterwijk, M.F., Versteeg, A., Filon, R., van Zeeland, A.A., and Mullenders, L.H. (1996). The sensitivity of Cockayne's syndrome cells to DNA-damaging agents is not due to defective transcription-coupled repair of active genes. Mol.Cell Biol. *16*, 4436-4444.

van Oosterwijk, M.F., Filon, R., de Groot, A.J., van Zeeland, A.A., and Mullenders, L.H. (1998). Lack of transcription-coupled repair of acetylaminofluorene DNA adducts in human fibroblasts contrasts their efficient inhibition of transcription. J.Biol.Chem. *273*, 13599-13604.

Veaute, X., Mari-Giglia, G., Lawrence, C.W., and Sarasin, A. (2000). UV lesions located on the leading strand inhibit DNA replication but do not inhibit SV40 T-antigen helicase activity. Mutat.Res. *459*, 19-28.

Venema, J., Mullenders, L.H., Natarajan, A.T., van Zeeland, A.A., and Mayne, L.V. (1990). The genetic defect in Cockayne syndrome is associated with a defect in repair of UV-induced DNA damage in transcriptionally active DNA. Proc.Natl.Acad.Sci.U.S.A. *87*, 4707-4711.

Waga, S., Hannon, G.J., Beach, D., and Stillman, B. (1994). The p21 inhibitor of cyclin-dependent kinases controls DNA replication by interaction with PCNA. Nature *369*, 574-578.

Wakasugi, M. and Sancar, A. (1999). Order of assembly of human DNA repair excision nuclease. J.Biol.Chem. *274*, 18759-18768.

Waldman, T., Kinzler, K.W., and Vogelstein, B. (1995). p21 is necessary for the p53-mediated G1 arrest in human cancer cells. Cancer Res. *55*, 5187-5190.

Waldman, T., Lengauer, C., Kinzler, K.W., and Vogelstein, B. (1996). Uncoupling of S phase and mitosis induced by anticancer agents in cells lacking p21. Nature *381*, 713-716.

Wallace, S.S. (1988). AP endonucleases and DNA glycosylases that recognize oxidative DNA damage. Environ.Mol.Mutagen. *12*, 431-477.

Walters, R.A. and Hildebrand, C.E. (1975). Evidence that x-irradiation inhibits DNA replicon initiation in Chinese hamster cells. Biochem.Biophys.Res.Commun. *65*, 265-271.

Warren, A.J., Ihnat, M.A., Ogdon, S.E., Rowell, E.E., and Hamilton, J.W. (1998). Binding of nuclear proteins associated with mammalian DNA repair to the mitomycin C-DNA interstrand crosslink. Environ.Mol.Mutagen. *31*, 70-81.

Weeda, G., Donker, I., de Wit, J., Morreau, H., Janssens, R., Vissers, C.J., Nigg, A., van Steeg, H., Bootsma, D., and Hoeijmakers, J.H. (1997). Disruption of mouse ERCC1 results in a novel repair syndrome with growth failure, nuclear abnormalities and senescence. Curr.Biol. *7*, 427-439.

Winkler, G.S., Sugasawa, K., Eker, A.P., de Laat, W.L., and Hoeijmakers, J.H. (2001). Novel functional interactions between nucleotide excision DNA repair proteins influencing the enzymatic activities of TFIIH, XPG, and ERCC1-XPF. Biochemistry *40*, 160-165.

Wold, M.S. (1997). Replication protein A: a heterotrimeric, single-stranded DNA-binding protein required for eukaryotic DNA metabolism. Annu.Rev.Biochem. *66:61-92.*, 61-92.

Wood, R.D. and Burki, H.J. (1982). Repair capability and the cellular age response for killing and mutation induction after UV. Mutat.Res. *95*, 505-514.

Wood, R.D., de Veciana, M., and Presson-Tincknell, B. (1982). Postirradiation properties of a UV-sensitive variant of CHO. Photochem.Photobiol. *36*, 169-174.

Wood, R.D. (1999). DNA damage recognition during nucleotide excision repair in mammalian cells. Biochimie *81*, 39-44.

Wu, H., Wade, M., Krall, L., Grisham, J., Xiong, Y., and Van Dyke, T. (1996). Targeted in vivo expression of the cyclin-dependent kinase inhibitor p21 halts hepatocyte cell-cycle progression, postnatal liver development and regeneration. Genes Dev. *10*, 245-260.

Wu, X., Bayle, J.H., Olson, D., and Levine, A.J. (1993). The p53-mdm-2 autoregulatory feedback loop. Genes Dev. *7*, 1126-1132.

Wu, X., Wilson, T.E., and Lieber, M.R. (1999). A role for FEN-1 in nonhomologous DNA end joining: the order of strand annealing and nucleolytic processing events. Proc.Natl.Acad.Sci.U.S.A. *96*, 1303-1308.

Wyllie, F.S., Haughton, M.F., Bond, J.A., Rowson, J.M., Jones, C.J., and Wynford-Thomas, D. (1996). S phase cell-cycle arrest following DNA damage is independent of the p53/p21(WAF1) signalling pathway. Oncogene *12*, 1077-1082.

Xanthoudakis, S. and Curran, T. (1992). Identification and characterization of Ref-1, a nuclear protein that facilitates AP-1 DNA-binding activity. EMBO J. *11*, 653-665.

Xanthoudakis, S., Miao, G., Wang, F., Pan, Y.C., and Curran, T. (1992). Redox activation of Fos-Jun DNA binding activity is mediated by a DNA repair enzyme. EMBO J. *11*, 3323-3335.

Xanthoudakis, S., Smeyne, R.J., Wallace, J.D., and Curran, T. (1996). The redox/DNA repair protein, Ref-1, is essential for early embryonic development in mice. Proc.Natl.Acad.Sci.U.S.A. 93, 8919-8923.

Xiao, W., Lechler, T., Chow, B.L., Fontanie, T., Agustus, M., Carter, K.C., and Wei, Y.F. (1998). Identification, chromosomal mapping and tissue-specific expression of hREV3 encoding a putative human DNA polymerase zeta. Carcinogenesis *19*, 945-949.

Xiong, Y., Zhang, H., and Beach, D. (1992). D type cyclins associate with multiple protein kinases and the DNA replication and repair factor PCNA. Cell *71*, 505-514.

Xu, H., Swoboda, I., Bhalla, P.L., Sijbers, A.M., Zhao, C., Ong, E.K., Hoeijmakers, J.H., and Singh, M.B. (1998). Plant homologue of human excision repair gene ERCC1 points to conservation of DNA repair mechanisms. Plant J. *13*, 823-829.

Zehfus, B.R., McWilliams, A.D., Lin, Y.H., Hoekstra, M.F., and Keil, R.L. (1990). Genetic control of RNA polymerase I-stimulated recombination in yeast. Genetics *126*, 41-52.

Zhang, H., Hannon, G.J., Casso, D., and Beach, D. (1994). p21 is a component of active cell cycle kinases. Cold Spring Harb.Symp.Quant.Biol. *59:21-9.*, 21-29.

Zhou, B.B. and Elledge, S.J. (2000). The DNA damage response: putting checkpoints in perspective. Nature *408*, 433-439.

Zhu, J., Woods, D., McMahon, M., and Bishop, J.M. (1998). Senescence of human fibroblasts induced by oncogenic Raf. Genes Dev. *12*, 2997-3007.

Nucleotide excision repair gene (ERCC1) deficiency causes G_2 arrest in hepatocytes and a reduction in liver binucleation: the role of p53 and p21

FATIMA NÚÑEZ,* MICHAEL D. CHIPCHASE,* ALAN R. CLARKE,† AND DAVID W. MELTON*,[1]

*Institute of Cell and Molecular Biology, Edinburgh University, King's Buildings, Edinburgh, Scotland, U.K.; and †Department of Pathology, Edinburgh University, Teviot Place, Edinburgh, Scotland, U.K.

ABSTRACT **A wide range of DNA lesions, both UV and chemically induced, are dealt with by the nucleotide excision repair (NER) pathway. Defects in NER result in human syndromes such as xeroderma pigmentosum (XP), where there is a 1000-fold increased incidence of skin cancer. The ERCC1 protein is essential for NER, but ERCC1 knockout mice are not a model for XP. In the absence of exogenous DNA-damaging agents, these mice are runted and die before weaning, with dramatically accelerated liver polyploidy and elevated levels of p53. Here we present a morphological, immunological, and molecular study to understand the mechanism for the unusual liver pathology in ERCC1-deficient mice. We show that the enlarged ERCC1-deficient hepatocytes are arrested in G_2 and that DNA replication and the normal process of binucleation are both reduced. This is associated with a p53-independent increase in expression of the cyclin-dependent kinase inhibitor p21. The most dramatic feature of the ERCC1-deficient liver phenotype, the accelerated polyploidy, is not rescued by p53 deficiency, but we show that p53 is responsible for the reduced DNA replication and binucleation. We consider that the liver phenotype is a response to unrepaired endogenous DNA damage, which may reflect an additional non-NER-related function for the ERCC1 protein.—Núñez, F., Chipchase, M. D., Clarke, A. R., Melton, D. W. Nucleotide excision repair gene (ERCC1) deficiency causes G_2 arrest in hepatocytes and a reduction in liver binucleation: the role of p53 and p21. *FASEB J.* 14, 1073–1082 (2000)**

Key Words: DNA repair · cancer · knockout mice · cell cycle arrest

UNREPAIRED DNA LESIONS can give rise to mutations, genome instability and carcinogenesis, or cell death. Nucleotide excision repair (NER) deals with a wide range of lesions, from UV-induced thymine dimers and (6–4) photoproducts to lesions caused by a variety of chemical agents (1, 2). NER is a multi-step process that involves damage recognition, dual incision of the damaged strand, followed by the removal of the lesion as part of an oligonucleotide, gap filling, and strand ligation (1, 2). Defects in the proteins involved in this mechanism are associated with three human disorders: xeroderma pigmentosum (XP), which is characterized by a high incidence of skin cancer in sun-exposed areas of the body; Cockayne's syndrome (CS); and trichothiodystrophy (TTD). ERCC1 (excision repair cross-complementing gene 1) was the first mammalian NER gene to be cloned by virtue of its ability to complement a UV-sensitive Chinese hamster ovary cell line (3). ERCC1 failed to correct the repair defect in any of the human NER-deficient cell lines tested (4, 5). Nevertheless, the ERCC1 gene product is known to play a critical role in NER, where it acts in a complex with XPF to make an incision 5′ to the damage site (6). This led to speculation that mutations in ERCC1 may be developmentally lethal. Alternatively, ERCC1 deficiency may be associated with a different human phenotype not represented among the known NER deficiency diseases. Some NER proteins, such as XPB and XPD, have additional non-NER-related functions, and defects in these have been linked to the neurological and other not obviously NER-related problems, such as retarded physical or sexual development and brittle hair, seen in some XP, CS, and TTD patients (reviewed in ref 7). There is evidence that ERCC1 may also have other key functions. Based on homology studies (8, 9), the ERCC1/XPF complex has been proposed to play a role in mitotic recombination as well as in NER. In addition, many ERCC1 and ERCC4(XPF) mutants are extremely sensitive to agents, such as mitomycin C, which cause interstrand cross-links and are repaired by a process involving homologous recombination (7). ERCC1

[1] Correspondence: Institute of Cell and Molecular Biology, Edinburgh University, Darwin Building, King's Buildings, Mayfield Road, Edinburgh EH9 3JR, Scotland, U.K. E-mail: David.Melton@ed.ac.uk

0892-6638/00/0014-1073/$02.25 © FASEB

has also been implicated in the processing of heteroduplex recombination intermediates in mammalian cells (10). However, recent experiments suggest that in mouse cells ERCC1 is not essential for the recombination-mediated repair of interstrand cross-links, but instead may have a role in S-phase-dependent chromosome exchange (11).

p53 has been studied extensively in relation to DNA repair and its role in cell cycle regulation. On the detection of DNA damage, p53 levels are elevated through an increase in the protein half-life. p53 induces the transcription of downstream genes, such as the cyclin-dependent kinase inhibitor p21 (12), resulting in cell cycle arrest at both G_1/S and G_2/M checkpoints; in some cell types it can also lead to apoptotic cell death (13, 14). p53 and p21 have also been implicated in cellular aging: p53 levels accumulate as diploid fibroblasts age, with a corresponding increase in p21 levels, which in turn correlate with a slowing of cellular growth (15, 16). Fibroblasts from p21 null mice cannot arrest in G_1 after DNA damage (17, 18), and human p21-deficient cells show similar characteristics (16, 19, 20). From studies of these human p21-deficient cells, another role for p21 has emerged in p53-mediated G_2 arrest and coupling of DNA synthesis and mitosis (19, 20).

Contrary to some expectations, the absence of ERCC1 did not result in an embryonic lethal phenotype (21, 22). However, unlike XPA and XPC knockout mice (23–25), animals deficient in ERCC1 do not present the typical phenotype associated with XP. Our ERCC1 knockout mice are severely runted at birth and die before weaning, probably due to hepatic failure, with elevated levels of p53 in their liver, brain, and kidney (21). The most striking pathology was seen in the liver, where there was a dramatic increase in hepatocyte nuclear size. FACS analysis showed that this was due to nuclei with greater than the normal diploid (2n) content, with both polyploid (4n, 8n) and aneuploid nuclei being present (21). Increased liver ploidy is normally only seen in older mice (see below) and increased p53 levels have been found in senescing fibroblasts (15), so the phenotype in our ERCC1-deficient mice is reminiscent of premature aging. We wanted to understand how such a phenotype can arise in the absence of exogenous DNA-damaging agents. A clue to the involvement of cell cycle arrest in the ERCC1-deficient phenotype came from a report that similar liver abnormalities occurred in mice overexpressing p21 in their liver (26). We also investigated the role of p53 in the phenotype. If elevated p53 levels are responsible for the increased DNA content, then the ERCC1-deficient liver phenotype might be rescued in mice deficient in both ERCC1 and p53. We carried out studies on 3-wk-old mice of the following genotypes: wild-type (wt), ERCC1-deficient, p53-deficient, and double null. The age of the mice for this study was determined by the severe phenotype of the ERCC1-deficient animals, which do not survive longer than 3 wk (21). Incorporation of 5-bromo-2′-deoxyuridine (BrdU) (as a marker for DNA synthesis) and morphological studies (nuclear area measurement and binucleate cell count) of liver sections were used to investigate the cell cycle status of the hepatocytes. The nuclear area of the hepatocytes is directly related to DNA content (27, 28), with the area increasing with increasing ploidy as the animals age.

MATERIALS AND METHODS

Mice

The origin of the ERCC1 (21) and p53 knockout (13) mice has been described. Both strains were maintained as heterozygotes and were crossed to produce double heterozygous mice. These were intercrossed to obtain the mice used in this study, which were genotyped for ERCC1 (21) and p53 (13) as described. All the animals were maintained on an outbred background segregating for several different genomes. To determine the DNA replication index, mice were injected intraperitoneally with a 10 mM BrdU solution (0.1 ml/10g body weight) and livers were removed 24 h later.

Northern analysis

Liver RNA samples (30 μg), prepared using the RNAzol method (Biogenesis Ltd., Bournemouth, U.K.), were subjected to Northern analysis as described (29). A 490 bp fragment of mouse p21 cDNA, produced by PCR amplification of total mouse embryonic cDNA with the following p21 primers, was used as a probe: p21F (5′) ACCATGTCCAATCCTGGTGATGTCCG; p21R (5′) GGGCACTTCAGGGTTTTCTCTTGCAG. Primers were derived from the complete mouse p21 cDNA sequence (GenBank Acc. No. U09507). The filter was then stripped and reprobed for glyceraldehyde-3-phosphate dehydrogenase (GAPDH) mRNA as a loading control using a 1.2 kb cloned fragment of GAPDH cDNA (30). Signals were visualized using a Molecular Dynamics (Sunnyvale, Calif.) PhosphorImager and analyzed with ImageQuant software.

Immunohistochemistry

Livers were removed and immersion fixed for 24 h in methacarn, followed by storage in 70% ethanol. For the morphometry studies, 3 μm sections were stained with hematoxylin/eosin (H&E). For immunohistochemistry, 3 μm sections were mounted on slides that had been coated with poly-L-lysine. For the BrdU antibody, cells were rendered permeable by incubating slides in 1N HCl at 60°C for 1 h. The slides were then washed in running water and rinsed in phosphate-buffered saline (PBS) for 5 min. The sections were subsequently blocked for endogenous peroxidase activity in 3% hydrogen peroxide for 10 min at room temperature and incubated in a 1:5 dilution of normal goat serum (Scottish Antibody Production Unit) for 10 min. After this, the samples were incubated in the primary antibody to BrdU (MAS250, Harlan SeraLab), diluted (1:50) in normal serum for 30 min at room temperature, washed, and incubated for 30 min in biotinylated secondary antibody diluted (1:50) in normal serum. After washing the secondary antibody off, the slides

were incubated in horseradish peroxidase-conjugated AB Complex (streptavidin/biotin, DAKO Ltd., Bucks, U.K.) for 30 min at room temperature. AB Complex was washed off and the positive nuclei were visualized in 3,3′-diaminobenzidine tetrahydrochloride solution. Finally, the slides were counterstained lightly in hematoxylin (Sigma Diagnostics, St. Louis, Mo.), rinsed in Scott's tap water (1% (w/v) K_2CO_3, 10% (w/v) $MgSO_4$), dehydrated, and mounted. Controls were carried out using preimmune serum in place of primary antibody.

Measurement of hepatocyte nuclear areas

The AxioHOME Morphometric System (Zeiss) was used to perform the study of BrdU incorporation and nuclear area size distribution (31). Typically, a 100× objective lens was used for the measurements; 10 fields, each containing 50–70 nuclei, were measured for the BrdU-stained sections. For the area measurements and binucleate hepatocyte counts, all the nuclei in a field were measured and five fields were assayed per animal.

Centromeric staining of hepatocytes

Fresh livers were gently pressed onto a glass coverslip. This method allows single hepatocytes to detach in a nondisruptive manner so that their nuclei remain intact. Liver cells were air-dried for 5 min and fixed in 4% paraformaldehyde/PBS. After washing in PBS, the cells were permeabilized in KB buffer (10 mM Tris-HCl pH 7.7, 0.15 M NaCl, 0.1% bovine serum albumin)/0.1% Triton, washed twice in PBS without Triton, and incubated for 30 min at room temperature in the primary antibody, NR antibody (32; kindly donated by William Earnshaw, Institute of Cell and Molecular Biology, Edinburgh University) and diluted (1:1000) in PBS/0.1% Triton/0.1% sodium azide. The coverslips were then washed twice in PBS/1% Triton/0.1% sodium azide and subsequently incubated in a dilution (1:1000) of the biotinylated secondary antibody (anti-human IgG) for 30 min at room temperature. Then they were washed again and incubated for another 30 min in the tertiary antibody solution (streptavidin/Texas red complex, 1:1000 dilution in PBS/0.1% Triton/0.1% sodium azide) at room temperature. Finally, the cells were washed and stained with 4,6-diamidino-2-phenylindole (DAPI; 0.5 μg/ml in PBS) for 5 min, mounted on slides with Vectashield mounting medium, and sealed with nail varnish. Red dots within the nucleus of the hepatocytes, corresponding to the centromeres, were scored on a fluorescence microscope (Axioplan 2, Zeiss) using a 100×NA 1.4 oil immersion objective lens. The images presented here were acquired using a Sedat/Agard deconvolution microscope (Applied Precision Inc., Issaquah, Wash.) with an Olympus IX70 inverted microscope, a 100×/NA 1.4 oil immersion objective lens, and a PXL CCD camera (Photometrics, Munich, Germany). This process was performed using DeltaVision software running on a Silicon Graphics computer. All pictures were processed using the Adobe PhotoShop or Powerpoint packages.

RESULTS

The absence of p53 does not rescue the ERCC1-deficient phenotype

Animals that were both ERCC1 and p53 deficient did not survive longer than their ERCC1-deficient counterparts. This was the first indication that the absence of p53 did not rescue the overall phenotype associated with ERCC1 deficiency. In total, seven double null mice were identified, all of which were runted and were either killed or died prior to weaning. Mice were routinely genotyped at 3 wk, when the number of double nulls was far below the expected mendelian ratio of 1:16 from doubly heterozygous matings. A similar deficiency was not observed at day 19 of gestation, indicating very high perinatal mortality of the double null mice. We have previously reported a similar high perinatal mortality for ERCC1-deficient animals (21). This imposed a technical limitation on the number of double null samples analyzed at 3 wk of age.

To see whether the ERCC1-deficient liver phenotype was affected by p53 deficiency, studies of nuclear morphology and binucleate frequency were carried out on H&E-stained liver sections. In normal mouse liver development, the number of binucleate and polyploid cells increases with age, concomitant with a decrease of mononucleate, diploid cells. The appearance of both the wild-type (**Fig. 1*A***) and the p53-deficient (Fig. 1*C*) livers was normal, but this nuclear uniformity was lost in ERCC1-deficient (Fig. 1*B*) and double null (Fig. 1*D*) livers, with both showing enlarged nuclei in addition to the smaller

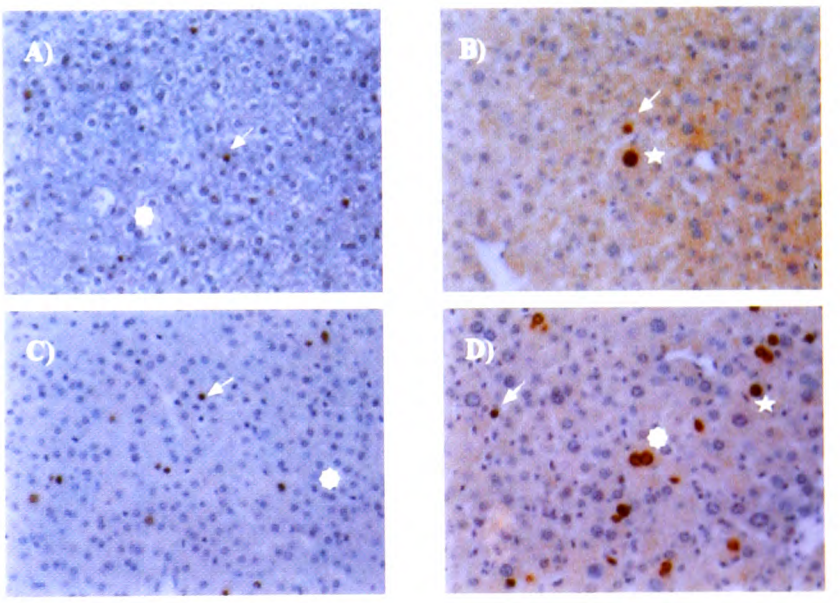

Figure 1. Liver morphology and typical BrdU staining patterns from 3-wk-old wild-type, ERCC1-deficient, p53-deficient, and double null mice. Photographs of liver sections were taken from BrdU-stained/hematoxylin- counterstained sections using a 40× objective lens. *A)* Wild-type, showing the typical uniform distribution of small nuclei seen in young animals. Eight-point star is situated immediately above a normal size binucleate cell. Arrow points toward a normal size BrdU-stained nucleus. *B)* ERCC1-deficient. Arrow points toward a normal size BrdU-stained nucleus. Star is situated next to an enlarged BrdU-stained nucleus. *C)* p53-deficient. Eight-point star is situated immediately above a normal size binucleate cell. Arrow points toward a normal-sized, BrdU-stained nucleus. *D)* Double null. Arrow points toward a normal size BrdU-stained nucleus. Star is situated next to a BrdU-stained enlarged nucleus and the eight-point star is situated next to a BrdU-stained binucleate cell with enlarged nuclei.

size characteristic of wild-type. Thus, the lack of p53 also failed to rescue the ERCC1-deficient liver phenotype. Despite overall similarities in the appearance of the ERCC1 null and the double null livers, initial observations suggested that the number of binucleate cells was elevated in the double null compared to the ERCC1-deficient livers (see Fig. 1*B, D*). To confirm these observations, the size of the hepatocyte nuclei and the number of binucleate cells were determined. Only cells that were unequivocally parenchymal in origin were counted, taking care to avoid the areas surrounding the portal veins, where there is an increased number of nonparenchymal cells. The distribution of the nuclear areas is shown in **Fig. 2**. The wild-type profile (top panel) shows a distribution of areas with a mode of 20–30 μm^2 and a maximum area of 70 μm^2. The number of nuclei that fall within the last two nuclear categories (from 50–70 μm^2 was so low (1% of the total) that >50 μm^2 was the cut-off area chosen to define abnormal, enlarged nuclei. We have previously demonstrated that this category comprises both polyploid and aneuploid nuclei (21). The p53-deficient livers showed the same size distribution as the wild-type (see Figs. 1 and 2), suggesting that p53 absence does not affect liver nuclear morphology, and this was confirmed by the observations made in the double null livers. In both the ERCC1-deficient livers and the double null livers the size distribution profiles were flatter and broader, indicating a clear shift to larger nuclear areas. We have previously reported this distribution for ERCC1-deficient mice (21) and it has also been observed by Weeda et al. (22). The mode in these two categories has increased from the wild-type value of 20–30 to 30–40 μm^2, and the biggest nuclei were up to 200 μm^2. Also, the percentage of nuclei >50 μm^2 has increased for both the ERCC1 null and the double null genotypes from the wild-type value of 1% to 34%. This percentage remained low (5%) for the p53 null livers. Using the Kolmogorov-Smirnov test, there was no significant difference in the distribution of nuclear areas in ERCC1-deficient and the double null livers, but both were significantly different (P=0.01) from wild-type.

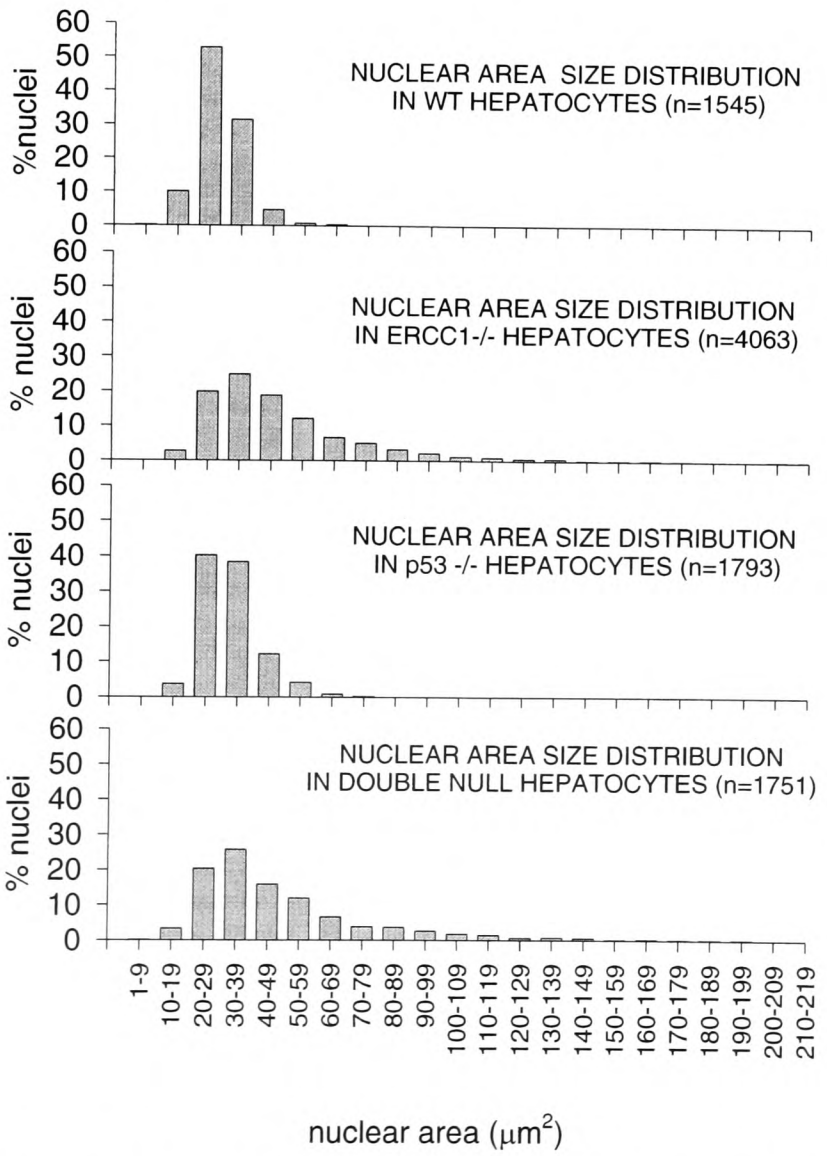

Figure 2. Hepatocyte nuclear area distribution in 3-wk-old wild-type, ERCC1-deficient, p53-deficient, and double null mice. The areas (μm^2) were calculated as described in Materials and Methods. The total number of nuclei counted per genotype is represented by *n*.

Binucleation is inhibited in ERCC1-deficient hepatocytes

The older the mouse, the higher the percentage of polyploid (4n, 8n) binucleate cells and the lower the number of diploid mononucleate cells. Binucleation arises from consecutive rounds of replication in the absence of cell division and is an essential step in the normal development of liver polyploidization (27). Therefore, a change in the pattern of binucleation in our mice would reflect changes in the regulation of liver development. Binucleate cells were counted and divided into two categories: normal (nuclear area <50 μm^2) and enlarged (area>50 μm^2). The percentage of binucleate hepatocytes in wild-type (8%) and p53-deficient livers (10%) was not significantly different (by the Mann-Whitney *U* test). In these two genotypes, there was no evidence of binucleate cells with enlarged nuclei (see **Fig. 3** and Fig. 1). In ERCC1-deficient livers, the percentage of binucleate cells (3%) was significantly lower than in all other genotypes (P=0.05 compared to wild-type), with 44% of the binucleates having enlarged nuclei. In the double nulls the total number of binucleate cells (7%) was significantly increased compared to ERCC1-deficient livers (P=0.05), being similar to that of the wild-type and p53-deficient tissues, with a high percentage (61%) of those binucleate cells having enlarged nuclei. Thus, binucleation seems to be impaired in the absence of ERCC1 and this block is rescued by the absence of p53.

The absence of p53 rescues the replication block in ERCC1-deficient liver

Sections of liver were stained with an anti-BrdU antibody to establish the replication index for each geno-

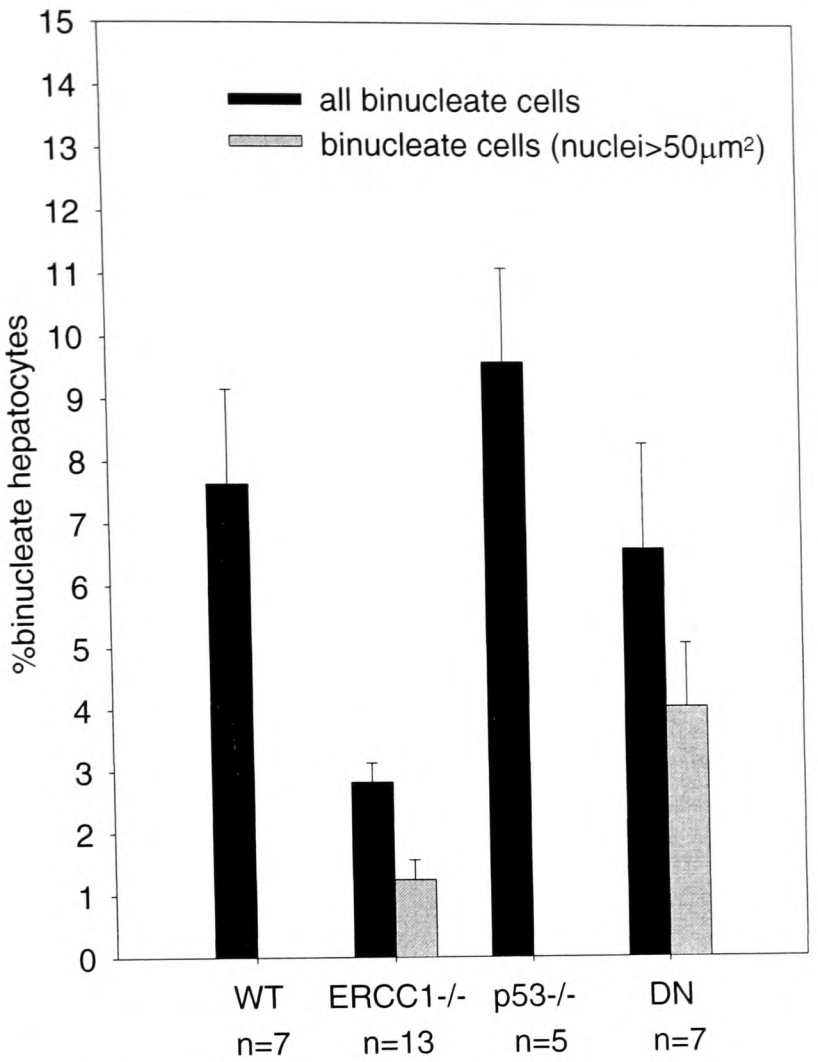

Figure 3. Percentage of binucleate hepatocytes in 3-wk-old wild-type, ERCC1-deficient, p53-deficient, and double null mice. Enlarged nuclei (when present) are represented by the second (gray) bar. DN, double null; WT, wild-type. Standard errors are shown. *n*, the number of animals sampled per genotype.

type (see **Fig. 4**). The DNA replication index is the percentage of cells labeled with BrdU during the 24 h before collection of liver samples. Because ERCC1-deficient and double null animals are always runted, it was decided to use rare, runted wild-type and p53 nulls as controls for this experiment. We have previously reported that the liver nuclear abnormalities in ERCC1-deficient mice are not observed in runted control animals (21). BrdU incorporation was also determined for normal (nonrunted) wild-type animals. Overall, the replication index for the runted wild-type, p53-deficient, and ERCC1-deficient livers was very low (<2%, see Figs. 1, 4), although these values were not significantly different (by the Mann-Whitney *U* test) from the higher value (4%) in the normal-sized wild-type animals. Lower values were expected since these groups all suffered from a growth impairment. Although replication levels in ERCC1-deficient livers were less than in nonrunted wild-type animals when compared to runted wild-type animals, there was no detrimental effect in terms of replication. In runted p53-deficient livers, the levels of replication were not rescued to normal wild-type (nonrunted) levels. However, in the double null livers the level of replication has significantly increased compared to all other runted genotypic classes (P=0.1 compared to ERCC1-deficient), reaching normal levels and demonstrating a bypass of the replication arrest typical of runted animals.

Once the difference in the liver DNA replication indices was established, we determined which subpopulation of hepatocytes (i.e., normal, or enlarged nuclei) was responsible for the increased BrdU incorporation in double null livers. The size distribution of BrdU-positive nuclei is shown in **Fig. 5**. When the size distribution of BrdU-stained nuclei is compared to the general nuclear size distribution, it is clear that although the distributions of BrdU-stained nuclei in the wild-type, p53 null, and ERCC1 null livers correspond with the general area distribution for the same genotypic classes, this is not the case for the double null livers. In this latter case, the distribution of sizes of BrdU-positive nuclei is significantly shifted (P=0.01 by Kolmogorov-Smirnov test) toward the enlarged nuclei (see also Fig. 1*D*). The replicative potential of the double null livers is concentrated in the subpopulation of hepatocytes with enlarged nuclei. Taken together with the earlier demonstration that the percentage of BrdU-stained nuclei in these livers is higher than in any of the other runted animals and has reached levels equivalent to normal wild-type livers, it is reasonable to think that those nuclei that have 'gained' a replicative status are the enlarged nuclei. This 'gain of replicative function' effect is not seen in p53-deficient liver.

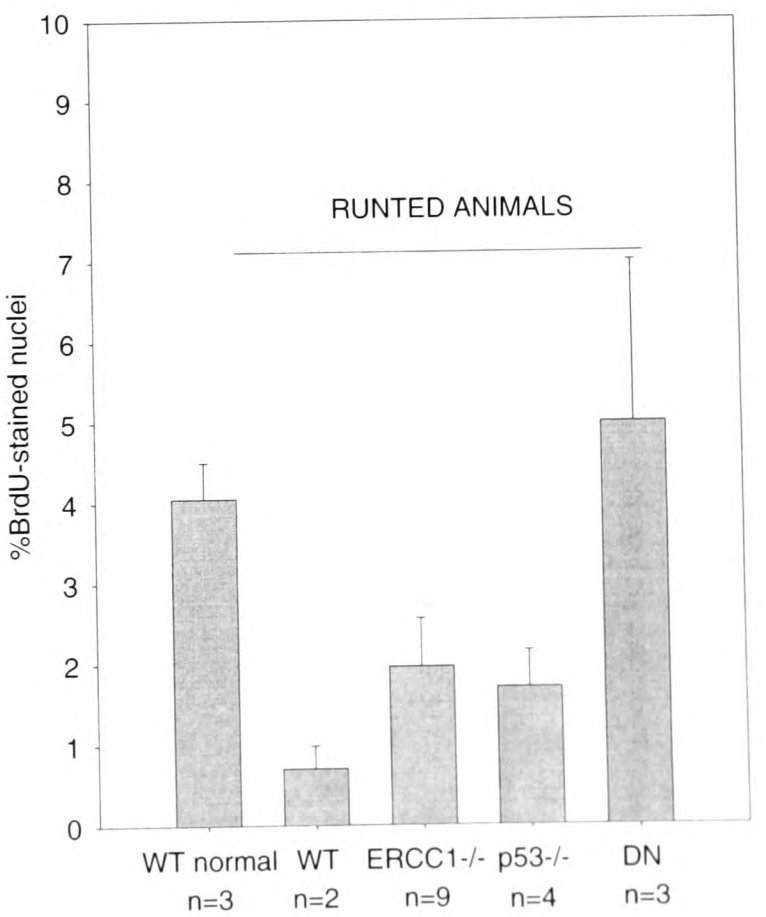

Figure 4. Percentage of BrdU-stained hepatocytes in 3-wk-old wild-type, ERCC1-deficient, p53-deficient, and double null mice. DN, double null; WT, wild-type. Standard errors are shown. *n*, the number of animals sampled per genotype.

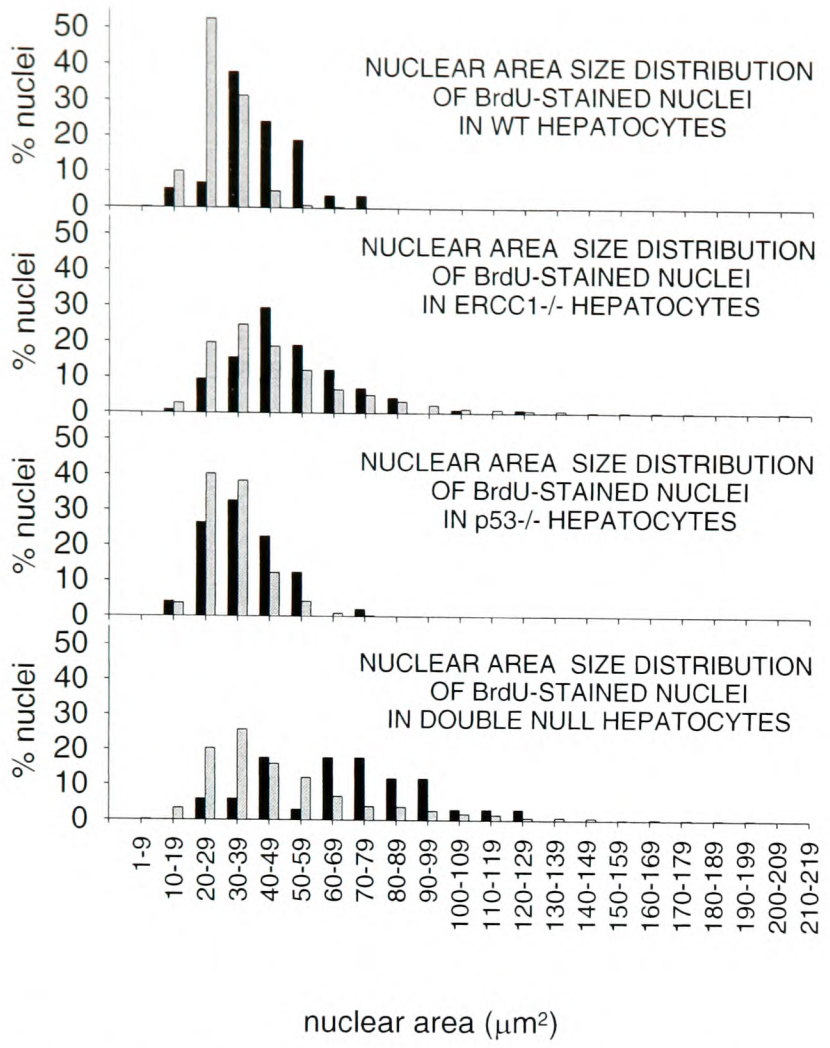

Figure 5. Nuclear area size distribution of BrdU-stained hepatocyte nuclei from 3-wk-old wild-type, ERCC1-deficient, p53-deficient, and double null mice. The BrdU-stained nuclear area size distribution is shown as black bars. For comparative purposes, the general nuclear area size distribution (from Fig. 2) is also shown (gray bars).

Enlarged ERCC1-deficient hepatocytes are arrested in G_2

ERCC1-deficient liver has a reduced growth rate and DNA replication index compared to normal control animals. Because of the increased hepatocyte DNA content and the presence of many nonhepatocyte cell types in young mouse livers, conventional FACS analysis of liver nuclear DNA content could not be used to obtain a simple indication of the stage of the cell cycle at which individual hepatocytes were; therefore, centromeric staining of hepatocytes was used to aid the determination (see **Fig. 6**). The autoimmune serum used stains mammalian centromeres (32). Each centromere appears as a single structure until centromere duplication occurs in G_2 and the structures become double (33). Thus, the presence of double centromere structures identifies cells in G_2. Fifty nuclei were scored from each 3-wk-old liver: six wild-type, five ERCC1-deficient, one p53-deficient, and one double null. The mean values (%) for hepatocytes in G_2 were wild-type 33 ± 2; p53-deficient 32; ERCC1-deficient, normal nuclei 36 ± 4; enlarged nuclei 62 ± 3; double null, normal nuclei 20; enlarged nuclei 50. A typical wild-type hepatocyte is shown in Fig. 6*A*. Each red spot represents a centromere; chromosomes appear blue. Since the majority of the centromeres appear as single structures (single red dots), it is concluded that this nucleus is not in G_2, but is instead in G_1 (or G_0), or S-phase. A typical enlarged ERCC1-deficient hepatocyte in G_2 is shown in Fig. 6*B*, identified by a prominence of double centromeric structures. The values for wild-type and normal ERCC1-deficient nuclei in G_2 are not significantly different (by Student's *t* test), but G_2 levels are significantly higher in enlarged ERCC1-deficient nuclei (P=0.01). We conclude there is a G_2 arrest in ERCC1-deficient and double null hepatocytes that is restricted to the enlarged hepatocyte population.

p21 is a possible mediator of the G_2 arrest and increased DNA content in ERCC1-deficient liver

A role for p21 in G_2 arrest and/or increased liver ploidy was supported by the finding that mice overexpressing p21 in their liver present a similar liver phenotype to our ERCC1-deficient mice (26). To see whether elevated levels of p21 were present in ERCC1 null mice, liver RNA was assayed for p21 mRNA levels. **Figure 7** corresponds to a sample Northern autoradiograph probed first with p21 and then reprobed with GAPDH as a loading control. A summary of the standardized p21 mRNA levels is shown in **Fig. 8**. The level of p21 mRNA in ERCC1-deficient and double null livers was 2- and 4.5-fold higher than that of the wild-type livers, respectively. Both values are significantly higher than wild-type (by the Mann-Whitney

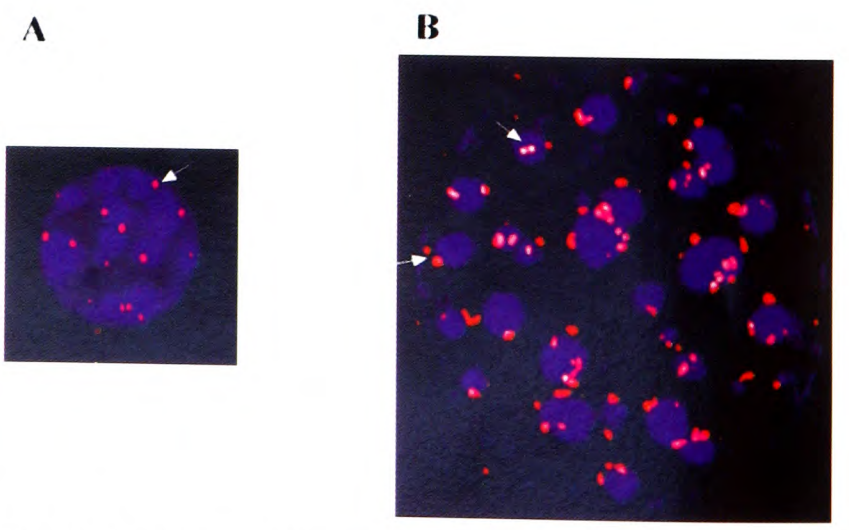

Figure 6. Centromeric staining in 3-wk-old wild-type and ERCC1-deficient hepatocytes. Binding of the NR antibody to centromeres was visualized with a Texas red-conjugated secondary antibody. Each centromeric structure is represented by a red spot. The DNA is stained with DAPI and presents a blue color. *A)* Wild-type, the majority of the centromeric structures, appear as single spots (arrow indicates a typical single spot). *B)* Enlarged ERCC1-deficient. Here the majority of the red dots appear as double spots (arrows indicate two typical double spots), so this nucleus is in G_2.

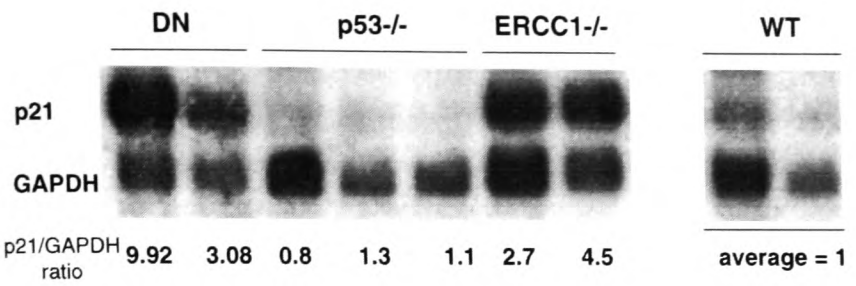

Figure 7. Northern analysis of p21 mRNA levels in liver from 3-wk-old wild-type, ERCC1-deficient, p53-deficient, and double null mice. The signal corresponding to p21 mRNA is shown. To obtain a loading control, the filter was reprobed with GAPDH and the ratio of p21/GAPDH signals for each sample was calculated using a PhosphorImage analysis system and expressed relative to the ratio for wild-type. DN, double null; WT, wild-type.

U test, $P=0.1$ for ERCC1-deficient, $P=0.05$ for double null), but not significantly different from each other. Since we have not measured p21 levels in individual hepatocytes and ERCC1-deficient liver contains both normal (diploid) and enlarged cells (arrested in G_2 with increased DNA content), we are unable to determine whether the elevated p21 levels are associated with the G_2 arrest, increased DNA content, or both. In p53-deficient livers (in the presence of proficient NER) the levels of p21 were equivalent to wild-type. Thus, in mouse liver, the expression of p21, both in the presence and absence of NER, is p53-independent.

DISCUSSION

The tumor suppressor p53 has a prominent role in cell cycle regulation and apoptosis in response to DNA damage (34, 35). Tight regulation of DNA repair and cell cycle progression is necessary for the cell to cope with genotoxic stress (36–38), and p21 has been shown to play an important role in this process via both p53-dependent and independent pathways (39, 40). The liver phenotype in the ERCC1-deficient mouse reflects a profound misregulation of the cell cycle. p53 levels had already been found to be elevated in ERCC1-deficient livers (21), making this a good model for the *in vivo* study of the relationship between p53, DNA repair and cell cycle control. We have previously reported that 3-wk-old ERCC1-deficient mice have a distribution of hepatocyte nuclear areas that is reminiscent of an aged wild-type (21), suggesting that the phenotype presented by the young ERCC1-deficient mice may also be related to premature aging. We have now investigated this further by carrying out an analysis of aspects of the hepatocyte's life cycle, such as nuclear size and binucleation rates, which change during liver development and differentiate young from old livers, in addition to studying the cell cycle regulation.

Binucleation

The normal binucleation process was impaired in ERCC1-deficient animals, but wild-type levels of binucleation were observed in p53 and ERCC1 double null livers, indicating a role for p53 in preventing binucleation in the absence of ERCC1. However, in repair-proficient normal circumstances, p53 absence did not affect binucleation. This p53-dependent suppression of binucleation in ERCC1-deficient cells can be understood in the context of the protective role of p53. If cells that cannot repair their damaged DNA proceed through either replication or binucleation (which involves a round of replication followed by an acytokinetic cell division), this could lead to the fixation of mutations and the creation of chromosomal aberrations.

DNA replication index

The protective effect of p53 in suppressing DNA replication in ERCC1-deficient liver can be seen from the BrdU labeling data. Except for the double null mice, all runted animals have lower replication indices than nonrunted wild-type animals, consistent with their intrinsic growth retardation. The values obtained for normal wild-type animals agree with results obtained by other groups (41, 42). These low

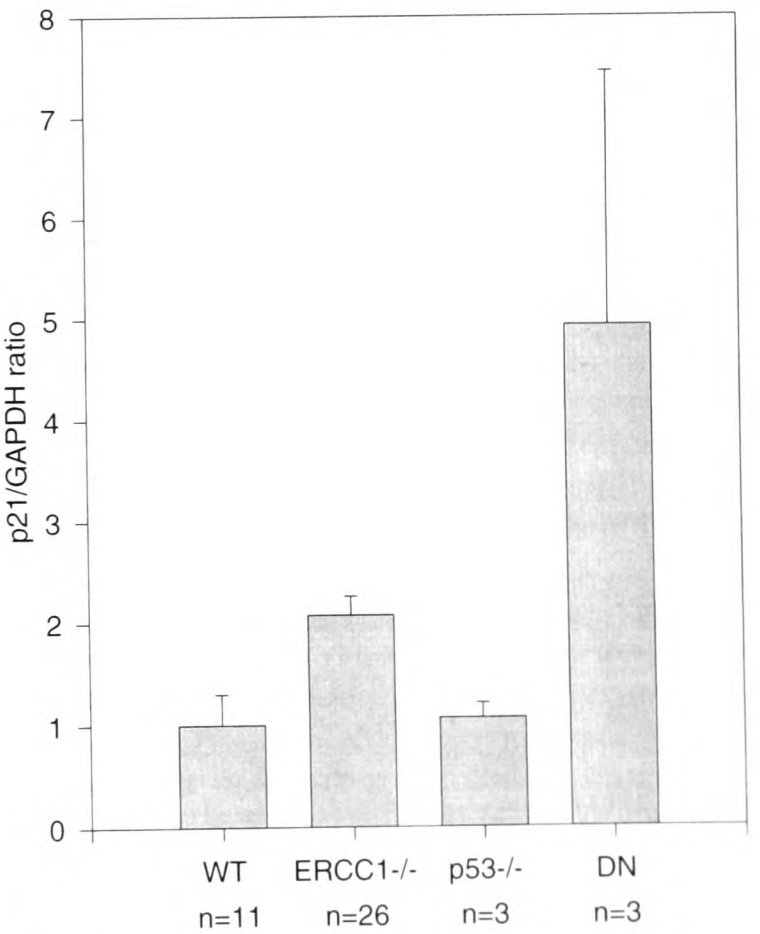

Figure 8. Summary of p21 mRNA levels in liver from 3-wk-old wild-type, ERCC1-deficient, p53-deficient, and double null mice. The mean p21/GAPDH ratio and standard errors are shown, expressed relative to a mean value of 1 for wild-type. DN, double null; WT, wild-type. *n*, the number of animals sampled per genotype.

runt-related levels in the ERCC1-deficient animals are rescued back to normal, higher levels in the absence of p53.

p21 in liver

p21 has a well-established role in cell cycle control and the regulation of cell growth; overexpression of p21 in liver has also been linked to an ERCC1 null-like phenotype (26). Elevated levels of p21 have been reported in primary fibroblasts derived from ERCC1-deficient mice (22), although no data were provided to support this affirmation. Our data demonstrate that increased liver p21 mRNA levels are associated with either the G_2 arrest or the premature increase in nuclear DNA content seen in ERCC1-deficient mice; furthermore, the p21 response is p53 independent. Another line of evidence comes from studies performed *in vitro* using a human colorectal carcinoma cell line (DLD1), where a p53-independent role for p21 in cell growth and DNA repair has been proposed (43). p21 has been shown to play a role in the control of the initiation of mitosis (G_2/M transition) through its inhibitory effect on cdk2 and cdk1-cyclin B (44). p21 has also been shown to bind and inhibit cdk1-cyclin A complexes, which play an important regulatory role in early mitosis (45). The ERCC1 null mouse may be a useful tool to understand the effect of p21-mediated growth arrest and its relationship with the DNA repair machinery *in vivo*.

Liver ploidy

The most striking feature of ERCC1-deficient liver is the increased hepatocyte DNA content at such an early age. Our previous studies have shown that the population of cells with enlarged nuclei comprises both polyploid and aneuploid cells (21). In normal mammals, polyploidization of hepatocytes is strongly correlated with age and the extent of genotoxic damage, but aneuploidy is not usually observed (28). Because hepatocytes absorb toxic products as part of their function, liver cells may accumulate genetic damage more rapidly than cells from other tissues. The absence of a special pool of nondifferentiated stem cells may make polyploidization a safer way to compensate for cellular losses than mitosis, which may result in a high incidence of chromosomal abnormality (28). Apart from its role in protecting against the deleterious cellular effects of endogenous DNA damage, polyploidization allows the liver to preserve its normal size and functional capability without the risk of accumulating through mitosis a large proportion of aberrant, aneuploid cells, which may increase the level of cellular transformation. Several hypotheses seek to explain the possible mechanism by which polyploidization exerts its protective role: by reiteration of vital genes, by making the cell more resistant to toxins and carcinogens, and by providing a morphogenetic strategy against aging in specialized diploid systems. However, the polyploidization of hepatocytes in later periods of life, particularly the progressive polyploidization observed in mouse liver during senescence, by formation of nuclei up to 32n in DNA content is apparently an integral part of the aging process; more than representing a real protection against aging, it could well be a tissue-specific adaptation to age-related cellular loss (28).

Endoreduplication

Polyploidization comes about by continuous rounds of DNA replication in the absence of mitosis (a process known as endoreduplication). p21 has also been implicated in the regulation of the checkpoints that prevent endoreduplication (20, 46). We have observed endoreduplication in the presence of elevated levels of p21, as opposed to its absence, so we propose that misregulation of p21 expression (either its absence or its overexpression) results in the uncoupling of the normal link between S-phase and mitosis, leading to cells in G_2 undergoing repeated rounds of replication in the absence of mitosis. Alternatively, elevated levels of p21, in response to nonrepaired, accumulating damage, may lead the hepatocytes down a terminal (and also protective) differentiation pathway. p21 has been reported to play an important part in the differentiation process of several cell types (47, 48). Since polyploidization is the natural state of 'aged' hepatocytes, the ERCC1 null phenotype could indeed be equivalent to a premature aging syndrome.

Greater levels of DNA replication were observed in enlarged G_2-arrested hepatocytes from animals deficient in both ERCC1 and p53. This observation would also predict higher DNA content (increased nuclear size) in double nulls compared to ERCC1-deficient, which was not observed. Perhaps the replication is only partial and not sufficient to result in higher levels of endoreduplication and a detectable increase in nuclear volume. However, it again illustrates the protective role of p53 in preventing DNA replication in ERCC1-deficient liver.

Model for the ERCC1-deficient liver phenotype

It is important to remember that the ERCC1-deficient liver phenotype arises spontaneously in the absence of exogenous DNA-damaging agents. The liver is required for a large number of metabolical processes such as lipid peroxidation, intermediate metabolism of carbohydrates and proteins, synthesis

of proteins and detoxification and removal of foreign material such as bacteria, drugs and other noxious substances. All this results in the liver cells being exposed to and producing large quantities of genotoxic agents, such as oxygen-free radicals and toxic metabolic byproducts. Many of these will result in bulky DNA adducts that are normally repaired by NER. However, given that the same liver phenotype is not observed in XPA (23, 25), XPC (24), or the recently reported XPG knockout mice (49), it has been suggested that other forms of damage, which are dealt with by the recombinational repair pathway, may be more significant (22). Probable involvement in this recombinational pathway distinguishes ERCC1 from most other NER proteins. The contribution that different forms of endogenous damage make to the ERCC1-deficient phenotype will be resolved when the DNA lesions are identified directly in ERCC1-deficient liver. The accumulation of unrepaired damage does not result in the normal cell cycle arrest at G_1/S. Instead, cells replicate and a population of cells arrested in G_2 with increased DNA content accumulates. This is associated with a p53-independent accumulation of p21. The premature polyploidization may be a protective response to the accumulation of damaged DNA. The development of polyploidy in young ERCC1-deficient mice is different from the normal situation in aging wild-type animals, where aneuploidy is not usually observed. ERCC1-deficient hepatocytes with increased, but aneuploid, DNA content may represent incomplete rounds of endoreduplication where replication has been physically prevented by unrepaired DNA lesions. p53 accumulates in ERCC1-deficient liver, but the main features of the phenotype are independent of p53. However, p53 does act to prevent binucleation and reduce the amount of DNA replication. FJ

Mouse genotyping was done by Carolanne McEwan. We would like to thank Prof. William Earnshaw (Institute of Cell and Molecular Biology, Edinburgh University) for his help with the deconvolution microscopy. We also want to thank Steve Mackell (Department of Pathology, Edinburgh University) for his help with the BrdU staining. F.N. was supported by a Ph.D. studentship from the Darwin Trust of Edinburgh. M.D.C. was supported by a Ph.D. studentship from the Medical Research Council. A.R.C. is a Royal Society University Research Fellow. This work was supported by a project grant (SP2095/0201) and a program grant (SP2095/0301) from The Cancer Research Campaign to D.W.M.

REFERENCES

1. Wood, R. D. (1996) DNA repair in eukaryotes. *Annu. Rev. Biochem.* **65,** 135–167
2. Wood, R. D. (1997) Nucleotide excision repair in mammalian cells. *J. Biol. Chem.* **272,** 23465–23468
3. Westerveld, A., Hoeijmakers, J. H. J., van Duin, M., Dewit, J., Odijk, H., Pastink, A., Wood, R. D., and Bootsma, D. (1984) Molecular cloning of a human DNA repair gene. *Nature (London)* **310,** 425–429
4. van Duin, M., Janssen, J. H., Dewit, J., Hoeijmakers, J. H. J., Thompson, L. H., Bootsma, D., and Westerveld, A. (1988) Transfection of the cloned human excision repair gene ERCC-1 to UV- sensitive CHO mutants only corrects the repair defect in complementation group-2 mutants. *Mutat. Res.* **193,** 123–130
5. van Duin, M., Vredeveldt, G., Mayne, L. V., Odijk, H., Vermeulen, W., Klein, B., Weeda, G., Hoeijmakers, J. H. J., Bootsma, D., and Westerveld, A. (1989) The cloned human DNA excision repair gene ERCC-1 fails to correct xeroderma pigmentosum complementation group-A through group-I. *Mutat. Res.* **217,** 83–92
6. Park, C. H., Bessho, T., Matsunaga, T., and Sancar, A. (1995) Purification and characterization of the XPF-ERCC1 complex of human DNA-repair excision nuclease. *J. Biol. Chem.* **270,** 22657–22660
7. Friedberg, E. C., Walker, G. C., and Siede, W. (1995) *DNA Repair and Mutagenesis,* ASM Press, Washington D.C.
8. van Duin, M., Dewit, J., Odijk, H., Westerveld, A., Yasui, A., Koken, M. H. M., Hoeijmakers, J. H. J., and Bootsma, D. (1986) Molecular characterization of the human excision repair gene ERCC-1 cDNA: cloning and amino acid homology with the yeast DNA repair gene rad10. *Cell* **44,** 913–923
9. Rodel, C., Kirchhoff, S., and Schmidt, H. (1992) The protein sequence and some intron positions are conserved between the switching gene swi10 of *Schizosaccharomyces pombe* and the human excision repair gene ERCC1. *Nucleic Acids Res.* **20,** 6347–6353
10. Sargent, R. G., Rolig, R. L., Kilburn, A. E., Adair, G. M., Wilson, J. H., and Nairn, R. S. (1997) Recombination-dependent deletion formation in mammalian cells deficient in the nucleotide excision repair gene ERCC1. *Proc. Natl. Acad. Sci. USA* **94,** 13122–13127
11. Melton, D. W., Ketchen, A.-M., Nunez, F., Bonatti-Abbondandolo, S., Abbondandolo, A., Squires, S., and Johnson, R. T. (1998) Cells from ERCC1-deficient mice show increased genome instability and a reduced frequency of S-phase-dependent illegitimate chromosome exchange but a normal frequency of homologous recombination. *J. Cell Sci.* **111,** 395–404
12. Fisher, P. B. (1996) p21 in differentiation. DNA-repair, tumor progression, and senescence. *Mol. Cell. Differ.* **4,** U7
13. Clarke, A. R., Purdie, C. A., Harrison, D. J., Morris, R. G., Bird, C. C., Hooper, M. L., and Wyllie, A. H. (1993) Thymocyte apoptosis induced by p53-dependent and independent pathways. *Nature (London)* **362,** 849–852
14. Lowe, S. W., Schmitt, E. A., Smith, S. W., Osborne, B. A., and Jacks, T. (1993) p53 is required for radiation-induced apoptosis in mouse thymocytes. *Nature (London)* **362,** 847–849
15. Atadja, P., Wong, H., Garkavtsev, I., Veillette, C., and Riabowol, K. (1995) Increased activity of p53 in senescing fibroblasts. *Proc. Natl. Acad. Sci. USA* **92,** 8348–8352
16. Brown, J. P., Wei, W. Y., and Sedivy, J. M. (1997) Bypass of senescence after disruption of p21(Cip1/Waf1) gene in normal diploid human fibroblasts. *Science* **277,** 831–834
17. Brugarolas, J., Chandrasekaran, C., Gordon, J. I., Beach, D., Jacks, T., and Hannon, G. J. (1995) Radiation-induced cell cycle arrest compromised by p21 deficiency. *Nature (London)* **377,** 552–557
18. Deng, C. X., Zhang, P. M., Harper, J. W., Elledge, S. J., and Leder, P. (1995) Mice lacking p21(Cip1/Waf1) undergo normal development, but are defective in G1 checkpoint control. *Cell* **82,** 675–684
19. Polyak, K., Waldman, T., He, T. C., Kinzler, K. W., and Vogelstein, B. (1996) Genetic determinants of p53-induced apoptosis and growth arrest. *Genes Dev.* **10,** 1945–1952
20. Waldman, T., Lengauer, C., Kinzler, K. W., and Vogelstein, B. (1996) Uncoupling of S phase and mitosis induced by anticancer agents in cells lacking p21. *Nature (London)* **381,** 713–716
21. McWhir, J., Selfridge, J., Harrison, D. J., Squires, S., and Melton, D. W. (1993) Mice with DNA-repair gene (ERCC-1) deficiency have elevated levels of p53, liver nuclear abnormalities and die before weaning. *Nat. Genet.* **5,** 217–224
22. Weeda, G., Donker, I., de Wit, J., Morreau, H., Janssens, R., Vissers, C. J., Nigg, A., van Steeg, H., Bootsma, D., and Hoeijmakers, J. H. J. (1997) Disruption of mouse ERCC1 results in a novel repair syndrome with growth failure, nuclear abnormalities and senescence. *Curr. Biol.* **7,** 427–439

23. de Vries, A., van Oostrom, C. T. M., Hofhuis, F. M. A., Dortant, P. M., Berg, R. J. W., Degruijl, F. R., Wester, P. W., van Kreijl, C. F., Capel, P. J. A., van Steeg, H., and Verbeek, S. J. (1995) Increased susceptibility to ultraviolet-B and carcinogens of mice lacking the DNA excision-repair gene XPA. *Nature (London)* **377,** 169–173
24. Sands, A. T., Abuin, A., Sanchez, A., Conti, C. J., and Bradley, A. (1995) High susceptibility to ultraviolet-induced carcinogenesis in mice lacking XPC. *Nature (London)* **377,** 162–165
25. Nakane, H., Takeuchi, S., Yuba, S., Saijo, M., Nakatsu, Y., Murai, H., Nakatsuru, Y., Ishikawa, T., Hirota, S., Kitamura, Y., Kato, Y., Tsunoda, Y., Miyauchi, H., Horio, T., Tokunaga, T., Matsunaga, T., Nikaido, O., Nishimune, Y., Okada, Y., and Tanaka, K. (1995) High-incidence of ultraviolet-B-induced or chemical carcinogen-induced skin tumors in mice lacking the xeroderma pigmentosum group-A gene. *Nature (London)* **377,** 165–168
26. Wu, H., Wade, M., Krall, L., Grisham, J., Xiong, Y., and van Dyke, T. (1996) Targeted in-vivo expression of the cyclin-dependent kinase inhibitor p21 halts hepatocyte cell-cycle progression, postnatal liver development, and regeneration. *Genes Dev.* **10,** 245–260
27. Epstein, C. J. (1967) Cell size, nuclear content, and the development of polyploidy in the mammalian liver. *Proc. Natl. Acad. Sci. USA* **57,** 327–334
28. Medvedev, Z. A. (1986) Age-related polyploidisation of hepatocytes: the cause and possible role. *Exp. Gerontol.* **21,** 277–282
29. Thompson, S., Clarke, A. R., Pow, A. M., Hooper, M. L., and Melton, D. W. (1989) Germ line transmission and expression of a corrected HPRT gene produced by gene targeting in embryonic stem cells. *Cell* **56,** 313–321
30. Fort, P., Marty, L., Piechaczyk, M., el Sabrouty, S., Dani, C., Jeanteur, P., and Blanchard, J. M. (1985) Various rat adult tissues express only one major mRNA species from the glyceraldehyde-3-phosphate dehydrogenase multigene family. *Nucleic Acids Res.* **13,** 1431–1442
31. Brugal, G. (1992) HOME: Highly optimised microscope environment. *Cytometry* **13,** 109–116
32. Earnshaw, W. C., and Rothfield, N. (1985) Identification of a family of human centromere proteins using autoimmune sera from patients with scleroderma. *Chromosoma* **91,** 313–321
33. Brenner, S., Pepper, D., Berns, M. W., Tan, E., and Brinkley, B. R. (1981) Kinetochore structure, duplication, and distribution in mammalian cells: analysis by human antibodies from scleroderma patients. *J. Cell Biol.* **91,** 95–102
34. Sanchez, Y., and Elledge, S. J. (1995) Stopped for repairs. *BioEssays* **17,** 545–548
35. Jacks, T., and Weinberg, R. A. (1996) Cell-cycle control and its watchman. *Nature (London)* **381,** 643–644
36. Kaufmann, W. K., and Paules, R. S. (1996) DNA-damage and cell-cycle checkpoints. *FASEB J.* **10,** 238–247
37. Murray, A. (1994) Cell cycle checkpoints. *Curr. Opin. Cell Biol.* **6,** 872–876
38. Pellegata, N. S., Antoniono, R. J., Redpath, J. L., and Stanbridge, E. J. (1996) DNA damage and p53-mediated cell cycle arrest: a re-evaluation. *Proc. Natl. Acad. Sci. USA* **93,** 15209–15214
39. Cox, L. S. (1997) Multiple pathways control cell growth and transformation: Overlapping and independent activities of p53 and p21(Cip1/Waf1/Sdi1). *J. Pathol.* **183,** 134–140
40. Savio, M., Stivala, L. A., Scovassi, A. I., Bianchi, L., and Prosperi, E. (1996) p21(Waf1/Cip1) protein associates with the detergent-insoluble form of PCNA concomitantly with disassembly of PCNA at nucleotide excision-repair sites. *Oncogene* **13,** 1591–1598
41. Soames, A. R., Lavender, D., Foster, J. R., Williams, S. M., Wheeldon, E. B., and Fornace, A. J. (1994) Image analysis of bromodeoxyuridine (BrdU) staining for measurement of S-phase in rat and mouse liver. *J. Histochem. Cytochem.* **42,** 939–944
42. Sakata, H., Takayama, H., Sharp, R., Rubin, J. S., Merlino, G., and LaRochelle, W. J. (1996) Hepatocyte growth factor/scatter factor overexpression induces growth, abnormal development and tumor formation in transgenic mouse livers. *Cell Growth Differ.* **7,** 1513–1523
43. Sheikh, M. S., Chen, Y. Q., Smith, M. L., and Fornace, A. J. (1997) Role of p21(Waf1/Cip1/Sd1) in cell death and DNA repair as studied using a tetracycline-inducible system in p53-deficient cells. *Oncogene* **14,** 1875–1882
44. Guadagno, T. M., and Newport, J. W. (1996) Cdk2 kinase is required for entry into mitosis as a positive regulator of cdc2-cyclin B kinase activity. *Cell* **84,** 73–82
45. Basi, G., and Draetta, G. (1995) The cdc2 kinase: structure, activation and its role at mitosis in vertebrate cells. In *Cell Cycle Control* (Hutchison, C., and Glover, D. M., eds) pp. 106–143, IRL Press at Oxford University Press
46. Bates, S., Ryan, K. M., Phillips, C., and Vousden, K. (1998) Cell cycle arrest and DNA endoreduplication following $p21^{Waf1/Cip1}$ expression. *Oncogene* **17,** 1691–1703
47. Jiang, H. P., Lin, J., Su, Z. Z., Collart, F. R., Huberman, E., and Fisher, P. B. (1994) Induction of differentiation in human promyelocytic HL-60 leukemia-cells activates $p21^{Waf1/Cip1}$ expression in the absence of p53. *Oncogene* **9,** 3397–3406
48. Parker, S. B., Eichele, G., Zhang, P. M., Rawls, A., Sands, A. T., Bradley, A., Olson, E. N., Harper, J. W., and Elledge, S. J. (1995) p53-independent expression of p21(Cip1) in muscle and other terminally differentiating cells. *Science* **267,** 1024–1027
49. Harada, Y. N., Shiomi, N., Koike, M., Ikawa, M., Okabe, M., Hirota, S., Kitamura, Y., Kitagawa, M., Matsunaga, T., Nikaido, O., and Shiomi, T. (1999) Postnatal growth failure, short life span, and early onset of cellular senescence and subsequent immortalization in mice lacking the xeroderma pigmentosum group G gene. *Mol. Cell. Biol.* **19,** 2366–2372

Received for publication August 4, 1999.
Revised for publication January 3, 2000.